No. 1 Vol.3 September 2020 - August 2021

The Proceeding of

ASEAN Bioenergy and Bioeconomy Conference 2020

ASEAN Bioenergy and Bioeconomy Conference 2020:

Sustainable Bioresources for Green Energy and Economy

September 24th, 2020

BITEC, Bangkok, THAILAND

With ASEAN Sustainable Energy Week 2020

September 23rd -26th, 2020

ISSN: 2586-9280

Organized by

Kasertsart Agricultural and Agro-Industrial Product Improvement Institute (KAPI),

Kasetsart University, Bangkok, THAILAND

E-mail: conference.abb@gmail.com

Website: www.abbconf.kapi.ku.ac.th

PROCEEDING OF

ASEAN Bioenergy and Bioeconomy Conference 2020

EDITED BY

SUMAPORN KASEMSUMRAN

PILANEE VAITHANOMSAT

ORGANIZING COMMITTEE MEMBERS

Advisors

Chongrak Wachrinrat, President of Kasetsart University
Sornprach Thanisawanyangkura, Vice President for Planning and Research, Kasetsart University
Araya Bijaphala, Director of International Affairs Division, Kasetsart University
Prasert Sinsukprasert, Ministry of Energy
Representative of Informa Markets (Thailand)
Pilanee Vaithanomsat, Director of Kasetsart Agricultural and Agro-Industrial Product Improvement Institute (KAPI), Kasetsart University
Maliwan Haruthaithanasan, Head of Special Research Unit of Biomass Management Technology for Energy and Energy Crops, Kasetsart Agricultural and Agro-Industrial Product Improvement Institute (KAPI), Kasetsart University

Chairman

Sumaporn Kasemsumran, KAPI, Kasetsart University

Vice-Chairman

Chakrit Tachaapaikoon, King Mongkut's University of Technology Thonburi (KMUTT)
Worajit Setthapun, Chiang Mai Rajabhat University

Members

Scientific Committee

Pathama Chatakanonda, KAPI
Rungsima Chollakup, KAPI
Patthra Pason, KMUTT
Pasinee Worachananant, KU
Chayanon Sawatdeenarunat, CMRU
Siriluck Liengprayoon, KAPI
Nattaporn Khanoonkon, KAPI
Jaruporn Rakmai, KAPI

Registration Committee

Prapassorn Rugthaworn, KAPI
Natedao Musigamart, KAPI
Phornphimon Janchai, KAPI
Jirachaya Boonyarit, KAPI

Coordination Committee

Tepa Phudphong, KAPI
Pussadee Sukpiboon, KAPI
Pavina Badan, KAPI

Secretariat Team

Preeyanuch Srichola, KAPI
Antika Boondaeng, KAPI
Thotsaphon Umamanit, KAPI

Reception Committee

Udomlak Sukatta, KAPI
Warapron Apiwatanapiwat, KAPI
Rattiya Weanukul, KMUTT
Prapaipid Chairattanamanokorn, KU

Exhibition Committee

Kasem Haruthaithanasan, KAP
Eakpong Tanavat, KAPI
Keowpetch Lobyam, KAPI
Jakkapong Vongtayan, KAPI

Information and Communication Committee

Warawut Suphamitmongkol, KAPI
Supansa Pakdeesrisontikul, KAPI

EDITORIAL BOARD MEMBERS

ASEAN Bioenergy and Bioeconomy Conference 2020: Sustainable Bioresources for Green Energy and Economy September 24th, 2020 Bangkok International Trade and Exhibition Centre (BITEC), Bangkok, Thailand

The first ABB conference was organized in 2017 with focus on sustainable management and partnership. Since then, ABB conference promoted the exchange of knowledge of bioenergy and bioeconomy, providing opportunities to update database, status and situation in ASEAN countries. The conference has a strong participation of researchers, private sectors, business developers and policy makers and has been an important platform for a dialogue between academic and industrial scientists and technologists.

Objectives

1) To exchange and transfer useful information on biomass and bioenergy database, status and situation, new knowledge and technologies and innovation among ASEAN countries
2) To enhance sustainable biomass for energy production and utilization in ASEAN region to relieve environmental crisis and increase competitiveness of biomass for energy from ASEAN countries to the world market
3) To strengthen the biomass and bioenergy network within ASEAN countries

Conference Topics

Bioenergy

- Biomass
- Biofuel

Bioeconomy

- Biorefinery
- Biocomposite
- Biopharmaceutical

Total 100 Participants

Organizing Committee

- Kasetsart Agricultural and Agro-industrial Product Improvement Institute (KAPI), Kasetsart University, Thailand
- Asian Development College for Community Economy and Technology, Chiang Mai Rajabhat University, Mae Rim Campus, Thailand
- King Mongkut's University of Technology Thonburi (KMUTT), Thailand
- Informa Markets (Thailand) Company Limited
- GFA-Certification Company Limited

PROGRAM

ASEAN Bioenergy and Bioeconomy Conference 2020:
Sustainable Bioresources for Green Energy and Economy
September 24th, 2020, BITEC, Bangkok, Thailand

PROGRAM (cont.)

ASEAN Bioenergy and Bioeconomy Conference 2020:
Sustainable Bioresources for Green Energy and Economy
September 24th, 2020, BITEC, Bangkok, Thailand

14.00-14.40	***Coffee break and Poster session***	
14.40-15.00	**Oral presentation 4-Bioeconomy** **O-EC4:** Isolation of mannanase-producing *Bacillus tequilensis* from pickled tea for mannooligosaccharides production **Waralee Suyama** School of Bioresources and Technology, King Mongkut's University of Technology Thonburi	30
15.00-15.20	**Oral presentation 5-Bioenergy** **O-EN1:** Lipase digestion by indigeneous bacteria for used frying oil-based biodiesel synthesis **Kanokwan Kamanake** Faculty of Science at Siracha, Kasetsart University Siracha Campus	37
15.20-15.40	**Oral presentation 6-Bioenergy** **O-EN2:** Catalytic reforming of synthesis gas from crude glycerol: Potential for rice husk catalyst study **Kamonrat Suksumrit** Expert Center of Innovative Clean Energy and Environment, Thailand Institute of Scientific and Technological Research	43
15.40-16.00	**Oral presentation 7-Bioenergy** **O-EN3:** Feasibility study of crude glycerol reforming to biomethanol **Kuntima Krekkeitsakul** Expert Center of Innovative Clean Energy and Environment, Thailand Institute of Scientific and Technological Research	49
16.00-16.15	**Best Oral Presentation and Poster Awards**	
16.15-16.30	**Conference Closing**	

POSTER

ASEAN Bioenergy and Bioeconomy Conference 2020

POSTER (cont.)

ASEAN Bioenergy and Bioeconomy Conference 2020

POSTER (cont.)

ASEAN Bioenergy and Bioeconomy Conference 2020

POSTER (cont.)

ASEAN Bioenergy and Bioeconomy Conference 2020

PREFACE

Dr. Chongrak Wachrinrat
President
Kasetsart University, Thailand

It is my great pleasure to extend to you all a very warm welcome to the *ASEAN Bioenergy and Bioeconomy Conference 2020* on behalf of Kasetsart University.

Allow me to extend a special welcome to the distinguished keynote speaker, Dr. Gary Denes, Head of Energy Technologies, Cenfura Limited, and to our honorable invited speakers, Dr. Yuji Yoshimura, AIST Emeritus Researcher, and Asst. Prof. Dr. Pruk Aggarangsi, Director at Energy Research and Development Institute Nakornping, Chiang Mai University. We would like to sincerely thank each of you for honoring our invitation in spite of your very busy and tight schedule.

We believe that today's symposium will open more opportunities for scientists, researchers, and technologists to share their insights and experience about innovation and research in the ASEAN Community, so that together can develop sustainable solutions to issues related to Biomass.

I would like to express my sincere appreciation to the organizing committee, led by Dr. Pilanee Vaithanomsat, Director of Kasetsart Agricultural and Agro-Industrial Product Improvement Institute (KAPI), for taking great efforts to organize the conference this year as well as to ensuring this event's continuity. My gratitude is given also to the many companies, universities, and organizations which have co-operated and contributed to this important event.

Finally, let me wish you fruitful discussions and a successful symposium. I am confident that this symposium will achieve its objectives and provide many tremendous rewards to society. I am delighted to declare this conference open.

Keynote Presentation

Dr.Gary Denes

Head of Energy Technologies, Cenfura Limited
www.cenfura.com
E-mail: gary@sigxi.com, gary.denes@cenfura.com

Dr. Gary Denes received his Ph.D. of Chemical Engineering in Sung Kyun Kwan University, Seoul, Korea. In 1984, he started his career as a Technical sales for formulations of fuel and lubricant in EXXON R&D, UK and Singapore, and hold his last position as the Asia fuel and lube technical marketing Director. In 1994, he stepped up to the Vice President of Texaco International Asia Ltd. President and CEO in 1997, and achieved the highest growth in sales and profit. In 1997, as the President and CEO of Taxaco International Asia Ltd., apart from his success in managing fuel, lubricant and its additives production and sales for Asian market, he successfully launched renewable energy projects such as bioethanol in China. Since then, he involved in various renewable energy projects in the US and other countries. In 2013, he was a Senior consultant of Kentec Energy which generate the electricity from gasification of municipal waste in Washington State. Based on his professional, he had associated in Steering Committee for ASIA Society of Automotive Engineers, Technical Committee of Korean EPA G-7 for Future technology and Senior Technical advisor of Indonesian Government in Ministry of Energy and Mining. Now, he is the Head of Energy Technologies, Cenfura Limited.

Mega Change of Global Energy Source

A. Renewable energy cost trends.

The cost of renewable energy has decreased dramatically over the past 10 years. However, the idea that fossil fuels produce cheaper power is still quite common. There are now solar and wind farms producing electricity at a lower cost than coal, which has been believed as the cheapest source of energy for last 50 years.

Renewable energy sources are becoming the definite energy option from the global point of view, Irrespective of environmental issue and climate change. In fact, many companies that use solar generation achieve the lower electricity costs than ever before. The residential area also got the benefits from renewable-energy generation.

The cost of renewable power is steadily decreasing around the world. According to the International Renewable Energy Agency (IRENA), all renewable sources showed cost decreases in 2018. As an example, solar and wind power costs decreased by 13%, hydroelectricity costs decreased by 11% and biomass power costs decreased by 14% vs. 2017.

When we compare the cost to cost between renewable energy and conventional energy source, we should consider the two below points.

1. Renewable energy that started operations recently are still calculated by finance cost which will show higher kilowatt hour cost.
2. But many existing power plants by fossil fuels like coals or heavy fuels must be paid off the financial costs. The Investors must have got the return on investment.

When the comparison is based on new renewable generation and new fossil fuel generation, the result will be in favor of renewable sources. In fact, there are now many solar and wind farms with lower kilowatt-hour costs than coal power plants.

The cheapest coal power is normally in the range of 3 to 4 cents per kilowatt-hour, but there are solar and wind power projects with contract prices below 3 cents/kWh.

Many fossil fuel power plants with low kWh prices are ending their service life. When new energy projects are considered, it is generally better for renewable sources. We consider that any corporates that depend on highly polluting energy sources must hurt their company image.

The electricity cost of clean energy sources is not only lower, but also more stable. This is a big advantage of most renewable sources of power.

As an example, sunlight shows a daily pattern, while wind and rainfall follow the local climate. Since renewable energy generation depends on stable inputs, electricity costs will remain stable in the long run – they only depend on maintenance. For example, if a power network relies heavily on gas turbines, price volatility in the natural gas market will have a strong effect on the kilowatt-hour price. On the other hand, renewable energy systems only have predictable maintenance costs, since their energy inputs are free in most cases.

We need to understand how renewable energy changed the electric business area.

For decades, the business model of power companies experienced almost no change. While the technical details are complex, the overall operation can be **summarized as follows:**

- Electricity production is centralized at power plants, which are owned by energy companies or private generators.
- Electricity is delivered to homes and businesses, using a transmission and distribution network.
- Consumption is measured for each user, and the bill is calculated by applying the corresponding tariff.

However, renewable energy sources have changed this business model, since they allow generation at the point of use. For example, homes and businesses can deploy solar power system and other technologies, assuming the role of both consumers and producers. Electricity flows in power grids had been in only one direction for decades, and now the movement is in both directions.

But while renewable energy sources have brought cheaper and cleaner electricity, they also come with technical challenges of their own. For example, both solar panels and wind turbines have a variable electricity production that depends on external inputs. Power companies only had to manage variability in consumption, but renewable sources have introduced variability to generation as well.

Fossil fuels are losing their cost advantage over clean energy sources, while having a higher environmental position. However, they still bring a key benefit to the table: being able to produce electricity on demand.

- Neither solar panels nor wind turbines can produce energy on a night without wind, but conventional power plants can continue operating if their fuel is available.
- Hydroelectricity is not affected by this, since water can be stored in a reservoir to generate power when needed. However, hydropower is demanding in site conditions, lacking the versatility of wind turbines and solar panels.

For this reasons, energy storage is important sector in the clean power industry, precisely because it eliminates the main limitation of solar panels and wind turbines.

Lithium batteries have existed for a long time, but they suffer from low efficiency and a short service life. Recent development technology batteries are much more promising in soon time, since they have the high efficiency and response speed required in the electricity sector. Batteries are still limited by their high price, but the International Renewable Energy Agency predicts price reductions of up to 60% by 2030 vs Price in 2020.

How new technologies can improve the Renewable energy sources.

Renewable generation can achieve synergy with technologies like blockchain and the Internet of things (IOT). These technologies must enhance the value of renewable energy power, like energy storage.

Blockchain has potential applications in energy trade and accountability. The technology can be used as part of a trading platform, where power grid users can sell and purchase energy freely. Homes and businesses who generate surplus energy become net producers, while those who purchase energy can optimize their mix based on the price and source.

Since blockchain keeps track of transactions, it can also be used to hold large consumers accountable for their energy consumption (if made non-anonymous). For example, blockchain transactions can reveal which large consumers are relying heavily on fossil fuel generation.

Solar panels and wind turbines depend on external inputs. They deliver power when possible, not necessarily when it is needed the most. However, an IoT platform can link multiple clean energy systems together, combining them with batteries:

- The generation and storage capacity connected to the system is aggregated, and the platform essentially becomes a virtual power plant.
- Even when capacity is distributed among multiple buildings, the system can mimic the operation of a conventional power plant.

Renewable generation can already compete with the cost of fossil fuels, and emerging technologies can add value in the near future. Energy storage systems can eliminate the variability of solar and wind power, while the IoT makes renewable generation smarter.

Renewable Energy sources from wind and solar

Renewable energy sources like wind and solar are already as cheap or cheaper than traditional fuels in about half of G20 countries, and are soon to be the cheapest form of electricity in every G20 country, according to a new report from Greenpeace in advance of the upcoming G20 Summit in Hamburg.

Published this week, before the G20 leaders meet in Hamburg, Germany, for their annual G20 Summit, the new report by Greenpeace Germany highlighted the decreasing costs of renewable energy sources, and their cost-competitiveness with traditional energy sources like coal and nuclear. Specifically, Greenpeace Germany highlighted a report by the United Nations Environment Programme and Bloomberg New Energy Finance that showed the average levelized cost of generating power from solar worldwide dropped by 17%, onshore wind dropped by 18%, and offshore wind costs fell by 28%. The report also highlighted the unsubsidized prices of renewable energy projects which are undercutting all other sources of new electricity generating capacity, such as “prices falling to nearly 26 €/MWh for a wind power project in Morocco and a bid of 24 €/MWh was made for a solar power plant in Abu Dhabi last year.”

The report, therefore, is an effort to substantiate these examples, and highlight the fact that “many G20 [countries] continue to favour fossil fuel and nuclear based power generation, which is economically unfounded.”

“There can be no excuses anymore,” **said Greenpeace Germany energy expert Tobias Austrup.**

“Climate protection increasingly makes economic sense across the G20 as renewable energy becomes cheaper than dirty coal and nuclear.”

“Any G20 country that is still investing in coal and nuclear power plants is wasting their money on technology that will not be competitive in coming years. The G20 now has a responsibility to send a clear signal that accelerating the clean energy transition is not only the right thing to do for the climate, but also for the economy.”

The report, *Comparing electricity production costs of renewables to fossil and nuclear power plants in G20 countries*, was conducted by the Finnish Lappeenranta University of Technology, and commissioned by Greenpeace Germany. The report calculated the electricity generation costs of all G20 countries between 2015 and out to 2030 and found that wind farms already generated the cheapest form of electricity in 2015 across large parts of Europe, South America, the United States, China, and Australia. Further, the report

concluded that due to significant technological innovation and progress leading and falling prices, solar energy in 2030 will be even cheaper than wind power in many G20 countries.

But even now, renewable energy across many G20 countries is already cost competitive with local grid prices, so it is unsurprising that by 2030 renewable energy will be far and away the cheaper option.

Unsurprisingly, however — for anyone who has paid even the slightest attention to these issues — there are still challenges to seeing this future come to pass without hindrance. Specifically, the report highlights the negative impact of subsidizing fossil fuels — highlighted in **another report published** in advance of the G20 Summit meeting in Hamburg. Specifically, this report showed that G20 countries averaged $70 billion in public finance for fossil fuels, totaling $215.3 billion in deals for oil, gas, and coal, between 2013 and 2015. The Greenpeace report further highlighted a study from the International Energy Agency which showed that countries spent close to $500 billion on consumption subsidies for fossil fuels in 2014 — 90% of which came from G20 governments.

In the end, the report's conclusions should be the definitive end for coal and other fossil fuel technologies, but entrenched interests across the world will continue to see coal and nuclear and other sources continue fighting for every scrap of financing and subsidies and years left to operate, further jeopardizing the planet's chances of keeping global warming within the limits set out in the Paris Climate Agreement.

B. Technologies and research direction for Renewable energy.

Technologies of Renewable energy allow us to be able to generate electricity, heat and fuel from various renewable sources.

Solar, wind, hydro, wave, heat-exchange, tidal, wave and bioenergy technologies are all derived from the sun, directly or indirectly.

Bioenergy technologies allow to convert the solar energy kept in plants, food, farm, forest and those wastes, sewage, and seaweed into electricity, heat (steam) and fuel using various technologies.These technologies allow us to warm and cool houses and buildings, generate electricity, and to transport by land, sea, and also by air possibly without generating dangerous toxic gases and other forms of pollutions any more.

Electricity from Renewable energy sources

Solar Photovoltaic (PV)

Wind

Large Hydro

Small Hydro and Run of River Hydro

Tidal

Wave

Geothermal

Fission and Fusion

Carbon Capture and Storage

Power Storage and Grid Stability

Fossil Fuels byproduct and Natural Gas

Best First Nations Policies and Practices

And so on…….

Types of Renewable Energy

1. Solar

Solar energy is derived by capturing radiant energy from sunlight and converting it into heat, electricity, or hot water. Photovoltaic (PV) systems can convert direct sunlight into electricity through the use of solar cells.

Benefits

One of the benefits of solar energy is that sunlight is functionally endless. With the technology to harvest it, there is a limitless supply of solar energy, meaning it could render fossil fuels obsolete. Relying on solar energy rather than fossil fuels also helps us improve public health and environmental conditions. In the long term, solar energy could also eliminate energy costs, and in the short term, reduce your energy bills. Many federal local, state, and federal governments also incentivize the investment in solar energy by providing rebates or tax credits.

Current Limitations

Although solar energy will save you money in the long run, it tends to be a significant upfront cost and is an unrealistic expenses for most households. For personal homes, homeowners also need to have the ample sunlight and space to arrange their solar panels, which limits who can realistically adopt this technology at the individual level.

2. Wind

Wind farms capture the energy of wind flow by using turbines and converting it into electricity. There are several forms of systems used to convert wind energy and each vary. Commercial grade wind-powered generating systems can power many different organizations, while single-wind turbines are used to help supplement pre-existing energy organizations. Another form is utility-scale wind farms, which are purchased by contract or wholesale. Technically, wind energy is a form of solar energy. The phenomenon we call “wind” is caused by the differences in temperature in the atmosphere combined with the rotation of Earth and the geography of the planet.

Benefits

Wind energy is a clean energy source, which means that it doesn’t pollute the air like other forms of energy. Wind energy doesn’t produce carbon dioxide, or release any harmful products that can cause environmental degradation or negatively affect human health like smog, acid rain, or other heat-trapping gases. Investment in wind energy technology can also open up new avenues for jobs and job training, as the turbines on farms need to be serviced and maintained to keep running.

Current Limitations

Since wind farms tend to be built in rural or remote areas, they are usually far from bustling cities where the electricity is needed most. Wind energy must be transported via transition lines, leading to higher costs. Although wind turbines produce very little pollution, some cities oppose them since they dominate skylines and generate noise. Wind turbines also threaten local wildlife like birds, which are sometimes killed by striking the arms of the turbine while flying.

3. Hydroelectric

Dams are what people most associate when it comes to hydroelectric power. Water flows through the dam’s turbines to produce electricity, known as pumped-storage hydropower. Run-of-river hydropower uses a channel to funnel water through rather than powering it through a dam.

Benefits

Hydroelectric power is very versatile and can be generated using both large scale projects, like the Hoover Dam, and small scale projects like underwater turbines and lower dams on small rivers and streams. Hydroelectric power does not generate pollution, and therefore is a much more environmentally-friendly energy option for our environment.

Current Limitations

Most U.S. hydroelectricity facilities use more energy than they are able to produce for consumption. The storage systems may need to use fossil fuel to pump water.[3] Although hydroelectric power does not pollute the air, it disrupts waterways and negatively affects the animals that live in them, changing water levels, currents, and migration paths for many fish and other freshwater ecosystems.

4. Geothermal

Geothermal heat is heat that is trapped beneath the earth's crust from the formation of the Earth 4.5 billion years ago and from radioactive decay. Sometimes large amounts of this heat escapes naturally, but all at once, resulting in familiar occurrences, such as volcanic eruptions and geysers. This heat can be captured and used to produce geothermal energy by using steam that comes from the heated water pumping below the surface, which then rises to the top and can be used to operate a turbine.

Benefits

Geothermal energy is not as common as other types of renewable energy sources, but it has a significant potential for energy supply. Since it can be built underground, it leaves very little footprint on land. Geothermal energy is naturally replenished and therefore does not run a risk of depleting (on a human timescale).

Current Limitations

Cost plays a major factor when it comes to disadvantages of geothermal energy. Not only is it costly to build the infrastructure, but another major concern is its vulnerability to earthquakes in certain regions of the world.

5. Ocean

The ocean can produce two types of energy: thermal and mechanical. Ocean thermal energy relies on warm water surface temperatures to generate energy through a variety of different systems. Ocean mechanical energy uses the ebbs and flows of the tides to generate energy, which is created by the earth's rotation and gravity from the moon.

Benefits

Unlike other forms of renewable energy, wave energy is predictable and it's easy to estimate the amount of energy that will be produced. Instead of relying on varying factors, such as sun and wind, wave energy is much more consistent. This type of renewable energy is also abundant, the most populated cities tend to be near oceans and harbors, making it easier to harness this energy for the local population. The potential of wave energy is an astounding as yet untapped energy resource with an estimated ability to produce 2640 TWh/yr. Just 1 TWh/yr of energy can power around 93,850 average U.S. homes with power annually, or about twice than the number of homes that currently exist in the U.S. at present.

Current Limitations

Those who live near the ocean definitely benefit from wave energy, but those who live in landlocked states won't have ready access to this energy. Another disadvantage to ocean energy is that it can disturb the ocean's many delicate ecosystems. Although it is a very clean source of energy, large machinery needs to be built nearby to help capture this form energy, which can cause disruptions to the ocean floor and the sea life that habitats it. Another factor to consider is weather, when rough weather occurs it changes the consistency of the waves, thus producing lower energy output when compared to normal waves without stormy weather.

6. Hydrogen

Hydrogen needs to be combined with other elements, such as oxygen to make water as it does not occur naturally as a gas on its own. When hydrogen is separated from another element it can be used for both fuel and electricity.

Benefits

Hydrogen can be used as a clean burning fuel, which leads to less pollution and a cleaner environment. It can also be used for fuel cells which are similar to batteries and can be used for powering an electric motor.

Current Limitations

Since hydrogen needs energy to be produced, it is inefficient when it comes to preventing pollution.

7. Biomass

Bioenergy is a renewable energy derived from biomass. Biomass is organic matter that comes from recently living plants and organisms. Using wood in your fireplace is an example of biomass that most people are familiar with.

There are various methods used to generate energy through the use of biomass. This can be done by burning biomass, or harnessing methane gas which is produced by the natural decomposition of organic materials in ponds or even landfills.

Benefits

The use of biomass in energy production creates carbon dioxide that is put into the air, but the regeneration of plants consumes the same amount of carbon dioxide, which is said to create a balanced atmosphere. Biomass can be used in a number of different ways in our daily lives, not only for personal use, but businesses as well. In 2017, energy from biomass made up about 5% of the total energy used in the U.S. This energy came from wood, biofuels like ethanol, and energy generated from methane captured from landfills or by burning municipal waste.

Current Limitations

Although new plants need carbon dioxide to grow, plants take time to grow. We also don't yet have widespread technology that can use biomass in lieu of fossil fuels.

Transportation from Renewable energy source

Transit and Light Rail Transit

Rail

Transportation Demand Management

Sustainable Urban transportation

Electric Vehicles

Biodiesel

Liquid Biofuels

Bioethanol

Hydrogen fuel cell with bus, truck, drone, heavy equipment and small flight

Ships with various size

And so on…..

Heat/cool and Buildings from renewable energy sources

Buildings consume a lot of energy, each of house and building are responsible for many CO_2 emissions. The challenge brings two parts of mission—: No 1. Creating new buildings that are zero carbon, and renovate all existing buildings to reduce and then eliminate their carbon footprint.

The first task is easier. Passive Homes need 90% less energy for heating and cooling by using super insulation and efficient heat recovery. There are Thousands homes in Europe built to Passive house specifications. Future building codes should maybe require that all new houses are built to this standard.

The challenge is tougher for existing buildings. Most building owners could achieve a 20% to 40% reduction in energy use by investing in new windows, super-insulation, heat-recovery systems, and efficient appliances and boilers.

Solar PV and solar hot water can be added to achieve more percentage even up to 90%, and zero-carbon heat can be obtained from heat exchange with the air, earth, water, and sewage.

General electrical consumption for House

Year-Round Solar Heating and Solar Cooling

Solar Cooking

And so on……

C. Wind, solar will be cheaper than fossil fuels in 2020.

Most forms of renewable energy are already cost competitive with fossil fuels and are often cheaper than lower end of costs of fossil fuel-based power across the world, a new report from the International Renewable Energy Agency (IRENA) found. However, by next year (2020), onshore wind and solar photovoltaics (PV) will be cheaper than fossil fuel power across the world without subsidies.

Based on previous cost reductions and anticipated future cost reductions, the latest report, Renewable Power Generation Costs in 2018, found that over three-quarters of the onshore wind and four-fifths of the utility-scale solar PV projects planned for the next year will cost less than the cheapest new coal-fired, oil, or natural gas option. Moreover, by 2020 the total lifetime costs of wind and solar and beyond will cost less than it will cost to existing coal fired plants

"We must do everything we can to accelerate renewables if we are to meet the climate objectives of the Paris Agreement. Today's report sends a clear signal to the international community: Renewable energy provides countries with a low-cost climate solution that allows for scaling up action," said IRENA's Director-General Francesco La Camera. "To fully harness the economic opportunity of renewables, IRENA will work closely with our membership and key partners to facilitate on-the-ground solutions and concerted action that will result in renewable energy projects."

In making its assessment IRENA undertook a comprehensive review of energy projects from around the world. It found that wind and solar PV costs fell by 13% and 14%, respectively, in 2017. Other forms of renewables also saw cost drops, the biggest being in concentrating solar power (CSP), which fell 26% and bioenergy, which fell by 14%. The report found that even the costs of hydropower fell by 12% in 2017.
The report also found that the costs of wind and solar projects are expected to fall further throughout the next decade, solidifying them as the lowest cost options for electric generation in the future. In solar power, some of those costs are likely to come as new generations of technology, like perovskite crystals, make solar power more affordable and efficient.

The falling costs of renewables also continue to best previous estimates, according to IRENA. In 2018 it projected that the weighted-average cost of electricity from onshore wind would be 4.9 cents per kilowatt hour and 5.5 cents per kWh for solar by 2020. Already it's fallen to 4.5 per kWh for wind and 4.8 per kWh for solar.

GOING 100 % RENEWABLE BETWEEN 2030 AND 2050

Some countries have set targets and goals to be run by 100 per cent renewable energy in the near future. At a 2016 United Nations Climate Change Conference, nearly 50 countries agreed to only use renewable energy by 2050. Countries like the Philippines and Colombia pledged to make their energy production 100 per cent renewable between 2030 and 2050, at the latest. The U.S. and Canada, however, are slowly catching up to the countries with such pledges that are leading the way. In the U.S. last year (2017), about 18 per cent of all electricity was from renewable sources. In Canada, the amount is about the same at 18.9 per cent, according to the Government of Canada.

The renewable energy market is expected to continue its upward growth, surpassing 2.9 trillion U.S. dollars on a global scale by 2027 – Market Research Future.

D. Summary

1. Refineries face with the significant production yield adjustment.
2. Current Crude oil suppliers throughout Chicken games will lose its main supplier position.
3. No more OPEC influence because of Shale oil/gas, LNG and cost competitive Renewable Energy source.
4. The Severer Governmental restriction/ regulation on emission control.
5. New technology of battery and Hydrogen fuel cell will replace or reduce consumption of Gasoline, Diesel fuel, Aviation fuel, heavy bunker fuels and even the transportation lubricant and its all feedstock and derivatives.
6. Energy will be distributed via transactive energy as renewable energy grows.
7. Energy distribution will be actively transacted through energy utility coins.
8. Traditional fossil fuels will be replaced by LNG, Shale gas and Renewable energy such as Wind, Solar, Hydro and ITER (Fusion technology based on heavy hydrogen. i.e. 2H and 3H.)
9. From year of 2020, the Wind and Solar energy will be cheaper than fossil fules. After Current Crude oil price structure settle down.

10. Future direction:
    A. Moving toward: more applied /cheaper/ developed renewable energy source and its technology.
    B. Significant reduction of crude oil and refineries produced fossil fuels.
    C. Recycling/gasification of waste/trash to generate electricity will be another major sector of technology movement.
    D. More energy transaction will be done via energy Utility Token Coins.

Changes in Delivery and sourcing

- New ways of managing networks
- Both non reliable and reliable sources need to be integrated
- Market demand for “peer to peer” trading
- Many more transactions makes traditional marketplaces expensive and almost unusable

How to Fix

- Transactive Energy model
    - Blockchain based/tokenized model for fast and trustable transactions
    - Smart contracts to do the heavy lifting
    - Peer to peer marketplace via tokens
    - FIAT End points for blind invoicing
- Integrated Renewables and storage
    - Storage to help smooth the peaks and troughs in consumption and production
    - Home based and large scale Renewables integrated seamlessly (smart contracts remove work)

Company Example – Cenfura Limited (www.cenfura.com)

- Cenfura marketplace at Cenfura.io along with external marketplaces for trading tokens (bilaxy)
- Blockchain based smart contracts
- Cenfura both owns and operates renewable energy production and storage facilities
    - System can also be extended to externally owned facilities
- Tokens used as interfacility payment method
- FIAT invoicing to End customers
- Software grid management

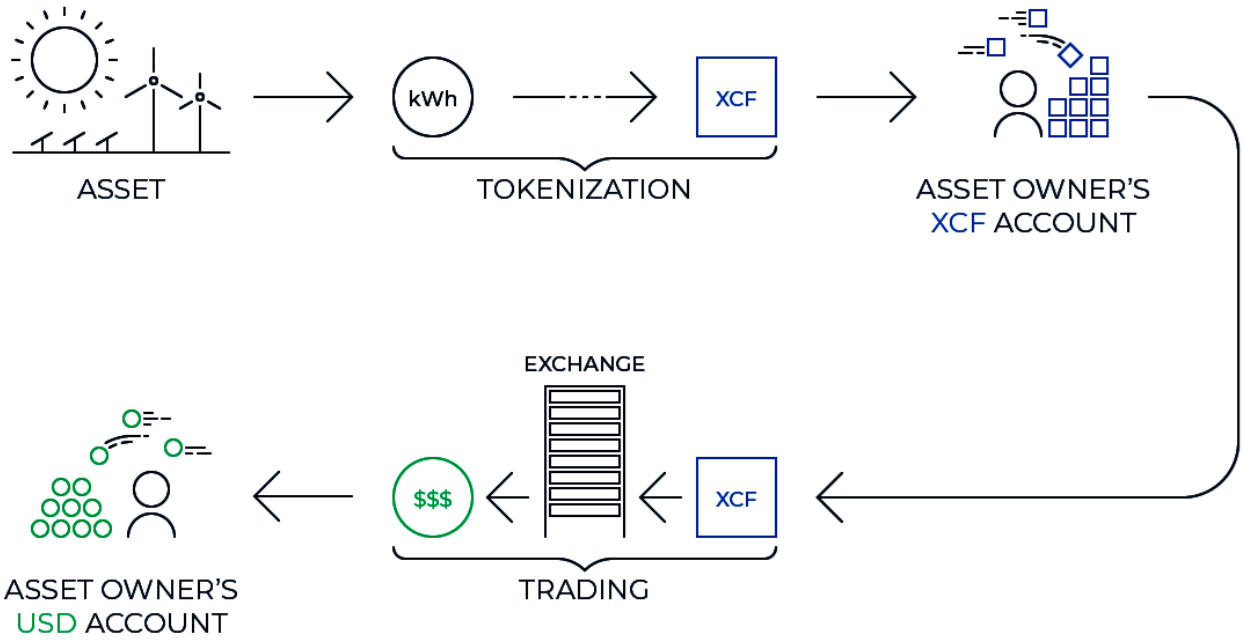

Invited Presentation

Dr. Yuji Yoshimura

AIST Emeritus Researcher, Japan
Visiting Senior, MTEC, Thailand
E-mail: y.yoshimura@opal.ocn.ne.jp

Dr. Yuji Yoshimura is now an Emeritus Researcher of National Institute of Advanced Industrial Science and Technology (AIST), Japan, and working for MTEC/NSTDA as a visiting senior researcher. He graduated from Kyushu University in 1975, and received a PhD degree (Chemical Engineering) from Kyoto University in 1981, and then joined in AIST. His work has mainly focused on catalysts related with energy and environment. He used to work as a Leader of Japan-Thailand JST-JICA SATREPS Project from 2010 to 2015, and after that work as a JICA senior volunteer related on H-FAME. He has published over 170 original research papers.

Upgrading Technology for Higher Blend of Biodiesel in ASEAN

ABSTRACT

Biodiesel has been used as a petrodiesel alternative, and its blending ratios in petrodiesel have increased gradually, e.g. B5, B7, B10, B20 and more in future in ASEAN, depending on the diesel engine/exhaust-gas-treatment systems. When these blending amounts increase, several issues will be getting dominant, e.g. fuel filter plugging with impurities such as monoglyceride (MG) and acids/sludge/polymers formation via thermo-oxidative degradation of biodiesel during the vehicle use. Impurities such as MG and water can be reduced via operational modification of biodiesel manufacturing process or distillation etc., while oxidation stability of biodiesel can increase via addition of antioxidants. However, there are concerns about the dosing amounts, life, cost, etc. of antioxidants during the vehicle use.

Thermo-oxidative degradation of biodiesel is mainly caused by decomposition of polyunsaturated fatty acid methyl ester (FAME). Whereas, monounsaturated FAME is relatively very stable with keeping an acceptable cold flow property. So, we have developed H-FAME (partially Hydrogenated FAME) to chemically convert polyunsaturated FAME into monoene for solving these thermo-oxidation stability issues without any antioxidants. After coupling with a wintering/crystallization system, we can get a thermo-oxidation stable and low MG of H-FAME with an economical feasible process. H-FAME technology can be applied to all of the FAME derived from any feedstock. I will introduce the details of H-FAME and H-FAME technology.

Keywords: Biodiesel, Higher blend, Polyunsaturated FAME, Thermo-oxidative degradation, Partial hydrogenation, H-FAME

Assistant Prof. Dr. Pruk Aggarangsi

Director
Energy Research and Development Institute Nakornping
Chiang Mai University, Thailand
E-mail: pruk.a@cmu.ac.th

Dr. Pruk Aggarangsi is currently the Director of Energy Research and Development Institute-Nakornping, Chiang Mai University and Assistant Professor in Mechanical Engineering, Chiang Mai University, Thailand. He has a wide scope of expertise in renewable energy, waste water treatment, numerical modeling, heat and energy simulation and mechanical vibration analysis. For the past 12 years, he has participated and in charge of energy projects including biogas / biomethane projects, digital energy audit and advanced energy efficiency projects. Dr. Pruk have had crucial roles in engineering of many renewable energy power plant projects as well as conducting many research projects in renewable energy related topics. He also plays an important role in driving Chiang Mai University's Smart City-Clean Energy Project aiming be the most energy efficient city in Thailand to encourage sustainable development for the communities around the world.

CMU Smart City Clean Energy Project

ABSTRACT

Biogas power plant has been gradually implemented in Thailand for the past 30 years. Currently, there are more than 1,500 biogas system in operations spreading across the countries of which more than 300 are designated as commercial scale renewable energy power plants ranging from 0.300 to 10.250 MW of installed capacity. The majority of existing biogas power plants is waste / waste water to energy through anaerobic digestion system for multiple benefits in social, environmental, energy and financial aspects. Recently, Thai Ministry of Energy has initiated a community power plant policy focusing on energy crop as feedstock for biogas and biomass incineration for electricity generation. While social and community benefit is clear for such program, overall financial and risk including issues in management still need to be addressed. Some technical figures and information will be presented for investors considerations.

Chiang Mai University is one of the most experienced renewable energy research and implementation.

Keywords: Biogas, Biomass, Biogas power plant

Oral Presentation

BIOECONOMY

O-EC1

ISOLATION AND CHARACTERIZATION OF COLD-ADAPTIVE CELLULASE PRODUCING BACTERIUM *CELLVIBRIO OSTRAVIENSIS* STRAIN C44 AND ITS ENZYMATIC PROPERTIES

Pantipa Prodbut[1]*, Patthra Pason[1, 2], Rattiya Weanukul[1,2], Khanok Ratanakhanokchai[1], and Chakrit Tachaapaikoon[1,2]*

[1] School of Bioresources and Technology, King Mongkut's University of Technology Thonburi, Bangkok, 10150, Thailand

[2] Pilot Plant Development and Training Institute, King Mongkut's University of Technology Thonburi, Bangkok 10150, Thailand

*E-mail: chakrit.tac@kmutt.ac.th; pantipa.pro@kmutt.ac.th

ABSTRACT

A cold-adaptive enzyme from psychrotrophs is a promising resource for the biotechnological industry. Among of cold-adaptive enzymes, cellulases are widely used in various industries including food, feed, brewing industries and bioconversion of lignocellulosic material. However, the cold-adaptive enzymes were a few reports and limited. In this study, we have isolated and characterized a psychrotrophic cellulase-producing bacterium, strain C44. The isolate was Gram-negative and non-spore forming. Cells are in a straight rod shape. The 16S rRNA gene analysis found that it has 98.83% similarity with *Cellvibrio ostraviensis*. The isolate was able to grow at temperature of 4-37 ^{o}C (optimum at 25 ^{o}C), additional pH of 6.0-10.0 (Optimum at 6.0). It utilized several polymeric substances, e.g., cellulose, xylan, starch, locus bean gum and pectin for growth. Besides, the crude enzyme produced from the strain C44 contains not only cellulase but also xylanase and mannanase activities, when cultured with phosphoric acid swollen cellulose (PASC) as sole carbon source. Moreover, the crude enzyme retained approximately 26.90% of cellulase activity at 10 ^{o}C compared to its optimal temperature. The result implied that the extracellular enzyme of the strain C44 was cold-adaptive and could apply in the biotechnological process under low heat. Therefore, the newly isolated *C. ostraviensis* strain C44 is an alternative bacterium to cold-adaptive enzyme producers for supply biotechnological industries.

Keywords: Cellulase, *Cellvibrio ostraviensis*, Cold-adaptive enzyme, Lignocellulosic material, Psychrotrophs

INTRODUCTION

Cold active enzyme or cold-adapted enzymes are interested in several biotechnological industries. Because the enzyme has the ability to catalyze the reaction at low temperature, it is produced from microorganisms that can adapt to grow under low temperature (a cold adaptive microorganism or psychrotrophs) (≥ 0 °C - 40 °C ≤) (Pulicherla, et al., 2011, Sarmiento et al., 2015). However, the cold-adaptive enzymes have a few reported and limited in the characterization of its properties. Among them, cellulases have been reported to use in many industries, e.g., food, feed, detergents, textiles, biofuel, paper, pharmaceuticals, molecular biology applications, etc. (Cavicchioli et al., 2011, Banerjee et al., 2016). Base on our knowledge, the genus *Cellvibrio* is a promising producer for lignocellulose degradation enzymes. This genus belonging to the Pseudomonadaceae family was first discussed by Blackall et al. in 1986. According to Xie et al. (2017), eight other species, namely, *Cellvibrio ostraviensis, C. vulgaris, C. mixtus, C. fibrivorans, C. gandavensis, C. japonicus, C. fulvus, and C. diazotrophicus*, have been identified to date (LPSN, https:// www.bacterio.net/-allnamesac.html). Moreover, the genus *Cellvibrio* are usually Gram-negative and aerobic, and these bacteria are known cellulose, xylan, starch, and chitin degraders (Blackall et al., 1986, DeBoy R. T., et al., 2008, Wu Y.-R., He J., 2015). In this study, we report a newly isolated strain that produces cold-adaptive cellulase from decayed biomass in the soil sample. The morphological features, 16S rRNA gene analysis, enzyme production and pattern of the extracellular enzyme of the isolate were also investigated, which built up a reasonable basis for exploring psychrotrophs in the tropical region.

MATERIALS AND METHODS

Isolation of cold-adaptive cellulase producing bacterial strain and culture condition

Soil samples were collected from the decayed lignocellulosic material mixing with soils, soil from the canal, Thailand. The samples were inoculated into the mineral salt medium (MS medium), pH7.0 containing $NaNO_3$ (20 g/L), $CaCl_2.2H_2O$ (0.2 g/L), K_2HPO_4 (5 g/L), $MgSO_4.2H_2O$ (0.2 g/L), $FeSO_4.7H_2O$ (0.2 g/L) and $MnSO_4.2H_2O$ (0.2 g/L), 0.5% (w/v) PASC and incubated at 16˚C for 7 days. Subsequently, the grown cultures were transferred to the fresh medium and then they were streaked on the CMC agar plate. The re-isolated step was repeated several times to obtain the pure culture. Cellulase-producing bacteria were detected by a clear zone around the colony.

Morphological of cold-adaptive cellulase producing bacterium

To observe cell shape and Gram staining of the cellulase producing bacterium, the selected strain was grown in the same above medium at 16^{o}C for 3 days. Traditional Gram staining was performed as described previously (Tachaapaikoon et al., 2012).

16S rRNA gene sequence analysis

The 16S rRNA gene was amplified using specific primers: 8F (5'-AGAGTTTGATCCTGGCTC AG-3') and 1492R (5'-GGTTACCTTGTTACGACTT-3') primers. The procedure for amplification and sequencing were followed by the previous report (Tachaapaikoon et al., 2012). The 16S rRNA gene sequence of the candidate was compared with other 16S rRNA gene sequences available in the GenBank database using the BLASTN program (http://blast.ncbi.nlm.nih.gov/Blast.cgi) to obtain highly similar sequences.

Enzyme production

The isolated strain was grown in MS broth (pH 6.0) containing 0.5% (w/v) PASC as the sole carbon source at 25°C for 72 hours in a shaker incubator (at 200 rpm). Afterward, the culture was centrifuged at 8,000 rpm for 15 min using a refrigerated centrifuge. Then, the culture supernatant was subjected to the Vivaspin20 column (10-kDa-cut off the membrane, GE Healthcare). The concentrated supernatant was used as the crude enzyme in the next step.

Enzyme assay

Cellulase, xylanase and mannanase activities were determined as previously described (Tachaapaikoon et al., 2012). The released sugars were determined using the Somogyi-Nelson method (Nelson, 1994) and its OD_{520} was measured in a spectrophotometer. One unit (U) of the enzyme activity was defined as the amount of enzyme that released 1 µmol of reducing sugars equivalent to glucose, xylose and mannose per minute during the reaction for cellulase, xylanase and mannanase, respectively.

Protein determination

Protein concentrations were measured by the Lowry method (Lowry, et al. 1951) using bovine serum albumin as the standard.

Effect of pH and temperature on the enzyme activity

The optimum pH of enzyme was determined using pH buffers: 100 mM citrate buffer (pH 3.0 to 4.0), 100 mM sodium acetate (pH 4.0 to 6.0), and 100 mM sodium phosphate buffer (pH 6.0 to 8.0). The optimum temperature was examined at different temperatures between 10°C to 70ºC with the optimum pH.

SDS-PAGE and Zymogram analysis

The molecular weight protein and active bands of the crude enzyme from an isolated cold-adaptive producing bacterium were run into the 10% SDS-PAGE (Laemmli,1970). After electrophoresis, the gel was stained with 0.1% Coomassie Blue R250 for detect the protein band. The molecular weight calibration kit (Pierce, Rockford, IL, USA) was used for standardization, while Zymogram (active-PAGE) contained CMC (0.1%) in the gel. Gel was run under the same condition of SDS-PAGE. Then, the CMCase Zymogram was stained with Congo-Red, and wash out the access dye by 1M NaCl until clear band appearance.

RESULTS AND DISCUSSION

Isolation of cold-adaptive cellulase producing bacteria

During the isolation, the pure fifteen colonies could grow on the CMC agar plate at 16^{o}C. However, the result revealed that only five isolates (namely C1S, C2B, C32, C43 and C44) showing the clear zone around the colony (Figure.1A). Five isolates produced extracellular CMCase at a low temperature. The result denoted that isolate C44 shows the highest clear zone when compared with another. Thus, the isolate C44 was selected to be the most appropriate bacterium for this purpose. Colonies on MS agar plated produced pale-yellow-pigmented (data not shown). Furthermore, the strain C44 was an aerobic, Gram-negative, non-spore forming. Cells were in a straight rod shape (Figure. 1B). It grew well between 4-37^{o}C, which was optimum 25^{o}C and no growth occurred at 45^{o}C. Optimum pH was 6.0, which can grow in the range of pH 6.0-10.0. Therefore, the isolated strain C44 is a psychrotrophic bacterium.

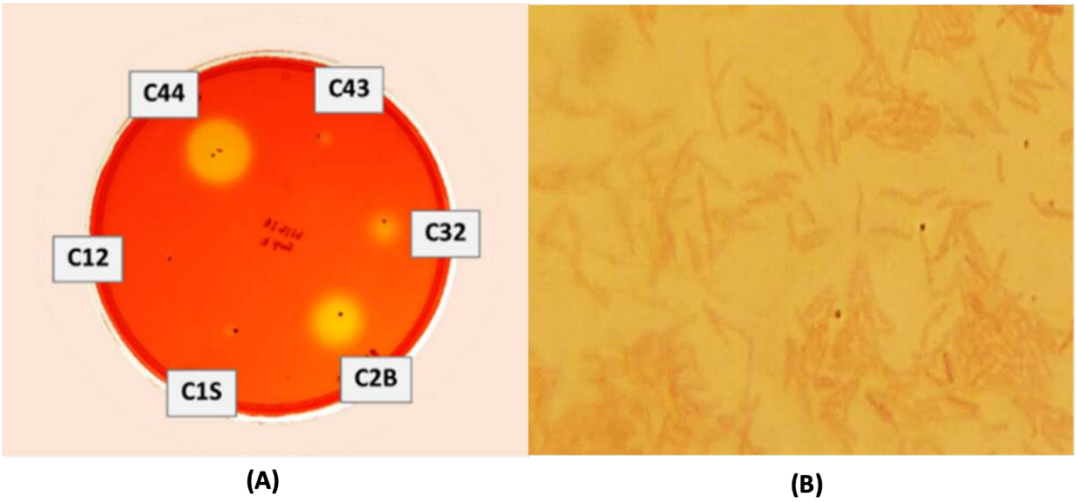

Figure 1. Clear zone of each isolate on MS agar plate containing CMC as the sole carbon source (A) and Gram-staining of the strain C44 under the microscope (B).

Identification of cold-adaptive cellulase producing bacterium

The 16S rRNA gene of the isolated strain C44 was amplified with the primer 8F and 1492R and then sequenced. The amplified sequence showed high similarity to the 16S rRNA gene fragment of *Cellvibrio ostraviensis* (98.83%), followed by *C. fibrivorans* (98.77%), *C. fulvus* (98.15%), *C. mixtus* (97.60%), *C. fontiphilus* (97.40%), *C. vulgaris* (97.27%) and *C. zantedeschiae* (96.39%), respectively (Table 1). The result exposed that the strain C44 resembles the member in the genus *Cellvibrio*. Consequently, the newly isolated strain C44 was permitted tentatively identified as *Cellvibrio ostraviensis* strain C44. Mergaert et al. (2003) reported a taxonomic study of *Cellvibrio* strains and a description the type strain of *Cellvibrio ostraviensis* sp. nov. Remarkably, the isolated strain C44 has some different biological properties compared with the type strain LMG18561^{T}, e.g., strain LMG18561^{T} cannot have a growth at 37^{o}C, but the isolated strain C44 can grow. Also, this isolated strain C44 is rapidly grown at 4^{o}C within 5 days. In contrast, the type of strain LMG18561^{T} needs at least 14 days for growth. The result indicated that the strain C44 probably is new strain in this group. However, other biochemical tests or genomic analyze should be performed in future studies.

SDS-PAGE and Zymogram of the crude enzyme

The protein and cellulase patterns of the crude enzyme from *C. ostraviensis* strain C44 was analyzed by SDS-PAGE and CMC-zymogram, respectively. The result was shown in Figure 2. The crude enzyme was subjected to SDS-PAGE, showed at least 18 proteins with molecular masses in the range of 250 to 22 kDa (Figure 2 lane1), of which 3 proteins (140, 100 and 75 kDa) had CMCase activity (Figure 2 lane 2). Although, the cellulolytic and dextranolytic Gram-negative bacteria had been reported to revive the genus *Cellvibrio* with the first report by Blackall et al. (1985). Subsequently, it was reclassified to a novel species as *C. ostraviensis* strain LMG18561T in 2003 (Mergaert et al., 2003). However, it did not

characterize the enzyme that was produced from this species. Herein, the enzyme-producing from the strain C44 was preliminarily observed on Zymogram that showed cellulase activity on the band protein. Therefore, this is the first report for the investigation of cellulase pattern in the crude enzyme of *C. ostraviensis*. Probably the characterization of the enzyme properties should also be done in a future experiment.

Table 1 Comparison of 16S rRNA gene from the isolated strain C44 with NCBI database.

Name	Microorganisms	Identity (%)
Strain C44	*Cellvibrio ostraviensis* strain LMG 19434	98.83
	Cellvibrio fibrivorans strain R-4079	98.77
	Cellvibrio fulvus strain NCIMB 8634	98.15
	Cellvibrio mixtus strain ACM 2601	97.60
	Cellvibrio fontiphilus strain MVW-40	97.40
	Cellvibrio vulgaris strain NCIMB 8633	97.27
	Cellvibrio zantedseschiae strain TPY-10	96.39

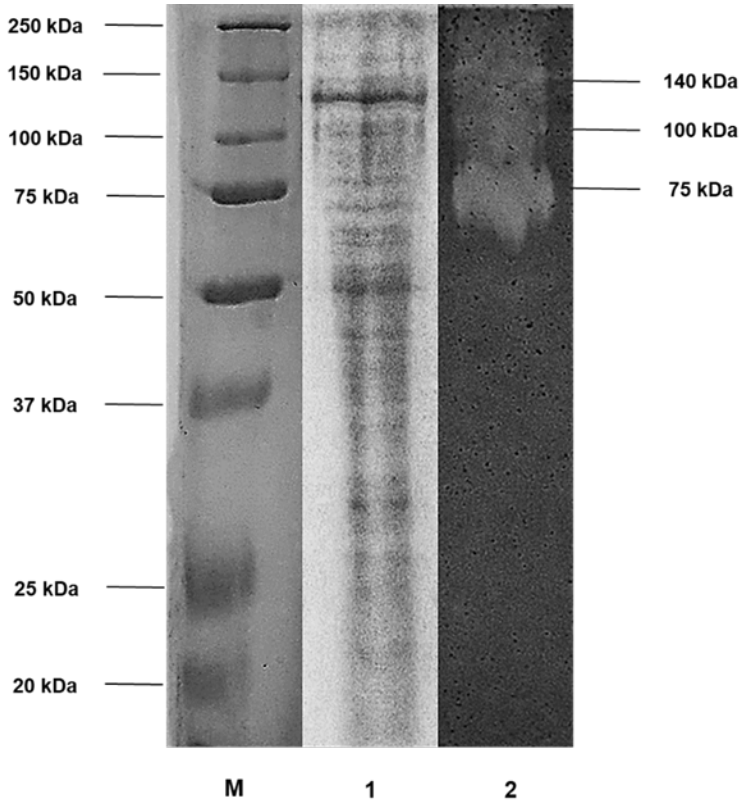

Figure 2. SDS-PAGE and Zymogram of the curde enzyme from *C. ostraviensis* strain C44. Lane M: Molecular marker, Lane 1: SDS-PAGE, Lane 2: CMCase zymogram.

Effect of temperature and pH on the cellulase activity

To address the crude enzyme that can be achieved in a suitable range of temperature and pH, the crude enzyme was incubated at a different temperature, as above mention. The result showed the optimum temperature as 50°C, however it can become active at low temperature (> 20% remaining relative activity at 10^{o}C) (Figure 3A). The result contrasted with other mesophilic bacteria such as *Peanibacillus curdlanolyticus* strain B-6, which is known as a high potential lignocellulose degrader at moderate and high temperature (Pason et al*.,* 2006, Teeravivattanakit et al*.,* 2017, Phakeenuya et al*.*, 2020). However, the crude enzyme of the strain B-6 was not active at low temperatures (< 20^{o}C, unpublished data). It implied that the isolated strain C44 can produce cold-adaptive cellulase, even grew at moderate temperature. Optimum pH of the crude enzyme from strain C44 was 7.0 (Figure 3B). The pH optimum of cellulases from bacteria is

mostly neutral. Because of amino acids in the active site are quite the same, therefore it will affect to hydrolysis mechanism. (Lombard et al., 2014).

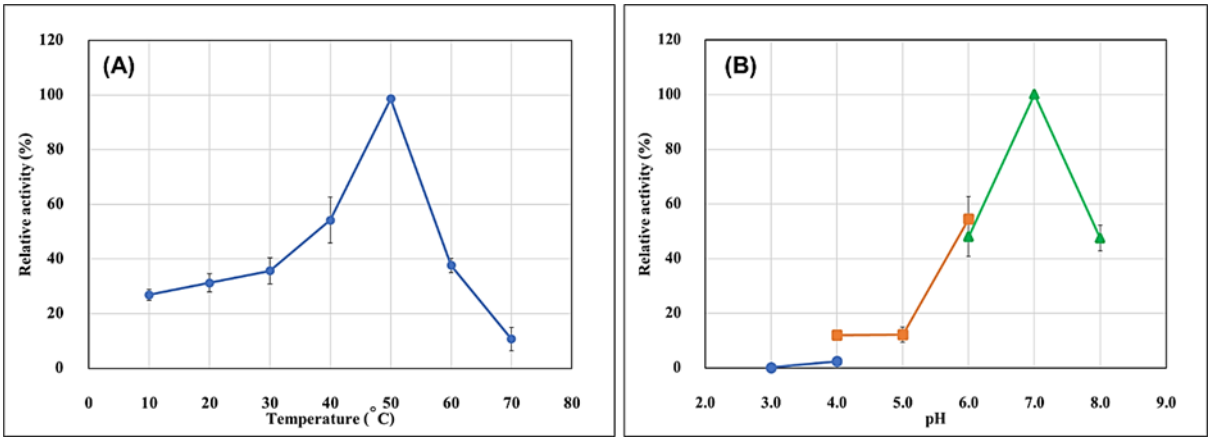

Figure 3. Effect of temperature (A) and pH (B) on the cellulase activity of the isolated strain C44 which citrate buffer (blue circle), sodium acetate (orange square), and sodium phosphate buffer (green triangle).

CONCLUSIONS

In this study, a psychrotrophic cellulase-producing bacterium was a success for screening and isolation. It can grow at 4-37^{o}C with the optimum temperature at 25^{o}C. The strain C44 was identified as *C. ostraviensis*, but was quite different from type strain LMG18561^{T}. The strain C44 is active at low temperature with remaining activity about 26.90% at 10^{o}C. Fascinatingly, this strain produces cold-adaptive cellulases, which has not reported in *C. ostraviensis* species before. Thus, *C. ostraviensis* strain C44 is an alternative cold-adaptive enzyme producer for the biotechnological process towards industrial applications.

ACKNOWLEDGEMENT

The authors acknowledge the financial support provided by King Mongkut's University of Technology Thonburi through the "KMUTT 60th Anniversary Commemorative Fund".

REFERENCES

Banerjee, R., A. Halder and A. Natta. 2016. Psychrophilic microorganisms: habitats and exploitation potentials. Eur. J. Mol. Clin. Med. 4: 16-24.

Blackall, L. L., A. C. Hayward and L. I. Sly. 1985. Cellulolytic and dextranolytic Gram-negative bacteria: revival of the genus *Cellvibrio*. J. Appl. Bacteriol. 59: 81-97.

Cavicchioli, R., T. Charlton, H. Ertan, S. M. Omar, K. S. Siddiqui and T. J. Williams. 2011. Biotechnological uses of enzymes from psychrophiles. Microb. Biotechnol. 4: 449–460.

DeBoy, R. T., E. F. Mongodin, and D. E. Fouts. 2008. Insights into plant cell wall degradation from the genome sequence of the soil bacterium *Cellvibrio japonicus*, J. Bacteriol. 190: 5455–5463.

Lombard, V., R. H. Golaconda, E. Drula, P. M. Coutinho and B. Henrissat. 2014. The carbohydrate-active enzymes database (CAZy) in 2013. Nucleic Acids Res. 42: D490–D495.

Mergaert, J., D. Lednika, J. Goris, M. C. Cnockaert, P. De Vos and J. Swings. 2003. Taxonomic study of *Cellvibrio* strains and description of *Cellvibrio ostraviensis* sp. nov., *Cellvibrio fibrivorans* sp. nov. and *Cellvibrio gandavensis* sp. nov." Int. J. Syst. Evol. Microbiol. 53: 465-471.

Pason, P., K. L. Kyu and K. Ratanakhanokchai. 2006. *Paenibacillus curdlanolyticus* strain b-6 xylanolytic-cellulolytic system that degrades insoluble polysaccharides. Appl. Environ. Microbiol. 72: 2483-2490.

Phakeenuya, V., K. Ratanakhanokchai, A. Kosugi, and C. Tachaapaikoon. 2020. A novel multfunctional GH9 enzyme from *Paenibacillus curdlanolyticus* B-6 exhibiting endo/exo functions of cellulase, mannanase and xylanase activities. Appl. Microbiol. Biotechnol. 104: 2079-2096.

Pulicherla, K. K., M. Ghosh, P. S. K. Ponnada and K. R. S. Sambasiva Rao. 2011. Psychrozymes-the next generation industrial enzymes. J. Marine Sci. Res. Development. 1: 1-7.

Sarmiento, F., R. Peralta and J. M. Blamey. 2015. Cold and hot extremozymes: industrial relevance and current trends. Front. Bioeng. Biotechnol. 3: 1-15.

Tachaapaikoon, C., S. Tanasupawat, P. Pason, S. Sornyatha, R. Waeonukul, K. L. Kyu and K. Ratanakhanokchai. 2012. *Paenibacillus xylaniclasticus* sp. nov., a xylanolytic-cellulolytic bacterium isolated from sludge in an anaerobic digester. J. Microbiol. 50: 394-400.

Teeravivattanakit, T., B. Baramee, P. Phitsuwan, S. Sornyotha, R. Waeonukul, P. Pason, C. Tachaapaikoon, K. Poomputsa, A. Kosugi, K. Sakka and K. Ratanakhanokchai. 2017. Chemical pretreatment-independent saccharifications of xylan and cellulose of rice straw by bacterial weak lignin-binding xylanolytic and cellulolytic enzymes. Appl. Environ. Microbiol. 83: 1-15.

Wu, Y.R. and J. He. 2015. Characterization of a xylanase-producing *Cellvibrio mixtus* strain J3-8 and its genome analysis, Sci. Rep. 5: 1-11.

Xie, Z., W. Lin, and J. Luo. 2017. Comparative phenotype and genome analysis of *Cellvibrio* sp. PR1, a xylanolytic and agarolytic bacterium from the pearl river, Bio. Med. Res. Int. 1: 1-10.

O-EC2

RUBBER FOAM: BETTER PERFORMANCE OF RECOVERY

Thridsawan Prasopdee[1], and Wirasak Smitthipong[1,2,3]*
[1] Specialized center of Rubber and Polymer Materials in agriculture and industry (RPM), Department of Materials Science, Faculty of Science, Kasetsart University, Bangkok, Thailand
[2] Office of research integration on target-based natural rubber, National Research Council of Thailand (NRCT), Bangkok, Thailand
[3] Office of natural rubber research program, Thailand Science Research and Innovation (TSRI), Bangkok, Thailand
*E-mail: fsciwssm@ku.ac.th

ABSTRACT
Natural rubber (NR) derived from the *Hevea brasiliensis* tree as liquid suspension called latex which is a bio-based elastomer. Rubber foam can be prepared from concentrated natural latex providing the specific characteristics such as density, compressive strength, and compression set, etc. The rubber foam has high compression set, thus it is suitable for making shape memory products. However, there are many customers requiring the natural rubber foam products with low compression set. This means the products can return back to its original shape in very short time. The main aim of this study is to prepare and develop the formula of rubber foam in order to study its recovery ability and other related characteristics by varying the vulcanizing chemicals. The results showed that the increasing of vulcanizing chemicals increased foam density as well as the compressive strength. The compression set of the rubber foam was decreased with the increasing of vulcanizing chemicals, indicates that the rubber foam has better property in returning back to its original shape when adding more vulcanizing chemicals. In another word, the recovery ability of rubber foam tends to increase as the vulcanizing chemicals increase, which is due to the greater of crosslinking density. Thus, the compression set is the best way to determine the ability of the recovering of rubber foams.
Keywords: Natural rubber, Rubber foam, Compressive strength, Compression set.

INTRODUCTION

Natural rubber (NR) is a bio-based elastomeric polymer which has been mainly applied in the rubber industry to manufacture products such as gloves, pillow and mattress, elastic band, etc. It is derived from the *Hevea brasiliensis* tree as a liquid suspension called latex in which the presence of other substances, to name a few, such as proteins, fatty acids, carbohydrates, etc., which contribute greatly to its properties. Moreover, latex is required to be chemically stabilized with ammonia prior to being processed because its properties can be environmentally affected during storage (Chollakup et al., 2019; Oliveira-Salmazo et al., 2016.)

Many products such as pillows and mattresses are made from rubber foam which is prepared from concentrated natural latex providing the specific characteristics. Generally, rubber foams are porous, elastic and they have ventilated surface. These foams are made into lightweight products that have been used for comfort applications such as in pillows and mattresses. From the mechanical properties point of view, rubber foam can be either soft or firm depending on the formula of compounded latex. Briefly, concentrated natural latex is mixed with chemical agents consist of blowing agent, vulcanizing agent, accelerators, activator, antioxidants, gelling agent, etc., in order to make the compounded latex (Chollakup et al., 2019; Suksup et al., 2019). All the chemical agents have to be grounded into micron scale because it is easier to mix with the concentrated natural latex.

Shape memory material has been categorized as smart material in which the smart material is the common name for a wide group of different substances. The general feature is the fact that one or more properties might be significantly changed due to external stimuli. It can receive, transmit, or process a stimulus and respond by producing a useful effect (Kamila, 2013). This ability offers opportunities for responsive materials including form-fitting, actuation, and sensing in industries including textiles, biomedicine, aerospace, and so on (Cavicchi, 2015). A basic mechanism of shape recovery can be

attributed to ‘shrinkage’ of oriented, extended chains triggered, for example, by melting or glass transition. Shape memory polymer (SMP) recovering by this mechanism can be defined as rubberlike SMP (Sedat Gunes et al., 2008). Moreover, there are many customers requiring the natural rubber foam products that can be back to its original shape in shorter time or have the lower compression set.

The main aim of this study is to prepare a rubber foam varying the vulcanizing chemicals in order to study its recovery ability and other related characteristics, this is a channel to develop the rubber foam products. It also increases the value of natural rubber which is a major economic crop in Thailand.

MATERIALS AND METHODS

Sample preparation

Three types of sample with different amounts of vulcanizing chemicals (10-14 %wt./wt.) were prepared in wet weight as following details.

Rubber foam sample was prepared from high ammonia concentrated natural latex (Num Rubber, Trang, Thailand) by weighing latex (200.4 g) then use the blender to spin the ammonia out at low speed (80 rpm) for 1 min. After that the speed of the blender was increasing up to 160 rpm, then Potassium Oleate (27.23 g of 20% aqueous dispersion preparing by Thanodom technology co., ltd.) was added and mixing for 10 min until the foam volume was increased. The blending speed was then reduced down to 80 rpm. Sulfur, zinc diethyldithiocarbamate, zinc-2-mercaptobenzothiazole (50% aqueous dispersion preparing by Thanodom technology co., ltd.) and zinc oxide (28% aqueous dispersion preparing by Thanodom technology co., ltd.) were varied as 27 g (10 %wt./wt.), 33 g (12 %wt./wt.), and 39 g (14 %wt./wt.) added and continue mixing for 1 min at each concentration. After that Wingstay L (3 g of 50% aqueous dispersion preparing by Thanodom technology co., ltd.) and diphenylguanidine (3.6 g of 28% aqueous dispersion preparing by Thanodom technology co., ltd.) were added then mixing for 1 min. Sodium silicofluoride (10.8 g of 23% aqueous dispersion preparing by Thanodom technology co., ltd.) was added at last then mixing for 3 minutes and test gel forming until reaching the gel point. The foam was then pouring into the mold and close the lids afterward then let the sample at room temperature for 45 min. After that, the sample was vulcanized in a hot air oven at 90°C for 2 h then removed from the mold, washed and dried at 70°C.

Characterizations of rubber foam

Density is determined from weight of the rubber foam sample and measure of volume of rubber foam sample, calculated as shown in Eq.1

$$\text{Density} = \frac{M}{V} \qquad \text{Eq.1}$$

where *M* is weight of the rubber foam sample (kg) and *V* is volume of rubber foam sample (m^3)

Compressive strength of the rubber foam sample is determined in 3 replications by Texture analyzer (TA.XT plus, United Kingdom), using platen probe with the diameter of 100 mm and speed of 0.1 mm/sec. The sample is 45 mm x 45 mm x 21.5 mm in dimension, compressed at 75% from the foam surface at room temperature adapted from ISO3386.

Compression set of the rubber foam sample is conducted according to ISO1856 method C by measuring the height of sample (d_o) then the sample is compressed at 75±4 %height for 72 h at room temperature. After that, the sample is released from the compression for 30 min then measuring the height of sample again (d_r) and %compression set (%c.s.) will be calculated as shown in Eq.2.

$$\%\text{Compression set} = \frac{d_o - d_r}{d_o} \times 100 \qquad \text{Eq.2}$$

Furthermore, %recovery of rubber foam can be calculated as shown in Eq.3

$$\%\text{Recovery of rubber foam} = 100 - \%\text{c.s.} \qquad \text{Eq.3}$$

RESULTS AND DISCUSSION

In this work, the effect of the system of vulcanizing chemicals on the recovery property was studied by varying vulcanizing chemicals into three formulae which are 10 %wt./wt., 12 %wt./wt., and 14 %wt./wt. According to Flory–Rehner theory (Flory and Rehner, 1943; Smitthipong et al., 2007), when adding more vulcanizing chemicals or expose to radiation, the crosslinking density of rubber is increased. The study results of all three formulae of rubber foam are as follow:

Firstly, the density of all three formulae rubber foams was investigated by using the sample with same volume. It was found that the increasing of vulcanizing chemicals tends to increase density of rubber foam as shown in Figure 1. At the vulcanizing chemicals 10 %wt./wt., 12 %wt./wt., and 14 %wt./wt., the density is 65.46 kg/cm^3, 68.34 kg/cm^3, and 73.97 kg/cm^3, respectively. This due to the increasing of crosslinking density within the same volume leading to significantly increase of density. Since in the same volume, the more of crosslink between rubber molecules, the more of weight, resulting in increasing of density of rubber foam.

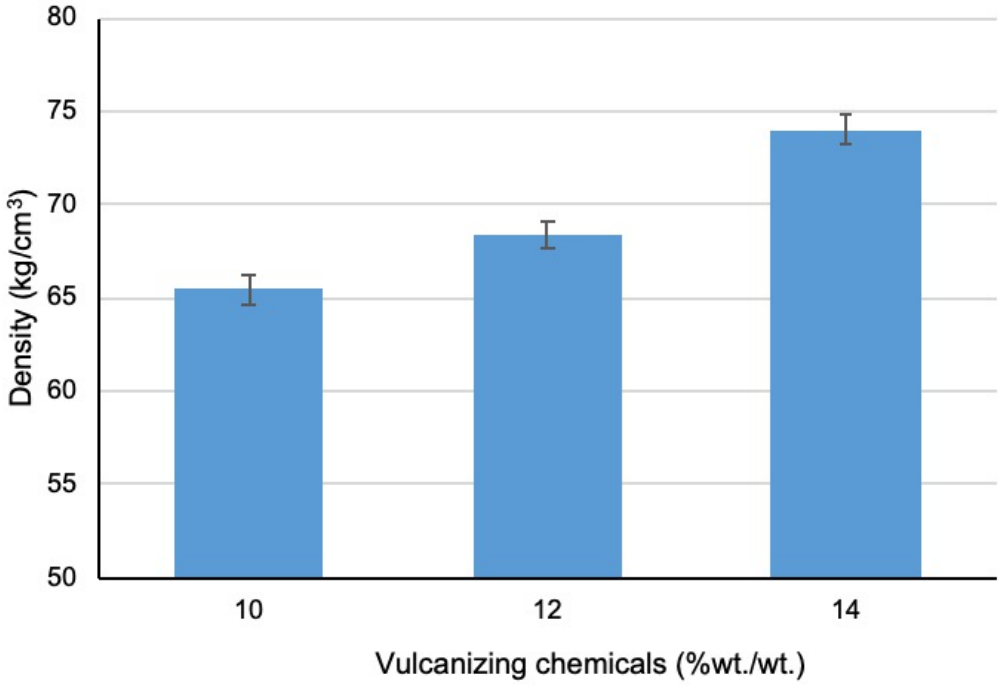

Figure 1. Density of rubber foam with various vulcanizing chemicals.

Consideration in mechanical property by compressive strength of all three formulae rubber foams as in Table 1, the increasing of vulcanizing chemicals that increases density of rubber foam also increases the compressive strength. When the rubber foam sample is compressed by 75% of its thickness, the applied force in equal area is higher in the sample with higher density. These results are in good agreement with the results of Suksup et al. (2019) in which they prepared rubber foam from two difference latex, centrifuged and creamed latex. Their results have shown that with the same formula, the density of the rubber foam from creamed latex is higher than the density of the rubber foam from centrifuged latex, and the compressive strength of the rubber foam from creamed latex is also higher than that of the rubber foam from centrifuged latex as well. However, the results in this present work indicate in the same tendency using the same matrix but different formulae.

Table 1 Compressive strength and compression set of rubber foam with various vulcanizing chemicals.

Vulcanizing chemicals (%wt./wt.)	Compressive strength (kPa) (±0.5 %)	Compression set (%) (±5 %)
10	6.54	5.35
12	6.43	5.02
14	10.11	2.70

Generally, natural rubber foam tends to be a memory foam. In this work, however, we are trying to enhance the recovery property by adjusting the chemicals in the rubber foam formula which is the cheapest and easiest way. Thus, the vulcanizing chemicals are studied, in order to see if they can be effective to the recovery property. In Table 1, when the vulcanizing chemicals in rubber foam are increased, the %compression set significantly decreases, in other words, the %recovery of rubber foam is increased from 94.65% to 94.89% and 97.30%, respectively. Deliberation in the results, the increasing of the vulcanizing chemicals must increase the crosslinking density within the structure of rubber foam, leading to the higher of compressive strength, in other words, ability to withstand higher force, and more recoverable ability. This means that the internal structure of rubber foam is related to the recovery property which is the interesting model in developing of recovery performance of rubber foam in the future.

CONCLUSIONS

In this work, rubber foam was prepared from three formulae using 10 %wt./wt., 12 %wt./wt., and 14 %wt./wt. of vulcanizing chemicals. The results showed that the increasing of vulcanizing chemicals tends to increase density of rubber foam which must due to the increasing of crosslinking density according to Flory–Rehner theory. The increasing of vulcanizing chemicals also increases the compressive strength when the sample is compressed by 75% of its thickness. Moreover, the %compression set significantly decreases or in other words, the %recovery is increased by the increasing of vulcanizing chemicals. This means that the internal structure of rubber foam is very important, and the better mechanical property and better performance of recovery can be achieved by increasing more vulcanizing chemicals. Thus, this is a development of the rubber foam products and also increases the value of natural rubber, certainly.

ACKNOWLEDGEMENT

This research is supported by graduate study development scholarship from the National Research Council of Thailand as of 2020 fiscal year. This research is also supported by Specialized center of Rubber and Polymer Materials in agriculture and industry (RPM), Faculty of Science, Kasetsart University, Bangkok, Thailand.

REFERENCES

Cavicchi, K. A. 2015. Shape Memory Polymers from Blends of Elastomers and Small Molecule Additives. Macromol. Symp. 358(1): 194-201.

Chollakup, R., P. Suwanruji, R. Tantatherdtam and W. Smitthipong. 2019. New approach on structure-property relationships of stabilized natural rubbers. J. Polym. Res. 26(2): 37.

Flory, P. J., J. Rehner, Jr. 1943. Statistical Mechanics of Cross-Linked Polymer Networks II. Swelling. J. Chem. Phys. 11(11): 521-526.

Kamila, S. 2013. Introduction, Classification and Applications of Smart Materials: An Overview. Am. J. Appl. Sci. 10: 876.

Oliveira-Salmazo, L., A. Lopez-Gil, F. Silva-Bellucci, A. E. Job and M. A. Rodriguez-Perez. 2016. Natural rubber foams with anisotropic cellular structures: Mechanical properties and modeling. Ind. Crops. 80: 26-35.

Sedat Gunes, I., F. Cao and S. Jana. 2008. Evaluation of Nanoparticulate Fillers for Shape Memory Polyurethane Nanocomposites. Polymer. 49: 2223-2234.

Smitthipong, W., M. Nardina, J. Schultza and K Suchiva. 2007. Adhesion and self-adhesion of rubbers, crosslinked by electron beam irradiation. Int. J. Adhes. Adhes. 27: 352-357.

Suksup, R., Y. Sun, U. Sukatta and W. Smitthipong. 2019. Foam rubber from centrifuged and creamed latex. J. Polym. Eng. 39(4): 336-342.

O-EC3

EFFECT OF THE MATRIX CONTENT ON PROPERTIES OF RUBBER FOAM

Supitta Suethao[1], Saree Phongphanphanee[1], Jirasak Wong-Ekkabut[1,2], and Wirasak Smitthipong[1,3,4]*
[1] Specialized center of Rubber and Polymer Materials in agriculture and industry (RPM), Department of Materials Science, Faculty of Science, Kasetsart University, Bangkok, Thailand
[2] Department of Physics, Faculty of Science, Kasetsart University, Bangkok, Thailand
[3] Office of natural rubber research program, Thailand Science Research and Innovation (TSRI), Bangkok, Thailand
[4] Office of research integration on target-based natural rubber, National Research Council of Thailand (NRCT), Bangkok, Thailand
*E-mail: fsciwssm@ku.ac.th

ABSTRACT
Current trends in the use of lightweight materials to replace conventional materials are of interest to the world. Rubber foam is porous and lightweight material that has two or more phases: a continuous phase is the part of polymer matrix and a gaseous phase is the part of gas bubble. For the Dunlop process, the porous structure is produced by a chemical blowing agent for gas bubble production in a polymer matrix. It can be used in many applications including pillows, mattress, dolls and flooring. The objective of this work is to study the effect of matrix content, as natural rubber, on the properties of rubber foam. Concentrated latex from centrifugation method (60% dry rubber content) was used to prepare a Dunlop-based rubber foam. The concentration of concentrated latex was varied in order to investigate the important properties of obtained rubber foam. We found that the density of rubber foam is increased with increasing of rubber content, this result is in good agreement with the compressive strength of rubber foam from the compression test. Interestingly, the morphological property of rubber foam from the scanning electron microscope corresponds to the density and compressive strength, higher rubber loading higher rubber interconnecting thus lower cell size of rubber foam. Our results are in good agreement with a previous study of styrene-acrylonitrile foam. A better understanding of this study leads to the development of tailor-made rubber foam with excellent properties, such as mechanical performance for a strong but light-weight product, etc.
Keywords: Rubber foam, Mechanical property, Morphological property

INTRODUCTION

Polymer foams are porous material that have two or more phases. The polymer matrix forms a continuous phase and the gaseous porosity phase is composed of gas bubbles. The porous structure is produced by either a chemical or a physical blowing agent for gas bubble production in a polymer matrix. In the case of chemical blowing agents, the gas bubbles are generated through a chemical reaction, usually thermal decomposition of a powder. On the other hand, physical blowing agents are inert gases or supercritical fluids (mostly CO_2 and N_2), which are dissolved into the polymer matrix during a saturation process, usually at high pressure (Mohebbi et al., 2015; Andrieux et al., 2018; Trofa et al., 2019).

Chemical blowing agents can be used for both liquid and solid polymers. For liquid polymers, especially natural latex, chemical blowing agent as potassium oleate is used in the Dunlop process in order to manufacture rubber foam for pillow and mattress applications (Suksup et al., 2019).

Generally, rubber foam is prepared from concentrated natural latex. It has been used to produce many products such as mattresses, pillows, dolls, cushions, flooring and upholstery foam, for many years. There are many processes that are used in natural rubber foam's production. But the two most popular processes are the Dunlop process and the Talalay process. Both processes have different foam characteristics which affect the latex foam properties.

The general properties of rubber foam are lightweight, buoyant, cushioning performance, flexible, thermal insulation, acoustic insulation and impact dampening (Najib et al., 2009). There is a great variety of properties. It is used in many applications. Many researchers have studied the factors affecting the foam

properties. But few have studied the relationship between the cell characteristics and the rubber foam properties.

The main aim of this work is to investigate the influence of matrix content on the rubber foam properties and the relationship between the cell characteristics and the rubber foam properties. A better understanding of this will lead to the development of tailor-made rubber foam with excellent properties, such as mechanical performance for a strong but light-weight product, etc.

MATERIALS AND METHODS

Materials

The concentrated natural latex, 60% dry rubber content, from *Hevea brasiliensis* was supplied from Num Rubber & Latex Co., Ltd., Trang, Thailand. The chemical agents consist of 10% potassium oleate solution, 50% sulfur dispersion, 50% zinc diethyldithiocarbamate (ZDEC) dispersion, 50% zinc-2-mercaptobenzothiazole (ZMBT) dispersion, 50% Wingstay L dispersion, 28% zinc oxide (ZnO) dispersion, 33% diphenylguanidine (DPG) dispersion and 12.5% sodium silicofluoride (SSF) dispersion were supplied from Thanodom technology Co., Ltd., Thailand.

The formulations of chemical agents for the rubber foam production were summarized in Table 1.

Table 1 Formulations of chemical agents for the rubber foam production.

Chemical agent	Formulation (g)		
	1	2	3
60% Concentrated natural latex	150.3	167.0	183.7
10% Potassium oleate	15		
50% Sulfur	4		
50% ZDEC	2		
50% ZMBT	2		
50% Wingstay L	2		
50% ZnO	10		
33% DPG	2		
12.5% SSF	8		

Rubber foam production

The rubber foam production was started by stirring the concentrated natural latex at a speed of 80 rpm for 1 min using the blender in order to remove ammonia content. Then potassium oleate was added with increasing the mixing speed to 160 rpm for 10 min. After that, the chemical agents including sulfur, ZDEC, ZMBT and Wingstay L were added into rubber compound with decreasing the mixing speed to 80 rpm for 1 min. Next, ZnO and DPG were added and continued to mix for 1 min. At the final step of mixing rubber foam, SSF was added into rubber compound and continued to mix until the rubber foam was close to the gel state. After that, the rubber foam was transferred into a mold and set in the mold for 45 min. Then it was cured in a hot air oven at 90°C for 2 h. The rubber foam was removed from the mold and then washed. The rubber foam was dried in a hot air oven at 70°C for 4 h.

Rubber foam characterization

Foam density is evaluated from weight of the rubber foam and volume of rubber foam. The density is calculated as shown in Eq.1

$$\text{Density} = \frac{M}{V} \qquad \text{Eq.1}$$

where M is weight of the rubber foam (kg) and V is volume of rubber foam (m^3)

Compressive strength is a mechanical property that indicates the ability of a material to resist the direct compressive force. The compressive strength of the rubber foam was evaluated by Texture analyzer (Stable Micro Systems, TA.XT plus) using platen probe with the diameter of 100 mm at the speed test of 0.1

mm/sec and room temperature. The three specimens (dimension of 45 mm x 45 mm x 24 mm) per rubber foam formulation were tested by compression at 75% from the rubber foam surface.

The morphology of rubber foam was examined using a scanning electron microscope (SEM) (FEI, Quanta 450). The rubber foam was cut into small pieces and coated with gold. Each rubber foam formulation was tested three replications. The ImageJ software was used to evaluate the average cell size and porosity of rubber foam. The average cell size was analyzed by measuring the diameter from at least three images and ten cells per image for each rubber foam. The porosity of the rubber foam was obtained from the ratio of pore area to SEM image area for each rubber foam formulation.

RESULTS AND DISCUSSION

The influence of the amount of concentrated natural latex, as matrix content, on the important properties and cell characteristics of rubber foam was investigated. In this work, the main components of concentrated natural latex consist of 60% of dry rubber content and 40% of water. The three formulations for rubber foam production were developed from varying the amount of matrix content, which included the 10% reduction in matrix content (formulation 1), the amount of matrix content of standard formulation (formulation 2) and the 10% addition in matrix content (formulation 3).

For investigating the density of rubber foam, we tested the rubber foam sample with the same volume. Each rubber foam sample was weighed to record its weight in kilograms. The results showed that the amount of matrix content has significant effect on the density of rubber foam. The density of rubber foam is decreased around 10% in the case of the 10% reduction in matrix content while the 10% addition in matrix content results in the increasing of density of rubber foam around 10% as well (Table 2).

Table 2 Density of rubber foam.

Formulation	Density (kg/m^3)	Compressive strength (kPa) ± 0.5%
1	98.93 ± 3.08	18.04
2	109.77 ± 0.44	24.67
3	123.06 ± 1.30	30.31

Concerning to the compressive strength, which is the maximum compressive stress at 75% from the rubber foam surface, we found that the compressive strength increases with the increasing of matrix content. This result is in good agreement with that of density. Generally, natural rubber exhibits the good mechanical properties because it represents high molecular weights (Smitthipong et al., 2004; Chollakup et al., 2019). Interestingly, the effect of matrix content is more sensitive to the mechanical property (compressive strength) than the density. The compressive strength of rubber foam was decreased around 37% in the case of the 10% reduction in matrix content while the 10% addition in matrix content results in the increasing of compressive strength of rubber foam around 23% (Table 2).

Table 3 Average cell size and porosity of rubber foam.

Formulation	Average cell size (μm) ± 1 μm	Porosity (%) ± 1.0%
1	555	52.6
2	522	47.3
3	352	44.7

From the morphological property point of view, we used the ImageJ software to determine the average cell size and porosity of rubber foam from SEM images. When the matrix content of rubber foam is increased, the average cell size and the porosity are decreased. This is due to the fact that the matrix content creates the interconnecting foam around the cell, higher matrix content higher interconnecting foam and thus lower average cell size and porosity (Table 3). This result is a good model to study the structure-property relationship of rubber foam using different formulations which is the economical way compared to the modification of processing.

CONCLUSIONS

We prepared rubber foam by varying the matrix contents in the formulation. The difference properties of rubber foam are due to the difference of its morphological property, the density and the mechanical property of rubber foam increase with the decreasing of average cell size and porosity. The morphology of rubber foam can be controlled by the matrix content, in particular the interconnecting foam and the overall air/rubber content. This is a good model to investigate structure-property relationship of rubber foam product at different grades.

ACKNOWLEDGEMENT

We wish to thank graduate school of Kasetsart University, Bangkok, Thailand for financial support. We also thank the Specialized center of Rubber and Polymer Materials in agriculture and industry (RPM), Faculty of Science, Kasetsart University, Bangkok, Thailand for supporting the knowledge, instruments, and places for this work.

REFERENCES

Andrieux, S., A. Quell, C. Stubenrauch and W. Drenckhan. 2018. Liquid foam templating – a route to tailor-made polymer foams. Adv. Colloid Interface Sci. 256: 276-290.

Chollakup, R., P. Suwanruji, R. Tantatherdtam and W. Smitthipong. 2019. New approach on structure-property relationships of stabilized natural rubbers. J. Polym. Res. 26.

Mohebbi, A., F. Mighri, A. Ajji and D. Rodrigue. 2015. Current issues and challenges in polypropylene foaming: A review. Cell. Polym. 34: 299-338.

Najib, N.N., Z. Ariff, N.A. Manan, A. Bakar and C. Sipaut. 2009. Effect of blowing agent concentration on cell morphology and impact properties of natural rubber foam. J. Phys. Sci. 20.

Smitthipong, W., M. Nardin, J. Schultz, T. Nipithakul and K. Suchiva. 2004. Study of tack properties of uncrosslinked natural rubber. J Adhes. Sci. Technol. 18, 1449-1463.

Suksup, R., Y. Sun, U. Sukatta and W. Smitthipong. 2019. Foam rubber from centrifuged and creamed latex, J. Polym. Eng. 39.

Trofa, M., E. Di Maio and P.L. Maffettone, 2019. Multi-graded foams upon time-dependent exposition to blowing agent. Chem. Eng. J. 362: 812-817.

O-EC4

ISOLATION OF MANNANASE-PRODUCING *BACILLUS TEQUILENSIS* FROM PICKLED TEA FOR MANNO-OLIGOSACCHARIDES PRODUCTION

Waralee Suyama[1], Khanok Ratanakhanokchai[1], Chakrit Tachaapaikoon[1,2], Rattiya Weanukul[1,2], and Patthra Pason[1,2]*
[1] School of Bioresources and Technology, King Mongkut's University of Technology Thonburi, Bangkok 10150, Thailand
[2] Pilot Plant Development and Training Institute, King Mongkut's University of Technology Thoburi, Bankok 10150, Thailand
*E-mail: patthra.pas@kmutt.ac.th

ABSTRACT
Miang (pickled tea), made from leaves of Assam tea (*Camellia sinensis* var. *Assamica*) fermented until sour, is a snack for refreshment in the north of Thailand. It is rich in probiotics and contains non-starch polysaccharides, especially cellulose and hemicellulose, including mannan. Thus, Miang is an interesting source of mannanase-producing bacterial for application in the food industry. Mannanase can hydrolyze mannan into manno-oligosaccharides (MOSs), a type of prebiotics commonly used in the poultry and aquaculture industry to improve the digestive system and stimulate the immune system. This research focused on the production of MOSs from locust bean gum using isolated mannanase-producing bacteria from Miang. The isolates were cultivated in a mineral salt medium supplemented with 2% locust bean gum at 37°C and selected by decreasing the viscosity. Afterward, single colonies were isolated by serial dilution. Twenty-one bacterial isolates of different sizes and colors were investigated for mannanase activity on agar plates containing 2% locust bean gum. The rod-shaped, Gram-negative, endospore-forming isolate M1 produced the highest mannanase activity, with a clear zone radius of 2.06 mm after 3 days at 37°C. In addition, M1 produced cellulase and pectinase with clear zones of 1.26 and 5.00 mm radii on 0.5% carboxymethyl cellulose (CMC) and pectin-containing agar plates, respectively. Based on 16S rRNA gene sequence analysis, M1 was identified to be *Bacillus tequilensis* with 99.93 percent similarity. Fermentable products of M1 using locust bean gum as a carbon source at 37°C for 16 h showed high molecular weight MOS (more than DP4) as a major product without monomers and dimers, and short-chain MOS (less than DP4). This process could reduce purification steps to eliminate fermentable sugars and short-chain oligosaccharides. This is the first report on high molecular weight manno-oligosaccharide production from *B. tequilensis.*
Keywords: *Bacillus tequilensis*, Mannanase, Mannan-oligosaccharides, Pickled tea

INTRODUCTION

Mannan-oligosaccharides (MOSs) become more popular because MOSs have been used as a prebiotic in the poultry and aquatics industry to improve the digestive system. MOSs increase the number and length of villi in the intestinal wall. Absorption of nutrients and stimulation of the immune was determined to significantly increase. Therefore, MOSs is an important alternative to reduce using of antibiotics in the animal feed and food industry for maceration and clarification (Chauhan et al., 2012; Jahanian et al., 2016; Chacher et al., 2017) MOSs is consisting of mannose in the main chain and produced from hydrolysis of mannan by acid, alkali or enzymes. (Kalidas et al., 2017) Enzymes from bacterial become important in MOSs production because they can hydrolysis complex polysaccharides from plant tissues into simple molecules such as short-chain polysaccharides and biosugar. In addition, Enzymatic hydrolysis has the following advantages: (1.) mild reaction (2.) no corrosion (3.) Non-toxic and (4.) less contaminated chemicals. Moreover, the enzymatic hydrolysis is very specific with the bond of structure in raw materials, the mannanase from bacteria has a specific reaction which high purity products and no toxic substances such as furfural and hydroxymethylfurfural etc. Miang (pickled tea) is a traditional fermented food in the north of Thailand. It is made from leaves of Assam tea (*Camellia sinensis* var. *Assamica*) fermented until sour and it is a snack for refreshment. Miang was reported it rich in probiotics such as lactobacilli *Bacillus spp.* yeast and the endospore forming bacteria. In addition, Miang contains non-starch polysaccharides, especially

cellulose and hemicellulose, including mannan. Thus, Miang is an interesting source of mannanase-producing bacterial for application in the food industry. This research focused on screening and isolation mannanase-producing bacteria from Miang for the production of MOSs from locust bean gum. We use locust bean gum as a model to study because it is the most structure found in the natural plant.

MATERIALS AND METHODS

Sample collection and bacterial isolation

Miang for isolation got from Chiang Mai (M) and Chiang Rai (M2). Sample was weighted about 3-5 g to locust bean gum (LBG) in Mineral salt medium (MS medium), incubated at 37℃ 200rpm 24h. Viscosity of medium should be reduced. The solution was made serial dilution and spread plates to 2% LBG agar plates for selection single colony that considerate from characterization, size and color of the colony. Then we transfer a new plant more than 10 or until the colony has the same character.

Screening of mannanase-producing bacteria

The mannanase-producing bacteria were selected on the agar plate by (Liu et al., 2018) method. A single colony was spotted to 2% w/v LGB agar plate, incubated at 37℃ 72 h. After that incubated at 55℃ 45 min. The agar plate was dyed in 1% v/w congo rad 15 min and washed in 1M NaCl solution 15 min. The color was fixed by 5% v/v acetic acid. The clear zone was found and measured.

Identification of bacterial strains by 16S rRNA

The bacteria have the highest clear zone, was inoculum to 1% LBG medium at 37℃ 200 rpm 24h. Centrifuge at 8,000 rpm 10 min to collet cell. Extracted DNA by DNeasy Blood & Tissue Kit and Increase a number by Polymerase Chain Reaction. The genomic was purified by QIaquick® PCR Purification Kit.16S rRNA was identified by Sanger Sequencing from 1st BASE DNA Sequencing Services. Use BioEdit version 7.3.3 to analyze the sequent data and compare the information on the BLAST® database. (website: https://blast.ncbi.nlm.nih.gov/Blast.cgi). Phylogeny was performed in MEGA software version X statistics on the Maximum Likelihood and use the Tamura-Nei model.

Morphology of isolated bacteria

The bacteria was measured the size, color, and shape under a microscope by gram-staining bacteria (Moyes et al., 2009) and endospore staining (Marise and Hussey 2007).

Production of the cellulolytic and hemicellulolytic enzyme of isolated bacteria

The production of cellulolytic and hemicellulolytic enzymes used the modified methods of (Liu et al., 2018). The bacteria were growth in agar plates that contain 5% v/w of differences hemicellulose such as galactomannan from locust bean gum for mannanase, pectin from oranges peel for pectinase, xylan from corn core for xylanase, and carboxymethyl cellulose for cellulose, incubated at 37℃ 72 h. The clear zone was detected the same as the selection of mannanase-producing bacteria.

Effects of Temperature, pH, and Culture Conditions

The optimum pH for mannan-oligosaccharide production in galactomannan from locust bean gum

The bacteria were cultured in MS medium containing 0.5% v/w of locust bean gum by adjusting the range of pH 5.0 to 9.0 incubated at 37℃ 200 rpm. All of the samples were inoculated at 37℃ 200 rpm for 24 hours. The solution was collected every 6 hours (0, 6, 12, 18, and 24 hours), the control is MS medium without bacterial. The examination growth of the cells by spreads plates. Count the single colonies that occurred and calculate the CFU/ml (Santana et al., 2008). The solution after that was boiled for 15 min to stop the reaction. The product was examined reducing sugar by Smogyi-Nelson (Nelson, 1944; Smogyi, 1952). Characteristics of products obtained by thin-layer chromatography (mobile phase is 2:1:1, butanol: acetic acid: water), mannose DP 1 to 6 and galactose are standard.

RESULTS AND DISCUSSION

The total 22 isolated from Miang, 4 isolated from Chiang Mai (M) and 18 isolated from Chiang Rai (M2). All of the sample growth on LBG but, only one isolated was found endo-β-D-mannanase; EC 3.2.1.78 which is M1, with a clear zone radius of 2.06 mm after 3 days at 37°C. The identification was carried out by

16S rRNA gene sequence analysis. The 16S rDNA fragment was amplified by PCR and then the nucleotide sequence of 16S rRNA gene was compared for similarities against the bacterial 16S rDNA sequence database in GenBank. The 16S rRNA gene sequence was deposited in GenBank this was clearly demonstrated that the isolate M1 showed the high similarity of 99% to *Bacillus tequilensis*. The phylogenetic tree from MEGA software version X statistics on Maximum Likelihood and use the Tamura-Nei model showing the relationships M1 with other bacterial strains in Figure 1. Gram staining B. tequilensis strain M1 under a microscope 100X magnification found that the shape is rod. Gram-positive is able to produce endospores (Figure 2).

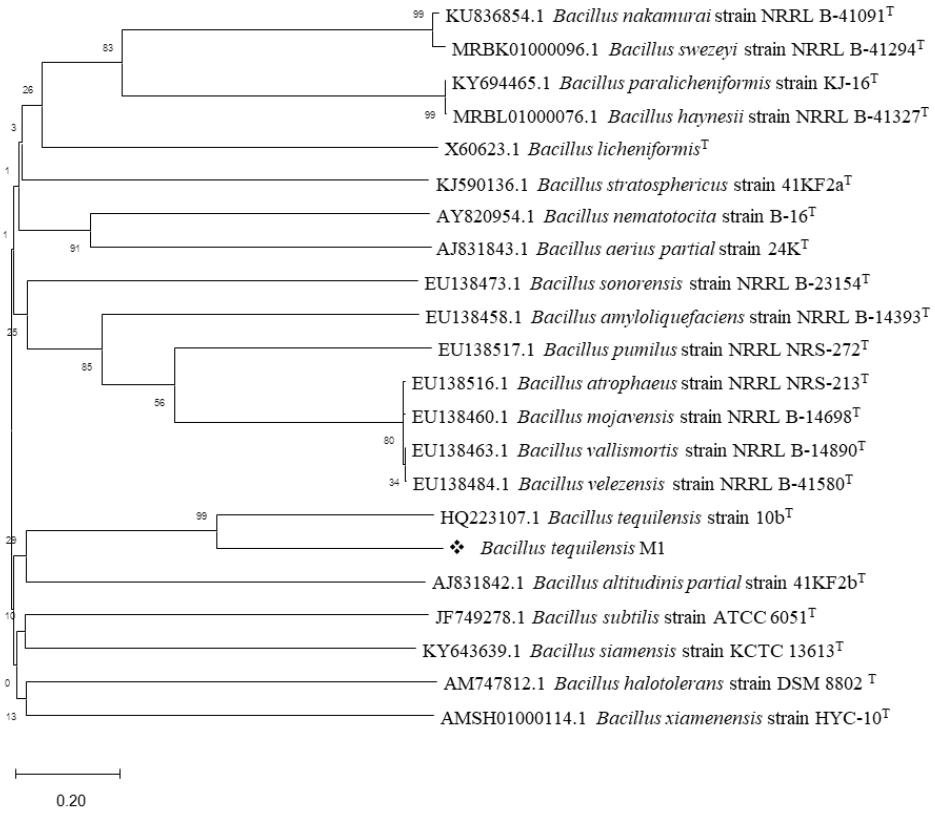

Figure 1. The phylogenetic tree of isolated M1 from MEGA software version X statistics on Maximum Likelihood and use the Tamura-Nei model.

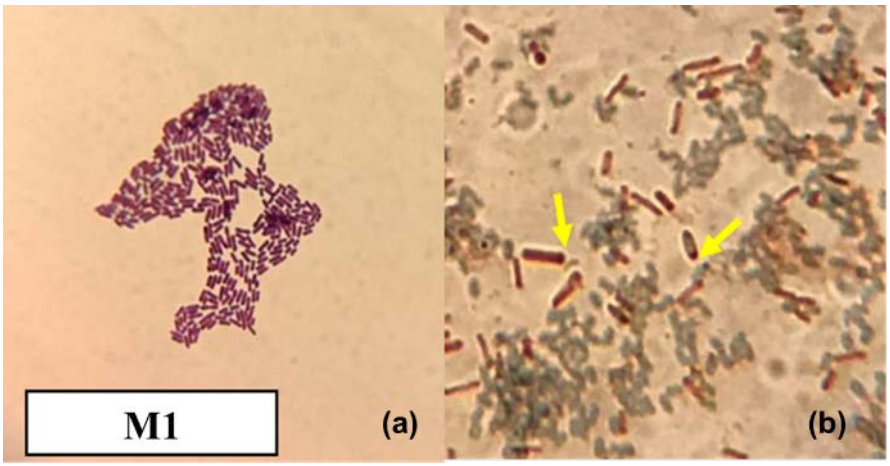

Figure 2. Gram staining *B. tequilensis* strain M1 under a microscope 100X magnification (a) and endospores forming (b).

Examination of cellulolytic and hemicellulolytic enzymes. There are different types of cellulose and hemicellulose each 0.5% w/v, galactomannan, pectin, xylan, and carboxymethyl cellulose (CMC) for monitoring the production of mannanase, pectinase, xylanase and cellulase respectively. The results showed that *B. tequilensis* M1 produced mannanase pectinase cellulase but did not produce xylanase (Figure 3). The maximum clear zone is pectin 5.00 mm, cellulase 1.26 mm, and mannanase 1.12 mm respectively.

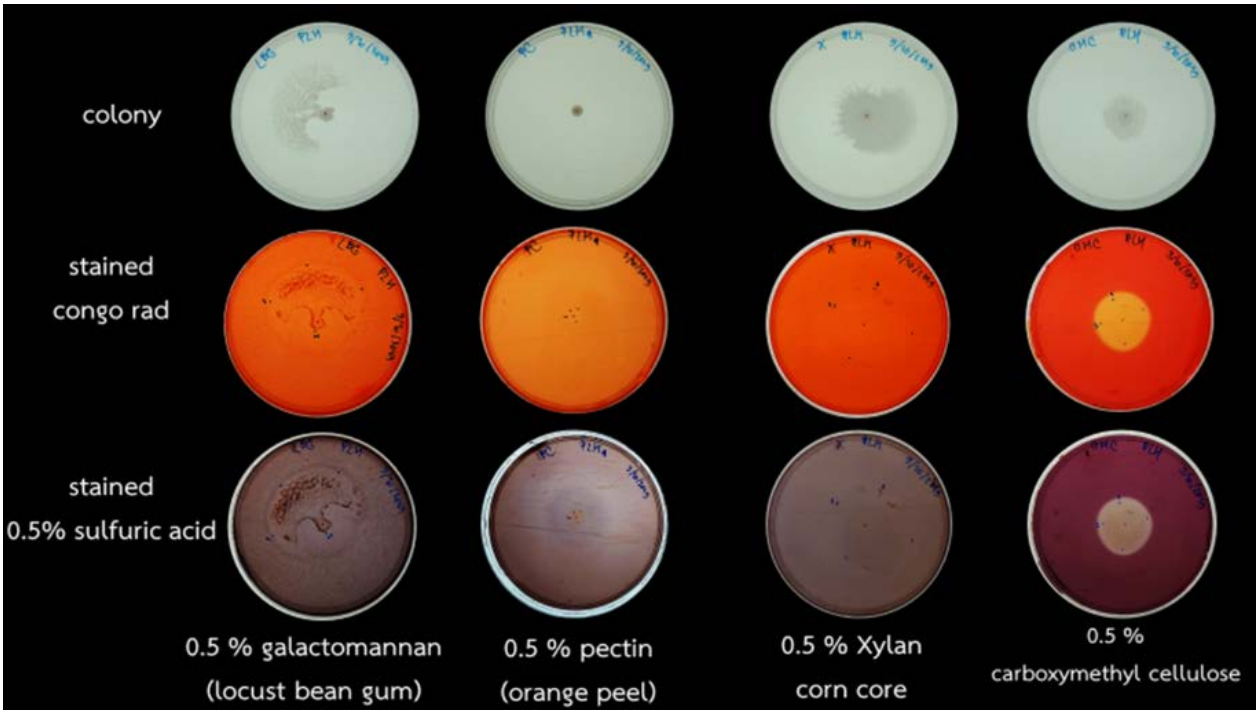

Figure 3. The production of mannanase, pectinase and cellulase of *B. tequilensis* M1 on a culture plate containing various types of hemicellulose after incubation at 37 ° C for 72 hours, then dye with congo red and fix with sulfuric acid.

B. tequilensis M1 in 0.5% w/v LBG as a carbon source, the pH starts at 5.0-9.0. The results showed *B. tequilensis* M1 has the highest growth rate at pH 6.0 with a cell volume of 3.5 ± 0.01 x 10^8 CFU / ml after 24 hours of incubation, followed by pH 7.0 (2.48 ± 0.01 x 10^8 CFU / ml) pH 8.0 (2.09 ± 0.06 x 10^8 CFU / ml) pH 9.0 (1.47 ± 0.02 x 10^8 CFU / ml) and pH 5.0 (1.24 ± 0.02 x 10^8 CFU / ml) respectively, showing that *B. tequilensis* M1 can grow well in a wide range of pH ($p > 0.05$). All of pH had the same growth rate, lag phage is appeared in 0 to 6 hours. During this period, the amount of reducing sugar remained unchanged. *B. tequilensis* M1 in pH 6.0 to 9.0 when entering 6 to 12 h, this period is the exponential phase or log phase. This phase the cells multiply rapidly and the amount of reducing sugar in the vitreous increased. The extracellular enzyme was produced outside the cell to be used to hydrolyzed galactomannan into short chain oligosaccharides or sugar molecules for use in growth. (Aderibigbe and Odunfa, 1990) At 12 to 24 h enter the stationary phase, growth cell growth and reducing sugar began to decrease and remained stable (Figure 3b).

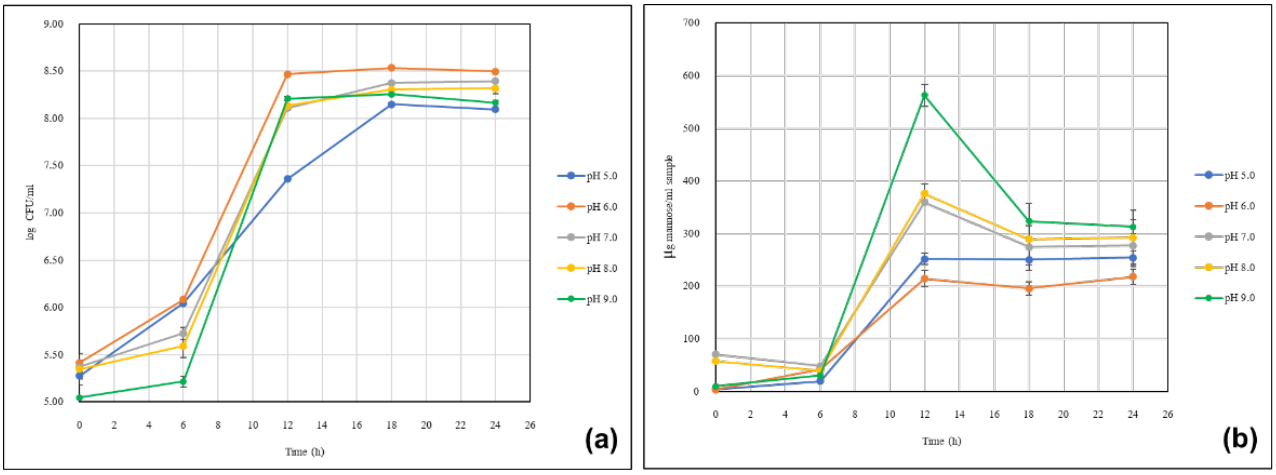

Figure 4. Growth of *Bacillus tequilensis* M1 (a) and reducing sugar (b) in 0.5% w/v LBG in pH range 5.0-9.0 at 37˚C for 24 h.

B. tequilensis M1 at pH 5.0 had the longest log phase, 6 to 18 hours and stationary phase in 18 to 24 hours (Figure 3a). Therefore, after 6 hours different DP of sugar production is commensurate with the slightly reduced sugar content, but then after entering in 12 hours. B. tequilensis M1 cultured in pH 6.0 and 7.0 the products remaining DP of sugar below 4 in solution (Figure 4), but *B. tequilensis* M1 in pH 5.0, 8.0 and 9.0 will take at least 18 hours to be able to use all the small sugar in the medium (low DP Than 4). The most of mannans, oligosaccharides with prebiotic capabilities have DP in the range of 2-10. (Singh et al., 2018) Moreover, the industry needs a short time production process to save energy and cost of production. Therefore, *B. tequilensis* M1, raised in pH 6.0 and 7.0 is a condition that takes quick time to produce sugar-free mannan-oligosaccharides when compare to other conditions. However, when considering the reducing sugar content was found that at 12 hours the reducing sugar content at pH 7.0 is higher than pH 6.0, which is 359.09 ± 34.69 and 214.24 ± 15.43 µg / ml, respectively. Thus, pH 7.0 is the condition that it is suitable for the production of mannan oligosaccharides due to the short production time and the highest production volume.

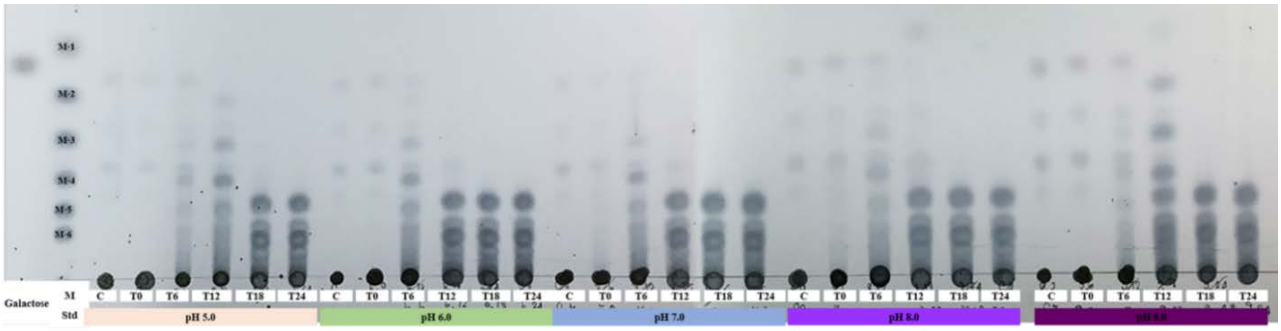

Figure 5. Chromatogram the product every 6 hours of *B. tequilensis* M1 cultured in 0.5% v/w LGB for 24 hours at 37˚C pH 5.0-9.0. Galactose and Mannan-oligosaccharides with DP 1-6 are standard (M1: mannose; M2: mannobiose; M3: mannotriose; M4: mannotetraose; M5: mannopentaose; M6: mannohexaose) by C is 0.5 % v/w LBG without *B. tequilensis*; T0 is 0.5 % v/w LGB with *B. tequilensis* M1 at zero hours; T6 is 0.5 % v/w LBG after adding *B. tequilensis* M1 for 6 hours; T12 is 0.5 % v/w LBG after adding *B. tequilensis* M1 for 12 hours; T18 is 0.5 % v/w LBG after adding *B. tequilensis* M1 for 18 hours and T24 is 0.5 % v/w LBG after adding *B. tequilensis* M1 for 24 hours.

CONCLUSIONS

Bacillus tequilensis M1 isolated from Miang produce MOSs from locust bean gum. At 37˚C, pH 7.0 is the optimum condition for the production. This condition M1 MOSs was found at least in 12 hours, which is the shortest time to hydrolysis galactomannan from locus bean gum when compare to other conditions used

in the study and the final product that has DP more than 4. In addition, M1 can produce pectinase and cellulase. Therefore, M1 is possible to be applied in the food industry and oligosaccharides from the plant.

ACKNOWLEDGEMENT

We acknowledge enzyme technology laboratory and systems biology and bioinformatics laboratory, King Mongkut's University of Technology Thonburi, Thailand. The authors acknowledge the financial support provided by King Mongkut's University of Technology Thonburi through the "KMUTT 55th Anniversary Commemorative Fund", and ASEAN Bioenergy and Bioeconomy Conference 2020.

REFERENCES

Aderibigbe, Y. E. and S. A. Odunfa. 1990. Growth and extracellular enzyme production by strains of *Bacillus* Species Isolated from Fermenting African Locust Bean, Iru. J. Appl. Microbiol. 69: 662-671.

Chacher, M. F. A., Z. Kamran., U. Ahsan., S. Ahmad., K. C. Koutoulis., H. G. Qutab Ud Din and Ö. Cengiz. 2017. Use of mannan oligosaccharide in broiler diets: An overview of underlying mechanisms. Worlds Poult Sci J. 73: 831-844.

Chauhan, P. S., N. Puri., P. Sharma and N. Gupta. 2012. Mannanases: microbial sources, production, properties and potential biotechnological applications. Appl Microbiol Biotechnol. 93: 1817–1830.

Jahanian, E., A. H. Mahdavi., S. Asgary and R. Jahanian. 2016. Effect of *dietary supplementation of mannanoligosaccharides on growth performance,Ileal Microbial Counts*, and Jejunal Morphology in broiler chicks exposed to aflatoxins. Livest. Sci. 190: 123-130.

Kalidas, N. R., M. Saminathan., IS. Ismai, F. Abas, P. Maity, S. S. Islam, N. Manshoor and K. Shaari. 2017. Structural characterization and evaluation of prebiotic activity of oil palm kernel cake mannanoligosaccharides. Food Chem. 234: 348-355.

Liu, J., A. Basit., T. Miao., F. Zheng., H. Yu., Y.Wang., W. Jiang and Y. Cao. 2018. Secretory expression of β-mannanase in *Saccharomyces Cerevisiae* and its high efficiency for hydrolysis of mannans to mannooligosaccharides. Appl. Microbiol. 102: 10027-10041.

Marise, A and A. Z. Hussey. 2007. Endospore stain protocol. ASMscience. 14: 1-11.

Moyes, R. B., J. Reynolds and D. P. Breakwell. 2009. Differential staining of bacteria: gram stain. Curr Protoc Microbiol.15: A.3C.1-A.3C.8.

Nelson, N. 1944. A photometric adaption of the Sumogyi method for the determination of glucose. J. Biol. Chem.153: 375-380.

Santana, M. A. and A. E. Gillis. 2008. *Bacillus Thuringiensis* improved isolation methodology from soil samples. J. Microbiol. Methods. 75: 0167-7012.

Singh, S., A. Ghosh and A. Goyal. 2018. Manno-oligosaccharides as prebiotic-valued products from agro-waste. In Biosynthetic Technology and Environmental Challenges. Springer Singapore, Singapor. 205-221.

Smogyi, M. 1952. Notes on sugar determination. J. Biol. Chem. 46: 19-23.

Oral Presentation

BIOENERGY

O-EN1

LIPASE DIGESTION BY INDIGENEOUS BACTERIA FOR USED FRYING OIL-BASED BIODIESEL SYNTHESIS

Soontree Khuntong*, **Kanokwan Kamanake**, Tippawan Jongdaeng, Jamnong Tanyasit, and Pattarawadee Sumthong Nakmee
Department of Resources and Environment, Faculty of Science at Siracha, Kasetsart University, Chonburi, Thailand
*E-mail: srcstk@ku.ac.th

ABSTRACT
Indigenous microorganisms provided potential oil digestion that was leading to the research objectives including microorganisms screening and culturing for improvement of used frying oil-based biodiesel synthesis. Indigenous microorganisms were collected from oil contaminated domestic wastewater from KUSRC canteen wastewater and Ao Udom fresh market sewerages. The pure culture of lipid digested microorganisms was performed by Enrichment culture in NA agar slant at 37 ^{o}C for 24 hr. Bacteria screened from mixed culture provided the dominant lipid digestion activities. The gram staining showed entirely 9 gram negative bacteria which provided high lipid digestion activities by comparing from clear zone on Tween-80 agar. The used frying oil was used as carbon source of selected bacteria with MSB broth for additional of mineral needs. The mixture (bacterial suspension, used frying oil and MSB broth) was shaken for 48 hr at room temperature. After digestion, each digested oil was separated and filtered through anhydrous Na_2SO_4 for water removal. Synthesis of biodiesel from digested oil with ethanol and H_2SO_4 (96%) at 80 ^{o}C for 4 hr was performed. Three highest lipase digestion activities were found in 2 strains from market wastewater and one strain in canteen wastewater. The highest biodiesel production yields via bacterial digested oil prior esterification were ranged from 99.74, 98.51 and 97.43%, respectively. The most lipase activity were significantly influenced the biodiesel production yield more than amount of free fatty acid. The optimum amount of free fatty acid from digestion was approximately 1%. The high amount of free fatty particularly caused saponification instead of esterification. The lipase activity form living cells provided more advantageous alternative method for biodiesel production because of (1) high cost of commercial lipase and (2) transesterification produced high yield of by-product (glycerol). Bacterial digestion prior esterification was benefit for biodiesel synthesis from used frying oil due to high production yield, less chemical reagents and waste. Moreover, the used frying oil was value added and decreased the cost of wastewater treatment.
Keywords: Indigenous bacteria, Used frying oil, Lipase activity, Biodiesel, Esterification

INTRODUCTION

Biodiesel; the renewable diesel from plant and animal lipid; is the methyl ester of fatty acid. Recently, it became commercially marketed in various fractions of petroleum-based diesel including PTT B10, B20, Bangchak B10, Shell diesel B10, ESSO B10 and B20 and Caltex diesel B10 and B20. It provided advantage properties over petroleum-based diesel for less sulfur content, renewable fuel high cetane number and so on. Since biodiesel was synthesized from plant or animal lipid which no sulfur contents in their molecular structure, the emission from the combustion of synthetic biodiesel did not contain sulfur dioxide in the exhaust. In terms of atmospheric pollutant, sulfur dioxide proceeded secondary pollutant causing particulate sulfate which was taken part of PM2.5 suspending in the air (SEPA, 2020). Biodiesel was chemically synthesized from palm oil and methanol via transesterification process. This kind of biodiesel was mostly added to petroleum diesel and formulated to improve high performance commercial diesel.

Biodiesel can be synthesized from cooking oil waste such as used frying oil by chemical transesterification, microbial lipase digestion or combined method. Since waste cooking oil causes serious impact to human health and environment. To environment, it inhibited atmospheric gaseous exchange to aqueous phase and distorted wastewater treatment system e.g. pumps, pipes, scrubber, filter. For health impact, the frying steps accompanied various chemical reactions including oxidation, hydrolysis, polymerization and fission which resulted in decreasing in unsaturated fatty acids of oils and increasing

foam, color, viscosity, density and specific heat from free fatty acids, polar hydrocarbon compounds and polymeric compounds (Cho and Min, 2007). The major components of used frying oil consist of triacylglycerols (TAG) (Zhang et al., 2012) and the complex products from oxidative degradation of TAGs and volatile organic compounds as their intermediates such as polycyclic aromatic hydrocarbons (PAHs) and heterocyclic amines. These compounds are known as carcinogens, they can increase the risk of developing lung cancer (Lee and Gany, 2013) and respiratory tract cancer (Cao et al., 2013).

The general primary removal of oily contaminated wastewater was gravity separation tank by overflow or sweeping the floating oil at the surface to the collecting tank. Oil residue was then treated with solvent extraction (Ahmad et al. 2003), emulsification (Eckenfelder 2002), flocculant aids (Welz et al., 2007), coagulation/flocculation (Santo et al., 2012), membrane filtration (Ochando-Pulido and Stoller, 2014) chemical oxidation (da Silva et al., 2015) in secondary or tertiary unit were costly and time consume. The alternative and beneficial method was performed the used frying oil as raw material for synthesis of biodiesel. Catalytic lipase from microorganisms was the advantageous step to digest triacylglycerol to optimum amount of free fatty acid which was the reactant together with alcohol forming alkyl ester or biodiesel. Lipase was supplied from various sources including commercial lipase or living lipase from living microorganisms. The former was very expensive while the later can isolate the indigenous the living cells from oil contaminated wastewater.

The studies were aimed to isolate and screen lipase produced bacteria from selected oil contaminated wastewater for degradation of lipid forming free fatty acid. The bacterial digestion was hypothesized to reduce FFA, the digested oil was then examined to produce biodiesel by esterification process. The goals of this research were to reduce the oily waste discharging to the environment and minimized the chemical use as well as energy requirement for esterification process.

MATERIALS AND METHODS

Isolation of lipase produced bacteria

Oil contaminated wastewater from the discharge of KUSRC canteen and the sewer of Ao Udom fresh market was collected. The enrichment culture was provided in jelly slant with NA media (Jelly 15 g, beef extract 3 g, peptone 5 g was mixed in 1 L of deionized water and let it boil for 15 min). Culture media was incubated at 37 ^{o}C for 24 hr. Gram staining of bacteria was performed by Differential staining techniques (Ahern, 2018). The cellular morphology was observed under compound microscope (Figure 1).

Lipase activity of bacteria

The isolated consortium from jelly slant was inoculum in Tween 80 media (Jelly 15 g, peptone 10 g, $CaCl_2$ 0.1 g, NaCl 5 g was mixed in 1 L of deionized water. After boiling for 15 min. The media was sterilized at 121 ^{o}C, 15 psi for 15 min). Lipase activity was observed by clear zone diameter within 3 – 5 days of incubation (Figure 2).

Lipid digestion of used frying oil by isolated bacteria

The MS broth (Dissolve K_2HPO_4 1.8 g, KH_2PO_4 1.2 g, NH_4Cl 10 g, $MgSO_4.8H_2O$ 0.2 g, NaCl 0.1 g, $Fe_2(SO_4)3$ 0.01 in 1 L of deionized water, adjust to pH 7) 80 ml was mixed into 20 ml of sterilized used frying oil. After shaken at 170 rpm for 48 hr the mixed solution was left for phase separation (oil and cultured media). The oil phase was filtered through anhydrous Na_2SO_4 for water removal. The yield (%) of digested oil was calculated.

Each media was sterilized at 121 ^{o}C, 15 psi for 15 min before bacterial culture. The percentage of free fatty acid (FFA) containing in bacterial digested used frying oil (BDUFO) was resulted from titration with standard NaOH solution (0.005 M). The digested oil (0.5 g) was dissolved in ethanol (10 ml) and diethyl ether (10 ml), the concentration of FFA was calculated from the volume of std. NaOH at the end point of phenolphthalein indicator.

Synthesis of biodiesel by esterification method

The esterification of BDUFO with ethanol resulted ethyl ester of fatty acid (biodiesel). The reaction was performed by mixing BDUFO (30 g), conc.H_2SO_4 (96% 0.45 ml) as catalyst, C_2H_5OH (95%, 90 ml), the mixed reactants were refluxed at 80 ^{o}C for 4 hr. After solvent removal, the remaining substance was removed by washing with deionized water, ethyl ester (biodiesel) was filtered through anhydrous Na_2SO_4 for water removal. The percentage yields of biodiesel were calculated.

All chemical used was analytical reagents except ethanol (commercial grade).

RESULTS AND DISCUSSION

Morphology and of bacteria isolated from oily contaminated wastewater

The gram-negative bacteria were found in wastewater both at KUSRC canteen and Ao Udom fresh market. Nine single colonies were isolated including seven bacillus isolates and two coccus isolates. Each single colony was temporally named as indicating the sample sites. The cellular morphology under 100 times compound microscope was given in Figure 1. It was observed that only gram-negative bacteria were grown up. They involved with the morphology of bacteria cell wall structure. Besides gram-negative bacteria, the three outermost layers consisted of lipopolysaccharides, phospholipid bilayer and thin layer of peptidoglycan while the cell wall of gram-positive bacteria consisted only thick peptidoglycan layer and teichoic acid (Pornchalermpong and Rattanapanon, 2020). In terms of chemical mechanisms, lipid consisted of glycerol and fatty acid which proposed no attraction with teichoic acid in gram-positive bacteria. Moreover, the ten times thicker of peptidoglycan layer my inhibit the exchange or absorb the large molecules of lipid into the cell. For gram-negative bacteria, lipopolysaccharide linkage to phospholipid layer may induce lipid closed to phospholipid which provided hydrophobic behavior as lipid.

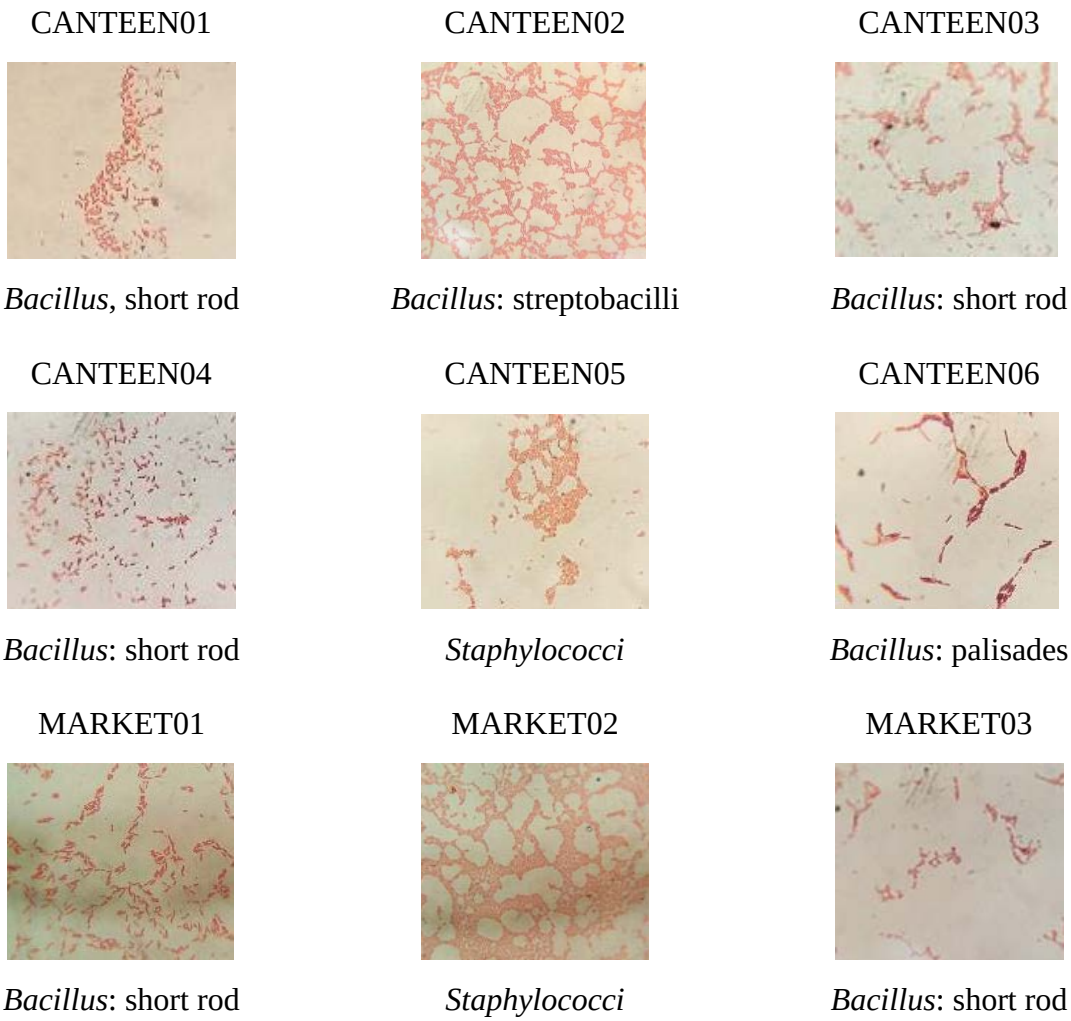

Figure 1. Morphology of isolated bacteria from the wastewater from KUSRC and wastewater from Ao Udom fresh market.

Lipase activities and free fatty acid contents from the isolated bacteria

The clear zones were observed after log phase from the bacterial growth curve since the clear zone could be seen within approximately 3-5 days. The clear zones occurred in Tween 80 from seven isolates except MARKET01 (Table 1). The ester linkage between glycerol and fatty acid was broken down by lipase enzyme. It supposed that the extracellular digestion produced glycerol and free fatty acids. The fatty acids were absorbed through cell membrane as carbon source for living cells. The white turbid precipitation was observed around the colony resulting from the reaction of Ca^{2+} in Tween 80 and fatty acids (digested products). Finally, the rest free fatty acids were found in oil phase after digestion. The appearance of bacterial digested oil and the final biodiesel products were compared in Figure 2. The more repeatability of frying oil was significantly influenced the digestion process (data not shown). During frying, many chemical reactions occurred increased foam, color, viscosity, density and specific heat of free fatty acids, polar hydrocarbon compounds and polymeric compounds (Cho and Min 2007). The major components of used frying oil were triacylglycerols (TGA) (Zhang et al., 2012) and the complex products from oxidative degradation of TAGs and volatile organic compounds as their intermediates such as polycyclic aromatic hydrocarbons (PAHs) and heterocyclic amines. Most products were considered as persistent organic compounds which was difficult to break down by bacteria themselves.

The lipase activities did not perform directly linear relationship with percentage of free fatty acids. It supposed that each isolate absorbs different amounts of fatty acid due to its need for increasing the cell numbers.

Table 1 Diameter of clear zones indicating lipase activities and percentage of free fatty acids over control after digestion.

Bacteria	Diameter of clear zone (cm)	Percentage of free fatty acid
CANTEEN01	1.35	0.64
CANTEEN02	1.2	0.44
CANTEEN03	1.4	0.31
CANTEEN04	1.2	0.45
CANTEEN05	1.5	0.37
CANTEEN06	1.45	0.79
MARKET01	No clear zone	0.36
MARKET02	1.4	1.4
MARKET03	2.2	0.39

Biodiesel synthesized from BDUFO

By visual inspection, the digested oil was clear pale liquid, less rancid smelling and viscosity comparing with the control oil. The appearance of BDUFO (in the flask) and biodiesel can be seen in Figure 2.

Figure 2. The appearance of BDUFO compared with biodiesel.

The percentage yields of biodiesel were significantly influenced by optimum amount of free fatty acids. The high percentage of fatty acid (approximately > 1%) performed saponification instead of esterification. The soap bubble was generated during washing step. The percentage yields of biodiesel from high to low was summarized in Table 2. Probably the highest percentage yield of biodiesel (91.87%) depended on the highest lipase activity of CANTEEN02. Lipase (triacylglycerol acylhydrolases, E.C.3.1.1.3) was one of the serine hydrolases that catalyzed triglycerides to glycerol and free fatty acids by hydrolysis of at an oil–water interface (Feng et al., 2013; Gupta et al., 2004; Kamini and Iefuji, 2001). Additionally, under suitable conditions, it can proceed many catalytic synthetic reactions including esterifi-cation and transesterification (Saxena et al., 2003) in both aqueous and non-aqueous media (Masaki et al., 2005). Due to the advantage of lipase, alkyl eater (biodiesel) was partially synthesized and completed by chemical esterification. The amount of free fatty acid from digestion was an additional the reactant for enhancement the esterification to increase the biodiesel yield. Indigenous lipase-produced bacteria seemed to propose better catalytic properties not only broken down of ester leakage to free fatty acid and glycerol, it might transferred the used oil to biodiesel. Moreover, all isolates were proved to be the lipophilic bacteria that were naturally tolerant and can be subjected to increase the bacterial numbers. Since the hydrolysis was active at an oil-water interface, lipase was alternatively suitable for treatment of oil-floating over water layer.

Table 2 Percentage yields of biodiesel products.

Biodiesel code[1]	Percentage yield (%)		
	BDUFO[2]	Biodiesel[3]	Overall[4]
CANTEEN03	87.48	99.74	87.25
CANTEEN05	86.23	98.51	84.95
MARKET03	89.46	97.43	87.16
CANTEEN04	86.52	97.37	84.24
MARKET02	75.97	97.21	73.85
CANTEEN02	94.98	96.73	91.87
MARKET01	85.74	96.73	82.94
CANTEEN06	82.00	94.87	77.79
Control	89.84	82.77	74.36
CANTEEN01	89.30	64.30	57.42

[1] Biodiesel codes were named analogous to bacteria. [2] The percentage yields of digested used frying.
[3] The percentage yields of biodiesel synthesized from BDUFO. [4] The net percentage yield from initially used frying oil.

CONCLUSIONS

Enzymatic hydrolysis and esterification were resulted from the excretion of lipase bacteria isolated KUSRC canteen wastewater and Ao Udom fresh market wastewater. The lipase activity was the significant factor for bacterial synthesis of biodiesel. The morphology of indigenous bacteria was gram-negative within 7 bacillus and 9 coccus types. The highest yield of biodiesel was exceeded 91.87% which was produced by CANTEEN02. The ongoing procedures were characterized and identified. The biochemical methods should be applied to confirm the digestion mechanism and the properties of biodiesel may be determined comparing to API standards. Finally, the ready-to-use bacteria will be developed for locally synthesis of biodiesel.

ACKNOWLEDGEMENT

We would like to appreciate our sincere thanks to Kasetsart University Research Development Institute (KURDI) for financial support. Thanks for Faculty of Science at Sriracha for additional matching fund and all beneficial facilities. Special thanks to Prof. Dr. Ngampong Kongkatip and Assoc. Prof. Vittaya Punsuvon; (KURDI experts) for very valuable comments particularly in indigenous bacterial sites.

REFERENCES

Ahmad, A. L., S. Ismail, N. Ibrahim and S. Bhatia. 2003. Removal of suspended solids and residual oil from palm oil mill effluent. J. Chem. Technol. Biotechnol. 78: 971 – 978.

Ahern, H. 2018. Microbiology: A laboratory experience. SUNY Textbooks, Milne Library State University of New York at Geneseo, Geneseo, NY 14454. https://milnepublishing.geneseo.edu/. July 13, 2020.

Cao, J., R. Ding. Y. Wang. D. J. Chen, D. M. Guo, C. M. Liang. 2013. Toxic effect of cooking oil fumes in primary fetal pulmonary type II-like epithelial cells. Environmental Toxicology and Pharmacology. 36: 320 – 331.

Choe, E. and D. B. Min. 2007. Chemistry of deep-fat frying oils. J. of Food science. 72: 77 – 86.

Da Silva S, S., O. Chiavone-Filho, E. L. de Barros Neto, and E. L. Foletto. 2015. Oil removal from produced water by conjugation of floatation and photo-Fenton processes. J. Environ. Manage. 147: 257 – 263.

Eckenfelder, W. W. 2000. Industrial Pollution Control. 3rd edition. McGraw-Hill.

Feng, X., D. A. Patterson, M. Balaban, E. A. C. Emanuelsson. 2013. Characterization of tributyrin hydrolysis by immobilizedlipase on woollen cloth using conventional batch and novelspinning cloth disc reactor. Chem. Eng. Res. Des. 91: 1684–1692.

Gupta, R., N. Gupta, P. Rathi. 2004. Bacterial lipases: an overview of production, purification and biochemical properties. Appl. Microbiol. Biotechnol. 64: 763–781.

Kamini, N. R. and H. Iefuji. 2001. Lipase catalyzed methanolysis of vegetable oils in aqueous medium by *Cryptococcus* spp. S-2. Process Biochem. 37: 405 – 410.

Lee, T. and F. Gany. 2013. Cooking oil fumes and lung cancer: A review of the literature in the context of the U.S. population. J. Immigr. Minor. Health. 15: 646 – 652.

Masaki, K., N. R. Kamini, H. Ikeda, H. Iefuji. 2005. Cutinase-likeenzyme from the yeast *Cryptococcus* sp. Strain S-2 hydrolyzespolylactic acid and other biodegradable plastics. Appl. Environ. Microbiol. 71: 7548 – 7550.

Ochando-Pulido, J. M. and M. Stoller. 2014. Boundary flux optimization of a nanofiltration membrane module used for the treatment of olive mill wastewater from a two-phase extraction process. Sep. Purif. Technol. 130: 124 – 131.

Pornchalermpong, P. and Rattanapanon N. 2020. Cell wall. Food Network Solution Co., Ltd. http://www.foodnetworksolution.com/. July 15, 2020.

Santo, C. E., V. J. P. Vilar, C. M. S. Botelho, A. Bhatnagar, E. Kumar and R. A. R. Boaventura. 2012. Optimization of coagulation-flocculation and floatation parameters for the treatment of petroleum refinery effluent from a Portuguese plant. Chem. Eng. J. 183: 117 – 123.

Saxena, R. K., A. Sheoran, B. Giri and W. S. Davidson. 2003. Purification strategies for microbial lipases. J. Microbiol. Methods 52: 1 – 18.

SEPA 2020. The chemistry of air pollutant. Scottish Environmental Protection Agency. https://www.sepa.org.uk/. July 13, 2020.

Welz, M., N. Baloyi and D. Deglong. 2007. Oil removal from industrial wastewater using floating in a mechanically agitated floatation cell. Water SA. 33.

Zhang, Q., A. S. M. Saleh., J. Chen and Q. Shen. 2012. Chemical alterations taken place during deep-fat frying based on certain reaction products. Chem. Phys. Lipids. 165: 662 – 681.

O-EN2

CATALYTIC REFORMING OF SYNTHESIS GAS FROM CRUDE GLYCEROL: POTENTIAL FOR RICE HUSK CATALYST STUDY

Kamonrat Suksumrit[1]*, Rujira Jitrwung[1], Kuntima Krekkeitsakul[1], Rujiroj Tamnitra[2], Jiraporn chalongtham[1], Mukrawee Maneewuthiworasakul[1], and Anantachai Wannajampa[1]
[1] Expert Center of Innovative Clean Energy and Environment, Thailand Institute of Scientific and Technological Research (TISTR), Khlong Luang, Pathum thani 12120, Thailand
[2] Department of Chemical Engineering, Faculty of Engineering and Industrial Technology, Silpakorn University, Sanam Chandra Palace, Nakhon Pathom 73000, Thailand
*E-mail :kamonrat@tistr.or.th

ABSTRACT
Crude glycerol is by product of biodiesel production that one of interesting feedstocks for valuable chemical such as bio-methanol. Pyrolysis and reforming are the approved processes for the catalytic conversion of glycerol. However, catalyst is one of limited factor for improvement and development of glycerol reforming technologies due to its deactivation such as coke formation. Therefore, this research aims to study the potential for agricultural catalyst such as rice husk catalyst which is substituting to Ni-base commercial catalyst. The catalyst was prepared by wetness impregnation method, then it was characterized before substituting in Ni-base commercial catalyst by mixing ratio of 25, 50, 75, and 100 wt%. The each 13 g mixtures of rice husk and Ni-base commercial catalyst were investigated their potential by using glycerol reforming in a continuous fixed-bed reactor under temperature 650 ^{o}C, atmospheric pressure, 35 wt% of crude glycerol solution with 0.1 ml/min flow rate combining with 15 ml/min CO_2 flow rate. The influence of acid treatment of rice husk catalyst using HCl and H_2SO_4 solutions was shown over 99.7% SiO_2 purity. Catalyst mixed ratio resulted the H_2/CO ratio 2.66, 2.58, 4.48, and 4.24, respectively. In addition, the potential for agricultural catalyst can decrease the catalyst cost resulting to reduce variable cost of bio-methanol synthesis from glycerol process 5.76, 11.52, 17.28, and 23.04%, respectively.
Keywords : Crude Glycerol, Rice husk catalyst, Reforming, Acid treatment, Catalyst mixed ratio

INTRODUCTION

In Thailand, biodiesel production has been promoted as an alternative fuel since 2005 that leads to supporting and increasing biodiesel production capacity every year. Generally, the transesterification reaction of triglycerides with methanol has crude glycerol as by-product. Previous researches have been considering viable processes for glycerol utilization because it can improve biodiesel industrial income.

Alternative technology of crude glycerol utilization had been studied such as hydrogen production by using photo catalysis process, catalytic reforming process, and biochemical conversion process: organic degradation process that used yeast or bacterial for fuel. Generally, crude glycerol is contaminated with other chemicals, it is expensive to purify for use in the food, pharmaceutical, or cosmetics industries. Methanol synthesis by reforming process of crude glycerol is the one of interested processes because world methanol demand is increasing every year which formaldehyde production is the majority consumption (HIS Markit, 2019). For Thailand methanol demand was consumed 0.855 million tons/year in year 2019 that up to 9.61% from previous years (Department of Industrial work, 2019). Base on biodiesel production, it found that 30% of methanol imported was used in biodiesel section and 70% for other application. Basically, glycerol can be transformed by two steps i) glycerol steam reforming and ii) methanol synthesis reaction. The first step, glycerol is converted to synthesis gas following glycerol steam reforming equation (1), glycerol decomposition equation (2), and water gas shift reaction equation (3).

$$C_3H_8O_3 + 3H_2O \leftrightarrow 3CO_2 + 7H_2 \quad (1)$$
$$C_3O_3H_8 \leftrightarrow 3CO + 4H_2 \quad (2)$$
$$CO + H_2O \leftrightarrow CO_2 + H_2 \quad (3)$$
$$CO + H_2 \leftrightarrow CH_3OH \quad (4)$$
$$CO_2 + 3H_2 \leftrightarrow CH_3OH + H_2O \quad (5)$$

The second step, synthesis gas is used as the primary feedstock for CO and CO_2 hydrogenation as shown in equation (4) and (5), respectively. Catalytic glycerol reforming process, the catalyst is a key factor for synthesis efficiency especially Ni-base catalyst is slightly expensive and effecting to glycerol reforming process. Therefore, some agricultural waste was applied for substituting Ni-base catalyst. Interesting agricultural wastes were investigated feasibility study and efficiency for reforming catalyst. Thailand generated abundant rice husk as agricultural waste which is potential for high grade silica producing (Adam F. et al., 2012 and Madduluri V.R. et al., 2020).

Therefore, this research will focus on rice husk by synthetic catalysts (rice husk) for substituting the Ni-base commercial catalysts. The potential of rice husk catalyst is investigated for reducing variable cost of bio-methanol synthesis from glycerol process in industrial scale.

MATERIALS AND METHODS

Materials

Crude glycerol feedstock was supported by Energy Absolute Pub. Co., Ltd (Thailand) which its composition consisted of glycerol (85.0%), methanol (2.2%) and other impurities (spent catalyst, ash and matter organic non-glycerol: 12.8%). Catalyst of synthesis gas production divided in two types of catalyst: as commercial catalyst (catalyst A) was obtained from Hutong Global Co., Ltd (China) and rice husk catalyst (catalyst B) was prepared by wetness impregnation method that using Nickel (II) nitrate hexahydrate from DAEJUNG Co., Ltd. (CAS NO. 13478-00-7) and rice husk from Phichit rice farm. Moreover, the glycerol steam reforming had used carbon dioxide (CO_2) as carrier gas that obtained from Thai Special Gas Co., Ltd. (Thailand).

Catalyst Preparation

The rice husk catalyst was prepared by wetness impregnation method. Initially, rice husk was washed with distilled water to remove particles and overnight drying at 383 K in an air oven. Then, acid leaching was applying clean rice husk by reflux boiling in HCl and H_2SO_4 at 353 K for 2 hours. The rice husk was filtered and washed by distilled water following overnight drying at 383 K. Pure amorphous white silica was obtained by burning at 873 K for 6 hours. After that, 3%Ni catalyst was prepared by white silica immersed in a Nickel (II) nitrate hexahydrate solution while stirring on a hot plate until complete dryness. The obtained catalysts were overnight drying at 383 K and calcined in air at 973 K for 4 hours.

Experimental Method

The glycerol steam reforming reactor was made from 304 stainless steel with the inside diameter of 16 cm and belonging dimension of 30 cm. The flow of carrier gas was controlled by mass-flow controller (Brooks, Model SLA5850) and Series II Isocratic HPLC pump (Scientific Systems, Inc) was used for glycerol solution feeding. The reactor was installed temperature control with K-type thermocouple for temperature measuring and controlling. The condition of the experiment was shown in Table 1 (5).

Table 1 Laboratory glycerol reforming experiment condition.

Reaction	Glycerol reforming
Feed flow rate	0.1 ml/min
Pre-heat	503 K
Carries Gas feed flow rate	15 ml/min
Reactor temperature	924 K
Crude glycerol	35 in distilled water basis %
Catalyst	13 g (catalyst A + catalyst B)

After reforming reaction, fluid product was sent to cyclone for removing contaminated solid. The fluid was cooled and liquid product was trapped by glycerol trap. Then, gas product was sent to analyze by gas chromatography (GC).

Characterization and Analysis

Rise husk and catalyst was characterized by using three instruments as following:

- X-ray fluorescence spectrometry (XRF): Pure amorphous white silica that derived from rice husk was characterized by using X-ray fluorescence spectrometry (XRF, FaBruker, Model S8 Tiger) instrument for element analysis.
- Scanning Electron Microscope (SEM): The Thermo Scientific Prisma E Scanning Electron Microscope (SEM) was used for scanning the integrity surface of pure white silica and catalyst.
- Surface area and Pore size analyser (BET): A Quantachrome Autosorp IQ instrument was measured by N_2 adsorption isotherm at -77.35 K and samples outgassing under vacuum at 573°C overnight.

Product Analysis

Gaseous product or synthesis gas was analyzed by online Gas Chromatograph (GC, Agilent Technologies 7890A) equipped with Thermal Conductivity Detector (TCD) and Flame Ionization Detector (FID).

Definitions

Silica Yield = weight of pure silica (g) / weight of rice husk (g) (6)

$$\text{Catalyst substitution percentage} = \frac{\text{Agricultural Catalysts from rice husk (g)}}{\text{Ni-base commercial catalyst (g)}} \quad (7)$$

RESULTS AND DISCUSSION

The effect of acid leaching for pure amorphous white silica

The preparations of pure amorphous white silica from rice husk had prepared with two types of acids leaching as i) 10% of sulfuric acid (H_2SO_4) and ii) 10% of hydrochloric acid (HCl). The results showed that the main product was pure silica or silicon dioxide (SiO_2) as detailed in Table 2. For H_2SO_4 acid leaching preparation, yields of pure silica was 15.45-16.12 wt.% with 99.69% of purity. Meanwhile, HCl acid leaching preparation exhibited higher yield and purity in range of 17.03-19.20 wt.% and 99.76%, respectively. The result is related with research that had studied silica from rice husk by using 3% of HCl and 10% of H_2SO_4 and results 95.14-99.66% of purity (Yalcin N., et al., 2001).

Table 2 Pure amorphous white silica by using acid leaching.

Acid Preparation	Yields (wt.%)	SiO_2 Purification (%)	Contaminant (wt.%)
10 %H_2SO_4	15.45-16.12	99.69	0.31
10 %HCl	17.03-19.20	99.76	0.24

In addition, SEM micrograph of amorphous white silica by HCl acid leaching preparation showed more regular geometry structure than silica by H_2SO_4 leaching preparation as shown in Figure 1. The particle size distribution was indicated in rage of 0.015-30 µm, and it is classified in macroporous silica.

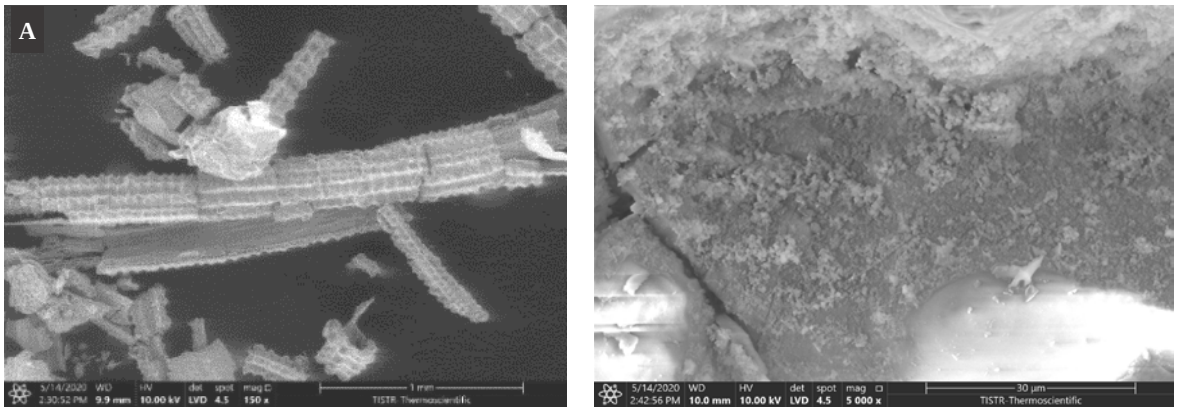

Figure 1. SEM micrograph of (a) H_2SO_4 acid leaching preparation.

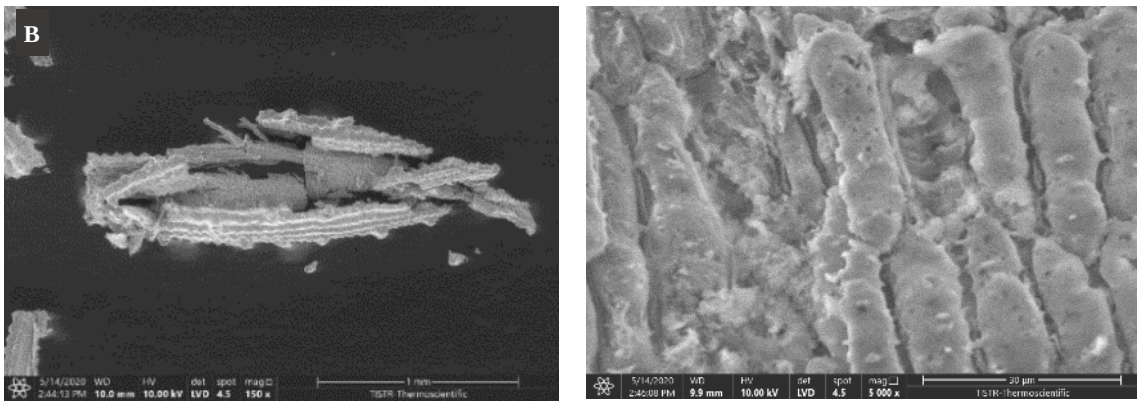

Figure 1. SEM micrograph of (b) HCl acid leaching preparation.

The pure amorphous white silica from calcination of rice husk was used as a support for Ni-base catalysts. The structure of Ni loading on amorphous white silica (catalyst B) by wetness impregnation method shown in Figure 2B. The SEM micrograph of catalyst B was more random size in geometry where while catalyst A had a regular particle as shown in Figure 2A.

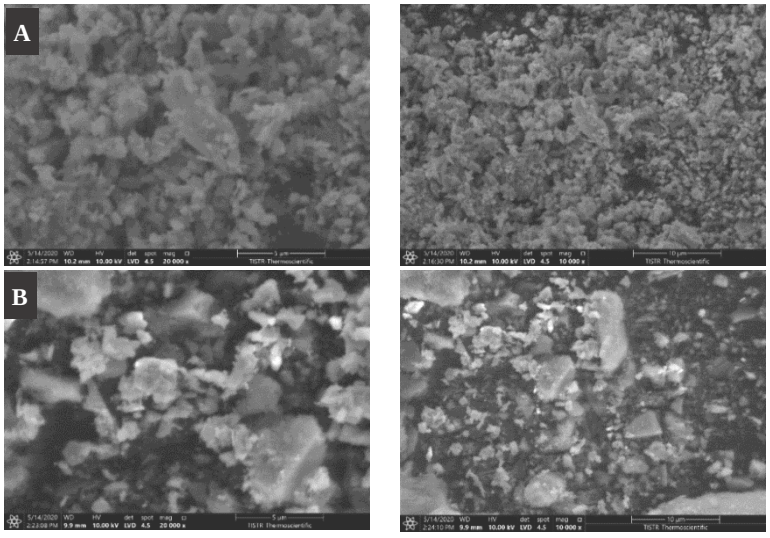

Figure 2. SEM micrograph of (a) Catalyst A (b) Catalyst B.

Surface area and pore size, the prepared rice husk silica was divided by using two different acid leaching HCl and H_2SO_4. HCl acid leaching was higher specific surface area and larger pore volume than silica obtained by H_2SO_4 acid leaching as detail in Table 3. In addition, pore diameter of silica from HCl and H_2SO_4 acid leaching was 5.11 x 10^{-3} and 6.05 x 10^{-3} µm, respectively.

Table 3 BET specific surface area, pore specific volume and diameter of rice husk samples.

Sample	Specific surface area (m^2/g)	Pore specific volume (cm^3/g)	Average pore diameter (µm)
Si from H_2SO_4	236.98	0.3584	6.05 x 10^{-3}
Si from HCl	1,893.93	2.4180	5.11 x 10^{-3}
Catalyst A	9.34	0.0444	1.91 x 10^{-2}
Catalyst B	208.48	0.3658	7.02 x 10^{-3}

Surface area after metal loading (catalyst B) were decreased approximately nine times comparing pure silica support (Si from HCl). Pore volume and average pore diameter were also reduced because of substituting on silica support by Ni metal.

The efficiency of agricultural materials catalyst

In this study, yields of synthesis gas were investigated by steam reforming process which catalytic conversion of glycerol by two type catalysts: i) Ni-base commercial catalyst (Catalyst A) ii) Agricultural Catalysts from rice husk (Catalyst B). These two catalysts were mixed in ratio of 25, 50, 75 and 100 percentage as following in equation (7).

The comparison of pure Catalyst A and Catalyst B, synthesis gas ratio was similar 4.31 and 4.42, respectively. The results were founded that the increasing of substitution percentage of catalyst B effected to the ratio of synthesis gas products (H_2/CO ratio). Replacement percentage of catalyst B by 25, 50, 75 and 100 were given H_2/CO ratio in 2.66, 2.58, 4.48 and 4.42, respectively. In addition, substituting catalyst B on catalyst A resulted in various products such as methane (CH_4) 0.4-2% and propane (C_3H_8) 0.52% as shown in Figure 3.

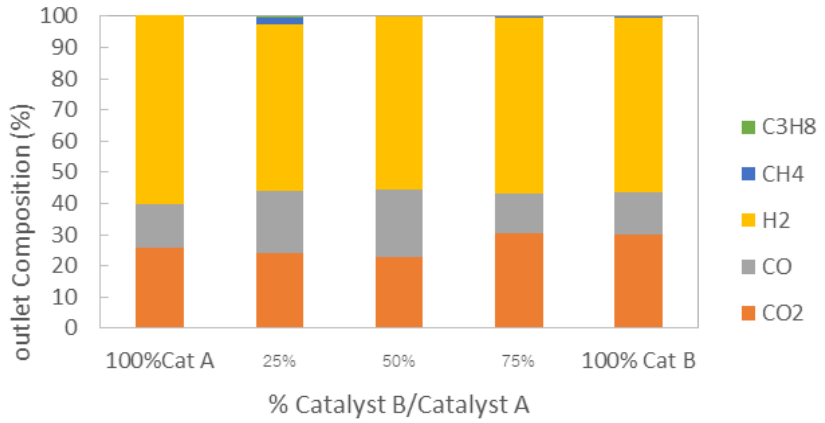

Figure 3. Composition of gas production from commercial Ni-base catalysts (Catalyst A) with agricultural materials (Catalyst B).

The potential for agricultural catalyst

Synthesis gas production from glycerol were used as the primary feedstock in the methanol synthesis process. Data obtained from laboratory experiment were combined with simulation in 26,000 kg/day of methanol production based on the previous simulation by Jitrwung et al., 2020. It resulted in variable cost that was divided by three main costs: raw material, energy and catalyst as shown in Table 4.

Table 4 Variable cost of methanol synthesis from crude glycerol.

Variable cost	USD/MT MeOH
Raw material	
Crude glycerol	132.72
Water	0.06
CO_2	15.24
Energy	
Electrical	72.19
Thermal	56.10
Catalyst	
Ni-base Catalyst	33.13
Cu/ZnO/Al_2O_3 Catalyst	23.42
Total variable cost	332.83

The possibility of cost reduction related to the catalyst cost. The price of Ni-base catalyst was 33.13 USD/MT MeOH and estimated 13.4% of total variable cost. In case of replacing Ni-base catalyst by rice husk catalyst by 25, 50, 75 and 100 % that variable cost can be reduced to 5.76, 11.52, 17.28 and 23.04%, respectively. Cost estimation of catalyst B was shown two sections which chemical and raw material as show in Table 5. and electricity costs as shown in Table 6.

Table 5 Chemical and raw material cost of agricultural catalyst from rice husk (catalyst B).

Chemical and raw material	USD/Kg catalyst
Rice husk	0.05-0.063
Hydrochloric acid	2.23-2.94
Distilled water	8.45
Nickel II (nitrate hexahydrate)	0.48-1.00
Total chemical and raw material cost	11.21-12.45

Table 6 Electricity costs of agricultural catalyst from rice husk (catalyst B).

Electricity costs		
Calcined pure white silica 873 K, 6h	21	unit
Furnace (3.5 kilowatt 250) 973K, 4h	14	unit
Total electricity	35	unit
Cost of electricity per unit	0.08-0.11	USD
Cost of electricity	2.912	USD/kg catalyst

The total cost of catalyst preparation (chemicals, raw materials and electricity) was price 14.43–15.36 USD per kilogram. As a result, the rice husk catalyst leads to the opportunity of using agricultural waste for catalyst in the methanol production from crude glycerol.

CONCLUSIONS

Rice husk is potential agricultural material for pure amorphous white silica which can be used as support for Ni-base reforming catalyst. The HCl acid leaching preparation gives the high yield and purity of silica however the catalyst synthesis needs the continuously improvement and development for techno-economic feasibility. The rice husk catalyst activity results 4.48 of H_2/CO ratio as same as H_2/CO ratio of commercial catalyst. For feasibility, the rice husk catalyst has efficiency for reducing variable cost of synthesis gas production by using glycerol steam reforming process in range of 5.76-23.04% by 25-100% substitution commercial catalyst.

ACKNOWLEDGEMENT

The authors would like to acknowledge the National Research Council of Thailand (NRCT) for the approval and financial support in this research.

REFERENCES

HIS Markit. 2019. Methanol: Emerging Global, Energy Markets, Methanol Institute.

Hazardous chemical. 2019. Petroleum Institute of Thailand, Department of Industrial work.

Adam, F., J. N. Appaturi and A. Iqbal. 2012. The utilization of rice husk silica as a catalyst: Review and recent progress, Catal. Today. 190: 2–14.

Madduluri, V. R., K. K. Mandari, V. Velpula, M. Varkolu, S. R. R. Kamaraja and M. Kang. 2020. Rice husk-derived carbon-silica supported Ni catalyst for selective hydrogenation of biomass-derived furfural and levulinic acid. Fuel. 261: 116339.

Yalcin, N. and V. Sevinc. 2001. Studies on silica obtained from rice husk. Ceram. Int. 27: 219-224.

Rujira, J., J. chalorngtham, K. Krekkeisakul, K. Suksumrit, M. Maneewuthiworasakul, A. Wannajumpa, R. Ramnita. 2020. Bio-methanol synthesis process from syngas derived from crude glycerol cooperation with CO_2, TIChe. 29: 197-203.

Radhika, T. and S. Suganan. 2006. Structural and catalytic investigateion of vanadia supported on ceria promoted with high surface area rice husk silica, J. Mol. Catal. A Chem. 250: 169-176

Aguiar, M., B. B. Cazula, L. M. S. Colpini, C. E. Borba, F. A. Siva, F. B. Noronha and H. J. Alves. 2019. Ai-MCM-41 obtains from different sources of silica and its application as support for nickel catalysts used in dry reforming of methane. Int. J. Hydrogen Energ. 44: 32004-32018.

O-EN3

FEASIBILITY STUDY OF CRUDE GLYCEROL REFORMING TO BIOMETHANOL

Kuntima Krekkeitsakul[1]*, Rujira Jitrwung[1], Rujiroj Tamnitra[2], Kamonrat Suksumrit[1], Mukrawee Maneewuthiworasakul[1], Jiraporn Chalongtham[1], and Anantachai Wannajampa[1]
[1] Expert Center of Innovative Clean Energy and Environment, Thailand Institute of Scientific and Technological Research (TISTR), Khlong Luang, Pathum thani 12120, Thailand
[2] Department of Chemical Engineering, Faculty of Engineering and Industrial Technology, Silpakorn University, Sanam Chandra Palace, Nakhon Pathom 73000, Thailand
*E-mail: kuntima@tistr.or.th

ABSTRACT
Crude glycerol is a valuable by-product obtained from biodiesel production process (transesterification of vegetable oils and fats with methanol in the presence of catalyst). In typically, biodiesel production generates about 10% (w/w) of glycerol which it is of low value and have impurities i.e. soap, methanol, ash, moisture etc. Therefore, crude glycerol must be purified before its applications (cosmetics, soap, and pharmaceuticals). There are various methods to upgrade crude glycerol; purification and reforming into valuable chemicals. Thus, this study was presented the reforming of crude glycerol into Biomethanol. The biomethanol as a methanol from bio-resources can be returned into biodiesel process resulting in circular economy. In this experiment, the feasibility study of variable cost for transforming crude glycerol to biomethanol (GTM) was compared with glycerol refinery process (GRP). In GTM process, 35% crude glycerol solution was run in a reforming reactor with temperature 650 °C and atmospheric pressure under commercial steam reforming catalyst obtaining syngas as a product. Next, the syngas was fed into the methanol synthesis reactor with 200 °C and 40 bar under methanol synthesis catalyst gaining 98% of biomethanol purity. The effects of economic feasibility had been studied in term of Net Present Value (NPV), Internal Rate of Return (IRR) and Payback period (PB), respectively. Base on this study, it was concluded that GTM was $ 0.39/Kg of crude glycerol comparing with glycerol refinery process spending $ 0.99/Kg of crude glycerol.
Keywords: Crude glycerol, Reforming, Biomethanol, Economic Feasibility

INTRODUCTION

Since the beginning of fossil fuel are depleted by environmental concerns, renewable energy is considered to be viable alternatives to conventional oil. Diesel is a kind of oil which is needed to substitute with renewable oil as biodiesel. Thailand government has set a target to replace by 30% of renewable fuel in 2036 and it is launched a policy that the conventional fuels should have an addition of at least 10% of Biodiesel (B10). Biodiesel is a mono alkyl ester of fatty acids obtained from vegetable oil or animal fats through esterification or transesterification reaction with alcohol (mostly methanol) in the presence of catalyst (NaOH, KOH or H_2SO_4) (Babajide, 2013) ; (Refaat, 2010) ; (Banerjee et al., 2014) ; (Zhang et al., 2015) ; (Neumann et al., 2016). The reaction is shown in Figure 1. (Nda-Umar et.al., 2019). The high production of biodiesel produces large volumes of glycerol as the major by product. Various literature have been reported that 10% of glycerol was generated from the total volume of biodiesel capacity. That means, for every 100 kg of biodiesel produced, 10 kg of glycerol is generated (Singhabhandhu et al., 2010) ; (Quispe et al., 2013). The rising demand of biodiesel will lead to surplus of glycerol, which is a low commercial value because of its low quality (Yazdani et al., 2007). Therefore, crude glycerol is necessary to be treatment into purify glycerol or other applications. There were several researches which attempted to convert glycerol into high value and useful products such as 1,3-propanediol (for production of polymer, cosmetic, food and pharmaceutical), acrolein also known as 2-propenal or acrylic aldehyde (for manufacture of paper) and hydrogen (via catalyst steam reforming, partial oxidation, autothermal reforming) (Fan et al., 2010).

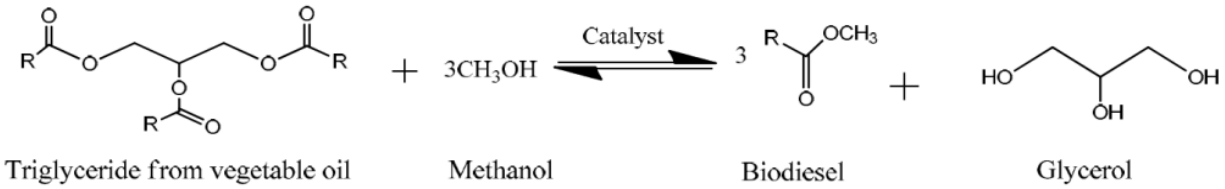

Figure 1. Conversion of glyceride to biodiesel and glycerol (Nda-Umar et al., 2019)

Crude glycerol obtained from biodiesel based is contained impurities such as alcohol, spent catalyst, ash, water, and fatty acid. The different processes create various impurities in crude glycerol with different purity, however it is generally contained from 60% to 70% (wt.) glycerol. The applications of crude glycerol are limited due to the presence of the salt and impurities and its fuel value is also with its current low market value (Comelli, 2011); (Gupta et al., 2012). To distribute crude glycerol in the market, crude glycerol is refined to more purity. Pure glycerol (> 99%) has a multitude of uses in pharmaceutical, cosmetic, and food industries. There are many techniques to purify crude glycerol such as distillation, membrane, filtration, chemical treatment, adsorption (using activated carbon), ion-exchange (using resin), extraction, decantation and crystallization which depending on glycerol resources. In generally, the distillation is used to remove water and methanol based on boiling point during glycerol purification. Distillation is a simple and efficient method to purify crude glycerol with high contents of salts and matter organic non-glycerol (MONG) (Katryniok et al., 2010).

The global glycerol market size was estimated at USD 3.04 billion in 2020 and was expected that reach to USD 3.5 billion by 2027 at an annual growth rate of 4.0%. In Thailand, the demand of refinery glycerol production was 0.127 MMT. (Food and Drug Administration, 2018) Purify glycerol was used in various applications such as drugs or pharmaceuticals, personal care, polyether, food, alkyd resins triacetin and others as shown in Figure 2 (Tan et al., 2013).

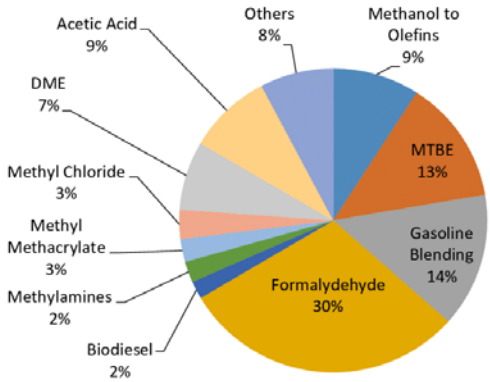

Figure 2. Glycerol industrial applications (Tan et al., 2013).

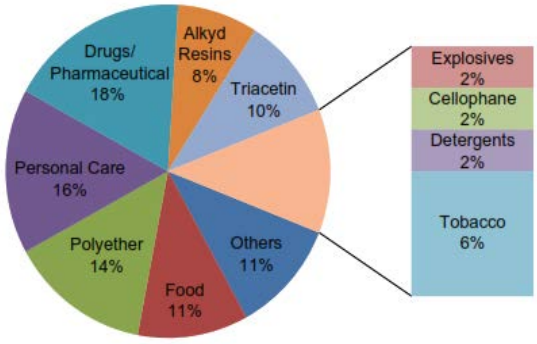

Figure 3. Methanol industrial applications (Matzen, 2015).

On the other side, crude glycerol can be converted into biochemicals such as “Biomethanol”. The biomethanol is methanol obtained from bio-resources and it can be returned into biodiesel process. There are two techniques carried out crude glycerol into methanol (GTM); (1) The solution of crude glycerol was soluble then used directly in the catalytic reaction to produce methanol and then (2) Crude glycerol was soluble and converted into synthesis gas (syngas) via reforming process. After that, the syngas was transformed to biomethanol. According to the direct glycerol to methanol in one step, process was gave various products mainly methanol and other alcohols. Hence, liquid product should be though separation before it is used. By the way, liquid product from reforming glycerol to methanol (GTM) yielded more purity of methanol. Methanol, as a basic chemical is mainly using for biodiesel and have many applications in traditional chemical derivatives and energy related such as formaldehyde, acetic acid, MTBE, DME, MTO as shown in Figure 3 (Matzen, 2015). Global methanol demand is rising an average of 5% to 6% each year by

63.96 MMT (2014), 92.30 MMT (2016), and forecasted 107 MMT (2023) (HIS Markit, 2017). (Jitrwung et al., 2019) Thus, this paper will focus only on indirect crude glycerol to biomethanol process which represented for GTM process.

The GTM process consists of two main steps: reforming of glycerol and methanol synthesis. First, glycerol can be digetesed and reformed to synthesis gas (syngas) which composing of carbonmonoxide (CO) hydrogen (H_2) and carbon dioxide (CO_2) by Steam reforming reaction (1) is glycerol and water reacting under steam reforming catalyst at 650 °C and 1 atm. The side reactions (2) - (6) might be occurred.

However, water gas shift reaction (7) can be appered to balance CO and CO_2 composition in syngas as a side reaction. Second, the CO or CO_2 are used to produce methanol under methanol synthesis catalyst at 170 °C and 40 bar. Methanol synthesis has occurred via two reactions: hydrogenation on carbon monoxide (8) and hydrogenation on carbon dioxide (9) (Bussche et al.,1996); (Skrzypek et al.,1991); (Snoeck et al.,1997).

Reforming reaction of glycerol;

Glycerol steam reforming:	$C_3H_8O_3+3H_2O$	↔	$3CO_2 + 7H_2$	ΔH = 123 kJ/mol	(1)
Glycerol decomposition:	$C_3H_8O_3$	↔	$3CO + 4H_2$	ΔH = 245 kJ/mol	(2)
Methanol reforming:	$CH_3OH+ H_2O$	↔	$CO_2 + 3H_2$	ΔH = 49 kJ/mol	(3)
Methanol decomposition:	CH_3OH	↔	$CO + 2H_2$	ΔH = 128 kJ/mol	(4)
Revert water gas-shift:	$CO_2+ H_2$	↔	$CO + H_2O$	ΔH = 41 kJ/mol	(5)
Methanation:	CO_2+4H_2	↔	CH_4+2H_2O	ΔH = -165 kJ/mol	(6)
Water gas-shift:	$CO + H_2O$	↔	$CO_2+ H_2$	ΔH = -41 kJ/mol	(7)

Methanol Synthesis;

CO Hydrogenation:	$CO + 2H_2$	↔	CH_3OH	ΔH = -90 kJ/mol	(8)
CO_2 Hydrogenation:	$CO_2 + 3H_2$	↔	$CH_3OH+ H_2O$	ΔH = -49 kJ/mol	(9)

The GTM process contained two reaction steps then GTM process diagram can be drawn as shown in Figure 4. Glycerol solution and CO_2 were fed into mixer1 and preheated until obtaining 650 °C, then reacted in Reforming reactor (RF). Fluid gas contained water and syngas came out and were reduced temperature by cooling water for separating water out and receiving syngas for next step .The syngas was compressed to reach pressure 40 bar, heated up to 170 °C, and was reaction in Methanol synthesis reactor (MS) Fluid products contained methanol and syngas were cooled and separated in M- Trap, then liquid methanol was drawn out and the syngas was given off or returning to the process.

The process feasibility and economic analysis are essential factors to conduct the view of research and industry. Aspen plus program is employed to obtain mass and energy balance for GRP and GTM process. The purpose of this article will be comparing the feasibility of crude glycerol upgrading not only glycerol refinery process (GRP) but also glycerol to biomethanol process (GTM) in case of economic factors, which are NPV, IRR and PB being reflection the opportunity in Thailand.

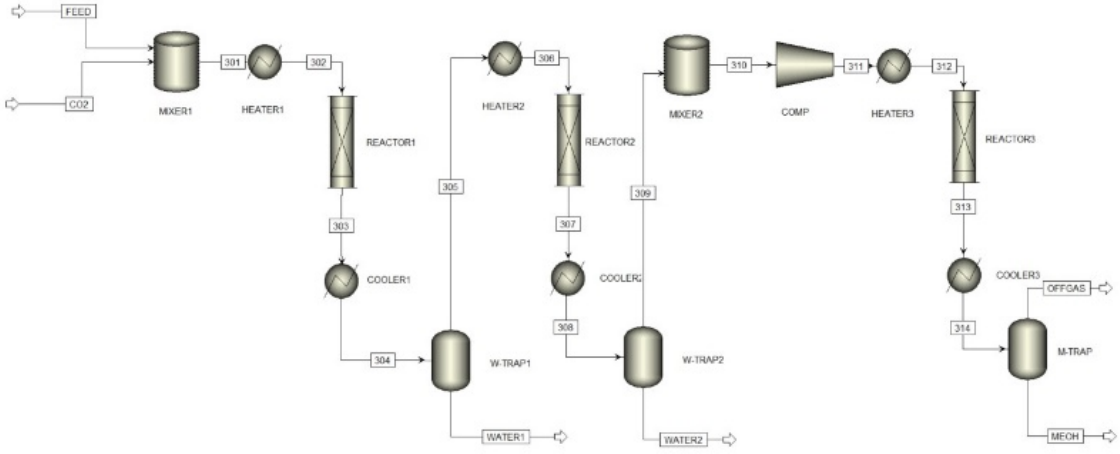

Figure 4. Process flow diagram of the crude glycerol reforming to biomethanol process. (Jitrwung et al., 2020)

MATERIALS AND METHODS

Data Collection

This study was compared 2 processes of crude glycerol application; (1) glycerol refinery process (GRP) data obtained from Arora et al., 2015 with kind permission and (2) glycerol to biomethanol process (GTM) process was collected information of Biodiesel process received from companies in Thailand (Crude glycerol with 80 %wt. of purity).

Data Analysis and Economic Feasibility

The above experimental data were used to design process simulation by Aspen Plus Software. After that, Excel program employed for Process economic evaluation (NPV, IRR, and PB). Basic economic calculation tools such as Net Present Value (NPV), Internal Rate of Return method (IRR) and Payback Period (PB) shown in the equation (10)-(12) (Benguerba et al., 2015); (Richardson et al.,1990).

$$NPV = \sum_{t=1}^{t} \frac{C_t}{(1+r)^t} - C_o \quad (10)$$

NPV =net present value r =Discount Rate

C_0 = initial investment t =duration

C_t = net cash flow over time

$$IRR = \left(\sum_{t=1}^{t} \frac{C_t}{(1+r)^t} - C_o\right) \quad (11)$$

Payback period = initial investment /net cash per year after tax (12)

RESULTS AND DISCUSSION

Glycerol - based biodiesel potential in Thailand

In 2020, biodiesel plants in Thailand, there are 13 registered companies, which were summarized in Table 1. The capacities were selected 3 sizes of biodiesel plants in Thailand which are 200,000, 500,000 and 1,000,000 L/D respectively, because the purpose of the distribution of three representatives for covering every capacity to predict the economic feasibility of glycerol to methanol. The data exhibited the biodiesel capacities, which were then evaluated quantities of raw materials (Triglycerides and methanol) and glycerol as a by-product in term of Kg/Day by using transesterification reaction composing with factory sample inquiry. The methanol was required over than 17% for completed reaction. As a result, the lowest row in Table 1 showed the average of each component which were biodiesel capacity 520 ton/day was produced from 575 ton/day of Triglycerides and 97 ton/day of methanol and generated 65 ton/day of 78.3% crude glycerol.

Table 1 Capacities of biodiesel plants (BD) in Thailand (2019).

No.	Biodiesel Capacity (L/D)	Biodiesel Capacity (Kg/D)	Triglycerides Used (Kg/D)	Methanol Used (Kg/D)	Crude glycerol 78.3% (Kg/D)
BD1	30,000	26,400	29,231	4,969	3,312
BD2	100,000	88,000	97,436	16,564	11,039
BD3	**200,000**	**176,000**	**194,872**	**33,128**	**22,079**
BD4	200,000	176,000	194,872	33,128	22,079
BD5	300,000	264,000	292,308	49,692	33,118
BD6	**500,000**	**440,000**	**487,179**	**82,821**	**55,197**
BD7	500,000	440,000	487,179	82,821	55,197
BD8	693,642	610,405	675,856	114,896	76,575
BD9	800,000	704,000	779,487	132,513	88,316
BD10	930,000	818,400	906,154	154,046	102,667
BD11	**1,000,000**	**880,000**	**974,359**	**165,641**	**110,395**
BD12	1,028,600	905,168	1,002,226	170,378	113,552
BD13	1,400,000	1,232,000	1,364,103	231,897	154,553
Total	**7,682,242**	**6,760,373**	**7,485,261**	**1,272,494**	**848,080**
Average	**590,941**	**520,028**	**575,789**	**97,884**	**65,237**

* BD = Biodiesel Plant

Crude glycerol to biomethanol process (GTM)

As mentioned previously, crude glycerol can be converted into value biochemical products. One of interesting product is “Biomethanol” cause of substituting methanol used in biodiesel process. This can encourage the green renewable energy from bio-resource from beginning to ending of process. Which are in consistent to the government policy and direction toward Bio-Circular-Green (BCG) Economy. Glycerol reformed into biomethanol via 2 steps following equation (1-9). The glycerol to biomethanol process design was referenced in Figure 4 then was computed and simulated by Aspen plus program. The material balance for each chemical was shown in Table 2. In this calculation, 3 biodiesel capacities were used as representative with size of small (200,000 L/day), medium (500,000 L/day) and large-scale (1,000,000 L/day). It was also resulted that amount of crude glycerol generating from the biodiesel process as of small, medium and large size of biodiesel capacity which generated crude glycerol 22,079, 55,197, and 110,395 kg/D respectively. These amounts of crude glycerol can produce 25,993, 64,982, and 129,965 kg/day of methanol (Table 2) which were compared 33,128, 82,821, and 165,641 kg/day of methanol requirement (Table 1). Biomethanol based glycerol was compensated in 78.46 % for methanol imported. However, the biodiesel process can normally recover 15% excess methanol from the process, the methanol may just be required 28,158, 70,398, and 140,795 kg/D for small, medium and large size of biodiesel capacity. Biomethanol would have an opportunity to compensate in 92.31% methanol consumption. It is also known that GTM process generated 1.17 kg methanol/kg crude glycerol.

Table 2 Material balance via 2 steps glycerol to methanol by Aspen plus.

Material Balance	BD3	BD6	BD11
Types	Small	Medium	Large
Biodiesel capacity	200,000	500,000	1,000,000
Crude Glycerol (kg/day)	22,079	55,197	110,395
Water (kg/day)	3,022	7,554	15,108
CO_2 (m^3/day)	12,669	31,673	63,347
MeOH (kg/day)	25,993	64,982	129,965
MeOH/ kg of crude glycerol	1.17	1.17	1.17

* BD = Biodiesel Plant

Table 3 Economic assumption and data simulation of crude glycerol to biomethanol (GTM).

Raw materials	USD /ton methanol
Crude glycerol (156.25 USD/ton)	13.28
Water (0.469 USD/ton)	0.05
CO_2 (0.031 USD/m^3)	15.31
Energy	
Heating (3.63 x 10^{-5} USD/kcal)	56.25
Electricity (78.13 USD/MWh)	72.19
Catalysts	
Steam Reforming Catalyst (18.75 USD/kg)	33.13
Methanol Synthesis Catalyst (17.09 USD/kg)	23.44
Total Variable cost	332.83
Products	
Methanol Price (USD/ton)	375
Depreciation (year)	20
Demand growth rate (%)	1.0%
Price growth rate (%)	2%
Incremental fixed costs (USD)	6250
SG&A growth rate (%)	1.0%
WACC (or interest rate) (%)	7.0%
Tax Rate (%)	20%
Cash conversion cycle (CCC) (Day)	50
Employees cost growth rate (%)	5.3%
Annual maintenance cost (%)	2.0%

Table 4 Feasibility result of crude glycerol to biomethanol (GTM).

Items	Unit	BD3	BD6	BD11
Types		Small	Medium	Large
Biodiesel capacity	L/day	200,000	500,000	1,000,000
Crude Glycerol	kg/day	22,079	55,197	110,395
Water	kg/day	3,022	7,554	15,108
CO_2	m^3/day	12,669	31,673	63,347
MeOH	kg/day	25,993	64,982	129,965
Economic Analysis				
Variable Cost	USD/kg	0.332	0.332	0.332
Fixed Cost	USD	5.40 M	8.94 M	13.08 M
NPV	USD	-0.68 M	6.24 M	20.04 M
IRR	%	6.0%	11.8%	16.2%
PAYBACK PERIOD	years	14.02 y	9.99 y	7.94 y

* BD = Biodiesel Plant

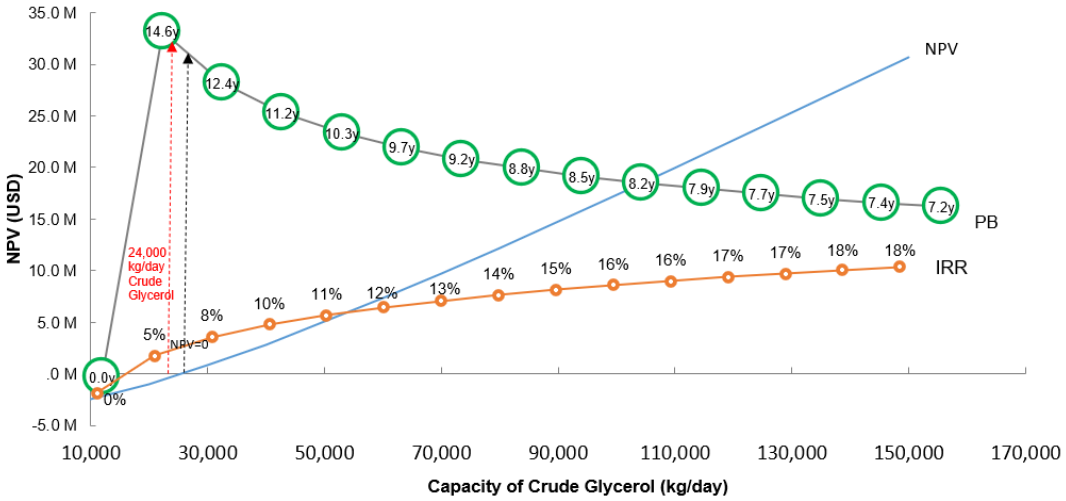

Figure 5. The sensitivity of crude glycerol for methanol production versus NPV, IRR and PB (Jitrwung et al., 2020).

The feasibility of GTM process were evaluated under economic assumption and simulation data shown in Table 3. The economic assumption inputs were based on the present situation (2020) and were simulated in data computation for the three biodiesel capacities as resulted in Table 4. It was found that the small size was negative NPV (-0.68 million USD, MUSD), but medium and large size were positive NPV as 6.24 MUSD and 20.04 MUSD respectively. It means that the small biodiesel capacities (200,000 L/day) were not economic for transforming crude glycerol to methanol, but medium and large were appropriate and obtaining IRR 11.8 % and 16.2 % also returning for PB were 9.99 and 7.94 years respectively. Moreover, the sensitivity of crude glycerol for methanol production was step 10,000 kg/day until 150,000 kg/day versus NPV, IRR and PB shown in Figure 5. The result detailed that the positive NPV started when crude glycerol was over than 26,000 kg/day. Whenever NPV reached positive, the IRR was 7% to 18% and PB returned 13 to 7.2 years from 26,000 kg/day to 150,000 kg/day crude glycerol.

Glycerol Purification Process (Arora et al., 2015).

The process for glycerol purification in this reference was compared two techniques (1) distillation process and (2) membrane separation process. In this work, the data obtained from (Arora et al., 2015) used simulated concentration of crude glycerol (50 %glycerol, 35 %methanol, 10 %potassium hydroxide, and 5 %methyl oleate) and reported two techniques for 24,000 kg/day of crude glycerol refiner

The vacuum distillation process was shown in Figure 6 .Crude glycerol input and sulfuric acid stream were mixed and heated up to 130 °C by passing through a heat exchanger, then the mixed stream was

flashed. The upper stream was flashed out in Flash 1 containing methanol and water. The lower stream was continually flashed in Flash 2. The lower stream of Flash 2 contained salt and the upper stream contained glycerol and FAME. The stream (GLY+FAME) was then sent to a vacuum distillation then glycerol come out from the top of distillation column and cooled down. The streams of crude glycerol, sulfuric acid and product glycerol of the vacuum distillation was shown in Table 5 (a).

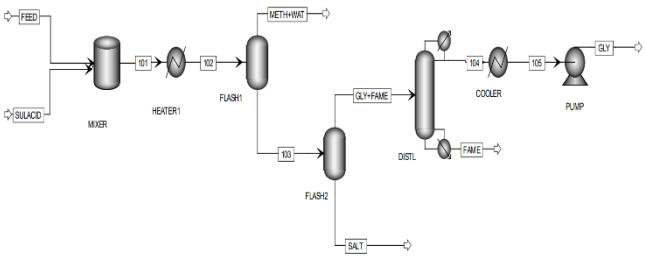

Figure 6. Flowsheet for Vacuum Distillation Process (Arora et al., 2015).

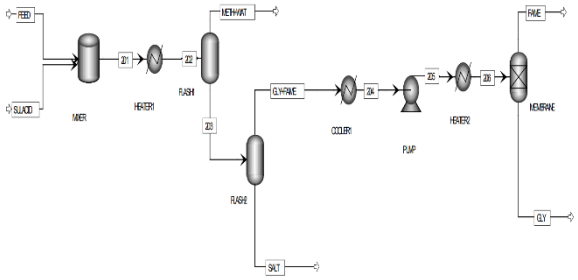

Figure 7. Flowsheet for membrane separation process (Arora et al., 2015).

The membrane separation process was shown in Figure 7. Crude glycerol input and sulfuric acid stream were processed the same as vacuum distillation technique (Figure 6) until receiving glycerol and FAME coming out the upper stream of Flash 2. The stream (GLY+FAME) was then passed through a cooler to reduce the stream temperature until obtaining liquid phase and then pumped to a heat exchanger to reach pressure 5 atm. for operating in a membrane separator. The top stream contained rich in FAME and the bottom contained rich in glycerol. The streams of crude glycerol, sulfuric acid and product glycerol of the membrane separation was shown in Table 5 (b).

Arora P. and research team summarized that (58.76%) IRR of membrane technique had better than IRR (51.12%) of vacuum distillation and had less environment impact. They also concluded that the selling price of purified glycerol should be $1.98/kg.

Table 5 Feed and product stream information for the vacuum distillation process (a) and membrane separation process (b) (Arora et al., 2015).

Items	Crude glycerol	Sulfuric acid	Product Glycerol (a)	Product Glycerol (b)
Temperature ˚C	25	25	25	25
Pressure (kPa)	101.32	101.32	101.32	101.32
Molar flow (kmol/h)	24.10	10.99	4.76	4.76
Mass flow (kg/h)	1200	283.78	436.90	436.90
Component mass fraction				
Methanol	0.35	0	0.00047	0.00047
KOH	0.1	0	0	0
H_2SO_4	0	0.37	$3.60x10^{-8}$	0
Glycerol	0.5	0	0.99	0.99
Water	0	0.63	0.00072	0.00072
FAME	0.05	0	$3.61x10^{-8}$	$3.61x10^{-8}$

Compare GRP and GTM process

The simulation data obtained from the vacuum distillation (VD) and membrane separation (MS) process were detailed for properly unit operations then calculated for sizing and brought about unit cost estimation which were compared with the GTM process. Therefore, the economic feasibility calculation based on 1,000 kg/h or 24,000 kg/D of crude glycerol for three techniques were compared in Table 6. NPV of the three processes (VD, MS, and GTM) were shown as 15.32, 16.31, and -0.33 MUSD, respectively. However, GTM showed negative when size of crude glycerol was 24,000 kg/day, it was positive when NPV was over 26,000 kg/day as previous mentioned in item 3.2. By the way, MS process was required 0.99 USD

for refinery crude glycerol to purify glycerol, but GTM process was just spent 0.39 USD for transforming crude glycerol to methanol.

Table 6 The economic feasibility in terms of NPV, IRR and PB of the GTM process compared with Vand MS process by using crude glycerol 24,000 kg/D.

Economic Feasibility	Arora et al. (2015), with kind permission		This work	
	Refinery Process by Vacuum distillation (VD)	Refinery Process by Membrane (MS)	Glycerol to Methanol (GTM)	
Crude glycerol (kg/D)	24,000	24,000	24,000	26,000-150,000
Net Present Value (NPV) (millions US)	15.32	16.31	-0.33	0 to 30.7
Internal rate of return (IRR)%	51.12	58.76	6.50	7 to 18
Discounted Payback Period (DPBP) (years)	1.6	1.4	13.54	13 to 7.2
Cost ($ US/ kg crude glycerol)	N/A	0.99	0.39	0.39

CONCLUSIONS

This work was studied of transforming crude glycerol to methanol (GTM) comparing with refinery crude glycerol by vacuum distillation (VD) and membrane separation (MS). The VD and MS process were carried out 24,000 kg/D of crude glycerol and obtaining higher IRR % 51.12 and 58.76, respectively. This previous work (VD and MS) carried on ideal simulation raw material of 50% pure glycerol mixed with other components. However, this work (GTM) was experimented by real crude glycerol sponsoring by private biodiesel factory, then the experimental data was used in simulation for scaling up. The economic feasibility showed IRR 7% to 18% and PB returned 13 to 7.2 years from 26,000 kg/day to 150,000 kg/day of crude glycerol. Refinery glycerol by MS process was required 0.99 $ US/ kg of crude glycerol comparing with methanol production by GTM process was just spent 0.39 $US/ kg of crude glycerol. Furthermore, the result of this study exhibited that an opportunity of crude glycerol application not only directly purify but also convert to biomethanol. It can be encouraged biodiesel industry to replace imported methanol for biodiesel production as well as supported Bio-Circular-Green Economy.

ACKNOWLEDGEMENT

The authors would like to acknowledge the National Research Council of Thailand (NRCT) for the approval and financial support in this research. We also appreciate Energy Absolute Public Company Limited (EA) to provide raw material as well as Biodiesel plants in Thailand gave the information for this research.

REFERENCES

Arora, P., C. Baroi and A. K. Dala. 2015. Feasibility study of glycerol purification process. J. Basic and Applied Engineering Research. 2: 60-63.

Babajide, O. 2013. Sustaining biodiesel production via value-added applications of glycerol. J. Energy. 178356.

Banerjee, N., R. Ramakrishnan and T. Jash. 2014. Biodiesel production from used vegetable oil collected from shops selling fritters in Kolkata. Energy Procedia. 54: 161-165.

Benguerba, Y., L. Dehimi, M. Virginie, C. Dumas and B. Ernst. 2015. Modelling of methane dry reforming over Ni/Al_2O_3 catalyst in a fixed-bed catalytic reactor. Reaction Kinetics, Mechanisms and Catalysis. 114: 109-119.

Comelli, R. A. 2011. Glycerol, the co-product of biodiesel :One key for the future bio-refinery. In Biodiesel-Quality, Emissions and By-Products; InTech : Rijeka, Crotia.

Fan, X. H., R. Burton. and Y. C. Zhou. 2010. Glycerol (byproduct of biodiesel production) as a source for fuels and chemicals-mini review. The Open Fuels and Energy Science Journal. 3: 17-22.

Food and Drug Administration. 2018. http//:thaiteci.com/chemicals.php .

Gupta, M and N.Kumar. 2012. Scope and opportunities of using glycerol as an energy source. Renew. Sustain. Energy Rev.16: 4551- 4556.

HIS Markit . 2017. Chemical Economics Handbook (CEH).

Jitrwung, R., K. Krekkeitsakul, K. Leeheng, R. Tamnitra and J. Chalongtham. 2019. Intergrated economic analysis of agricultural waste-biogas to inverstment of bio-methanol industry. 87-94

Katryniok, B., S. Paul., V. Bellier-Baca and P. Rey. 2010. Dumeigni F. Glycerol dehydration to acrolein in the context of new uses of glycerol. Green Chemitry.12: 2079-98.

Matzen, M. 2015 .Sustainability Assessment for Energy Systems and Chemical Process Industries . Chemical & Biomolecular Engineering Theses, Dissertations, & Student Research. Paper 27.

Nda-Umar, U. I., I. Ramli., Y. H. Taufiq-Yap and E. N, Muhamad. 2019. An Overview of REscent Research in the Conversion of Glycerol into Biofuels, Fuel Additives and other Bio-Based Chemicals. Catalyst. 15.

Neumann, K., K. Werth, A. Martin and A. Grak. 2016. Biodiesel production from waste cooking oils through esterification :Catalyst screening, chemical equilibrium and reaction kinetics. Chem. Eng.Res. Des.107: 52-62.

Quispe, C. A., C. J. Coronado and J. A. Carvalhor. 2013. Glycerol: Production, consumption, prices, characterization and new trends in combustion. Renew. Sustain. Energy Rev. 27: 475-493.

Refaat, A. 2010. Different techniques for the production of biodiesel from waste vegetable oil. Int. J. Environ. Sci .Technol. 7: 183-213.

Richardson, J. T. and S. A. Paripatyadar.1990. Carbon dioxide reforming of methane with upported rhodium. Applied Catalysis. 61: 293-309.

Singhabhandhu, A and T. Tezuka. 2010. A perspective on incorporation of glycerin purification process in biodiesel plants using waste cooking oil as feedstock. Energy. 35: 2493-2504.

Skrzypek, J., M. Lachowska and H. Moroz. 1991. Kinetics of methanol synthesis over commercial copper/zinc oxide/alumina catalysts. ChEnS. 46: 2809-2813.

Snoeck, J. W., G. F. Froment and M. Fowles. 1997. Kinetic study of the carbon filament formation by methane cracking on a nickel catalyst. J .Cat. 169: 250-262.

Stamatelatou, K. 2011. Advanced oil crop biorefineries. Cambridge :RSC.

Tan, H. W., A. R. Abdul Aziz and M. K. Aroua. 2013. Glycerol production and its applications as a raw material : A review. Renewable and Sustainable Energy Reviews. 27:118-127.

Yazdani, S. S. and R. Gonzalez. 2007. Anaerobic fermentation of glycerol: A path to economic viability for the biofuels industry. Curr. Opin. Biotechnol. 18: 213-219.

Zhang, F., Z. Fang and Y. T. Wang. 2015. Biodiesel production direct from high acid value oil with a novel magnetic carbonaceous acid. Appl. Energy. 155: 637-647.

Poster

EN-P001

ADEVELOPMENT OF A NEAR-INFRARED SPECTROSCOPIC ANALYSIS METHOD TO EVALUATE SUGARCANE GERMPLASM RESOURCES FOR MAJOR CHEMICAL COMPONENTS

Sumaporn Kasemsumran[1]*, Sunee Jungtheerapanich[1], Kraireuk Ngowsuwan[1], and Satoru Miyata[2]
[1] Laboratory of Non-destructive Quality Evaluation of Commodities, Kasetsart Agricultural and Agro-Industrial Product Improvement Institute (KAPI), Kasetsart University, Bangkok 10900, Thailand
[2] Japan International Research Center for Agricultural Sciences, Tsukuba 305-8686, Japan
*E -mail: aapspk@ku.ac.th

ABSTRACT
In this study, near-infrared (NIR) spectroscopy was employed to determine cellulose in terms of glucan, hemi-cellulose in terms of xylan, and lignin contents in sugarcane bagasse as biomass for energy purpose utilization. 20 simulated samples prepared by mixing of 3 standard biomasses were prepared in many ratios to expand the range of contents for those analyzes, 47 sugarcane bagasse samples of wild species and their hybrids were obtained from Khon Kaen and others, and 70 sugarcane bagasse samples were collected from various sugar factories in Thailand. All samples were measured in the NIR region of 1100 – 2500 nm. Partial least square (PLS) regression models for the quantitative determination of glucan, xylan, and lignin contents in sugarcane bagasse samples were calculated from data of NIR spectra and of analyzed contents detected by reference methods. The best PLS calibration models for cellulose (correlation coefficient (R)=0.94; root mean squared error of prediction (RMSEP) =4.34%), xylan (R=0.88, RMSEP=1.50%) and lignin (R=0.94, RMSEP=2.11%) in sugarcane bagasse samples obtained from the model using real bagasse samples, in which they developed from multiplicative scattering correction (MSC), 2nd derivative and 2nd derivative pretreated spectra, respectively. This study shows that NIR spectroscopy can be used to predict the necessary chemical constituents of sugarcane bagasse prior to converting biomass to substitute energy with fast detecting and reducing the use of chemicals.
Keywords: Near-infrared, Biomass, Cellulose, Lignin, Sugarcane bagasse

INTRODUCTION

The sugarcane is a member of the Gramineae (Poaceae) family, tribe Andropogenae and the genus Saccharum, which is the most substantial harvest for sugar production and energy production. In Thailand, the industry of sugarcane production growth to 127 million metric tons per year and become the world's second-largest sugar exporter (Ratanasumarn and Chitprasert, 2020). Biomass from sugarcane production can be divided into top trashier and bagasse. However, the sugarcane mill produces a lot of bagasse as residue, in which it is easy to collect and deliver to a renewable energy factory. Therefore, bagasse has a high potential to utilize as renewable source of energy. There are many advantages to generating bioenergy using bagasse when compared to fossil fuels, including lower greenhouse gas emissions, energy cost savings and waste management**.** Bagasse can be converted into electricity through several methods. In a direct combustion system, bagasse is burned in a furnace to generate heat, which is then fed into a boiler to generate steam used to generate power (Khaenson, 2018). Sugarcane bagasse is used to produce power as a fuel to generate electricity and to produce ethanol, (Dias et al., 2012; Espirito Santo et al., 2018). Chemical compositional changes in sugarcane bagasse are subjected to different resources and their impacts on the conversion process to bioenergy. Therefore, it is necessary to know the chemical composition of sugarcane bagasse. The conventional methods used to determine the chemical composition of bagasse are combined with a several methods such as the chemical extraction and CHONS analyser, in which these methods are time-consuming, expensive, labor-intensive and not practically feasible for the analysis of large populations of samples. On the other hand, near-infrared (NIR) spectroscopy is a powerful technique owing to rapid analysis, non-destructive, and minimal sample preparation. For example, NIR has

been used for predicting soluble sugars in sugarcane, the fibre content of sugarcane stalk, stalk soluble sugar, bagasse hydrolyzed sugar (Phuphaphud et al., 2019; Wu et al., 2015).

However, no research attempt has been made to determine cellulose (glucan), hemicelluloses (xylan), and lignin contents in sugarcane bagasse using NIR. Hence, the objective of this research is to demonstrate the possibility to employ NIR spectroscopic method for the determination of glucan, xylan, and lignin contents in sugarcane bagasse. This process could be further associated with bio-ethanol productivity by sugarcane germplasm.

MATERIALS AND METHODS

Sample preparation

Three groups of sugarcane bagasse samples were employed in this study. One was the simulated samples prepared by mixing of cellulose and xylan from birch wood and lignin powder from beech wood in many ratios to expand the range of contents for those three analyzed, the second was the samples obtained from wild species and their hybrids obtained from Khon Kaen and others and the last one was the samples collected from various sugar factories in Thailand. The sugarcane bagasse samples were dried, ground, and sieved. Before NIR measurement, the samples were again ground with a Cyclotec 1093 (FOSS) to obtain the regular size of the sample.

Chemical analysis

Samples were packed in a closed cup for the powder sample. The NIR spectra were recorded by the InfraAlyzer 500 (BRAN+LUEBBE) spectrometer in the region of 1100-2500 nm, at 2 nm resolution. Each sample was scanned triplicate and the averaged NIR spectral data were used for data analysis.

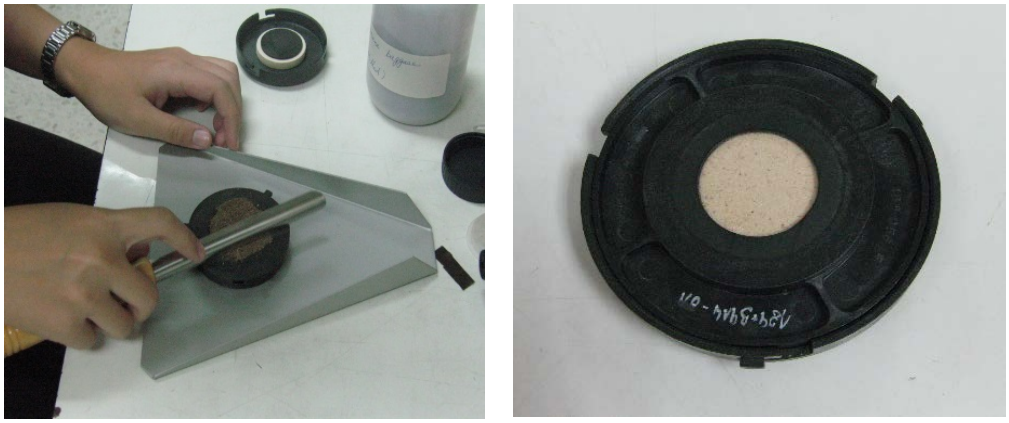

Figure 1. Sample preparations for NIR measurement.

Reference analysis

The contents of glucan and xylan were determined by using the method of the US National Renewable Energy Laboratory (Sluiter et al., 2008). The quantitative analysis method for lignin content was the Acetyl bromide method (Iiyama and Wallis 1989). The distribution contents of glucan, xylan, and lignin in three groups of samples are shown in Table 1.

Data analysis

The NIR spectra were pretreated with 2nd derivative and multiplicative scatter correction (MSC) before developing the calibration models and then do the comparisons. Calibration models were calculated by the partial least square regression (PLSR) method and validated by a separate test set of samples using Unscrambler (Ver. 9.8). Two calculation types were carried out, type I consisted of 100 samples from groups of A, B, and C for a calibration set and 37 samples from a group of C for a prediction set, in which they were randomly selected. Type II contained 80 samples from groups of B and C for a calibration set and employed the same samples as type I for prediction set. Table 2 shows the distribution of glucan, xylan, and lignin contents in the samples for the calibration set and prediction set. Note that the maximum and minimum contents of analysts were kept in the calibration set.

Table 1 Distribution of the analyze contents in the sugarcane bagasse sample for three groups.

Sample group	Analyze	Min (%)	Max (%)
mixing standard samples (n=20)	Glucan	14.82	35.16
	Xylan	14.84	30.00
	Lignin	35.14	64.84
wild species and their hybrids (n=47)	Glucan	11.82	42.81
	Xylan	7.74	26.15
	Lignin	7.08	23.15
sugarcane bagasse from sugar factories (n=70)	Glucan	34.90	47.53
	Xylan	17.20	26.95
	Lignin	17.20	28.30

Table 2 Distribution of the analyze contents in the sugarcane bagasse samples for model development.

Type	Sample group	Analyze	Min (%)	Max (%)
I	Calibration ABC (n=100)	Glucan	11.82	47.53
		Xylan	7.74	30.00
		Lignin	7.08	64.84
	Prediction C (n=37)	Glucan	35.00	47.08
		Xylan	19.30	26.20
		Lignin	18.40	27.13
II	Calibration BC (n=80)	Glucan	11.82	47.53
		Xylan	7.74	26.95
		Lignin	7.08	28.30
	Prediction C (n=37)	Glucan	35.00	47.08
		Xylan	19.30	26.20
		Lignin	18.40	27.13

RESULTS AND DISCUSSION

Figure 2 shows a second derivative spectrum of averaged sugarcane bagasse samples. The O-H stretching bands clearly showed at 1430 and 1916 nm. The assignment for cellulose peaks at 2275 and 2334 nm corresponding to O-H/C-O in glucose molecule and C-H stretching/CH2 deformation combination in polysaccharide structure, respectively. The band at 1670 nm, which arises from C-H aryl in the aromatic structure was varied with the percentage of lignin. The other peak at 1370 nm relates to the C-H vibration of the methyl group (Workman and Weyer, 2007). The statistical results of PLS calibration models for determination of glucan, xylan, and lignin content in sugarcane bagasse obtained by different pretreated NIR spectral data for calculation types I and II were compared in Tables 3 and 4, respectively. The highest predictive performance of the PLS model was selected by considering a model that yielded the lowest values of root mean square error of prediction (RMSEP), the bias of prediction. In calculation type I, the best PLS calibration models for glucan, xylan, and lignin in sugarcane bagasse samples were developed from MSC pretreated spectra using factor numbers of 7, 10, and 6, respectively. As for calculation type II, the best PLS calibration models for glucan, xylan, and lignin in sugarcane bagasse samples were developed from MSC pretreated spectra (6-factor number), 2nd derivative pretreated spectra (8-factor number) and 2nd derivative pretreated spectra (3-factor number), respectively. These models yielded the lowest RMSEP (type I: glucan 4.53%; xylan 1.64%; lignin 2.74%, type II: glucan 4.34%; xylan 1.50%; lignin 2.11%) and bias values with high correlation coefficient (R) (Tables 3 and 4).

The difference between calculation types of I and II was that types I contained a set of simulated samples which was prepared by mixing standard powder of glucan, xylan, and lignin. They were not authentic sugarcane bagasse. The ranges of analyst content were expanded by including a simulated sample set, in which illustrated the developed model with higher R-value than those obtained from models in calculation type II. However, the RMSEP values obtained from the best models in type I were higher than

those obtained from the best models in type II. It was maybe that the matrix of the simulated sample was different from the authentic sugarcane bagasse sample, which may raise the prediction error. Therefore, the best PLS calibration models for prediction glucan, xylan, and lignin content in bagasse were obtained from type II with the lowest RMSEP value, in which all samples in type II were only authentic sugarcane bagasse.

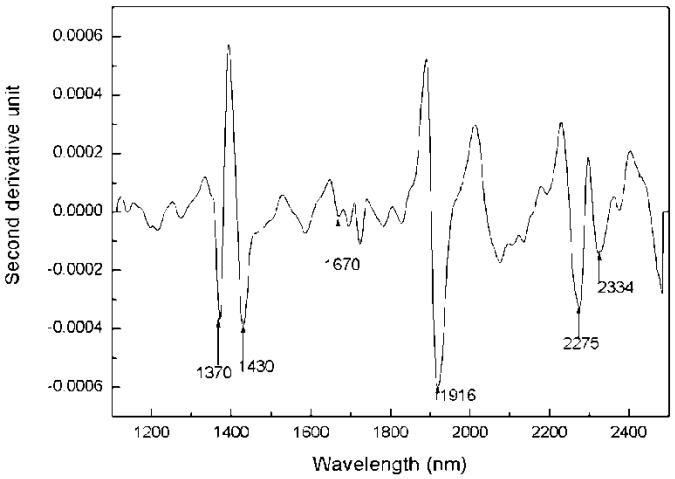

Figure 2. A second derivative spectrum of sugarcane bagasse samples in the region of 1100 – 2500 nm.

Table 3 PLS calibration results of calculation type I for predicting contents of glucan, xylan, and lignin in sugarcane bagasse samples.

Analyze	Pretreatment	F	Calibration			Prediction	
			R	RMSEC (%)	Bias (%)	RMSEP (%)	Bias (%)
Glucan	Original	4	0.90	4.20	-1.53×10^{-7}	4.72	-1.11
	MSC*	7	0.93	3.41	-1.11×10^{-6}	4.53	-0.10
	2nd Derivative	4	0.90	4.06	-6.29×10^{-7}	4.68	-0.83
Xylan	Original	13	0.90	1.83	-1.92×10^{-5}	2.04	0.49
	MSC*	10	0.88	1.97	-4.31×10^{-6}	1.64	0.23
	2nd Derivative	7	0.88	1.94	1.34×10^{-7}	1.69	0.42
Lignin	Original	5	0.98	3.16	2.07×10^{-6}	4.08	-1.54
	MSC*	6	0.99	2.42	5.00×10^{-6}	2.74	-0.38
	2nd Derivative	4	0.98	2.81	6.39×10^{-7}	2.98	-0.68

F: factor number, RMSEC: root mean squared error of calibration, RMSEP: root mean squared error of prediction,
*: selected model

Table 4 PLS calibration results of calculation type II for predicting contents of glucan, xylan, and lignin in sugarcane bagasse samples.

Analyze	Pretreatment	F	Calibration			Prediction	
			R	RMSEC (%)	Bias (%)	RMSEP (%)	Bias (%)
Glucan	Original	8	0.95	3.04	5.38×10^{-6}	4.41	-0.40
	MSC*	6	0.94	3.22	1.13×10^{-9}	4.34	-0.51
	2nd Derivative	4	0.92	3.82	2.02×10^{-6}	4.61	-1.16
Xylan	Original	11	0.88	1.75	4.34×10^{-6}	1.84	0.02
	MSC	9	0.86	1.87	-6.76×10^{-6}	1.85	-0.10
	2nd Derivative*	8	0.88	1.71	1.55×10^{-7}	1.50	0.02
Lignin	Original	4	0.94	1.97	-1.15×10^{-7}	2.44	-0.74
	MSC	3	0.94	1.93	-4.41×10^{-7}	2.56	-0.81
	2nd Derivative*	3	0.94	1.94	-1.43×10^{-7}	2.11	-0.38

F: factor number, RMSEC: root mean squared error of calibration, RMSEP: root mean squared error of prediction,
*: selected model

CONCLUSIONS

In this study, we have demonstrated the possibility to employ NIR spectroscopic method for the quantitative determination of glucan, xylan, and lignin in sugarcane bagasse. The PLS calibration models developed from pretreated NIR spectra (MSC for glucan and 2nd derivative method for xylan and lignin) of real sugarcane bagasse in the whole NIR region provided the best predictive performance with high correlation and lowest RMSEP values of 4.34, 1.50 and 2.11% for glucan, xylan and lignin predictions, respectively. These developed calibration models are recommended to employ for quantitative analysis of the unknown samples with the range of those calibration set for glucan of 11.82-47.53%, xylan of 7.74-26.95% and lignin of 7.08-28.30%.

ACKNOWLEDGEMENT

We grateful to thank Japan International Research Center for Agricultural Sciences to support research funding and coordination, and to Khon Kaen Field Crops Research Center for their support for samples.

REFERENCES

Dias, M. O. S., T. L. Junqueira, O. Cavalett, M. P. Cunha, C. D. F. Jesus, C. E. V. Rossell, R. M. Filho and A. Bonomi. 2012. Integrated versus stand-alone second generation ethanol production from sugarcane bagasse and trash. Bioresour. Technol. 103: 152-161.

Espirito Santo, M., C. A. Rezende, O. D. Bernardinelli, N. Pereira Jr., A. A. S. Curvelo, E. R. deAzevedo, F. E. G. Guimarães and I. Polikarpov. 2018. Structural and compositional changes in sugarcane bagasse subjected to hydrothermal and organosolv pretreatments and their impacts on enzymatic. Ind Crops Prod. 113: 64-74.

Iiyama, K. and Wallis, A.F.A. 1989. Effect of acetyl bromide treatment on the ultraviolet spectra of lignin model compounds. Holzforschung, 43: 309-316.

Khaenson, W., S. Maneewan, and C. Punlek. 2018. Assessment of the environmental impact of biomass electricity generation in Thailand. Int. J. Renew. Energy Res. 8(1) : 302-312.

Phuphaphud, A., K. Saengprachatanarug, J. Posom, and K. Maraphum. 2019. Prediction of the fiber content of sugarcane stalk by direct scanning using visible-shortwave near infrared spectroscopy. Vib. Spectrosc. 101: 71-80.

Ratanasumarn, N. and P. Chitprasert. 2020.Cosmetic potential of lignin extracts from alkaline-treated sugarcane bagasse : Optimization of extraction conditions using response surface methodology. Int. J. Biol. Macromol. 153: 138-145.

Sluiter, A., B. Hames, R. Ruiz, C. Scarlata, J. Sluiter, D. Templeton and D. Crocker. 2008. Determination of structural carbohydrates and lignin in biomass. US National Renewable Energy Laboratory.

Workman, J. and Jr. L. Weyer. 2007. Practical Guide to Interpretive Near-Infrared Spectroscopy, CRC Press, 239-263.

Wu, L., M. Li, J. Huang, H. Zhang, W. Zou, S. Hu, Y. Li, C. Fan, R. Zhang, H. Jing, L. Peng and S. Feng. 2015. A near infrared spectroscopic assay for stalk soluble sugars, bagasse enzymatic saccharification and wall polymers in sweet sorghum. Bioresour. Technol. 177: 118-124.

EN-P002

EFFECT OF THE PHOTOPERIOD AND SALINITY ON GROWTH AND BIOMASS OF *DUNALIELLA SALINA* KU11

Wipawee Dejtisakdi*
Faculty of Science, King Mongkut's Institute of Technology Ladkrabang, 1 Chalongkrung Rd., Ladkrabang, Bangkok, Thailand 10250
***E-mail: wipawee.de@kmitl.ac.th

ABSTRACT
Dunaliella salina is a promising green microalga for pharmaceutical and nutraceutical production since *D. salina* produces a high amount of beta-carotene, an anti-oxidant and vitamin-A precursor. To increase the amount of beta-carotene accumulation, we need to improve some factors that affected its growth and biomass. In this research, we aim to investigate the effects of photoperiod and salinity on the growth and biomass of *Dunaliella salina* strain KU11. In our experiments, the *Dunaliella* was cultured in Modified Ramaraj Medium (RM) under three different photoperiod (12Light:12Dark, 16Light:8Dark, 24Light:0Dark) and NaCl concentration (1M, 1.5M, 2M NaCl). Under three different photoperiods, we found that *D. salina* KU11 cultured under 16L:8D showed the fastest growth accumulation by entering the log phase after 24 hours (on day 1) and the culture also showed cell accumulation at the stationary phase approximately 1.5 fold higher than 12L:12D and 24L:0D, respectively. Under three different NaCl concentrations (1M, 1.5M and 2M), we found that the *D. salina* culture adding 1M NaCl showed the highest *D. salina* cell accumulation approximately 9.91 x 10^6 cells/mL at the stationary phase followed by 1.5M and 2M NaCl. In the next experiment, we then measured the *D. salina* biomass under the photoperiod of 12L:12D, 16L:8D, 24L:0D with adding 1M NaCl. The result showed that the culture under 16L: 8D with adding 1M NaCl was the most efficient medium by showing the highest biomass accumulation up to 0.16 g/L. This finding suggested us to use the culture condition of 16L:8D with adding 1M of NaCl in our further study of *D. salina* KU11 application.
Keywords: *Dunaliella salina* KU11, Growth, Biomass, Photoperiod, Salinity

INTRODUCTION

Dunaliella salina is a halophile unicellular green microalga and typically found in sea salt or saline soil (Hosseini and Shariati, 2009; Wu et al., 2016). This microalga is known for high accumulation of the important antioxidant, beta-carotene (more than 10% of the dry weight), under stress conditions such as high light intensity, high NaCl concentration, suitable temperatures, or nitrate deficiency (Ben-Amotz and Avron, 1983, 1990; Wu et al., 2016). Importantly, beta-carotene plays a significant role as pro-vitamin A that is benefit for humans and animals (Choudhari and Singhal, 2008; Wu et al., 2016). Moreover, *Dunaliella* can produce some other biomolecules such as lipids up to 55% of its dry weight under hypersaline conditions (Chen and Jiang, 2009; Liang M. H. and J. G. Jiang, 2013; Wu et al., 2016).

To increase the naturally the beta-carotene and the other products, we need to improve *Dunaliella*'s growth and biomass. In this research, we tested the effects of photoperiod and salinity on the growth and biomass of *Dunaliella salina* strain KU11 and found that the suitable condition for increasing its growth and biomass was to use the photoperiod 16 hours of light and 8 hours of the dark with adding 1M NaCl into the medium.

MATERIALS AND METHODS

Microalgal strain and Growth condition

Dunaliella salina strain KU11 was delivered from Prof.Dr. Niran Juntawong and it was isolated from saline soil in Nakorn Ratchasrima province. In experiments, it was grown by using Modified Ramaraj medium (RM) (Sathasivam and Juntawong, 2013) under light intensity 4,210 lux, temperature 28°C at 110 rpm on the rotary shaker.

For the experiment of different light and dark periods (L:D), 100 mL of *D. salina* KU11 culture was grown under L12:D12, L16:D8, L24:0 in the RM with adding 1.5 M of NaCl. After 10-day culturing, cell count was used to determine *Dunaliella*'s growth.

For the experiment of different concentrations of NaCl, 100 mL of *D. salina* KU11 culture was grown under 1M, 1.5M and 2M of NaCl under L12:D12, L16:D8, L24:0 condition in the RM. After 10-day culturing, cell count and specific growth rate were used to determine *Dunaliella* growth.

For the biomass measurement, 500 mL of *D. salina* KU11 culture was grown under L12:D12, L16:D8, L24:0 condition in the RM with adding 1M of NaCl and 10 mL of each culture was collected on day 4 (log phase), 6 and 9 (stationary phase) to measure dry weight by filtering on glass microfiber filter GF/C 47 mm and dried in an oven at 70°C overnight. We then weighed the filter after loading cells compared with before loading cells.

Cell count

Cultures in all experiments were counted every 24 hours until 10 days of culturing. Cell count was determined by using a haemacytometer with 10-µL-culture loading. The two biological replications were done in every experiment and each cell count (every 24 hours) was done in the triplicates.

The specific growth rate measurement

The specific growth rate was determined by using the equation below.

$$\mu = \frac{\ln (N - N_0)}{\Delta t}$$

RESULTS AND DISCUSSION

To compare different light and dark periods (L12:D12, L16:D8, L24:0) for *D. salina* growth, we found that the culture grew under L16:D8 was entering in the log phase after 24 hours and could reach the highest cell number accumulation up to 1.55 fold compared with L24:0 and L12:D12, respectively (Figure 1).

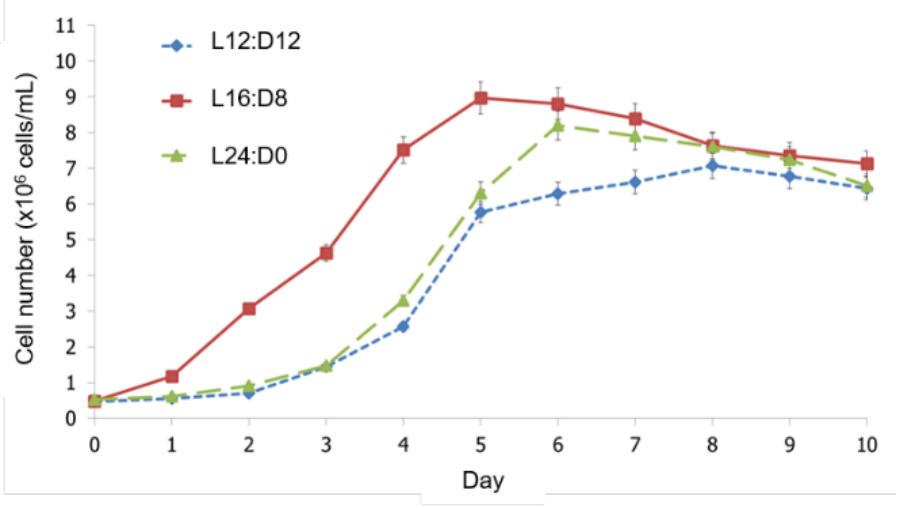

Figure 1. Growth development of *Dunaliella salina* KU11 cultures under three different Light:Dark periods (L12:D12, L16:D8, L24:0) under growing in the RM with adding 1.5 M of NaCl.

We set up the next experiment by varying the NaCl concentration (1M, 1.5M, 2M) to find out what concentration was suitable for *Dunaliella* growth determined by using cell count and specific growth rate measurement. We found that *Dunaliella* grew in the RM under L16:D8 with adding 1M of NaCl showed the highest cell number accumulation up to 9.91 x 10^6 cells/mL and the most suitable NaCl concentration was 1M under L16:D8 growing condition (Figure 2). Moreover, we found that the specific growth rate was related to *Dunaliella*'s growth. To illustrate, the specific growth rate in the Light:Dark period at 16:8 was 0.2138, the highest number, compared with other growth conditions as shown in Table 1. This finding result was corresponding to Ben-Amotz and Avron's report, they found that *Dunaliella*'s growth decreased while the salinity concentration was increasing (Ben-Amotz and Avron, 1981). Moreover, in the high salinity, cells started accumulating beta-carotene and this could make cell division was decreased (Richmond, 1986; Juntawong and Sathasivam, 2015).

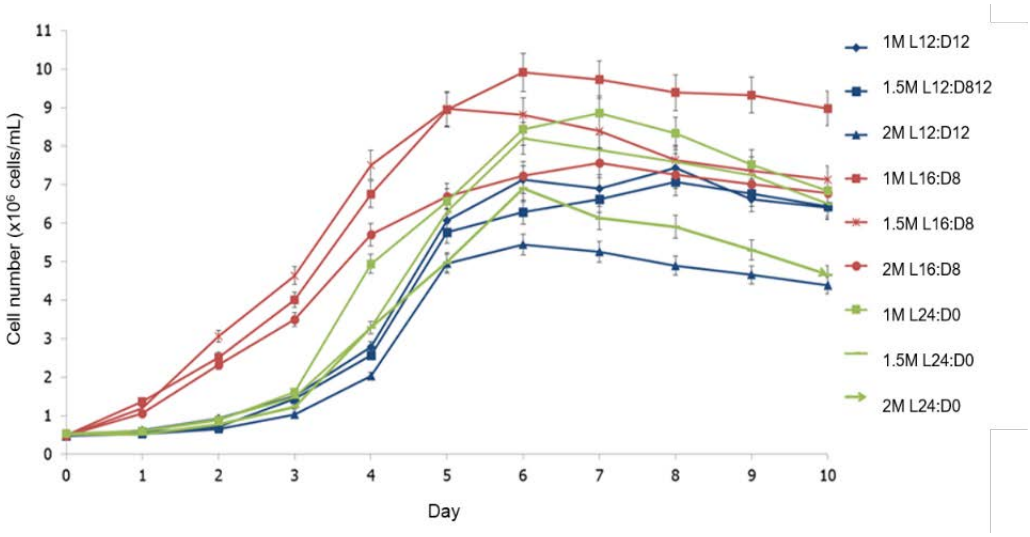

Figure 2. Growth development of *Dunaliella salina* KU11 cultures under three different Light:Dark periods (L12:D12, L16:D8, L24:0) and NaCl concentrations (1 M, 1.5 M, 2 M).

Table 1 Comparison of the specific growth rate of *D. salina* KU11 culture under different concentration of NaCl and Light:Dark period.

Light:Dark period	Specific Growth Rate (cells/day)		
	1M NaCl	1.5M NaCl	2M NaCl
12:12	0.1780	0.1786	0.1363
16:8	0.2138	0.1894	0.1842
24:0	0.1841	0.1788	0.1422

In the next experiment, we then measured *Dunaliella*'s biomass under L12:D12, L16:D8, L24:0 with adding 1M NaCl in day 4 (log phase), day 6 and day 9 (stationary phase). We found that *Dunaliella* culture grew in day 6 under L16:D8 showed the highest biomass accumulation up to 0.16 g/L following by the growth condition at L24:D0 (approximately 0.14 g/L) (Figure 3). In the light exposure 24 hours, cells were performing photosynthesis and dividing all the time and also we found cells showed small size compared with L16:D8 photoperiod. This finding might suggest that biomass in L16:D8 was less than L24:D corresponding to Fogg and Thake's study (Fogg and Thake, 1987).

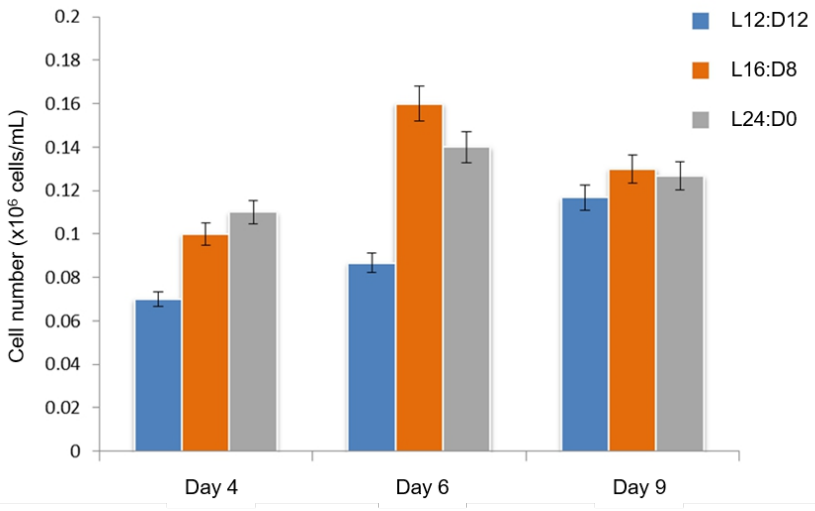

Figure 3. Comparison of *Dunaliella salina* KU11's biomass grown under L12:D12, L16:D8, L24:0 periods and all cultures were collected and measured on day 4 (log phase), day 6 (early stationary phase) and day 9 (stationary phase) in the RM with adding 1M of NaCl.

CONCLUSIONS

In this study, we aim to find the best suitable of growth condition in Modified Ramaraj medium (RM) by varying Light:Dark periods (L12:D12, L16:D8, L24:0) and NaCl concentrations (1M, 1.5M, 2M) and also to find the highest biomass accumulation in each growth condition. We found that L16:D8 photo period with adding 1M NaCl in the RM was the suitable condition for growing *Dunaliella salina* KU11 as shown in its growth (cell number accumulation) and biomass accumulation.

ACKNOWLEDGEMENT

I would like to thank for the Faculty of Sciences for the project funding (2561-01-05-38) and Prof.Dr. Niran Juntawong for *Dunaliella* strain KU11 strain. I am also greatly appreciated Ms. Chorpaka Bunlert and Ms. Dhittita Chanphayap, my students, who worked hard for the project.

REFERENCES

Ben-Amotz, A. and M. Avron. 1981. Glycerol and betacarotene metabolism in the halotolerant alga *Dunaliella*: a model system for biosolar energy conversion trends. Biochem. Sci. 6: 297-299.

Ben-Amotz, A. and M. Avron. 1983. On the factors which determine massive beta-carotene accumulation in the halotolerant alga *Dunaliella bardawil*. Plant Physiol. 72(3):593-597.

Ben-Amotz, A. and M. Avron. 1990. The biotechnology of cultivating the halotolerant alga *Dunaliella*. Trends Biotechnol. 8: 121–126.

Chen, H. and J. G. Jiang. 2009. Osmotic Responses of *Dunaliella* to the changes of salinity. J. Cell. Physiol. 219: 251–258.

Choudhari, S. and R. Singhal. 2008. Media optimization for the production of b-carotene by Blakeslea trispora: A statistical approach. Bioresour. Technol. 99: 722–730.

Fogg, G.E. and B. Thake. 1987. Algae cultures and phytoplankton ecology. 3rd Edition, The University of Winsconsins Press Ltd., London.

Hosseini, T. A. and M. Shariati. 2009. *Dunaliella* biotechnology: method and applications. J. Appl. Microbiol. 107, 14–35.

Juntawong, N. and R. Sathasivam. 2015. Identification and comparison of culture medium for high betacarotene production by *Dunaliella salina* KU11 isolated from salt soil samples collected from Northeastern parts of Thailand. The Proceeding of 53rd Kasetsart University Annual Conference. 3-6 February, 2015.

Liang, M. H. and J. G. Jiang. 2013. Advancing oleaginous microorganisms to produce lipid via metabolic engineering technology. Prog. Lipid Res. 52(4): 395–408.

Richmond, A. 1986. Handbook of Microalgal Mass Culture. CRC Press, Inc. Boca Raton, Florida.

Sathasivam, R. and N. Juntawong. 2013. Modified medium for enhanced growth of *Dunaliella* strains. Int. J. Curr. Sci. 5: 67-73.

Wu, Z., W. Dejtisakdi, P. Kermanee, C. Ma, W. Arirob, R. Sathasivam and N. Juntawong. 2016. Outdoor cultivation of *Dunaliella salina* KU11 using brine and saline lake water with raceway ponds in northeastern Thailand. Biotechnol. Appl. Biochem. 64(6): 938-943.

EN-P003

EFFICIENCY OF MICROORGANISM AND CHEMICAL FOR ANAEROBIC CONDITION CREATION IN BUTANOL PRODUCTION

Chalida Daengbussadee[1], Lakkana Laopaiboon[2,3], and Pattana Laopaiboon[2,3]*
[1] Graduate School, Khon Kaen University, Khon Kaen 40002, Thailand
[2] Department of Biotechnology, Faculty of Technology, Khon Kaen University, Khon Kaen 40002, Thailand
[3] Fermentation Research Center for Value Added Agricultural Products, Khon Kaen University, Khon Kaen 40002, Thailand
*Email :patlao@kku.ac.th

ABSTRACT
Biobutanol can be produced by Clostridia via the acetone-butanol-ethanol (ABE) fermentation under strictly anaerobic condition. In laboratories, oxygen free nitrogen (OFN) gas is used to create anaerobic condition for ABE fermentation. However, this method is not suitable and costly for a large-scale fermentation. The aim of this work was to study the feasibility of anaerobic condition creation using strictly aerobe bacterium, *Arthrobacter* sp. and a chemical, sodium dithionite, for butanol production by *Clostridium beijerinckii*. Sweet sorghum juice (SSJ) containing 60 g/L of total sugar and 1.27 g/L of ammonium sulfate was used as a butanol production (BP) medium in 1-L air-locked bottles. *Arthrobacter* sp. or sodium dithionite (SDTN, 0.25 mM to 0.20 M) was added into the BP medium to create anaerobic condition. After 4 h, *C. beijerinckii* was inoculated into the BP medium to start the fermentation. The results showed that the highest butanol titer (P_B = 8.51 g/L), yield ($Y_{B/S}$ = 0.26 g/g) and productivity (Q_B = 0.10 g/L·h) were obtained under using 0.25 mM at 84 h of fermentation time. In the experiments using *Arthrobacter* sp. for anaerobic condition creation, the P_B of 10.62 g/L, $Y_{B/S}$ of 0.33 g/g and Q_B of 0.22 g/L·h were obtained at the fermentation time of 48 h. These values were higher than those using SDTN and the control experiment using OFN gas flushing to create anaerobic condition (P_B = 9.79 g/L, $Y_{B/S}$ = 0.30 g/g, Q_B = 0.21 g/L·h at 48 h). The results indicated that *Arthrobacter* sp. is an effective bacterium to create anaerobic condition for batch butanol production from SSJ by *C. beijerinckii*.
Keywords: *Arthrobacter* sp., Biobutanol, *C. beijerinckii*, Sodium dithionite

INTRODUCTION

Butanol or butyl alcohol (C_4H_9OH) is a linear 4-carbon aliphatic saturated alcohol. Biobutanol has been considered as a better transportation fuel than bioethanol, mainly due to its higher number of carbon atoms and consequently in higher energy content, miscibility in diesel, and blending capacity (Li et al., 2018). Biobutanol can be produced by Clostridia via ABE (acetone-butanol-ethanol) fermentation under strictly anaerobic condition. In laboratories, anaerobic condition for ABE fermentation by OFN gas flushing is used. However, it is not suitable in a large scale fermentation. Camacho et al. (2014) reported that sodium dithionite (STDN, 0.005-0.20 M) could absorb oxygen in a stirred-tank bioreactor and Jhaveri and Sharma (1968) reported that the heterogeneous reaction between oxygen and dithionite diffusion is likely to play an important role. In addition, Hayatsu et al. (1999) reported that *Arthrobacter* sp., a Gram positive, rod-shaped and non-spore forming bacteria, is able to consume oxygen. Eschbach et al. (2003) stated that *Arthrobacter* sp., strictly aerobic bacterium, can consume rapidly oxygen within the 20 min. Therefore, the addition of SDTN or *Arthrobacter* sp. has potential to create anaerobic condition creation for ABE fermentation.

In present, the effective performance of butanol production depends on processes and substrates. The substrates for butanol production include starch, sugars and hydrolysates (Cascon et al., 2011). Sweet sorghum [*Sorghum bicolor* (L.) Moench] is a non-competitive substrate with less water requirement and tolerance to salinity and drought. The juice from sweet sorghum stalk consists of fermentable sugars, such as sucrose, glucose and fructose, which can be directly fermented to produce acetone, butanol and ethanol by *Clostridium* spp. Sirisantimethakom et al. (2018) reported that sweet sorghum juice supplemented with $CaCO_3$ (7.14 g/L), $(NH_4)_2SO_4$ (1.27 g/L) and butyric acid (5.18 g/L) was a suitable substrate for butanol production giving the butanol titer (P_B) of 16.91 g/L. $CaCO_3$ was used as a buffer and $(NH_4)_2SO_4$ was used

as a nitrogen source, whereas butyric acid was used as one of carbon sources for butanol production. However, sweet sorghum juice supplemented with only $(NH_4)_2SO_4$ was applied in this study.

The aim of this research was to study the feasibility of anaerobic condition creation using a chemical (STDN) and a strictly aerobe bacterium (*Arthrobacter* sp.) for butanol production from sweet sorghum juice supplemented with $(NH_4)_2SO_4$ by *C. beijerinckii.*

MATERIALS AND METHODS

Raw material

Sweet sorghum juice (*cv.* KKU 40) extracted from its stalks using a sugarcane extractor was obtained from Faculty of Agriculture, Khon Kaen University, Thailand. Then, it was concentrated to obtain total soluble solids of 67 °Bx and stored at -20 °C (Laopaiboon et al., 2009).

Butanol production medium preparation

Concentrated sweet sorghum juice (SSJ) was thawed at room temperature and diluted with distilled water to obtain total sugar at 60 g/L. The juice was supplemented with 1.27 g/L of $(NH_4)_2SO_4$ (BDH, UK), autoclaved at 110 °C for 28 min (modified from Sirisantimethakom et al., 2018) and used as butanol production medium.

Microorganism and inoculum preparation

Clostridium beijerinckii TISTR 1461 was purchased from Thailand Institute of Scientific and Technology Research (TISTR) Khlong Luang, Pathumthani, Thailand. It was maintained as a spore suspension and stored at 4 °C in sterile distilled water. The spore suspension was activated by heat shocked in a water bath at 80°C for 1 min, then immediately cooled in an iced water bath for 1 min. The spore suspension was transferred into sterile cooked meat medium (CMM: 1 g CMM and 0.08 g glucose in 10 mL distilled water) (Oxoid, UK). CMM was purged with OFN gas to create strictly anaerobic condition and incubated at 37 °C for 16-19 h. The vegetative cells of 5% (v/v) were inoculated into sterile tryptone-glucose-yeast extract (TGY) medium (Oxoid, UK) and incubated at 37 °C for 4-6 h to obtain 0.5 OD (optical density at 600 nm) before use as an inoculum for ABE fermentation (Wechgama et al., 2017).

Arthrobacter sp. was purchased from Thailand Bioresource Research Center (TBRC), Khlong Luang, Pathumthani, Thailand). Cells were grown in a sterile nutrient broth (NB) medium under shaking condition at 200 rpm and 30 °C for 6-7 h. Then, it was transferred to a fresh NB medium at the same conditions to get 0.5 OD (optical density at 600 nm) before use as an inoculum for anaerobic condition creation. The NB medium consists of 10 g/L peptone (Himedia, India), 10 g/L beef extract (Bacto, France) and 5 g/L NaCl (Ajax, New Zealand) (modified from Sliva et al., 2012).

Anaerobic condition creation and fermentation conditions

The fermentation medium with working volume of 700 mL in a 1-L screw-capped bottle was used (Sirisantimethakom et al., 2016). Under control experiment, the medium was purged with OFN gas to create anaerobic condition before fermentation was performed. *C. beijerinckii* TISTR 1461 with 5% (v/v) from TGY was transferred to the butanol production media and incubated at 37 °C with agitation rate of 150 rpm until the end of fermentation. Samples were collected at time intervals for analyses.

Sodium dithionite (SDTN, BKKchemi, Thailand) concentrations in the range of 0.25 mM-0.20 M were spiked into the fermentation media for 4 h. Then, *C. beijerinckii* TISTR 1461 was inoculated to start butanol production and incubated at 37 °C until the end of fermentation.

Arthrobacter sp. (5%, v/v) was inoculated in the fermentation medium for 4 h at 30 °C and 150 rpm. After that, *C. beijerinckii* TISTR 1461 was transferred into the medium and incubated at 37 °C until the end of fermentation.

Analytical methods

Acetone, butanol, ethanol, acetic and butyric acids were analysed by gas chromatograph (Shimadzu, GC-2014, Japan) using a Porapak Q column (80/100 mesh, 3 m×2 mm, Resteck, USA) (Areesirisuk et al., 2010). pH was measured by pH meter. Total sugar concentration was determined by a phenol-sulphuric acid method (Mecozzi, 2005). The kinetic parameters (butanol productivity, Q_B: butanol yield, $Y_{B/S}$ and ABE yield, $Y_{ABE/S}$) were calculated.

RESULTS AND DISCUSSION

Butanol production from SSJ by C. beijerinckii

Butanol production from SSJ supplemented with 1.27 g/L of $(NH_4)_2SO_4$ were carried out under anaerobic condition using OFN gas flushing as a control treatment. The batch ABE profiles are shown in Figure 1. The results showed that pH was decreased in the first 12 h of fermentation, corresponding to high acids were produced. This phase is called acidogenesis phase. After 12 h of fermentation, acids were converted to solvents, and pH were slightly increased. This phase called solventogenesis phase. Under this condition, the P_B of 9.79 g/L, $Y_{B/S}$ of 0.30 g/g and Q_B of 0.21 g/L·h were obtained (Table 1) at 48 h of fermentation. The results demonstrated that SSJ supplemented with only $(NH_4)_2SO_4$ is a potential raw material for butanol production by *C .beijerinckii* TISTR 1461.

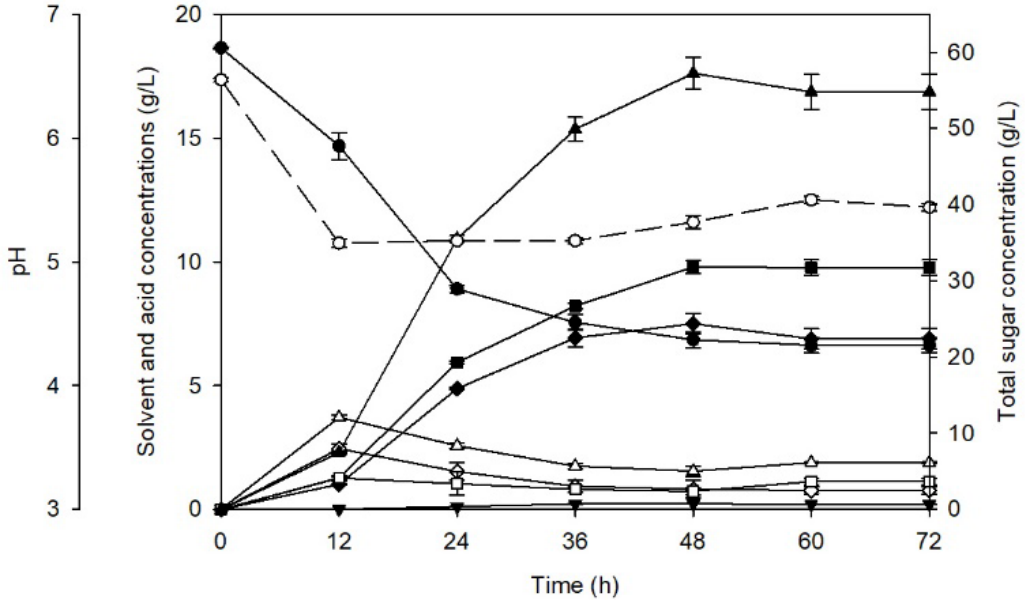

Figure 1. Batch ABE fermentation profiles from sweet sorghum juice supplemented with 1.27 g/L $(NH_4)_2SO_4$ under using OFN gas flushing :acetone (♦), butanol (■), ethanol (▼), ABE (▲), acetic acid (◊), butyric acid (□), total acids (∆), pH (○) and total sugar (●).

Anaerobic condition creation by SDTN for butanol production

To test the possibility of SDTN for anaerobic condition creation, the butanol production from SSJ supplemented with $(NH_4)_2SO_4$ and SDTN (0.25 mM-0.20 M) without OFN gas flushing was operated. The results indicated that butanol was not produced under using SDTN concentrations in the range of 0.75 mM-0.20 M (Table 1). These may be due to SDTN toxicity (Yang and He, 2008). However, P_B of 4.94 g/L was obtained at 0.50 mM STDN, suggesting that SDTN can be used to creation anaerobic condition for ABE fermentation. Under this condition, low sugar utilization (~30%) was observed. At 0.25 mM STDN, P_B and $Y_{B/S}$ increased to 8.51 g/L and 0.26 g/g, respectively. Lower concentration of SDTN (<0.25 mM) was not tested because longer fermentation time was obtained at low SDTN concentration, resulting in low Q_B. The results illustrated that STDN could absorb oxygen in the system to create ABE fermentation condition. However, the results obtained indicated that 0.25-0.50 mM had negative effect on butanol production efficiency. The P_B, P_{ABE}, $Y_{B/S}$, Q_B and $Y_{ABE/S}$ under this condition were lower than those under the control treatment ~9 to 52%. Hence, an alternative for anaerobic condition creation using *Arthrobater* sp., a strictly aerobe bacterium, was used to test the possibility for ABE fermentation in the subsequent experiments.

Table 1 Kinetic parameters of batch ABE fermentation from the sweet sorghum juice by *C. beijerinckii* TISTR 1461 under using OFN gas flushing and SDTN.

Parameter	Control treatment*	STDN		
		0.25 mM	0.50 mM	0.75 mM – 0.20 M
Butanol (g/L)	9.79±0.31[a]	8.51±0.44[b]	4.26±0.09[c]	0±0.00[d]
Total ABE (g/L)	17.61±0.63[a]	14.07±0.52[b]	5.80±0.16[c]	0±0.00[d]
Total acids (g/L)	1.54±0.21[b]	1.25±0.05[b]	5.00±0.19[a]	0±0.00[c]
Sugar utilization (g/L)	32.18±0.01[b]	33.89±0.14[a]	17.10±0.30[c]	ND[d]
Fermentation time (h)	48	84	72	-
$Y_{B/S}$ (g/g)	0.30±0.01[a]	0.26±0.00[b]	0.25±0.00[c]	-
Q_B (g/L·h)	0.21±0.01[a]	0.10±0.00[b]	0.06±0.00[c]	-
$Y_{ABE/S}$ (g/g)	0.45±0.00[a]	0.41±0.01[b]	0.34±0.00[c]	-

[a, b, c, d] Means followed by the same letter within the same row are not significantly different using Duncan's multiple range test at the level of 0.05 .The results in the table were performed in at least triplicate experiments and expressed as mean values ± SD.
SDTN: sodium dithionite
ND: not detected
$Y_{B/S}$ = butanol yield, $Y_{ABE/S}$ = ABE yield, Q_B = volumetric butanol productivity
*****Control treatment **:**using OFN gas flushing

Anaerobic condition creation by Arthrobacter sp. *for butanol production*

To evaluate the possibility of *Arthrobacter* sp. for anaerobic condition creation, the butanol production from SSJ supplemented with $(NH_4)_2SO_4$ by mixed cultures of *Arthrobacter* sp. and *C. beijerinckii* TISTR 1461 without OFN gas flushing were performed. *Arthrobacter* sp. was transferred into SSJ medium in 1-L screw-capped bottle for 4 h. Thereafter, active growing cells of *C. beijerinckii* TISTR 1461 were inoculated into the medium to start ABE fermentation. The batch ABE profiles are shown in Figure 2. It was found that the fermentation results were similar to those of the control treatment. The pHs under mixed cultures slightly decreased at the end of fermentation. This might be due to no buffering agents in the medium. However, the rates of sugar consumption, butanol production and ABE production under the mixed culture were higher than those of the control treatment, suggesting that the use of *Arthrobacter* sp. promoted ABE fermentation because *C. beijerinckii* TISTR 1461 showed the capability to produce butanol at the conditions tested. Thus, it implied that no or little oxygen left on the headspace before *C. beijerinckii* TISTR 1461 started to produce butanol.

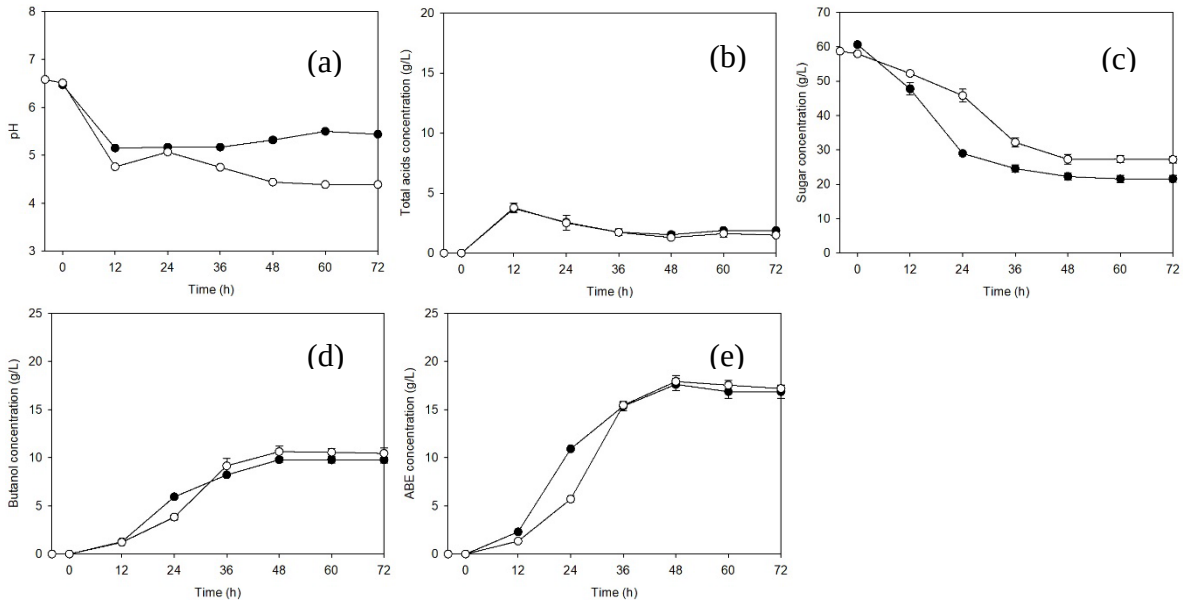

Figure 2. Batch ABE fermentation profiles for (a) pH, (b) total acids, (c) sugar concentration, (d) butanol and (e) (ABE of anaerobic condition creations for 4 h by *Arthrobacter* sp. (○) and OFN gas flushing (●).

Comparison of anaerobic condition creations for ABE fermentation under OFN gas flushing, SDTN and Arthrobacter sp.

The comparison of butanol fermentation results in our studies is shown in Figure 3. It was found that the highest butanol production efficiency (P_B = 10.62 g/L, $Y_{B/S}$ = 0.33 g/g and Q_B = 0.22 g/L·h) was obtained at 48 h using the mixed cultures. These values were higher than those under using SDTN ~25 to 120% and control treatment ~5 to 10%. Therefore, *Arthrobacter sp.* is a potential bacterium to be used to create anaerobic condition for butanol production.

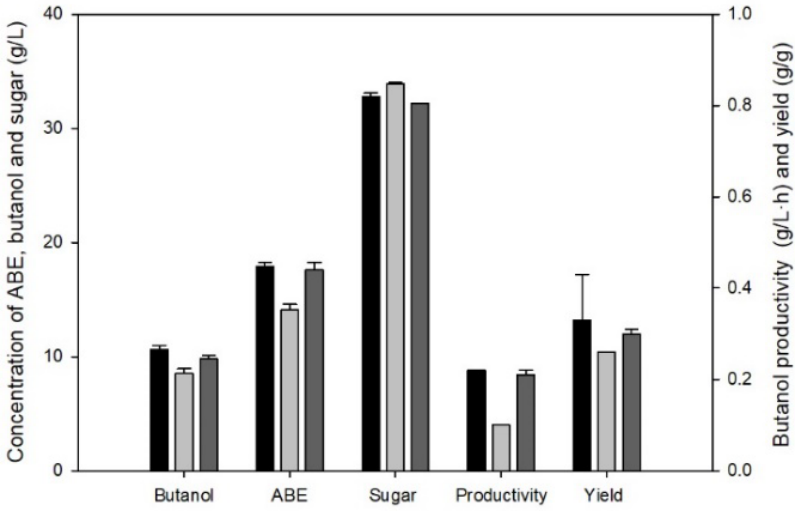

Figure 3. Butanol, ABE, sugar utilization, butanol productivity and yield for ABE fermentation from sweet sorghum juice supplemented with $(NH_4)_2SO_4$ (1.27 g/L) under anaerobic condition creations by OFN gas flushing, *Arthrobacter* sp .and optimal SDTN.

CONCLUSIONS

Sweet sorghum juice supplemented with 1.27 g/L of $(NH_4)_2SO_4$ can be used as a substrate for butanol production. SDTN is not suitable to be used to create anaerobic condition for butanol production due to low butanol productivity. *Arthrobacter* sp. is an efficient bacterium for anaerobic condition creation in batch butanol production from sweet sorghum juice by C. *beijerinckii* TISTR 1461. However, using this technique in full scale butanol fermentation requires steps of inoculum preparation of *Arthrobacter* sp. under optimum aeration.

ACKNOWLEDGEMENTS

This research was financially supported by the Fermentation Research Center for Value Added Agricultural Products (FerVAAP) and Faculty of Technology, Khon Kaen University, Thailand.

REFERENCES

Areesirisuk, A., L. Laopaiboon, N. Khongsay and P. Laopaiboon. 2010. Improvement of gas chromatographic analysis for organic acids and solvents in acetone–butanol–ethanol fermentation from sweet sorghum juice. Afr. J. Biotechnol. 9: 6422–6429.

Cascon, H. R., K. Choudhari, G. M. Nisola, L. Vivas, D. J. Lee and W. J. Chun. 2011. Partitioning of butanol and other fermentation broth components in phosphonium and ammonium-based ionic liquids and their toxicity to solventogenic clostridia. Sep. Purif. Technol. 78: 164–174.

Camacho, R. F., D. M. P. Paez, G. G. Blazquez and M. J. M. Garrido. 1992. Oxygen absorption in alkaline sodium dithionite solutions. Chem. Eng. Sci. 47: 4305-4314.

Eschbach, M., H. Möbitz, A. Rompf and D. Jahn. 2003. Members of the genus *Arthrobacter* grow anaerobically using nitrate ammonification and fermentative processes: Anaerobic adaptation of aerobic bacteria abundant in soil. FEMS Microbiol Lett. 223(2): 227–230.

Hayatsu M., M. Hirano and T. Nagata. 1999. Involvement of two plasmids in the degradation of carbaryl by *Arthrobacter* sp. strain RC100. Appl. Environ. Microbiol. 65: 1015–1019.

Jhaveri, A. S. and M. M. Sharma. 1968. Absorption of oxygen in aqueous alkaline solutions of sodium dithionite. Chem. Eng. Sci. 23(1): 1–8.

Laopaiboon, L., S. Nuanpeng, P. Srinophakun, P. Klanrit and P. Laopaiboon. 2009. Ethanol production from sweet sorghum juice using very high gravity technology: Effects of carbon and nitrogen supplementations. Bioresour. Technol. 100: 4176–4182.

Li, S., Y. Zhou, Z. Luo, Y. Cui, Y. Xu, L. Lin, M. Zhao, Y. Guo and Z. Pang. 2018. Dual function of ammonium acetate in acetone-butanol-ethanol fermentation by *Clostridium acetobutylicum*. Bioresour. Technol. 267: 319-325.

Mecozzi, M. 2005. Estimation of total carbohydrate amount in environmental samples by the phenol-sulphuric acid method assisted by multivariate calibration. Chemom. Intell. Lab. Syst. 79: 84–90.

Silva, C. R., J. C. Souza, L. S. Araujo, E. Kagohara, T. P. Garcia, V. H. Pelizzari. 2012. Exploiting the enzymatic machinery of *Arthrobacter atrocyaneus* for oxidative kinetic resolution of secondary alcohols. J. Mol. Catal. B Enzym. 83: 23-28.

Sirisantimethakom, L., L. Laopaiboon, P. Sanchanda, J. Chatleudmonkol and P. Laopaiboon. 2016. Improvement of butanol production from sweet sorghum juice by *Clostridium beijerinckii* using an orthogonal array design. Ind Crops Prod. 79: 287-294.

Sirisantimethakom, L., T. Thanapornsin, L. Laopaiboon and P. Laopaiboon. 2018. Enhancement of butanol production efficiency from sweet sorghum stem juice by *Clostridium beijerinckii* using statistical experimental design. Chiang Mai J. Sci. 45(3): 287-294.

Wechgama, K., L. Laopaiboon and P. Laopaiboon. 2017. Biobutanol production from agricultural raw materials by *Clostridium* spp. Chiang Mai J. Sci. 44(2): 394-405.

Yang, C. Y. and L. He. 2008. Neuroprotective effects of sinapine on PC12 cells apoptosis Induced by sodium dithionite. Chin. J. Nat. Med. 6(3): 205–209.

EN-P004

A FEASIBILITY STUDY OF THE MONITORING OF CELLULOSE, XYLAN AND LIGNIN CONTENTS IN ARTIFICIAL BIOMASS SAMPLES USING NEAR-INFRARED SENSOR

Sumaporn Kasemsumran[1]*, Sunee Jungtheerapanich[1], Kraireuk Ngowsuwan[1], and Satoru Miyata[2]
[1] Laboratory of Non-destructive Quality Evaluation of Commodities, Kasetsart Agricultural and Agro-Industrial Product Improvement Institute (KAPI), Kasetsart University, Bangkok 10900, Thailand
[2] Japan International Research Center for Agricultural Sciences, Tsukuba 305-8686, Japan
*E-mail: aapspk@ku.ac.th

ABSTRACT
The utilization of biomass has been continuously increasing importance. Because of the uncertainty of energy from petroleum and the impact on environmental pollution. Cellulose plant material is an appropriate raw material agent for use as bioenergy. However, the physical, chemical, structure, and composition are factors that hinder the process of biomass conversion. To increase the efficiency of biomass processing for energy purposes, it is necessary to know the chemical composition of complex biomass materials. Near-infrared (NIR) spectroscopy has shown that it is an effective way to characterize the organic composition of biomass. The objective of this research was to determine the variation of chemical composition across artificial biomass mixture to probe the potential of NIR technique in quantitatively analyzing chemical compositions. The artificial biomass mixtures of twenty were prepared and analyzed by the NIR sensor. Partial least square regression (PLS) models for cellulose, xylan as hemi-cellulose and lignin in mixture samples were developed from the wavelength region of 1100-2500 nm. The different types of spectra pretreatments were analyzed for reducing the spectra effects. The best calibration model of cellulose, xylan, and lignin in artificial samples were developed from the combination of multiplicative scatter correction (MSC) and the first derivative pretreated spectra. All obtained PLS models giving the correlation coefficient (R) of 0.99 and the standard error of cross-validation (SECV) of models for cellulose, xylan and lignin were 0.81, 0.65, 0.92 %w/w. This feasibility study was useful for further study to develop the calibration model for predicting the real biomass materials.
Keywords: Near-infrared, Biomass, Cellulose, Xylan, Lignin

INTRODUCTION

Thailand is one of the important agricultural countries in the world. We produce many kinds of agricultural products for human and animal consumption. By-products from agriculture and agro-industry are agricultural and industrial wastes, such as bagasse and rice husk, which can be converted into energy (Soccol et al., 2010). These materials are called "biomass". Due to petroleum oil considered the main fuel source of the world, is reducing and has a higher price every year. Finding alternative energy from oil is therefore absolutely essential. Biomass energy is therefore renewable energy, which Thailand has many advantages in the world because we have a high potential for biomass production. Before converting biomass into energy, it is necessary to know the chemical composition in order to lead to the selection of suitable energy production processes. These chemical compositions include cellulose, hemicellulose, and lignin. However, quantitative analysis of this chemical composition is a very complex and time-consuming method. Therefore, finding a rapid analysis method is very important. The near-infrared (NIR) method is a fast and low-cost chemical composition analysis method based on the method of creating a calibration model by using NIR spectral data of the samples and the required quantity of components to be predicted detecting using standard methods. The objective of this research is to individual analyze the amount of cellulose, hemicellulose in the form of xylan, and lignin in bagasse, a type of biomass by using the NIR sensor. Matt et al. (1996) employed the NIR technique to analyze components in biomass raw materials by creating various predictive equations including ethanol extractives, ash, lignin, uronic acids, arabinose, xylose, mannose, galactose, glucose, C, H, N and O from wood biomass feedstocks. Nicole et al. (2008) applied NIR method for classification biomass samples including red oak, yellow poplar tree, walnut family tree, switch grass, corn cob, and bagasse. Edward and Amie (2009) studied to improve the quality of NIR

model for prediction of chemical composition in dilute-acid pretreated corn stover. In Thailand, there was a report on the use of NIR techniques for analyzing the amount of cellulose, hemicellulose and lignin in bagasse as agricultural waste materials for use in renewable energy production in 2010 by Kasemsumran et al. Xu et al. (2012) reported by comparison of NIR technique and chemical methods for the determination of lignocellulosic biomass properties. Recently, the rubber wood properties testing by mean of the visible and NIR spectroscopic prediction for the hemicellulose, cellulose, N, C, H and moisture contents in waste rubber wood as biomass for energy utilization were reported (Phumichai et al., 2020).

In this study, the artificial biomass samples were prepared and employed as the preliminary study. Three major components, cellulose, xylan as hemi-cellulose and lignin, were mixed as the modeling samples, in which they are generally consisting of natural wood and non-wood plant. Cellulose is the main component of biomass resources which refers to the value of the product. Xylan or arabinoglucuronoxylans are found in the all based plants and a backbone of poly-β-(1→4)xylose which involves to hemicellulose component. Lignin is the complex polymers that compose of phenyl propane structure. It is an important component for binder or hole the fiber together in a natural plant (Biermann, 1996).

MATERIALS AND METHODS

Sample preparation

Cellulose, xylan, and lignin powder were weighted by an electronic analytical balance AE200 with 0.1mg readability (Mettler Toledo, Switzerland) and mixed in a zipper plastic bag for 20 samples. Cellulose and xylan from birch wood were purchased from Sigma-Aldrich (Steinheim, Germany). Lignin powder was extracted from beechwood according to the Bjorkman procedure (Bjorkman, 1956).

Spectra measurement

The NIR spectra were recorded by a NIR sensor named InfraAlyzer 500 (BRAN+LUEBBE, Norderstedt, Germany) in the region of 1100-2500 nm, at 2 nm resolution. Each sample was scanned triplicate.

Data analysis

The NIR spectra were pretreated with 1st derivative, 2nd derivative, multiplicative scatter correction (MSC), and their combinations before develop the calibration models and then do the comparisons. The calibration model was calculated by the partial least square regression (PLSR) method and validated by the full cross-validation method by using Unscrambler (Ver. 9.7: CAMO AS, Trondheim, Norway).

RESULTS AND DISCUSSION

The percents of each component were depicted in Table 1. The cellulose of 35-54% represented the percentage of the non-wood plant. The 2nd derivative spectra of mixture samples are shown in Figure 1. The O-H stretching bands clearly shown at 1426 and 1920 nm. Moreover, the assignment for cellulose peaks at 2274 and 2336 nm corresponding to O-H/C-O in glucose molecule and C-H stretching/CH2 deformation combination in polysaccharide structure, respectively. Moreover, the band at 1670 nm, which arises from C-H aryl in the aromatic structure was varied with the percentage of lignin. Another peak at 1372 nm relates to C-H vibration of the methyl group (Workman and Weyer, 2008). The summary of statistic results is shown in Table 2. From the results, the calibration model using MSC and 1st derivative pretreated NIR spectra yielded a suitable model for predicting all components, cellulose, xylan, and lignin. The PLS models provided a high correlation and a small error of validation. The scatter plots of the best calibration model for the determination of cellulose, lignin, and xylan in the mixed samples were given in Figure 2.

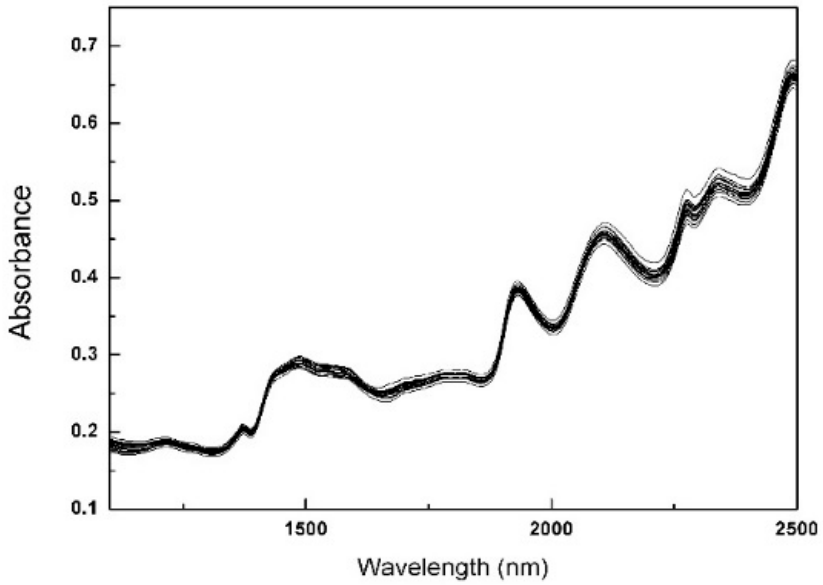

Figure 1. The spectra of 20 artificial biomass samples in the region of 1100 – 2500 nm.

Table 1 The statistical summary of artificial biomass samples.

Components	Min	Max	Standard deviation
Cellulose	35.14	64.58	8.23
Xylan	14.84	30.00	5.44
Lignin	14.82	35.16	6.91

Unit : %w/w

Table 2 The statistic results of the calibration model of components in artificial biomass samples.

Components	F	R	SEC	SECV	Bias
Cellulose	6	0.99	0.29	0.81	0.01
Xylan	6	0.99	0.28	0.65	0.02
Lignin	8	0.99	0.13	0.92	-0.02

F: The number of factors; R: correlation coefficient; SEC: standard error of calibration; SECV: standard error of cross-validation, Unit : %w/w

CONCLUSIONS

NIR technique can be used to the quantitative determination of cellulose, hemi-cellulose, and lignin in the artificial biomass samples. The NIR spectra significantly showed peaks of important chemical structure, which is the fundamental information of authentic biomass material. Moreover, the PLS calibration models provided a high correlation and low SECV values. These calibration models may be possible for estimating the contents of cellulose, hemi-cellulose, and lignin in authentic biomass material. However, more samples are needed and the calibration model may be better than this by investigating real biomass samples.

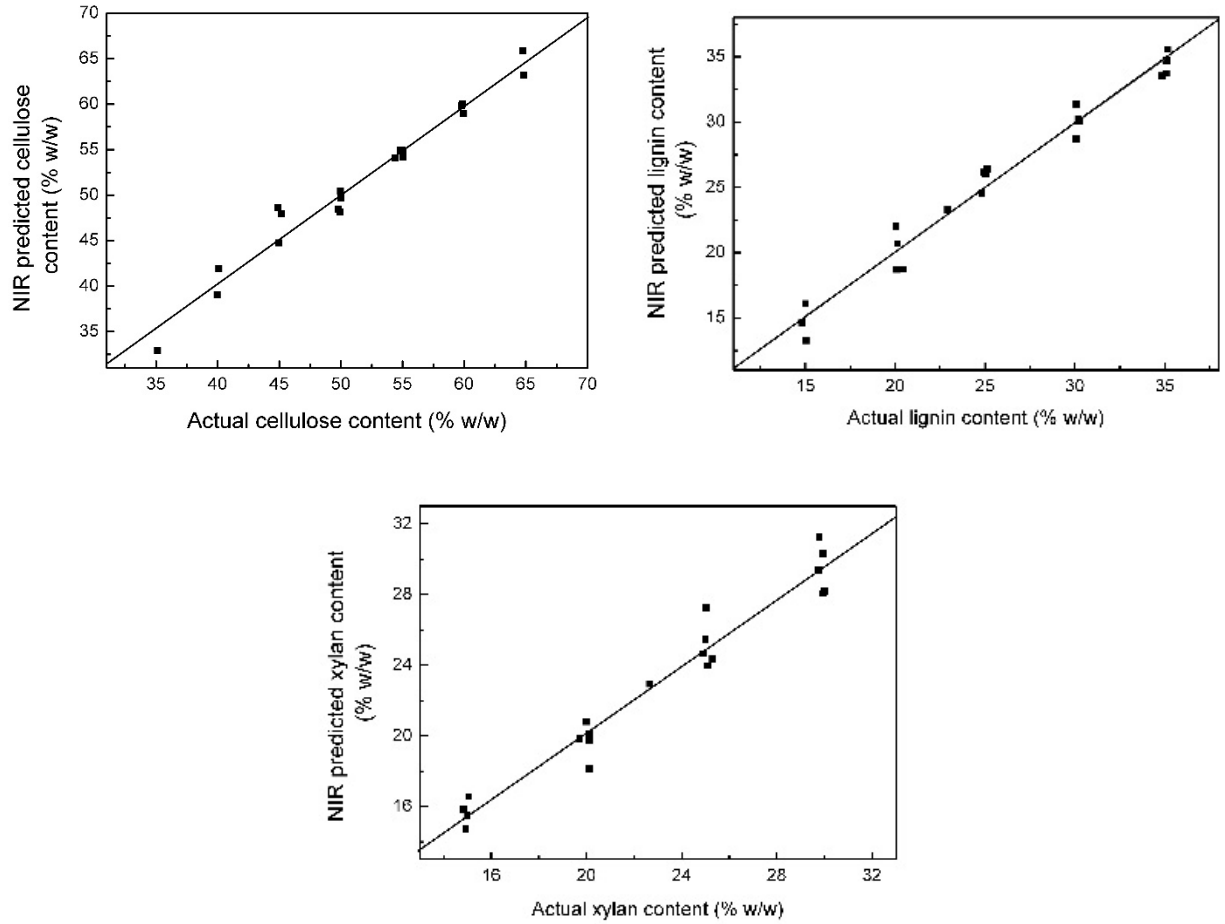

Figure 2. Scatter plots for the relationship between actual content and NIR predicted contents by using the best calibration models, which obtained in the calibration sample set.

ACKNOWLEDGEMENT

The authors would like to thanks the Japan International Research Center for Agricultural Sciences (JIRCAS) for financial support.

REFERENCES

Biermann, C. J. 1996. Handbook of Pulping and Papermaking, 2nd edition, Academic Press.

Bjorkman, A. 1956. Studies on finely divided wood I. Extraction of lignin with neutral solvents. Svensk Papperstidn, 59: 477- 485.

Edward J. W., and A. D. Sluiter. 2009. Improved multivariate calibration models for corn stover feedstock and dilute-acid pretreated corn stover. Cellulose. 16: 567-576.

Kasemsumran S., N. Suttiwijitpukdee, J. Prasatsrisupub, W. Thanapase and S. Miyata. 2010 Quantitative determination of chemical constituents in biomass for substitute energy utilization by using near infrared spectroscopy. Agric. Sci. J., 41(3/1): 65-68. (in Thai)

Phumichai, T., T. Tonusin, R. Rungtumnan, S. Chotchutima and S. Kasemsumran. 2020. Rubber wood properties testing for biomass energy by using visible–near infrared spectroscopy. Thai J. Agri. Sci. . 53(2): 67-75.

Soccol, C. R., L. P. S. Vandenberghe, A. B. P. Medeiros, S. G. Karp, M. Buckeridge, L. P. Ramos, A. P. Pitare-lo, V. Ferreira-Leitão, L. M. F. Gottschalk, M. A. Ferrara, E. P. S. Bom, P. Moraes, J .A. Araújo and F. A. G. Torres. 2010. Bioethanol from lignocelluloses: status and perspectives in Brazil. Bioresour. Technol. 101: 4820-4835.

Workman, J. and Jr. L. Weyer, 2008. Practical Guide to Interpretive Near-Infrared Spectroscopy, CRC Press, Inc., FL, United State.

EN-P005

RECOMMENDED FAST GROWING TREE SPECIES FOR ENERGY PLANTATION IN THAILAND: A LITERATURE REVIEW

Maliwan Haruthaithanasan*, Pussadee Sukpiboon, Eakpong Tanavat, Pavina Badan, Orracha Sae-tan, Kasem Haruthaithanasan, and Yuttana Banchong
Kasetsart Agricultural and Agro-industrial Product Improvement Institute (KAPI), Kasetsart University
Bangkok, Thailand
***E-mail: maliwan.t@ku.th

ABSTRACT
Fast growing tree planting in Thailand has been increasing due to higher quality and stability as biomass fuel compared to that of agricultural waste. The Alternative Energy Development Plan (AEDP) launched to increase the biomass utilization for energy sector. There are not so many researches on fast growing tree recently. Some private companies are doing their research and development in fast growing tree planting, and attempt to reduce establishment cost and as well as secure sustainable supply of raw material. Following are potential fast growing tree species in Thailand: *Leucaena leucocephala* (Lam.) de Wit, *Acacia* hybrid (*mangium* x *auriculiformis*), *Eucalyptus* spp., *Casuarina junghuhniana* Mig., and *Melaleuca cajuputi* Powell. The most important properties are heat value and ash content. High heating value (HHV) of those of five genera ranges from 4,200 to 4,900 cal/g, ash content being between 2 to 3%. The average annual yield (green weight) is 18.8 – 31.2 ton/ha depending upon site quality, while common planting spaces are 2x2, 2x3, 3x3 m. Farmers will clear cut when the trees are 3 – 7 years old depending upon the purpose of utilization. The farmers prefer to plant nitrogen-fixing trees such as Acacia and Leucaena, some farmers are still aware of environmental impact, soil and water in particular, from eucalyptus planting.
Keywords: Fast growing species, Energy plantation, Thailand

INTRODUCTION

Regarding to the national policy on renewable energy, biomass energy has been promoted seriously due to benefits to the environment and local economy. Fast growing tree (FGT) plays an important role as a raw material to generate heat and electricity in factories and biomass power plants. There are a number of FGT species in Thailand which are both native and exotic species, being used for energy generation. Almost of these FGT are collected and harvested from natural stands in public land and farmland, their productivity is not enough to supply all factory and power plant. Therefore, FGT plantation is recommended to provide large scale and good quality of biomass fuel.

FGT can be harvested every year under clear cutting cum coppice system with 5-year rotation, with annual diameter growth of about 4-5 cm or 15.6 cm^3/ha/year, and tree coppices can be harvested every 5 years (crop) for 3 crops before replanting (Corvanich, 1982, Thaiutsa, 1994). For FGT plantation, the right species on the right planting site is the key importance. There are many species that can found as plantation in Thailand such as *Gmelina arborea*, *Melia azedarach*, *Casuarina equisetifolia*, and exotic species such as *Casuarina junghuhniana*, *Acacia auriculiformis*, *Acacia mangium*, *Eucalyptus* spp (Corvanich, 1982). However, these plantations are focused on wood and pulp industries with higher value than that for energy industry. Therefore, FGT for energy plantation needs to be studied for supporting energy security as well as to support farmers and investors who what to establish energy plantation.

This report includes literature review about FGT both in Thailand and elsewhere in order sources to find out the appropriate species for energy plantation based on growth rate, coppicing ability, yield per ha, cutting rotation (1-3 years), wood properties (heating value, ash content), and environmental issues.

RESULTS AND DISCUSSION

It can be suggested from literature review that 5 species of fast growing trees be used for energy plantation in Thailand, i.e., *Leucaena leucocephala* (Lam.) de Wit, *Acacia* hybrid (*A.mangium x A.auriculiformis*), *Eucalyptus* spp*., Casuarina junghuhniana* Mig., and *Melaleuca cajuputi* Powell.

Leucaena leucocephala (Lam.) de Wit

L. leucocephala (Lam.) de Wit is exotic species, its origin is in Central America and Pacific island. The distribution area is in tropical and subtropical zone and high rainfall area such as Africa and Asia. *L. leucocephala* (Lam.) de Wit has more than 100 varieties (Haque et al., 2007; Pandey and Kumar, 2013). *L. leucocephala* (Lam.) de Wit was first introduced to grow in Thailand in 1966 because its rapid growth in all regions and it can be cut in short time about 5-10 years (Ruaysungnern,1982). *L. leucocephala* (Lam.) de Wit is medium hardwood, drought tolerance and nitrogen-fixing tree from rhizobium in their roots, moreover mychorrhiza also in root zone helps to decompose phosphorus and some other elements to promote growth rate of *L. leucocephala* (Lam.) de Wit (Pandey and Kumar, 2013; Chaplot, 2014).

L. leucocephala (Lam.) de Wit can grow well in all regions especially in soil with pH 5.5. Moreover, *L. leucocephala* (Lam.) de Wit grows in calcareous soil provide very high growth rate and yield (Chotchutima et al., 2013). The mass propagation usually uses seed because it is cheapest and easiest way. However, stem or shoot cutting can be done to keep identical quality as their parent (Pandey and Kumar, 2013).

Leaves of *L. leucocephala* (Lam.) de Wit contain high protein which is good to produce cattle feed, wood can supply for pulp industry and use as biomass fuel, heating value of 4 years wood was about 4,370 – 4,410 cal/g (Pandey and Kumar, 2013). While, Haruthaithanasan *et al.* (2010) reported that total height and DBH in 2 years old of *L. leucocephala* (Lam.) de Wit were 6.59 m and 3.56 cm. Their heating value was 4,652 cal/g and green biomass yield was 35.35 ton/ha.

Wannaarpha (2010) reported that cost of *L. leucocephala* (Lam.) de Wit planting was 30,997 THB/ha while the wood price for biomass fuel was 650 – 750 THB/ton (Thaibiomass, 2015).

L. leucocephala (Lam.) de Wit plantation was found by Limlikhitaksorn (2007) that it can promote soil quality from his study in comparison of soil properties in *L. leucocephala* (Lam.) de Wit plantation and soil outside the plantation, his result obviously showed higher amount of organic matter, total N, K and Mg in *L. leucocephala* (Lam.) de Wit plantation (Figure 1).

Figure 1. *Leucaena leucocephala* at Wang Chin plantation, Phrae Province.

Acacia hybrid (*A.mangium* x *A.auriculiformis*)

In the 1970 natural *Acacia* hybrid between *Acacia mangium* and *Acacia auriculiformis* was first reported in Sabah, Malaysia (FAO 1982). *Acacia mangium* was identified as the female parent and *Acacia auriculiformis* as the male parent of the natural Acacia hybrid (Kha et al. 1993).

Acacia hybrid is a medium-sized tree that looks similar to *Acacia mangium*. In 2 years, the tree can reach 8 -10 m and 7.5 - 9.0 cm DBH. The species grow on sandy loam or sandy clay loam soils however, it also thrives on lateritic crude soils. *Acacia* hybrid is found where temperatures range from 12 - 35 °C, annual precipitation is 1,200 - 1,850 mm, and elevation is 50 - 350 m (Kijkar, 2003). *Acacia* hybrids have able to fix atmospheric nitrogen. Based on assessments of the number of nodules and nitrogen-fixing bacteria per plant, Acacia hybrids have marked better fixing able than *Acacia mangium* and *Acacia auriculiformis*. It showed that *Acacia* hybrid can improve the physical and chemical properties of the soil. (Kha, 2001).

Growth at the 8 years old, the total height and DBH Acacia hybrid were 15.2 cm and 18.2 m (Kha et al., 2012) nearly seemed as found by Kha and Ha (2017) that they were 18.8-20.7 m and 15.2-17.6 cm. While, Haruthaithanasan et al. (2010) reported total height and DBH in 2 years old of *Acacia* hybrid were 7.30 m and 4.41 cm. Their heating value was 4,734 cal/g and green biomass yield was 42.32 ton/ha. Artkla (2012) reported the cost of *Acacia* hybrid planting was 71,775 THB/ha at 3 years while the wood price for biomass fuel is 650 – 750 THB/ton, depending on the season and sites.

Acacia hybrids have become major plantation tree species in Southeast Asia because it having faster growth rates, higher productivity, a high measure of wood utilization, and greater paper strength. Planting acacia hybrids is not only for reforestation and short - term harvest but also for increasing local people's income, it has also contributed significantly to environmental improvement (Kha and Ha, 2017) (Figure 2).

Figure 2. 2nd rotation of *Acacia* hybrid (*A.mangium x A.auriculiformis*) (A; 3 months old after harvest, B; 5 months old after harvest) at Kanchanaburi Province**.**

Eucalyptus spp.

There are more than seven hundred species of eucalypts and most eucalypts are native to Australia, a few number are found in New Guinea and Indonesia. Eucalypts vary in size and habit from shrubs to tall trees. For several decades, eucalypts have been planted in Thailand to supply pulpwood and pole. With the increasing interest in bioenergy from renewable resources, Eucalypts are among priority tree species due to their fast growth, good coppicing ability and high heating value which are considered prerequisite for bioenergy crop on short rotation of 2-3 years (Figure 3).

Eucalyptus camaldulensis is the main species was recommended to grow in Thailand. It is a medium-sized to large tree. It grows under a wide range of climatic condition from warm to hot (3 - 40 °C). Annual precipitation is 600 - 1,250 mm, and altitude is 20 - 700 m (Doran and Turnbull, 1997). This species has the widest geographical range of any eucalypt. Its tolerance of extreme drought and high temperature combined with rapid growth when water available, tolerance of periodic water logging and salinity soil. Numerous companies have been breeding the Eucalypts between *E. camaldulensis* and other species such as *E. urophylla*, *E. pellita* and *E. brassiana* to support pulp and paper industry. Therefore, the *E*. hybrid is suitable for paper pulp industry. However, they are also used in bioenergy sector.

Haruthaithanasan et al. (2019) reported pure *E. camaldulensis* clones, which are most widely planted in Thailand, grew faster than *E. urophylla* x *E. pellita* and *E. pellita* x *E. brassiana* hybrids in Fang, northern Thailand. Growth performance in term of height and DBH in 2 years old of *E. camaldulensis* was 8.19 m height with 4.57 cm DBH. Their heating value was 4,602 cal/g and green biomass yield was 80.38 ton/ha (Haruthaithanasan et al., 2010). Eakpong et al. (2011) recorded green biomass productivity for bioenergy of pure species *E. camaldulensis* at 3 years old (97.66 ton/ha) higher than *A.* hybrid and *L. leucocephala* (52.18 and 36.82 ton/ha, respectively).

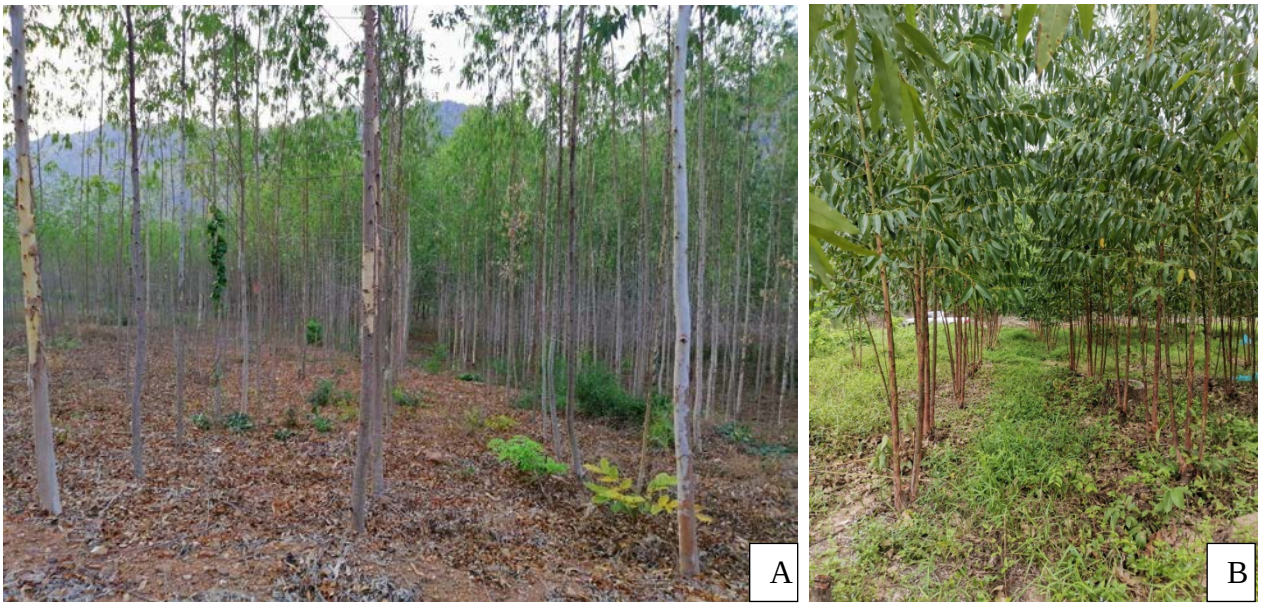

Figure 3. A; *Eucalyptus camaldulensis* 2 years old in drought area, B; 2nd rotation of *Eucalyptus* hybrid *(E.camaldulensis x E. pellita)* in wet area**.**

Casuarina junghuhniana

Casuarina junghuhniana of the Casuarinaceae family is a deciduous tree, 25–35 m tall and 50–80 cm in diameter. The natural distribution is restricted to the eastern part of the Indonesian Archipelago where it occurs on Java, Bali, Lombok, Sumbawa, Flores, Alor, Sumba, Timor and Wetar Islands (Pinyopusarerk and Boland, 1991; Mile, 1996). The ability of Casuarina species to fix nitrogen through endosymbiotic association with the actinomycete Frankia as well as associate with other ectomycorrhizal and endomycorrhizal fungi (Pinyopusarerk and House, 1993; Zhong et al., 1995) is another desirable property that lends them to environmental and ameliorative plantings. In southern India, the species has been increasingly planted by farmers over the past ten years to supply wood to the paper industry, replacing the better-known and extensively planted *C. equisetifolia* (Rawat et al., 2011; Varghese et al., 2011). Plantations can be harvested at age 4–5 years for pulpwood and poles, providing a quick return to small land-holders. *Casuarina junghuhniana* hybridises readily with *C. equisetifolia* and a male hybrid clone has been cultivated for fuelwood and pulpwood in India and used mainly for pole production in Thailand (Chittachumnonk, 1983).

The field trials of *C. junghuhniana* for identifying genetically improved planting material have been established in Kanchanaburi Province. In this study genetic parameters were estimated for nine growth traits using 29 novel clones of *C. junghuhniana* planted in Thailand. In addition, a widely planted commercial hybrid clone of *C. junghuhniana* x *C. equisetifolia* was included as a performance benchmark. The resulted showed that stand had attained a mean annual increment of 20.8 m^3 per hectare in 6 years old stand, the most productive clone was double the average and four times greater than the hybrid benchmark clone. Based on the growth and stem form traits, up to 11 clones are considered suitable for commercial plantation establishment (Luechanimitchit et al., 2017). The field trials for enegy plantation were conducted in saline soil area in Nakorn Ratchashima Province. The survival rate at 18 months old of *C. junghuhniana* in high and modulated salinity soil were 76% and 77% respectively. The heights at 18 months old were 2.0 and 3.7 meters respectively. The diameters at ground level were 2.5 and 4.1 centimeter respectively. The heating value were 4,500 – 4,700 cal/g (Mwihomeket et al., 2012) (Figure 4).

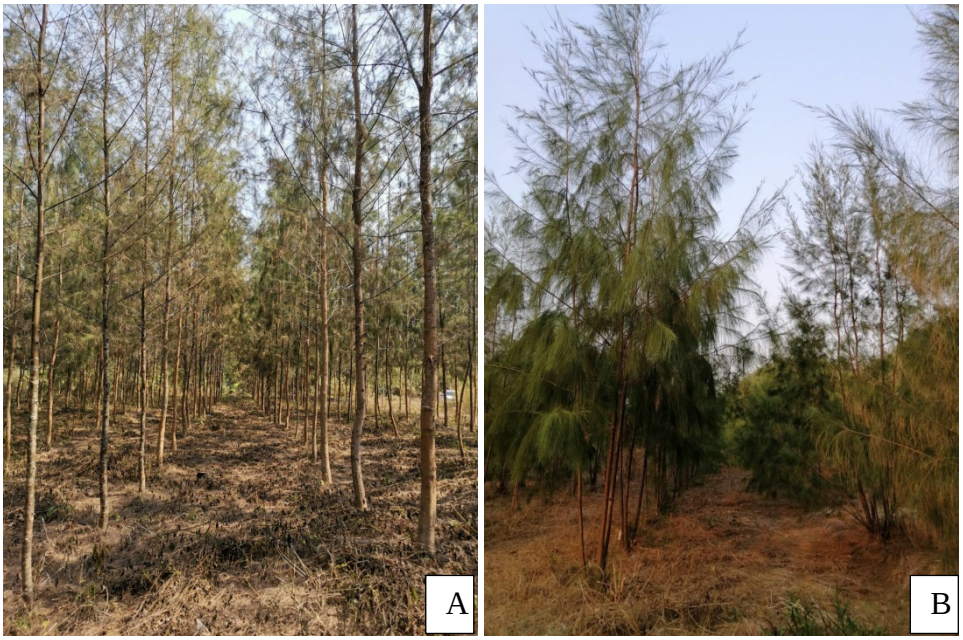

Figure 4. A; *Casuarina junghuhniana* 4 years old at Phrae Province, B; 2nd rotation of *Casuarina junghuhniana* at Kanchanaburi Province.

***Melaleuca cajuputi* Powell**

Melaleuca cajuputi Powell is a fast-growing tree species considered as a multipurpose species in South-East Asia. Three subspecies are recognised in this species, namely subsp. *cajuputi*, subsp. *cumingiana* (Turcz.) Barlow and subsp*. platyphylla* Barlow. There are distinguished by the Leaves length, stamens number and chemotype of essential oils (Brophy et al., 2013). *M. cajuputi* Powell is a multipurpose tree as it can be used for fuelwood, piles and frame poles in construction, leaves are used for essential oil distillation, flowers attract honey bees (Doran and Turnbull,1997), timber is used for pulp and paper, fiber and particle board, producing quality charcoal and potentially sawn timber (Trung, 2008). M. *cajuputi* plantation can be harvested on 5 – 7 years rotation for wood products (Trung, 2008, Nuyim, 2001) and two years for leaf oil distillation. The species is adapted to tropical environments with high salinity and high aluminium levels (Brinkman and Xuan, 1991), fire and drought tolerance (Tran et al., 2013), flooding and low pH (Nuyim, 2001, Osaki et al.,1998), seasonal inundation and acid-sulphate soils, which are difficult for tree plantation establishment (Chuong et al., 1996, Doran and Turnbull, 1997). *M. cajuputi* subsp. *cumingiana* was evaluated previously as a top priority tree species in reforestation efforts in the Mekong delta of Vietnam (Doran, 1999, Kha et al., 1999) and also widely planted (Kim et al., 2005).

The growth and yield of *M. cajuputi* showed the best resulted when compare with 13 tree species at the field trial in secondary peat swamp forest, Narathiwat province. The height of *M. cajuputi* at first to five years were 1.4, 2.3, 3.5, 5.0, 5.7 meters, respectively. The diameters at 10 cm above ground were recorded at 2.1, 3.6, 6.0, 7.9, 10.2 centimeters, respectively. The stem, twig and leaves biomass at five years were 12.9, 4.9 and 2.6 ton per hectare, respectively. The 2x2 meters spacing was recommended for plantation (Nuyim, 2001). The field experiment of *M. cajuputi* at high and modulated salinity soil in Nakorn Ratchashima Province showed the high potential of this species for plantation in salinity soil area. The height at 18 months old were 0.99 and 1.17 meters for high and modulated salinity soil respectively. The Diameter at ground level were 1.54 and 1.98 centimeter, respectively. Their heating value were 4,400 – 4,500 cal/g (Haruthaithanasan et al., 2014).

M. cajuputi is considered to be one of the potential tree species for development of the economic plantations in the peat swamp areas. The species consider to be plant in a wide range of environment disadvantages including high acid soil, saline soil, arid soil, and water-locked soil (Nuyim, 2001) (Figure 5).

Figure 5. *Melaleuca cajuputi* 5 years old at Lat Krathing plantation, Chachoengsao Province.

Table 1 Summary of important data of recommended FGT for energy plantation

	L. Leucocephala	***A.* hybrid**	***Eucalyptus.* spp.**	***C.Junghuhniana***	***M. cajuputi***
Plant spacing (m)	1x1, 1.5x1.5, 1x2	2x1, 2x2, 3x3	2x1, 2x2, 2x3,2x4	2x2, 2x3	2x2
Rotation (year)	2 – 3	3	3 - 5	4-5[/4]	5-7
Planting cost (THB/ha)	42,187 – 48,750	62,725	67,375 – 94,787	60,850-70,600	68,125-85,562
*First income (THB/ha)	43,488 - 65,232	75,600	93,360 - 155,600	85,344 - 106,680	87,280 - 122,192
Green Yield (ton/ha/year)	21.87-32.5	31.5[/1]	33.33-44.5	20-33.3	21.82[/5]
Heating value (cal/g)	4,200 – 4,600[/1]	4,734[/1]	4,200 – 4,500[/1]	4,500 – 4,700[/3]	4,400 – 4,500[/2]

* By calculated in the case of wood price was 800 THB/ton

Remark: [/1] Haruthaithanasan et al. (2010)
[/2] Haruthaithanasan et al. (2014)
[/3] Mwihomeket et al. (2012)
[/4] Chittachumnonk (1983)
[/5] Nuyim (2001)

CONCLUSIONS

Regards to this study, the important data of five potential FGT are *Leucaena leucocephala* (Lam.) de Wit, *Acacia* hybrid (*mangium* x *auriculiformis*), *Eucalyptus* spp., *Casuarina junghuhniana* Mig., and *Melaleuca cajuputi* Powell. It is discovered to support farmers and investors who plan to secure their biomass fuel to sustainably establish energy plantation. Although there are a number of FGT plantations but those plantations are not for energy. Therefore, research on silvicultural practices is needed to get more important and specific data for energy plantation. The research results can be used as a guideline to improve productivity of energy plantation as well.

ACKNOWLEDGEMENT

This project was financially supported by The Thailand Research Fund (TRF) and Electricity Generating Authority of Thailand (EGAT) to develop research roadmap on the fast growing species for energy plantation in Thailand during 2017 - 2018.

REFERENCES

Brinkman, W. J. and V. T. Xuan.1991. Melaleuca leucadendron, a useful and versatile tree for acid sulphate soils and some other poor environments. Int. Tree Crops J. (6): 261-274.

Brophy, J. J., L. A. Craven and J. C Doran. 2013. Melaleucas: their botany, essential oils and uses. ACIAR Monograph No. 156. Australian Centre for International Agricultural Research, Canberra.

Chaplot, P. C. 2014. Effect of planting geometry on biomass partitioning and productivity of *Leucaenaleucocephala*. Annals Agri-Bio Res. 19(4): 703 – 705.

Chittachumnonk, P. 1983. Silviculture of *Casuarina junghuhniana* in Thailand. In: Midgley, S.J., Turnbull, J.W., Johnston, R.D. (Eds.), 1st International Casuarina Workshop, Canberra, Australia.

Chotchutima, S., K. Kangvansaichol, S. Tudsri and P. Sripichitt. 2013. Effect of spacing on growth, biomass yield and quality of Leucaena (*Leucaenaleucocephala* (Lam.) de Wit.) for renewable energy in Thailand. J. Sustain Bioeng Sys. 3: 48 – 56.

Chuong, H., J. C. Doran, K. Pinyopusarerk and C. E. Harwood. 1996. Variation in growth and survival of Melaleuca species in the Mekong Delta of Vietnam. Tree improvement for sustainable tropical forestry, QFRI-IUFRO Conference. Caloundra, Queensland, Australia.

Corvanich A. 1982. Fast growing tree species and concept for forest plantation in Thailand. Forest of Thailand Association, Bangkok.

Doran, J. C. and J. W. Turnbull. 1997. Australian Trees and Shrubs: species for land rehabilitation and farm planting in the tropics. ACIAR Monograph No. 24. Australian Centre for International Agricultural Research, Canberra.

Doran, J. C. 1999. Cajuput oil. In: Southwell, I. and Lowe, R.(eds.) Tea tree: the genus Melaleuca. Harwood Academic Publishers, The Netherland.

FAO. 1982. Seed sources establishment and tree improvement project, Sabah, Malaysia. In Variation in *Acacia mangium* Willd. (ed. L. Pedley), pp. 41–42.

Haruthaithanasan, M., K. Haruthaithanasan, E. Tanavat, S. Phromlert and A. Baysangchan. 2010. The potential of *Leucaena leucocephala*, *Eucalyptus camaldulensis*, *Acacia mangium* and *Acacia spp.* (*mangium x auriculaeformis*) as plantation crops for energy. *In* Proceedings of 48th Kasetsart University Annual Conference: Plants, 3-5 February 2010, Kasetsart University, Bangkok.

Haruthaithanasan, M., E. Tanavat, N. Laksanaaree and K. Haruthaithanasan. 2014. Potential of salt tolerance Fast growing tree for energy plantation in Thailand (Final report). PTT public company limited, Bangkok.

Kha, L. D., D.H. Nguyen and V.T. Nguyen. 1993. Natural hybrid between *Acacia mangium* and *Acacia auriculiformis* (in Vietnamese). Forest Journal 7: 18-19.

Kha, L. D. 2001. Studies on the use of natural hybrids between *Acacia mangium* and *Acacia auriculiformis* in Vietnam. Agriculture Publishing, Hanoi.

Kha, L. D., C. E. Harwood, N. D. Kien, B. S. Baltunis, N. D. Hai and H. H. Thinh. 2012. Growth and wood basic density of *Acacia* hybrid clones at three locations in Vietnam. New For. 43: 13–31.

Kha, L. D. and H. T. Ha. 2017. Research and development of acacia hybrids for commercial planting in Vietnam. Vietnam Int. J. Eng. Sci. Technol. 59(1): 36-42.

Kijkar, S. 2003. Part II – Species Descriptions Acacia hybrid (*A. mangium x A. auriculiformis*). Available Source:https://rngr.net/publications/ttsm/species/Accacia%20hybrid.pdf/at_download/file,4 September 2019.

Kim, J., K. Liu, Y. Yoon, Y. Sornunwat, T. Kitiratirakarn and C. Anantachoke. 2005. Essential leaf oils from Melaleuca cajuputi. Acta Hortic. (680): 65-72.

Limlikhitaksorn, C. 2007. Soil properties after limestone mountain area reclamation by using *leucaena leucocephala* (Lam.) de Wit the Royal-initiated Nang Phan Thu Rat mountain area conservation and rehabilitation project, Phetchaburi Province. Master Thesis, Kasetsart University.

Luechanimitchita, P., V. Luangviriyasaenga, S. Laosakula, K. Pinyopusarerk and D. Bush. 2017. Genetic parameter estimates for growth, stem-form and branching traits of *Casuarina junghuhniana* clones grown in Thailand. For. Ecol. Manag. 404: 251-257

Mile, Y. 1996. Notes on the distribution of *Casuarina junghuhniana*. In: Pinyopusarerk, K., Turnbull, J. W., Midgley, S. J. (Eds.), Recent Casuarina Research and Development, Da Nang, Vietnam.

Mwihomeket, S. T., A. G. Mugasha, S. A. O. Chamshama, M. A. Mgangamundo, O. C. Kumburu and Z. Lupala. 2012. Early performance of *Casuarina junghuhniana* provenances/land races at Lushoto, Tanzania. South African Forest 194(1): 7 – 14.

Nuyim, T. 2001. Potentiality of *Melaleuca cajuputi* powell cultivation to develop for economic plantation purpose. The Proceedings of the 7th Silvicultural Seminar, Bangkok, Thailand.

Osaki, M., T. Watanabe, T. Ishizawa, C. Nilnond, T. Nuyim, C. Sittibush and T. Tanano. 1998. Nutritional characteristics in leaves of native plants grown in acid sulfate, peat, sandy podzolic, and saline soils distributed in Peninsular Thailand. Plant. Soil. 201: 175-182.

Pandey, V. C. and A. Kumar. 2013. *Leucaena leucocephala*: an underutilized for pulp and paper production. Gent Resour Crop Evol. 60: 1165 – 1171.

Pinyopusarerk, K. and D. Boland. 1991. *Casuarina junghuhniana* – an Indonesian species of promise for the tropics. *In* El-Lakany, M.H., Turnbull, J.W., Brewbaker, J.L. (Eds.), Proceedings of the 2nd International Casuarina Workshop, Cairo, Egypt.

Pinyopusarerk, K. and A. House. 1993. Casuarina: An annotated bibliography. International Centre for Research in Agroforestry, Nairobi, Kenya.

Rawat, G. S., N. K. Krishna and A. Nicodemus. 2011. Research and development of casuarinas in India. In: Zhong, C., Pinyopusarerk, K., Kalinganire, A., Franche, C. (Eds.), Fouth International Casuarina Workshop. China Forestry Publishing House, Haikou, Hainan, China.

Ruaysungnern,S. 1982. *Leucaena leucocephala* selected species for reforestation to improved soil properties. Royal Forest Department. Ministry of Agriculture and Cooperatives, Bangkok.

Tanavat, E., M. Haruthaithanasan, L. Puangchit, B. Thaiutsa and K. Haruthaithanasan. 2011. Nutrient storage in aboveground biomass and nutrient return in fast growing tree species planted for bio-energy. *In* Proceedings of 49th Kasetsart University Annual Conference: Plants, 1st-4th February 2011, Kasetsart University, Bangkok.

Thaibiomass. 2015. *Leucaena lencocephala*. Available Source: http://www.thaibiomass.com/uploads//3/4/6/3/3463780_leucaena_lencocephala_.20140515pdf, 25 February 2015.

Thaiutsa, B. 1994. *Acacia mangium* species for degraded heavy rainfall and saturated area. *In* Forestry Articles 1995. Forestry Research Center Faculty of Forestry Kasetsart University, Bangkok.

Tran, D. B., P. Dargusch, P. Moss and T.V. Hoang. 2013. An assessment of potential responses of Melaleuca genus to global climate change. Mitigation and Adaptation Strategies for Global Change, 18: 851-867.

Trung, N. Q. 2008. Melaleuca Timber- Resource potential and its current use in Kien Giang Province. Project "Conservation and Development of the Biosphere Reserve of Kien Giang Province. Technische Zusammenarbeit (GTZ) GmbH.

Varghese, M., A. Nicodemus and N. Ravi. 2001. Genetic and ecological variation in wood properties of Casuarina species. In: Gurumurthi, K., Nicodemus, A., Siddappa (Eds.), Casuarina: Improvement and Utilization. Institute of Forest Genetics and Tree Breeding, Coimbatore, India.

Wanida, A. 2012. Economic feasibility study of fast-growing acacia hybrids plantation and effecting factors on decision to adopt plantation for using in power generation. Thesis, Kasetsart University.

Wannaarpha, P. 2010. A financial and economic feasibility study of biomass power plant using giant leucaena as fuel. M.S. Thesis, Kasetsart University.

Zhong, C., M. Gong, Y. Chen and F.I. Wang. 1995. Inoculation of Casuarina with mycorrhizal fungi and Frankia. In: Brundrett, M., Dell, B., Malajczuk, N., Gong, M. (Eds.), Mycorrhizas for plantation forests in Asia, ACIAR Proceedings No. 62, Canberra.

EC-P001

EFFECTS OF DIFFERENT PINEAPPLE CULTIVARS AND CULTIVATED AREAS ON CHEMICAL COMPOSITIONS OF PINEAPPLE LEAF FIBERS AND THEIR RESIDUES FORAGE QUALITY

Chaiyaporn Sampoompuang, Keowpatch Lobyam, Nattaporn Khanoonkon, and Preeyanuch Srichola*
Kasetsart Agricultural and Agro-Industrial Product Improvement Institute, Kasetsart University, Bangkok, Thailand
***E-mail: aappua@ku.ac.th

ABSTRACT
The aims research was focus on study the effect of different pineapple cultivars on chemical compositions of pineapple leaf fibers and their residues forage quality. Pineapple leaves from 3 different pineapple cultivars collected from 8 different areas of Thailand were study. The chemical compositions of pineapple fibers, i.e. extractives, lignin, holocellulose, alpha-cellulose, hemi-cellulose, were investigated. The results showed that the chemical compositions of pineapple leaf fibers were affected by the cultivars and areas of cultivation. The pineapple leaf residues after fiber extraction of 'Pattavia' cultivar collected from Amphoe Kui Buri, Prachuap Khiri Khan Province, can be used as forage due to high values of protein content and TND, whereas low values of moisture content, NDF and ADF were detected.
Keywords: Pineapple leaf, Fibers, Morphology, Chemical compositions, Forage quality

INTRODUCTION

Pineapple (*Ananas comosus*), one of fruits cultivated in tropical and sub-tropical countries including Thailand. Pineapple cultivars were classified into 5 groups due to their leaf and fruit characteristics. 'Trad sri thong' and 'Thong Rayong' cultivars were divided in Queen group, whereas 'Pattavia' or 'Smooth Cayenne' was the Cayenne group (Rattanathawornkiti et al., 2016). Pineapple waste residues, i.e. peel, core, stem, crown, and leaves, from canned pineapple and pineapple juice industries, were totally 50% (w/w) of pineapple waste (Ketnawa et al., 2012). These wastes could be used as compost or animal feed for agricultural application or used as substrates for production of bioethanol and bio-manure and bioactive compounds (Correia et al., 2004: Mainoo et al., 2009: Zainuddin et al., 2014: Chintagunta, et al., 2017). Pineapple leaf wastes were utilized in many applications due to their rich of cellulose (69.5-83%) (Todkar et al., 2019). The pineapple leaf fibers could be used for paper (Sibaly et.al., 2017), textile (Hazarika et al., 2017), as well as composite (Ketnawa et.al., 2012: Todkar et al., 2019). applications (Hazarika et al., 2017: Sibaly et al., 2017: Todka et al., 2019). However, the different cultivation areas and various cultivars affected on morphology and chemical composition of fibers (Najeeb et al., 2020). Moreover, after extraction of pineapple leaf fibers by mechanical process, the residues of pineapple leaves were not utilized. The utilization of pineapple leaf residues after fiber extraction as fertilizer or feed might be the good way to solve this problem and brought this extraction process to zero waste.

MATERIALS AND METHODS

Materials

Three commercial cultivars of pineapple leaves from 8 different areas of Thailand were collected. The height and the weight of pineapple leave samples with ages of 1 year and 2 months were collected, and the cultivation areas were shown in Figure 1. The cultivar 'Pattavia' or 'Smooth Cayenne' was collected form 6 areas, i.e. i) Amphoe Ban Kha, Ratchaburi Province (Central region), ii) Amphoe Ban Chang, Rayong Province (Eastern region), iii) Amphoe Mueang, Lampang Province (Northern region), iv) Amphoe Cha-am, Phetchaburi Province (Central region), v) Amphoe Pranburi , Prachuap Khiri Khan Province (Central region) and vi) Amphoe Kui Buri , Prachuap Khiri Khan Province (Central region). The cultivar 'Trad Sri Thong' was obtained from Amphoe Khao Saming, Trad Province (Eastern region) and the cultivar 'Thong Rayong' was cultivated from Amphoe Pluak Daeng, Rayong Province (Eastern region). Ethanol, acetic acid, and acetone were purchased from Rci Labscan, Thailand. Sodium chorite and sodium hydroxide were obtained from Ajex

Finechem, Australia. Benzene, Sulphuric acid and sodium hydroxide were brought from Loba chemie (India), Qrec (New Zealand) and Ajax Finechem (Australia), respectively.

Figure 1. Cultivation areas of pineapple leaf samples.

Methods

The collected fresh pineapple leaves were extracted using fiber's extractor machine. After extraction, pineapple leaf fibers (Figure 2a) were washed using tap water and sun dried for 2 days to remove the water content of fiber prior to treatment. The residues after extraction (Figure 2b) was collected for proximate and forage quality analyses. After mechanical extraction, pineapple leaf fibers were cut into 2-3 cm-length. Fibers were immerged in the bottle containing the mixture of H_2O_2 and glacial acetic acid with the volume ratio of 1:1 prior to heat at 80-90 °C for 3 h prior to wash with distill water for 3 times. The fibers were separated by hand and keep at room temperature until dried. Chemical compositions of pineapple leaf fibers were determined according to the Technical Association of Pulp and Paper Industry (TAPPI) standard methods. Proximate analysis of pineapple leave residues after fibers separations was determined following the Official Methods of Analysis of Association of Official Analytical Chemists (AOAC, 2010). Moisture, protein, lipid, fiber, and ash contents were analyzed according to the method 934.01, method 984.13, method 2003.05, method 962.09 and method 942.05, respectively. The neutral detergent fiber (NDF), acid detergent fiber (ADF) and acid detergent lignin contents were characterized according to the Forage Fiber Analysis (Goering et al., 1970). The total energy (calories/gram) was determined using Analytical method (Bomb calorimeter).

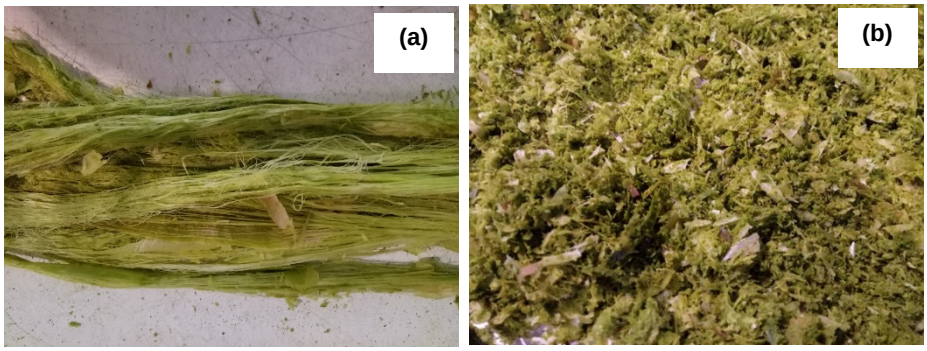

Figure 2. Appearances of (a) Pineapple leaf fibers and (b) pineapple leaf residues after extraction.

RESULTS AND DISCUSSION

Chemical compositions of pineapple leaf fibers

By considering, alcohol-benzene extractives of 3 pineapple leaf cultivars collected from 8 different areas of Thailand (Table 1). Alcohol extractives of 'Trad Sri Thong' (sample 2) and 'Thong Rayong' exhibited lower values as compared with 'Pattavia' cultivar. This result indicated that 'Pattavia' cultivar or the pineapple leaf in Cayenne group containing of aliphatic parts, fatty acids or triglycerides including fatty alcohols and waxes, more than the other cultivars. The 'Pattavia' cultivars collected from different areas showed different content of alcohol-benzene extractive. The highest content of alcohol-benzene extractive was from the samples of 'Pattavia' cultivar from Amphoe Ban-Kha, Ratchaburi Province (17.00%). The high values of lipophilic extractives caused the inherent tendency of processing equipment and deteriorated the final product properties, especially in papers making process.

Table 1 Extractive contents of pineapple leaf fibers after extract by several solvents.

Sample No.	Extractive content (%)			
	Alcohol-benzene	Alcohol	Hot-water	Total
1	17.00±0.71 ^{a}	1.15±0.07^{c}	5.81±0.63^{cd}	23.96 ±0.16^{a}
2	4.92 ±1.16 ^{d}	4.52 ±0.40^{a}	5.37 ±1.57^{d}	14.81 ±0.81^{c}
3	6.09 ±0.64 ^{d}	4.80 ±0.30^{a}	8.43 ±1.51^{abc}	19.32 ±1.56^{b}
4	11.14 ±1.35 ^{b}	4.95 ±0.65^{a}	7.11 ±1.15^{bcd}	23.20 ±0.45^{a}
5	10.79 ±1.01 ^{b}	2.21 ±0.30^{b}	10.06 ±1.47^{a}	23.06 ±0.76^{a}
6	8.17±0.13^{c}	1.43±0.32^{bc}	5.44±0.02^{d}	15.04±0.47^{c}
7	10.61±0.16^{b}	1.22±0.14^{c}	11.04±0.22^{a}	22.87±0.24^{a}
8	9.29±0.11^{bc}	1.87±0.01^{bc}	9.09±0.93^{ab}	20.25±0.80^{b}

The total extractive contents of all sample were in the range of 14.81-23.96%. The lowest contents were found in the samples of 'Trad Sri thong' cultivar (sample 2), 'Pattavia' cultivars collected from Amphoe Cha-am, Phetchaburi Province and Amphoe Ban-Kha, Ratchaburi Province, respectively. The highest value of total extractive was the samples of 'Pattavia' cultivar from Amphoe Ban-Kha, Ratchaburi Province. This highest value corresponded to highest contents of lipophilic substances. Lignin contents of all pineapple leaf fibers were in the range of 2.90-4.17% (Table 2). The three cultivars collected from eastern region of Thailand, i.e. 'Pattavia' culrivar from Amphoe Ban Chang, Rayong Province (sample 4), 'Trad Sri Thong' cultivar from Trad Province (sample 2) and 'Thong Rayong' from Rayong Province (sample 3) exhibited higher content of lignin than the cultivars from other regions. The low contents of lignin found in the sample collected from the province of the south-central region (Phetchaburi Province (sample 6), and Prachuap Khiri Khan Province (sample 7 and 8). These results suggested that the area of cultivars affected on the lignin contents of pineapple leaf fibers. In general, mechanical treatment or extraction of agricultural or agro-industry wastes could defibration of the raw material; however, this process could not remove some

substances, e.g. lignin from those raw material. Lignin plays important role in mechanical properties as well as in color of final product, especially in pulp and paper products. Alpha-cellulose content in this study were in the range of 48.20-58.97% (Table 2). The review of Todkar and Patil (2019) reported that pineapple leaf fibers contained 67-83% of cellulose. This implied that pineapple leaf fiber contents of our sample were lower than those of samples, which might be due to the different cultivar and areas of cultivation as well as the different extraction methods. More than 54% of alpha-cellulose found in the sample of 'Trad Sri Thong' and 'Thong Rayong') cultivated from eastern region (sample 2 and 3, respectively) and the 'Pattavia' cultivated from south-central region (sample 6, 7 and 8). These could be pointed that the areas of cultivated had more affected on cellulose content than the cultivars done. By considering hemi-cellulose contents, all fiber samples exhibited these values in the range of 13.67-18.49%. The lowest hemicellulose content found in 'Pattavia' cultivars from Phetchaburi Province (sample 6), whereas the highest one found in the same cultivar collected from Lampang province (sample 5). The results indicated that the hemicellulose content did not depended on cultivars and the area of cultivation. Moreover, it was found that the highest content of ash found in 'Pattavia' cultivar in sample 6 (Phetchaburi Province) followed by the same cultivar of sample 5 (Lampang province). It can be considered that the area of cultivation affecting on ash content, while the cultivar did not.

Table 2 Chemical components of pineapple leaf fibers.

Sample No.	Chemical components (%)				
	Lignin	Holocelluluse	Alpha-cellulose	Hemi-cellulose	Ash
1	3.98±0.23^{b}	67.71±0.07^{d}	49.58±0.24^{d}	18.13±0.17^{ab}	2.63±0.01^{b}
2	4.17±0.11^{ab}	74.61±1.01^{a}	56.97±0.84^{b}	17.64±0.17^{b}	2.21±0.23^{b}
3	4.05±0.04^{ab}	70.83±0.57^{c}	54.04±0.28^{c}	16.79±0.29^{c}	2.14±0.10^{b}
4	4.61±0.61^{a}	66.33±0.72^{d}	48.20±0.05^{d}	18.13±0.77^{ab}	2.60±0.01^{b}
5	3.94±0.01^{b}	67.88±0.67^{d}	49.39±0.54^{d}	18.49±0.13^{a}	3.68±0.02^{a}
6	2.90±0.05^{c}	72.64±0.91^{b}	58.97±0.98^{a}	13.67±0.06^{d}	3.86±0.81^{a}
7	2.83±0.09^{c}	70.76±0.94^{c}	54.29±1.18^{c}	16.47±0.24^{c}	2.56±0.19^{b}
8	3.31±0.06^{c}	71.60±0.64^{bc}	55.10±0.69^{c}	16.50±0.05^{c}	2.05±0.10^{b}

Proximate chemical composition and forage nutritional quality of pineapple leaf residues

The chemical compositions of pineapple leaf residues after extraction were determined according to AOAC standard and the results were shown in Table 3. The values of chemical residues contained 4-91-10.25% of protein, 17.55-26.71% of crude fiber, 1.43-2.93% of crude lipid, 4.27-7.40% of moisture, and 4.76-7.66% of ash. There is no relationship between cultivar or cultivation areas on chemical compositions of pineapple leave residues found in this study.

Table 3 Proximate chemical contents of pineapple leaf residues.

Sample No.	Chemical components (%)				
	Protein	Crude fiber	Crude Lipid	Moisture	Ash
1	7.22	22.29	1.43	4.15	6.47
2	8.78	23.10	1.61	5.08	5.86
3	8.34	24.96	1.69	5.67	6.31
4	4.91	26.71	1.45	5.63	5.68
5	5.31	22.12	1.65	7.40	7.32
6	7.81	20.78	1.89	4.32	7.66
7	8.57	21.28	2.93	4.81	5.18
8	10.25	17.55	1.80	4.27	4.76

The important indicators of forage nutritional quality, i.e. moisture content, crude proteins (CP), acid detergent fiber (ADF), neutral detergent fiber (NDF) and total digestible nutrient (TDN) were studied and the results were shown in Figure 3 Moisture contents of pineapple leave residues were in the range of 4.15-7.40 % (Table 4), indicating low moisture contents and good forage Quality (moisture content < 12%) (Figure 3A). The highest moisture content was presented in the sample collected from Lampang province (Pattavia cultivar). The protein content, one of the most desirable components in forage quality, of eight sample were shown in Figure 3B. A good quality forage, the amounts of CP must be higher than 7% to guarantee adequate N supply for effective rumen microbial fermentation. The protein contents of all residues were in the ranges of 4.9-10.25%. The highest protein content (10.25%) was exhibited in Pattavia cultivar, which growing in Amphoe Kui Buri, Prachuap Khiri Khan Province (Figure 3Bh), whereas the lowest protein content of this cultivar (5.31%) was observed when the cultivar was grown in Lampang province (Figure 3Be). Trad Sri Thong had protein content of 8.78% (Figure 3Bb), while protein content of Thong Rayong (Rayong province) was 8.35% (Figure 3Bc). Almost Pattavia cultivars showed high protein content with good quality, excepting the samples grown in Amphoe Ban Chang, Rayong province (4.91%, Figure 3Bd) and Amphoe Mueang, Lampang province (5.31%, Figure 3Be). These results indicating that not only cultivar but also the growing area were affected in protein content of pineapple leaf residues.

The fiber content, i.e. NDF and ADF affected in forage quality. The NDF value represents the intake potential and energies of the forage or animal feed. NDF of a good forage quality with high digestibility was less than 55%. NDF values of pineapple leaf residues were in the range of 54.49-62.93% (Figure 3C). Almost sample exhibited medium quality of forage, excepting Pattavia cultivars grown in Ratchaburi (Figure 3Ca) and Phetchaburi provinces (Figure 3Cf) and Trad Sri Thong from Trad province (Figure 3Cb) which showed poor forage quality. The best for age quality of these pineapple leaf residue samples was shown in Pattavia cultivar which collected from Amphoe Kui Buri, Prachuap Khiri Khan Province (Figure 3Ch). The ADF is an inverse correlation of digestibility; the more content of ADF the less digestibility (Moreno-Reséndez et al., 2017). This value used for estimating the animal feed energy as well as its digestibility. The high digestibility and good quality of forage containing ADF of 26—34% (Nadeem et al., 2019). The ADF of pineapple leaf residues were analyzed and the values were shown in Figure 3D. ADF of all samples were in the range of 26.71-36.17%, indicating all sample is the good quality of forage (Figure 3Db-h), excepting the sample of Pattavia grown in Amphoe Ban Kha, Ratchaburi Province which ADF value was in the medium Quality (Figure 3Da). These results might indicate that the pineapple leaf residues grown in eight areas of Thailand could be used as a forage with a good quality of ADF.

The sum of CP, digestible fat, digestible NFC, and NDF was known as total digestible nutrient (TDN) which representing the forage energy and digestibility. The forage with superior quality and nutritive value exhibited TDN value equal or greater than 65% (Nadeem et.al., 2019). In this study the TND values of pineapple leaf residues were in the ranges from 60.72-70.63% (Figure 3E). The greatest value of TND came from the ‘Pattavia’ cultivar which collected from Amphoe Kui Buri, Prachuap Khiri Khan Province (70.63%, Figure 3Eh), whereas the lowest one was from the same cultivar collected from Ban Kha, Ratchaburi province (60.72%, Figure 3Ea).

From the above results, the most suitable of the pineapple leaf residues for forage application was the sample of ‘Pattavia’ cultivar which collected from Amphoe Kui Buri, Prachuap Khiri Khan Province, which reached the all value standards with high values of protein content and TND, whereas showed low values of moisture content, NDF and ADF.

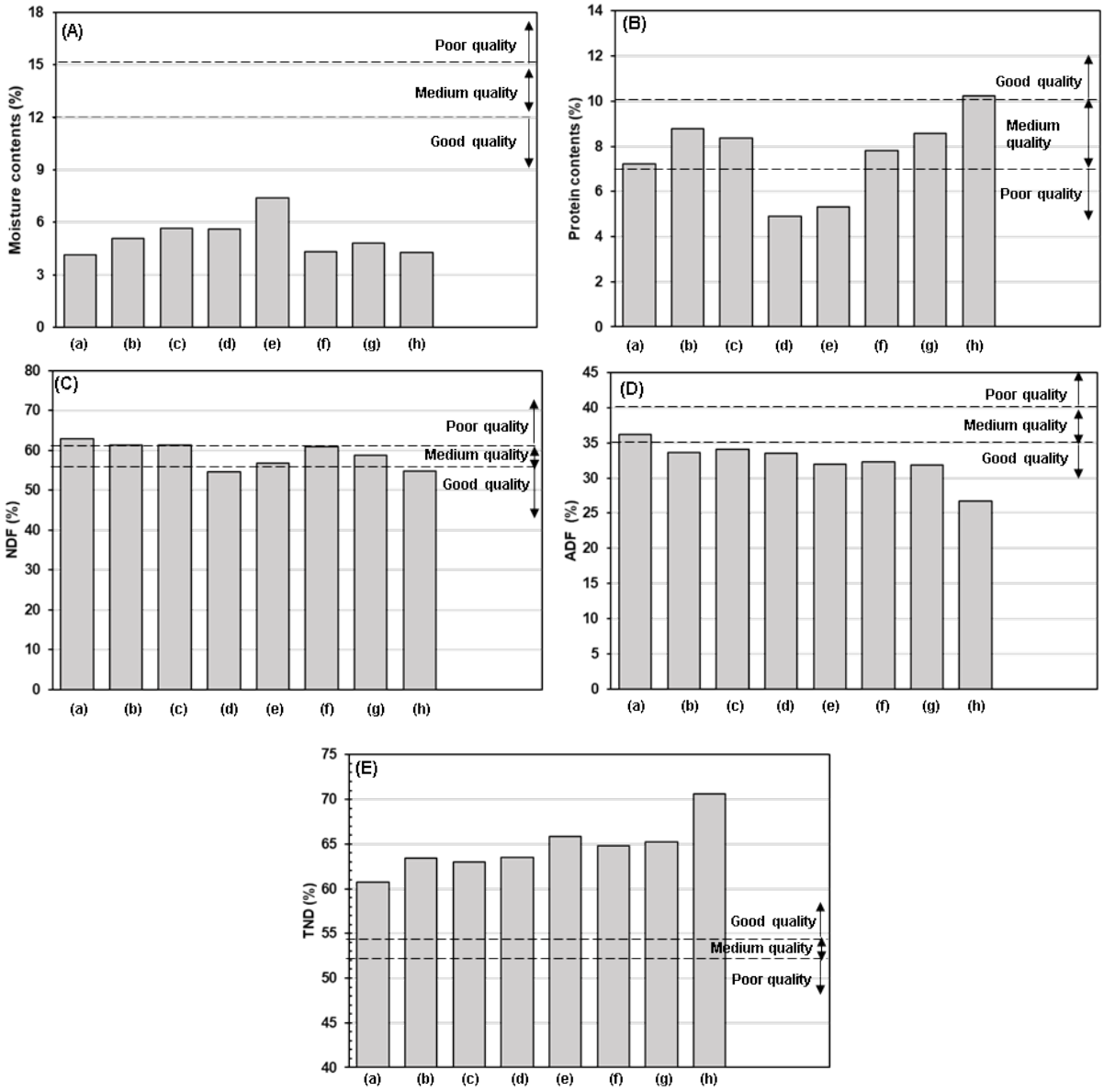

Figure 3. Forage compositions (A) moisture content, (B) protein content, (C) NDF, (D) ADF and (E) TND of extracted pineapple leaf resides from different samples; (a) sample 1, (b) sample 2, (c) sample 3, (d) sample 4, (e) sample 5, (f) sample 6, (g) sample 7 and (h) sample 8.

CONCLUSIONS

Chemical compositions of pineapple leaf fibers were affected by the cultivars and areas of cultivation. Alcohol-benzene extractives were influenced by the cultivar, while alcohol extractives were depended on the areas of cultivars. There is no observation of the relationship between of both cultivars or cultivated areas and the hot-water extractive. High lignin contents found in the samples grown in Eastern region without the influence of the cultivars. The high content of holocellulose and the alpha-cellulose were found in the Eastern and south-central region of Thailand. Ash and hemi-cellulose content did not change by the effect of cultivar and area of cultivation. The study of the proximate chemical composition of pineapple leaf residues for forage application found that there is no relationship between cultivar or cultivation areas on chemical compositions of pineapple leave residues found in this study. Moreover, pineapple leaf residues after fiber extraction can be used as forage, especially the sample of 'Pattavia' cultivar which collected from Amphoe Kui Buri, Prachuap Khiri Khan Province. It showed that application of pineapple leaf residues after fiber extraction reached all standards with good forage quality.

ACKNOWLEDGEMENT

The authors would like to thank the Kasetsart University Research and Development Institute (KURDI), Kasetsart University, Bangkok, Thailand for financial support.

REFERENCES

AOAC, 2010. Official Methods of Analysis of Association of Official Analytical Chemists. 18 ed. Washington DC.

Chintagunta A. D., Ray S. and R. Banerjee. J. Clean. Pro. 2017. 165: 1508-1516. DOI 10.1016/j.jclepro.2017.07.179.

Correia R. T. P., P. McCue, M. M. A. Magalhães, G. R. Macêdo and K. Shetty. 2004. Process. Biochem. 39(12): 2167-2172. DOI 10.1016/j.procbio.2003.11.034.

Goering H. K. and P. J. Van Soest. 1970. Forage fiber analyses: apparatus, reagents, procedures, and some applications. Agricultural Research Service, US Department of Agriculture.

Hazarika D., N. Gogoi., S. Jose, R. Das and G. Basu. 2017. J. Clean Pro. 141: 580-586. DOI 10.1016/j.jclepro.2016.09.092.

Ketnawa S., P. Chaiwut and S. Rawdkuen. 2012. Food. Bioprod. Process. 90(3): 385-391. DOI 10.1016/j.fbp.2011.12.006.

Mainoo N. O., S. Barrington, J. K. Whalen and L. Sampedro. 2009. Bioresour. Technol. 100(23): 5872-5. DOI 10.1016/j.biortech.2009.06.058.

Moreno-Reséndez A., J. E. Cantú Brito, J. L. Reyes-Carrillo and V. Contreras-Villarreal. 2017. Sci. Agr. 8(2): 127-135. DOI http://dx.doi.org/10.17268/sci.agropecu.2017.02.05.

Nadeem M., T.H. Pham, A. Nieuwenhuis, W. Ali, M. Zaeem, W. Ashiq, S.S.M. Gillani, C. Manful, O.A.
Adigun, L. Galagedara, M. Cheema and R. Thomas. 2019. Plant. Sci. 283: 278-289. DOI 10.1016/j.plantsci.2019.03.014.

Najeeb M. I., M. T. H. Sultan, Y. Andou, A. U. M. Shah, K. Eksiler, M. Jawaid and A. H. Ariffin. 2020. J. Mater. Res. Technol. 9(3): 3128-3139. DOI 10.1016/j.jmrt.2020.01.058.

Rattanathawornkiti K., T. Kanchanaketu, A. Suwanagul and V. Hongtrakul. 2016. Genomics and Genetics. 9(2&3): 56-65. DOI 10.14456/gag.2016.8.

Sibaly S. and P. Jeetah 2017. J. Environ. Chem. Eng. 5(6): 5978-5986. DOI https://doi.org/10.1016/j.jece.2017.11.026.

Todkar S. S. and S. A. Patil. 2019. Compos. Part B: Eng. 174: 106927. DOI 10.1016/j.compositesb.2019.106927.

Zainuddin M. F., S. Rosnah, M. M. Noriznan and I. Dahlan. 2014. Agric. Agric. Sci. Procedia. 2: 224-230. DOI 10.1016/j.aaspro.2014.11.032.

EC-P002

STIMULATION OF β-GLUCAN PRODUCTION FROM EDIBLE MUSHROOM BY DIFFERENT LIGHT WAVELENGTH

Waraporn Apiwatanapiwat[1], Udomlak Sukatta[1], Prapassorn Rugthaworn[1], Antika Boondaeng[1], Phornphimon Janchai[1], Nutthamon Boonlum[1], Supatchalee Sophonthammaphat[2], and Pilanee Vaithanomsat[1]*

[1] Kasetsart Agricultural and Agro-Industrial Product Improvement Institute, Kasetsart University, Bangkok, Thailand

[2] Department of Alternative Energy Development and Efficiency, Ministry of Energy, Thailand

*E-mail: aappln@ku.ac.th

ABSTRACT

Light wavelengths affect the mycelial mushroom. Mushrooms contain polysaccharides, identified as beta-glucan (β-glucan) which are the functional polysaccharides capable of reducing blood cholesterol, glucose levels, as well as possessing anti-tumor and anti-microbial activities. This experiment aimed to identify a suitable light wavelength for stimulating growth and β-glucan production in *Auricularia delicata* (RSPG00622). To accomplish this, samples were irradiated with the red LED (620-645 nm), the green LED (515-545 nm), the blue LED (460-475 nm) and the white LED (380-760 nm) light color in solid and submerged cultures at room temperature to induce the growth of mycelium and β-glucan productions. The light intensity consisted of 50, 100 and 150 Lux, respectively. The results showed that the diameter (7.37 cm) of *A. delicata* (RSPG00622) mycelium under the blue LED at the intensity of 150 lux provided maximum growth in solid culture followed the white, red and green light (6.76, 6.73, 6.66 cm., respectively). In submerged culture, the blue light was the best condition for biomass and β-glucan productions. The highest β-glucan production was at 41.47% (w/w), while the biomass production was 4.67 g/L.

Keywords: β-glucan, Edible mushroom, Light-emitting diode

INTRODUCTION

Mushrooms can be divided into edible and non-edible mushrooms. Non-edible mushrooms are poisonous mushrooms such as some species of Death cap mushroom, causing intoxication. Mushrooms contain polysaccharides such as β-glucan that can be found not only in the cell wall of fungi, but also in the cell wall of plants and bacteria (Gawronski et al., 1999). In general, when comparing the protein content in dried mushrooms and vegetables, it was found that dried mushrooms contained much higher protein content than vegetables. In addition, mushrooms are rich in essential amino acids, vitamins B1, B2, B12, C, D, E, riboflavin, niacin and fiber but low in calories, carbohydrate, fat and sodium. Besides the above mushroom properties, it also has medicinal properties such as antioxidant, anticancer, antidiabetic, antiallergic, immunomodulating, cardiovascular protector, anticholesterolemic, antiviral, antibacterial, antiparasitic, antifungal, detoxification, and protect against tumor development and inflammatory processes (Valverde et al., 2015). Polysaccharides have been found in many kinds of mushrooms. It could be able to reduce the blood pressure and cholesterol in the blood, against the occurrence of cancer cells and prevent abnormalities of the coronary arteries. β-glucan is a water-soluble polysaccharide consisting of monomer sugar such as glucose. It is connected with cellulose (β-(1 → 4)-glucan) by a glycosidic bond which is naturally found in plants such as oats, barley and microbes such as bacteria, fungi, algae and yeast (Gawronski et al., 1999: Goodridge et al., 2009). β-glucan is used as cancer prevention, immune adjustment, antimicrobial resistance, antioxidant and anti-inflammatory agent (Rieder and Samuelsen, 2012). The clinical study has shown that β-glucan is linked to the activation of macrophages, NK-cells, T-cells, B-cells from the body's natural defense system (Lindequist et al., 2005). According to previous research, *Auricularia delicata* (RSPG00622) was isolated from natural resources and it contained the highest β-glucan. Therefore, in this study, growth and β-glucan production were stimulated by light-emitting diode (LED) at different wavelengths and intensities in solid-state and submerged cultures.

MATERIALS AND METHODS

Microorganism and culture conditions

The *Auricularia delicata* (RSPG00622) was isolated from natural resources at Amnat Charoen province. The mycelium was cultivated on a PDA plate for 7 days at room temperature and used as the seed culture. The seed culture was transformed to 300 ml PDA media broth in 1000 ml flasks and incubated in different light wavelengths at room temperature with shaking at 100 rpm for 5 days. The mycelia were harvested and separated from the media by filtration through Whatman No.1 filter paper. About 300 ml of distilled water was used to wash the filtered mycelia 3 times. The filtered mycelia were dried overnight by a hot air oven. The dried mycelia were kept at -20 ºC until use. The mycelia were used for glucan extraction and mycelium extraction.

LED light sources

For mycelium growth, the size of the LED growth chamber was 60 x 40 x 25 cm, and this chamber was divided into 5 zones with 5 different light wavelengths including darkness treatment. Four LEDs emitting red, green, blue and white in the respective wavelengths 620-645 nm, 515-545 nm, 460-475 nm and 380-760 nm were chosen as light sources for *A. delicata* (RSPG00622). All LEDs were set at the quantity of light at 50, 100 and 150 lux. For β-glucan and mycelium extract, the different LED lights were set under the shaker platform with quantity at below 150 lux.

Determination of β-glucan content

The β-glucan content was determined according to the instruction of Mushroom and Yeast beta-glucan (Megazyme), as follows:

Total β-glucan determination

Two milliliters of 12 M sulfuric acid were added into a culture tube which contains dried mycelia 90 mg and then closed with a cap. The sample was mixed well by vortex mixer and place it in ice water bath for 2 h with interval mixing by vortex mixer. Four milliliters of distilling water were added into the tube and then mix well for 10 seconds. Water was added more 6 ml and incubated at 100 ◦C in a water bath for 5 min. The mixture was continue incubated for 2h. The samples were cool down at room temperature and added 6 ml of 10.0M KOH. The samples were adjusted the volume in 100 ml volumetric flask by 200 mM Sodium acetate buffer, pH 4.5 and then centrifuged to separate supernatant for D-glucose assay. A 0.1 ml exo-1,3- β-Glucanase and β-Glucosidase was added to 0.1 ml aliquot of sample and the mixture was again mixed thoroughly. The mixture was incubated at 40 °C for 60 min then added 3 ml GOPOD in the test tube and continue incubated at 40 °C. After 20 min in a water bath, the absorbance was measured at 510 nm.

α-glucan determination

Milled mycelia sample approximately 100 mg were added to the culture tube then added 2 ml of 1.7M NaOH to each tube and suspend the pellets by stirring for 20 min in an ice water bath. The 8 ml of 1.2M sodium acetate buffer (pH 3.8) was added to each tube with stirring and then immediately added 0.2 ml of amyloglucosidase plus invertase, mix well and place the tubes in a water bath at 40 °C. The samples were incubated at 40 °C for 30 min with intermittent mixing on a vortex stirrer and then centrifuged to separate supernatant. Transfer 0.1 ml aliquots of either the diluted or undiluted supernatants into a glass test tube then added 0.1 ml of 200mM sodium acetate buffer (pH 4.5) plus 3.0 ml of GOPOD reagent and incubated at 40 °C for 20 min. the absorbance was measured at 510 nm.

Calculation of β–glucan

β–glucan (%w/w) = Total glucan (%w/w) - α-glucan (%w/w)

RESULTS AND DISCUSSION

Effect of light wavelength and intensity on the mycelial growth of Auricularia delicata (RSPG622)

LEDs with different wavelengths and intensities were utilized in *Auricularia delicata* (RSPG622) solid-state culture to observe the mycelium growth. The maximum diameters of 3 mycelia colonies were measured every day and the mean values were calculated. Although the mycelia were stimulated by blue LED (5.91 cm) at intensity 50 lux as seen in Figure 1, there was no significant difference in growth between green LED, white LED and red LED which were 5.88, 5.88 and 5.77 cm, respectively after 7 days.

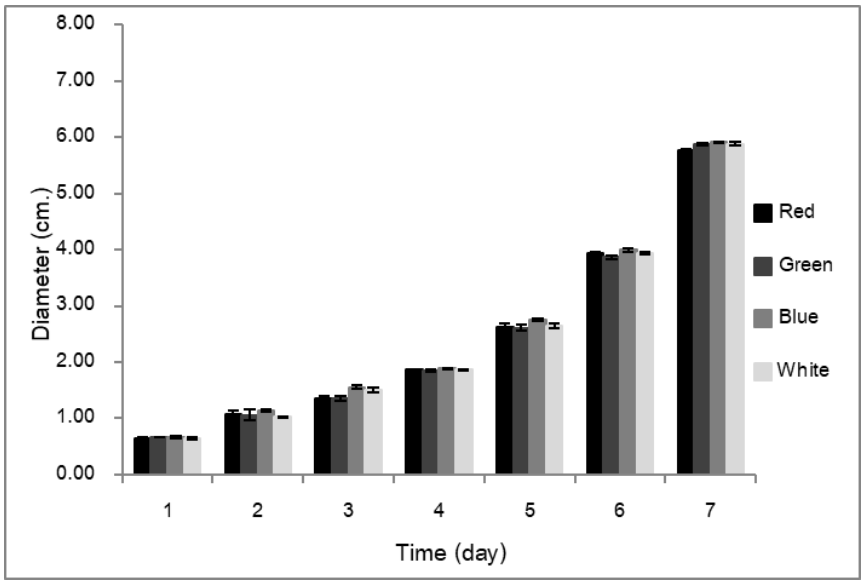

Figure 1. Effect of light-emitting diode (LED) sources in different wavelengths on the growth of *Auricularia delicata* (RSPG622) at intensity 50 lux.

When the applied lighting intensity was 100 lux, the blue light encouraged the best growth of *A. delicata* (RSPG622) then white, red and green light are the maximum growths of 7.10, 6.80, 6.35 and 6.35 cm. respectively as shown in Figure 2.

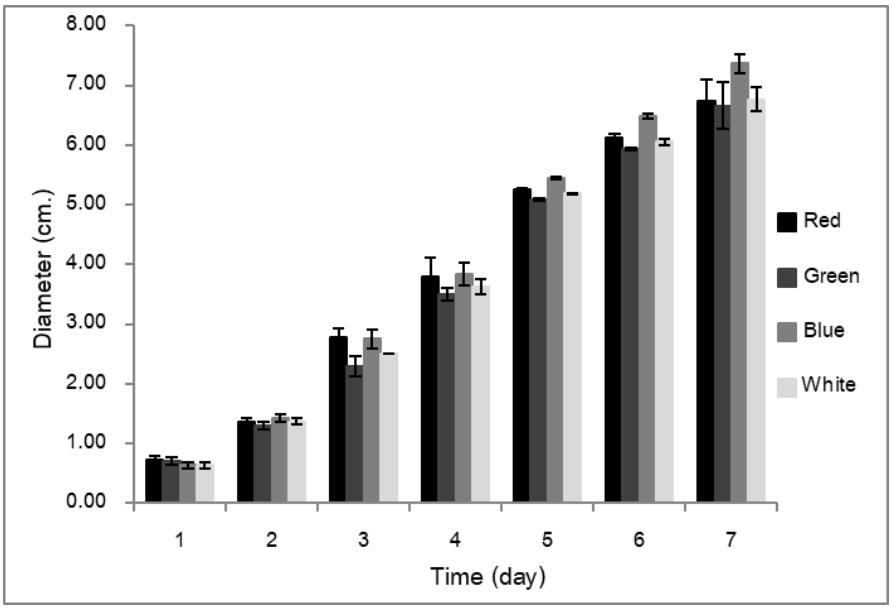

Figure 2. Effect of light-emitting diode (LED) sources in different wavelengths on the growth of *Auricularia delicata* (RSPG622) at intensity 100 lux.

The suitable color of light at intensity 150 lux for growth of *A. delicata* (RSPG622) on agar medium was a blue color. It showed higher growth than white, red and green color which were 7.37, 6.76, 6.73 and 6.66 cm, respectively as shown in Figure 3. On the other hand, Wu et al., (2013) found that using blue light had a negative effect on mycelium growth of *Pleurotus eryngii* in solid culture.

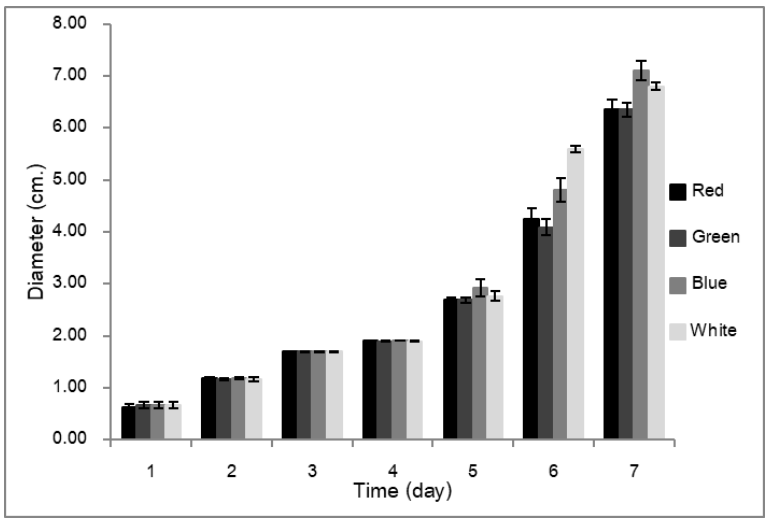

Figure 3. Effect of light-emitting diode (LED) sources in different wavelengths on the growth of *Auricularia delicata* (RSPG622) at intensity 150 lux.

The growth of *A. delicata* (RSPG622) under the blue LED at various intensities was compared. It found that the highest growth was detected at intensity 150 lux as shown in Table 1. The results showed that the widest diameter and maximum growth rate of mycelium were recorded under light intensity 150 lux with a maximum diameter of 7.37 cm at 7 days and growth rate 1.09 cm/day.

Table 1 Diameter of *Auricularia delicata* (RSPG622) colony on agar medium under blue light at 50, 100 and 150 lux.

Density of light (Lux)	Day1	Day2	Day3	Day4	Day5	Day6	Day7
50	0.67±0.02	1.14±0.02	1.55±0.03	1.89±0.01	2.76±0.02	4.00±0.03	5.91±0.01
100	0.67±0.06	1.19±0.02	1.70±0.01	1.91±0.00	2.92±0.17	4.81±0.22	7.10±0.19
150	0.63±0.06	1.43±0.06	2.75±0.16	3.84±0.19	5.44±0.02	6.49±0.04	7.37±0.16

Effect of light wavelength on biomass yield and β-glucan production of Auricularia delicata (RSPG622) in the liquid medium

Mycelial biomass yield under four LED lamps was conducted in liquid medium at intensity 150 lux. The results showed that the highest mycelial biomass of 4.67 g/L was obtained under blue LED after incubated for 5 days as shown in Figure 4. Higher mycelia biomass was obtained as 4.47 and 4.00 g/L under respective illumination of red and white LEDs while the lowest biomass production was found under green LED (2.54 g/L).

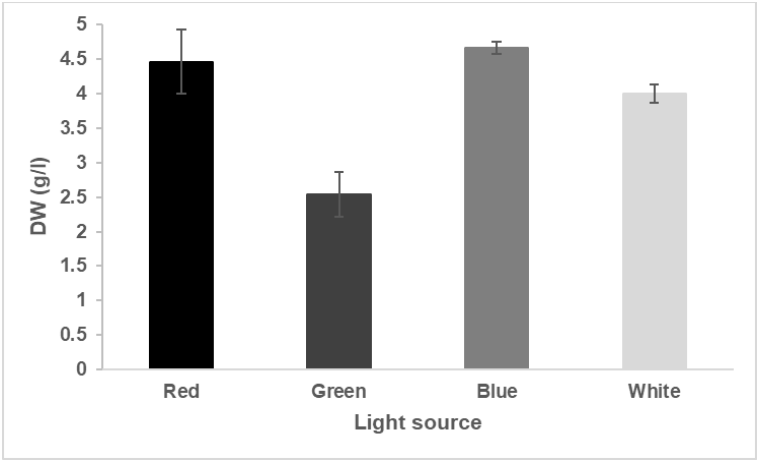

Figure 4. Effect of light -emitting diode (LED) sources in different wavelength on biomass yield of *Auricularia delicata* (RSPG622) at intensity 150 lux.

The total glucan, α-glucan and β-glucan from *A. delicata* (RSPG622) under various LEDs were analyzed and explored at intensity 150 lux. It was found that maximum total glucan and β-glucan production was obtained (42.55 and 41.47%(w/w)) under blue LED while the maximum α-glucan was detected under green LED (4.62%(w/w)) (Table 2).

Table 2 Effect of the light-emitting diode (LED) sources in different wavelengths on total glucan (A), α-glucan (B) and β-glucan (C) of *Auricularia delicata* (RSPG622) at intensity 150 lux.

Light source at 150 Lux	Total glucan (%w/w)	α-glucan (%w/w)	β-glucan (%w/w)
Red	36.99±0.58	0.77±0.01	36.10±0.79
Green	37.65±0.16	4.62±0.02	33.03±0.16
Blue	42.55±0.38	1.09±0.02	41.47±0.37
White	40.56±0.37	2.49±0.05	38.07±0.32

CONCLUSIONS

In conclusion, the stimulation of *Auricularia delicata* (RSPG622) growth could be achieved with LED at different wavelengths and intensity. The blue light with wavelengths between 460-475 nm at 150 lux could stimulate the growth of *Auricularia delicata* (RSPG622) in both solid and liquid medium. In a solid medium, the mycelia growth rate was up to 0.96 centimeters per day when incubated under blue light at intensity 150 lux. In liquid medium, the dry weight of this species under the same condition gave the highest dry weight when compared with other colors and intensity. The light had a significant impact on the total glucan, α-glucan and β-glucan production of *A. delicata* (RSPG622). The cultivation of *A. delicata* (RSPG622) under blue LED provided the highest β-glucan while the white LED gave the highest total glucan and α-glucan.

ACKNOWLEDGEMENT

This work was supported by Science and Technology Research Grants from Toray Science Foundation (TSF).

REFERENCES

Gawronski, M., J. T. Park, A. S. Magee and H. Conrad. 1999. Microfibrilla structure of PGG-glucan in aqueous solution as triple-helix aggregates by small angle X-ray scattering. Biopolymers 50(6): 569-578.

Goodridge, H. S., A. J. Wolf and D. M. Underhill. 2009. β-glucan recognition by the innate immune system. Immunol. Rev. 230(1): 38-50.

Lindequist, U., T. Niedermeyer and W. D. Jülich. 2005. The pharmacological potential of mushrooms. Evid. Based Complementary Altern. Med. 2(3): 285-299.

Rieder, A. and A. B. Samuelsen. 2012. Do cereal mixed-linked β-glucans possess immunemodulating activities? Mol. Nutr. Food Res. 56: 536-547.

Valverde, M. E., T. Hernández-Pére and O. Paredes-López. 2015. Edible mushroom: Improving human health and promoting quality life. International Journal of Microbiology. http://dx.doi.org/10.1155/2015/376387.

Wu, J-Y., H-B. Chen, M-J. Chen, S-C. Kan, C-J. Shief, Y-C. Liu. 2013. Quantitative analysis of LED effects on edible mushroom *Pleurotus eryngii* in solid and submerged cultures. J. Chem. Technol. Biotechnol. 88: 1841-1846.

EC-P003

COMPARISON OF CONVENTIONAL AND ACCELERATED SOLVENT EXTRACTION METHODS ON BIOACTIVE COMPOUNDS AND ANTIOXIDANT ACTIVITIES FROM RICEBERRY BRAN

Supatchalee Sirichokworrakit[1], Udomlak Sukatta[2]*, Hathairat Rimkeeree[1], Withida Chantrapornchai[1], and Prapassorn Rugthaworn[2]
[1] Department of Product Development, Faculty of Agro-Industry, Kasetsart University 50 Ngam Wong Wan Rd, Latyao, Chatuchak, Bangkok 10900, Thailand
[2] Kasetsart Agricultural and Agro-Industrial Product Improvement Institute, Kasetsart University 50 Ngam Wong Wan Rd, Latyao, Chatuchak, Bangkok 10900, Thailand
*E-mail: aapuls@ku.ac.th

ABSTRACT
Riceberry bran, a byproduct of the rice milling process, is one of the bioactive compound sources with potential health benefits. The purpose of this study was to compare the bioactive compounds extraction methods from Riceberry bran using accelerated solvent extraction (ASE) and conventional solvent extraction (CSE) methods. The experimental conditions studied included extraction temperatures (60, 70 and 80 °C) for 15 min using CSE method and extraction temperatures (60, 70 and 80 °C) for 5 min using ASE method. The extracts were measured for their total phenolic content (TPC), total anthocyanin content (TAC) and free radical scavenging activity using the DPPH, ABTS, and FRAP assays. The highest value of TPC was 19.70±0.68 mgGAE/g using ASE method at 80°C for 5 min and it was not significantly different in the CSE extract (80 °C for 15 min) and the highest value of TAC was 88.54±0.29 mg/100g using ASE method at 80 °C for 5 min which was not significantly different in the CSE extract (80 °C for 15 min). The highest value of % scavenging activity (DPPH and ABTS assays) and FRAP value were 57.94±0.31, 26.39±0.27 and 85.06±0.28 mmol/g, respectively) using ASE method (80 °C for 15 min). The main phenolic acids and anthocyanins found in Riceberry extract were vanillic acid, 4-hydroxybenzoic acid, cyanidin 3-glucoside and peonidin 3-glucoside that were found in ASE extract rather than CSE extract. Therefore, the results show significant difference in bioactive compounds and antioxidant activities between the two extraction methods, which indicate that the ASE method gave more effective extract than the CSE method.
Keywords: Riceberry bran, Conventional solvent extraction, Accelerated solvent extraction, Bioactive compounds

INTRODUCTION

Rice, *Oryza sativa* L., is one of the most important cereal crops and the staple food source consumed by over half of the world's population (Chatthongpisut et al., 2015). Riceberry, deep purple grain, is well known as containing high antioxidant properties and Khao Dawk Mali 105, well known as fragrant rice (Leardkamolkarn et al., 2011). Riceberry bran is a byproduct of the rice milling process. It is always extracted oil and defatted Riceberry bran is used as an ingredient in animal feed. Riceberry bran is a source of antioxidants such as phenolic acid and anthocyanin. The main bioactive compounds of Riceberry bran are phenolic acids and anthocyanins, which have been recognized as health-enhancing substances because of their antioxidant anti-inflammatory, antiartheriosclerosis, anticancer, hyperlipidemia and hypoglycaemic effect (Chatthongpisut et al., 2015). The extraction method is important in the extraction of bioactive substances which affect the quality of the extract. CSE method using water bath is an indirect heating method used for decades. Compare to CSE, ASE methods have been developed as an alternative to current extraction methods such as soxhlet, maceration, percolation offering advantages with respect to solvent consumption, extraction yields, extraction time and reproducibility. The purpose of this work was to compare the extraction efficiency of phenolic anthocyanin and antioxidant activity from Riceberry bran using CSE and ASE methods.

MATERIALS AND METHODS

Sample preparation

Defatted Riceberry bran was obtained from Sunfood Corp Limited (Samutprakan, Thailand). The bran was previously dried at 80°C for 60 min, and later it was sieved through 20 –100 mesh screen. The defatted Riceberry bran with a moisture content of 5.65% was sealed in a plastic bag and kept in the dark at -20°C until use, so as to slow down anthocyanins degradation in the raw material.

Sample extractions

For the CSE method, the studied factor was extraction temperatures (60, 70, and 80 °C) for 15 min in a temperature-controlled water bath with shaker Schutzart DIN 40050 – IP 20 (Memmert GmbH + Co. KG, Schwabach, Germany) with a shaking speed of 120 rpm. The Riceberry bran (10 g) was extracted in 200 mL of 70% ethanol. For the ASE method, it was performed on a Dionex ASE 350 system (Thermo Scientific, USA). The Riceberry bran (10 g) was mixed with diatomaceous earth (DE) in a proportion of 1:1 and placed in a 100 mL stainless steel extraction cell. A cellulose D28 filter (Dionex Corporation) was placed at the bottom of the extraction cell to avoid the collection of suspended particles in the collection vial. The extraction cells were arranged in the sample carousel and prefilled with the solvent (70% ethanol). The studied factor was extraction temperatures (60, 70, and 80 °C) for 5 min (Abdel-Aal et al., 2014). The extraction was done using 1 cycle and the cell was rinsed with 120% flush of extraction cell. The extract was collected in 250 mL collection vials. The resulting extracts from CSE and ASE method were filtered through a Whatman No. 5 filter paper and stored at -18 °C until use.

Determination of total phenolic content

TPC was measured using a modified Folin-Ciocalteu method (Wolfe et al., 2003). Different concentrations (0-200 µg/mL) of Gallic acid was used as standard with some modifications. The absorbance of the mixtures was determined at 760 nm in a spectrophotometer (UV mini-1240, Shimadzu, USA). TPC in the extract was expressed in mg Gallic acid equivalent/g.

Determination of total anthocyanin content

The TAC of the extract was measured by pH-differential method described by Giusti et al. (2011). The absorbance of the samples was measured at 510 nm and 700 nm in pH 1.0 and 4.5 using a spectrophotometer (UV mini-1240, Shimadzu, USA). The TAC was measured in term of cyaniding-3-glucoside equivalent using a molar extinction coefficient of 26,000 and molecular weight of 449.2

$$A = (A_{510} - A_{700})_{pH1.0} - (A_{510} - A_{700})_{pH4.5} \quad (1)$$

$$\text{TAC (mg/100g)} = (A \times MW \times DF \times V \times 100) / (\varepsilon \times 1 \times G) \quad (2)$$

Where, DF is dilution factor, MW is the molecular weight of cyaniding-3-glucoside, V was the volume of solvent, ε is the molar absorptivity of the reference anthocyanin and G was the weight of sample.

HPLC analysis of phenolic acids

HPLC analysis was performed using Shimadzu system (Japan) with an Inertsil ODS-3 C18 packed column (ID 5 µm, 250 × 4.6 mm). The mobile phase consisted of acetonitrile (solvent A) and 1% formic acid (solvent B) at a flow rate of 1 mL/min which took 60 min with a linear gradient of 6-6% A (0-9 min), 6-15% A (9-10 min), 15-15% A (10-20 min), 15-23% A (20-21 min), 23-23% A (21-35 min), 23-50% A (35-36 min), 50-50% A (36-45 min), 50-6% A (45-47 min) and 6-6% A (47-60 min). A standard solution of phenolic acids (vanillic acid and 4-hydroxybenzoic acid) suspended in methanol (99%), was injected to evaluate the area under the curve of phenolic acids. Operating conditions were as follows: column temperature, 40 °C; injection volume, 20 µL; UV-diode array detection at 280 nm. Phenolic acids in the samples were identified by comparing their relative retention times and UV spectra with those of authentic compounds.

HPLC analysis of anthocyanins

Cyanidin-3-O-glucoside and Peonidin 3-glucoside were quantified using HPLC with an Inertsil ODS-3 C18 packed column (ID 5 µm, 250 × 4.6 mm). The mobile phase consisted of acetic acid (solvent A) and 0.85% phosphoric acid (solvent B) at a flow rate of 1 mL/min which took 55 min with a linear gradient of 0-7% A (0-5 min), 7-12% A (5-10 min), 12-23% A (10-20 min), 23-35% A (20-25 min), 35-100% A (25-30 min),

100% A (30-35 min), 100-0% A (35-45 min) and 0% A (45-55 min). A standard solution of anthocyanins (cyanidin 3-glucoside and peonidin 3-glucoside) was injected to evaluate the area under the curve of phenolic acids. Operating conditions were as follows: column temperature, 40 °C; injection volume, 20 µL; UV-diode array detection at 520 nm. Anthocyanins in the samples were identified by comparing their relative retention times and UV spectra with those of authentic compounds.

Radical DPPH$^{\cdot}$ scavenging activity (DPPH)

The free radical scavenging activity of Riceberry bran extracts was evaluated using the stable radical DPPH according to the method of Re et al. (1999). The analysis was done in triplicates for each extract. The absorbance of the mixtures was determined at 517 nm relative to the control (as 100%) using a spectrophotometer.

Radical ABTS$^{\cdot+}$ scavenging activity (ABTS)

ABTS radical scavenging activity was determined according to Re et al. (1999) with some modifications. A stable stock solution of ABTS radical cation was produced by reacting to a 7 mM aqueous solution of ABTS with potassium persulfate in the dark at room temperature for 12-16 h before use. The absorbance of the mixtures was determined at 734 nm relative to the control (as 100%) using a spectrophotometer.

Ferric reducing antioxidant power (FRAP)

FRAP assay was based on the reduction of Fe^{3+}–TPTZ to a blue-coloured Fe^{2+}–TPTZ. The FRAP assay was adapted from Kubola and Siriamornpun (2008). The antioxidant potential of sample was determined from a standard curve plotted using the $FeSO_4.7H_2O$ linear regression equation to calculate the FRAP values of the sample expressed as mmol of Fe (II)/kg.

Statistical Analysis

The experiment was conducted in a completely randomized design (CRD) with 6 treatments. Chemical data obtained from each samples were analysed using the analysis of variance (ANOVA) for significant variables ($p \leq 0.05$) using the SPSS statistical program version 12. Differences between means were determined with Duncan's new multiple range test (DMRT). All measurements were done in triplicate.

RESULTS AND DISCUSSION

TPC of the extracts from Riceberry bran using CSE and ASE methods shows in Figure 1. The results showed that there were significant differences in TPC of the extracts. The ASE extract (80 °C for 5 min) had the highest TPC (19.70±0.68 mgGAE/g). TPC of the CSE extract (80 °C for 15 min) was not significantly different from the ASE extracts (70 °C and 80 °C for 5 min). In addition, TPC of the ASE extracts (60 °C and 70 °C for 5 min) had higher content than the CSE extracts at the same extraction temperature.

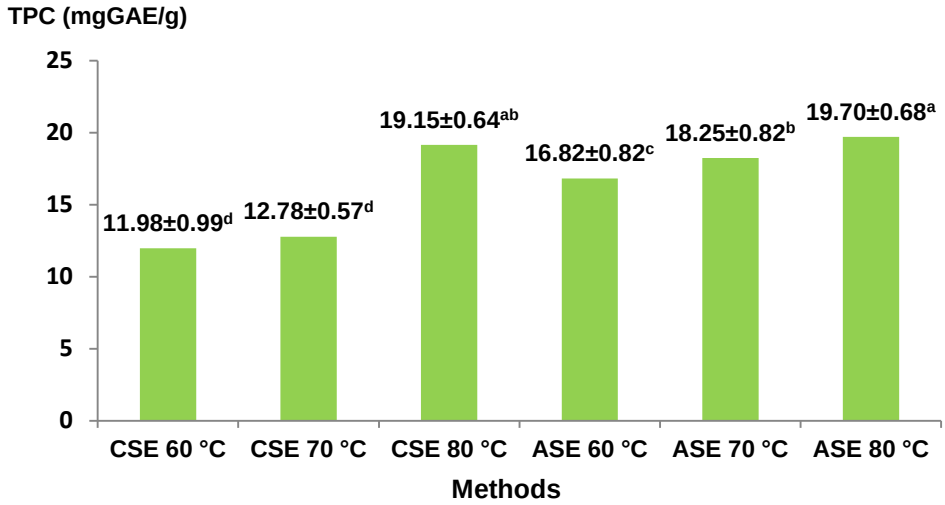

Figure 1. TPC of the Riceberry bran extracts using CSE and ASE methods.

The results indicated that ASE method at low extraction temperature and time could extract TPC higher than CSE method because to use high pressure during the extraction process of ASE method helps the solvent in a liquid state at elevated temperatures far above the boiling point. Moreover, high pressure increases the extraction efficiency by "pushing" the solvent into the pores, which results in antioxidant can be released from the matrix into the solvent (Sun et al., 2012).

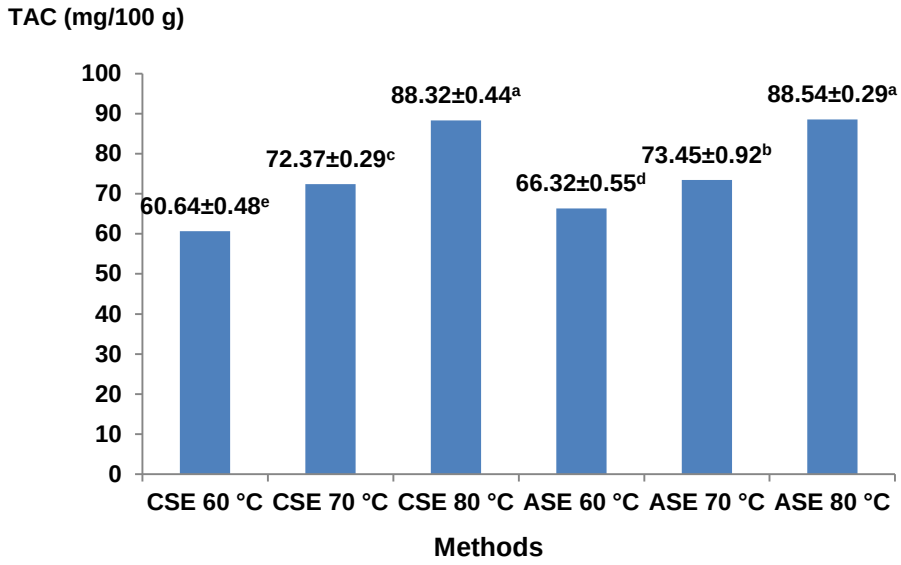

Figure 2. TAC of the Riceberry bran extracts using CSE and ASE methods.

TAC of the extracts from Riceberry bran using CSE and ASE method shows in Figure 2. The results found that there were not significant differences between the ASE extract (80 °C for 5 min) and the CSE extracts (80 °C for 15 min). The ASE extract (80 °C for 5 min) and the CSE extracts (80 °C for 15 min) had the highest TAC (88.54±0.29 and 88.32±0.44 mg/100g, respectively). In comparison, the ASE extracts had higher TAC than the CSE extracts at the same extraction temperature. The result revealed that the ASE method had effective TAC extraction and it was shorter extraction time than the CSE method. This result was supported by the works of Cai et al. (2016), which reported that the extraction efficiency of anthocyanins from purple sweet potato using ASE compared with CSE the results indicated that ASE method gave higher anthocyanins than and the CSE method.

Table 1 Effect of extraction methods on radical scavenging activities (DPPH, ABTS and FRAP assay).

method	Temperature(°C)	DPPH (%scavenging)	ABTS (%scavenging)	FRAP (mmole/kg)
CSE	60	47.95±0.71^{e}	19.35±0.70^{e}	63.47±0.65^{f}
	70	51.14±0.74^{d}	21.22±0.78^{d}	68.55±0.75^{e}
	80	55.24±0.51^{b}	25.01±0.97^{b}	81.95±0.32^{b}
ASE	60	53.63±0.16^{c}	23.13±0.41^{c}	73.65±0.13^{d}
	70	55.81±0.26^{b}	24.39±0.27^{b}	77.52±0.57^{b}
	80	57.94±0.31^{a}	26.39±0.27^{a}	85.06±0.28^{a}

$^{a-f}$ Means in same columns followed by different letters are significantly different ($p \leq 0.05$).

The extraction method and temperature affect radical scavenging activities (Table 1). The results indicated that there were significant differences in radical scavenging activities. The ASE extract (80 °C for 5 min) had the highest% scavenging of DPPH, ABTS assays and FRAP value. In comparison, the CSE extracts had lower radical scavenging activities than the ASE extracts at the same extraction temperature. This result was supported by the works of Li et al. (2019) which reported that ASE method was more effective compared to CSE method for TPC, TAC and radical scavenging activities. This enhancement

phenomenon could be attributed to the combined pressure and temperature. Therefore, the ASE method appears to be technically promising and economically viable in extracting natural antioxidants.

Table 2 Chemical composition of Riceberry bran extract by HPLC**.**

Compounds	CSE	ASE
Phenolic acids (μg/g)		
Vanillic acid	109.42±17.99[b]	153.05±15.17[a]
4-Hydroxybenzoic acid[ns]	131.16±31.01	183.55±17.11
Anthocyanins (μg/g)		
Cyanidin 3-glucoside	202.67±29.44[b]	292.99±19.01[a]
Peonidin 3-glucoside[ns]	43.70±6.59	52.89±1.68
Total bioactive compounds	487.14±65.56[b]	654.50±25.10[a]

[a-b] Means in same rows followed by different letter are significantly different ($p \leq 0.05$).
[ns] Means no significant difference.

Phenolic acids and individual anthocyanins contents of Riceberry bran extract from CSE extract (80 °C for 15 min) and ASE extract (80 °C for 5 min) are shown in Table 2. The main phenolic acids in Riceberry extract were vanillic acid and 4-hydroxybenzoic acid and the main anthocyanins were cyanidin 3-glucoside and peonidin 3-glucoside. The results show that vanillic acid, 4-hydroxybenzoic acid and cyanidin 3-glucoside of ASE extract had significantly higher content than CSE extract while peonidin 3-glucoside of CSE and ASE extracts were not significantly different.

CONCLUSIONS

To compare the extract from Riceberry bran which used CSE and ASE methods, the results obtained suggest that ASE extract had high TPC and TAC at all extraction temperatures. The efficiency of Riceberry bran ASE extracts had the highest radical scavenging activities. Furthermore, Phenolic acids and individual anthocyanins contents of ASE extract (80 °C for 5 min) had higher contents than CSE (80 °C for 15 min) excepted Peonidin 3-glucoside content. From the information mentioned above, it can be concluded that the ASE method seems to be more appropriate in extracting phenolic acid and anthocyanin from Riceberry bran as being comparable with the CSE method because the ASE was a pressured-liquid and short-time extraction and used the small solvent lower than CSE method.

ACKNOWLEDGEMENT

The authors gratefully acknowledge use of the services and facilities of Kasetsart Agricultural and Agro-Industrial Product Improvement Institute, Kasetsart University and department of product development, faculty of agro-industry, Kasetsart University.

REFERENCES

Abdel-Aal, E., H. Akhtar, I. Rabalski and M. Bryan. 2014. Accelerated, microwave-assisted, and conventional solvent extraction methods affect anthocyanin composition from colored grains. J. Food Sci. 79(2): C138-C145.

Chatthongpisut, R., Schwartz, S. J. and Yongsawatdigul, J. 2015. Antioxidant activities and antiproliferative activity of Thai purple rice cooked by various methods on human colon cancer cells. Food Chem. 188: 99-105.

Cai, Z., Z. Qu, Y. Lan, S. Zhao, X. Ma, Q. Wan and P. Li. 2016. Conventional, ultrasound-assisted, and accelerated-solvent extractions of anthocyanins from purple sweet potatoes. Food Chem. 197: 266-272.

Giusti, M. M. and R. E. Wrolstad. 2005. Characterization and measurement of anthocyanins by UV-visible spectroscopy. Current Protocols in Food Analytical Chemistry, 1, F1.2.1-F1.2.13.

Li, J., S. Zhang, M. Zhang and B. Sun. 2019. Novel approach for extraction of grape skin antioxidants by accelerated solvent extraction: Box–Behnken design optimization. J. Food Sci. Tech. 56(11): 4879-4890.

Leardkamolkarn, V., W. Thongthep, P. Suttiarporn, R. Kongkachuichai, S. Wongpornchai and A. Wanavijitr. 2011. Chemopreventive properties of the bran extracted from a newly developed Thai rice: The Riceberry. Food Chem. 125(3): 978-985.

Re, R., N. Pellegrini, A. Proteggente, A. Pannala, M. Yang and C. Rice-Evans. 1999. Antioxidant activity applying an improved ABTS radical cation decolorization assay. Free Radic. Biol. Med. 26(9-10): 1231- 1237.

Sun, H., X. Ge, Y. Lv and A. Wang. 2012. Application of accelerated solvent extraction in the analysis of organic contaminants, bioactive and nutritional compounds in food and feed. J. Chromatogr. A. 1237: 1-23.

Wolfe, K., X. Wu and R. H. Liu. 2003. Antioxidant activity of apple peels. J. Agric. Food Chem. 51: 609-614.

EC-P004

STUDY OF NEUTRALIZING AGENT TOLERANCE ON *BACILLUS COAGULANS* DSM1 FOR LACTIC ACID PRODUCTION

Rachaneekorn Klinsalee, Piraporn Pim-on, Phattharawan Yaemkaew, and Nilnate Assavasirijinda*
Department of Biology, Faculty of Science, King Mongkut's Institute of Technology Ladkrabang, Bangkok, Thailand
*E-mail: Nilnate.as@kmitl.ac.th

ABSTRACT
Nowadays, researchers are interested in the use of sodium hydroxide (NaOH) and potassium hydroxide (KOH) as a neutralizing agent for producing lactic acid. The advantages are no formation of precipitated waste which environmental friendly process and also reduced time and operation cost. *Bacillus coagulans* DSM1 is a thermophile that can produce L-lactic acid with a purity of 99.8% at 50-55 °C and using calcium carbonate as a neutralizing agent. The aim of this study is to determine level of sodium and potassium ion tolerance of *B. coagulans* DSM1 and preliminary apply NaOH as a neutralizing agent for lactic acid production. First, the tolerant abilities against NaOH, sodium chloride (NaCl), KOH, and potassium chloride (KCl) were determined. The results showed that *B. coagulans* DSM1 can tolerant to NaCl, KCl and KOH at a maximum concentration of 1 M, 1 M and 0.1 M on GYC agar, respectively. The NaOH tolerance was at a maximum concentration of 1 M at 1 minute in the solution before plating on GYC agar. Thus, the *B. coagulans* DSM1 seems sensitive to sodium and potassium ions. The growth of *B. coagulans* DSM1 in GYC and GY medium, with and without NaOH as a neutralizing agent were investigated. The GYC and GY medium showed the highest OD600 at 0.7741 and 0.3353, respectively. While the added NaOH in GY medium at 6 hr shown the highest OD600 of 0.5567. Thus, the neutralizing agent is still needed for cell growth and lactic acid fermentation. So, the further studies have to find the method for developing the *B. coagulans* DSM1 to tolerant to sodium hydroxide.
Keywords :*Bacillus coagulans* DSM1, Neutralizing agent, Lactic acid

INTRODUCTION

Polylactic acid (PLA) is a lactic acid polymer that can be used to produce biodegradable plastics (Bozell and Petersen, 2010). Lactic acid can be produced in both chemical and biological methods (Garlotta, 2001). However, the production of PLA needs to use high-purity L-lactic acid or D-lactic acid otherwise the resulting polymer would be amorphous polymer, which is not accepted for industrial used (Nair and Laurencin, 2007; Södergård and Stolt, 2002). The production of lactic acid by biological methods can produce either L-lactic or D-lactic acid with a high purity. Thus, the high purity of lactic acid provides facilitations for further industrial used. On the contrary, chemical methods production produces lactic acid in a mixture of L-and D-lactic (racemic mixture) (John et al., 2007).

B. coagulans are thermophilic bacteria that can produce L-lactic acid with a high purity up to 99.8% at a temperature of 50-55 °C and can also use cheap carbon sources, no need complex nitrogen sources as well as fermentation in anaerobic condition (Peng et al., 2013; Jiayang et al., 2009; Limin et al., 2010). In addition, the *B. coagulans* can also utilize agricultural waste as an energy source. The use of such species is cost effective when producing lactic acid at an industrial level (Limin et al., 2013). For example, Limin (2013) produced lactic acid at 50 °C from thermophilic *B. coagulans* using Jerusalem artichoke powder as a carbon source and corn steep powder as a nitrogen source. In the fed-batch fermentation, it can produce lactic acid up to 134 g/l with a productivity of 2.5 g/l/hr and the yield of 0.96 g/g of reducing sugar. However, the production of lactic acid by *B. coagulans* was used calcium carbonate as a neutralizing agent which causing waste from the production process.

Some microorganism can use sodium hydroxide as a neutralizing agent in lactic acid fermentation which can take the advantages of non-waste production, low cost and simplified process. Example, an alkaliphilic *Bacillus* sp. N16-5 can tolerant to sodium chloride up to 15% and sodium lactate up to 38.35% (Nilnate et al., 2016). Belong to the mechanism of sodium ions elimination through the cell walls and the

maintenance of alkaline pH cell, the strain can used sodium hydroxide as a neutralizing agent during the production process.

The aim of this study is to determine level of sodium and potassium ion tolerance of *B. coagulans* DSM1 and preliminary apply NaOH as a neutralizing agent for lactic acid production. If the *B. coagulans* DSM1 can uses NaOH as a neutralizing agent, lactic fermentation by the strain will be improved and also taken the advantages from the strain abilities, reduced cost, simplified process as well as environmental friendly.

MATERIALS AND METHODS

Ion-resistance ability test and sodium hydroxide tolerance test

B. coagulans DSM1 was grown on GYC medium which includes glucose 50 g/l, yeast extract 10 g/l and calcium carbonate 30 g/l. The 24 hr of single colony was sub-cultured on GYC agar with NaCl concentration of 0, 0.17, 0.34, 0.51, 0.68, 0.86 and 1 M, KCl concentration of 0, 0.40, 0.67, 1.0, 1.34 and 2.01 M and KOH concentration of 0, 0.1, 0.2, 0.5, 1.0 M. Then, the plates were incubated at 45 °C for 48 hr and growth colonies were observed.

For NaOH tolerance test, the single colony was cultured in GYC broth for 24 hr. The 1 ml of cultures were pipetted into 5 ml of sodium hydroxide solution at concentrations of 0, 0.1, 0.2, 0.5, 1.0, 2.5, 5.0, 10.0 M and lefted at room temperature for 0, 1, 5 and 10 minutes before streak on GYC agar plate. The GYC agar plates were incubated at 45 °C for 48 hr and growth colonies were observed. All experiments were repeated 2 times. All experiments were performed in duplicate and repeated twice.

Observation growth of B. coagulans DSM1 on GYC medium with and without neutralizing agent

The 48 hr single colonies were cultured in 5 ml GYC broth and Incubated at 45 °C for 48 hr, then transferred to 100 ml of GYC broth and incubated at 45 °C for 48 hr. The culture was used as starter culture. The 10% inoculum were inoculated into GYC, GY (glucose 50 g/l, yeast extract 10 g/l) and GY with NaOH)GYN (with 100 ml medium in 250 ml conical flaks. For GYN medium, 5 molar NaOH will be added at after 6 hr of incubation until the pH value reach to 7.0 (approximate 0.2 ml). The growth was cultured at 45 °C and observed Optical Density at 600 nm (OD600) every 6 hr for 24 hr. The sample from GYC medium was spinned down in microcentrifuge tube for 10-15 sec at 5000 rpm and then the supernatant was transferred into new tube and added 4 M hydrochloric acid in a ratio of 10 µl per 1 ml of supernatant for eliminating trace of calcium carbonate. The pH value was also observed.

RESULTS AND DISCUSSION

Ion-resistance ability test

To observe Ion-resistance ability of *B. coagulans* DSM1, the colonies was grown on NaCl, KCl and KOH added GYC agar plates with various concentrations. The results have shown that *B. coagulans* DSM1 can growth normally on 0.17 M of NaCl and higher concentration of NaCl show slightly growth. However, it can tolerant up to 1 M of NaCl on GYC ager plate (Figure 1). The effect of KCl resistance ability shown that *B. coagulans* DSM1 can slightly growth on 0.40, 0.67, 1.0 M of KCl added GYC agar plates (Figure 2). For KOH resistance ability, *B. coagulans* DSM1 can only slightly growth on 0.1 M of KOH added GYC agar plates (Figure 3). At higher concentration of KCl and KOH, it cannot growth (data not shown).

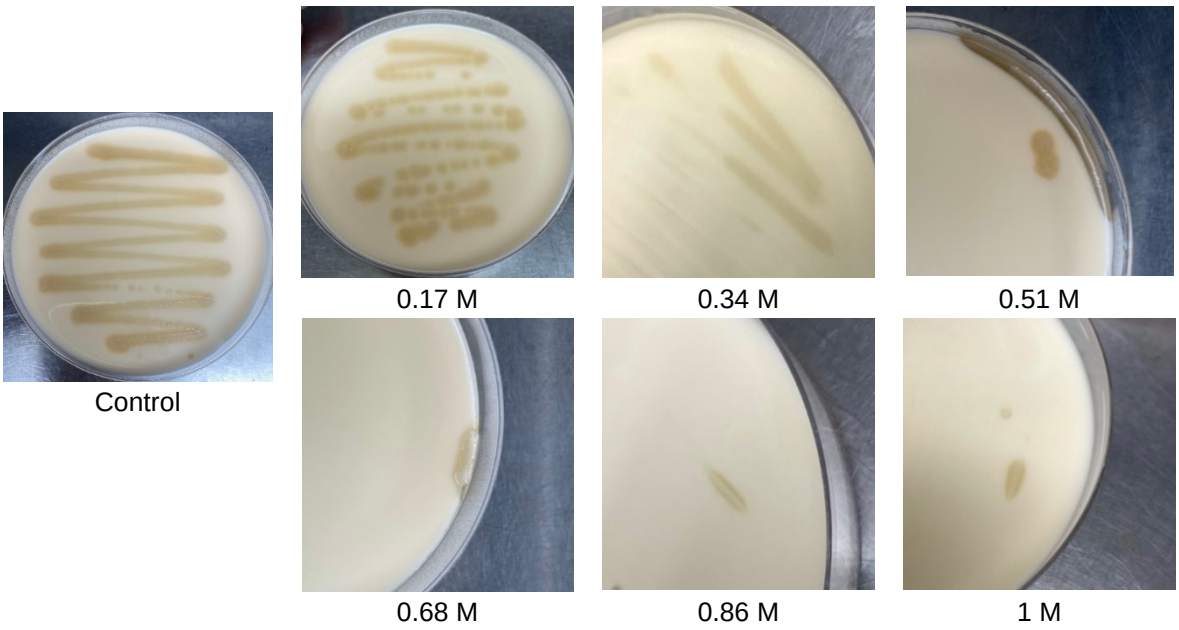

Figure 1. Growth of *Bacillus coagulans* DSM1on GYC agar (control) and GYC agar with NaCl at the concentration of 0, 0.17, 0.34, 0.51, 0.68, 0.86 and 1 M.

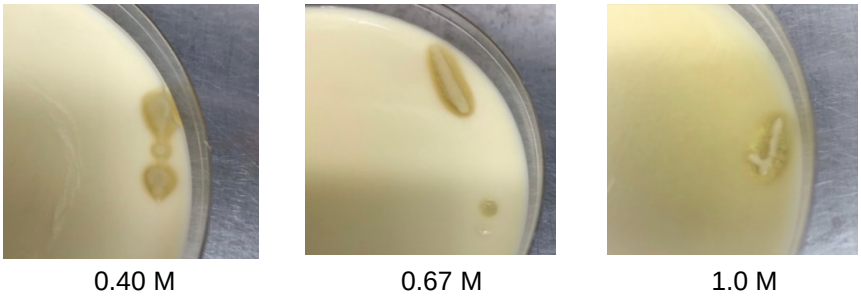

Figure 2. Growth of *Bacillus coagulans* DSM1 on GYC agar with KCl at the concentration of 0.40, 0.67, 1.0 M.

Figure 3. Growth of *Bacillus coagulans* DSM1 on GYC agar KOH at the concentration of 0.1 M.

The NaOH resistance of *B. coagulans* DSM1 was observed by contracting the cell with NaOH solution at each concentration. The results have shown that the strain is less tolerant to NaOH since 0.1 M of NaOH had an effect on cell growth at every contract times. However, the DSM1 strain can withstand and survive up to 1 M of NaOH for 1 minute. The results have shown in Figure 4.

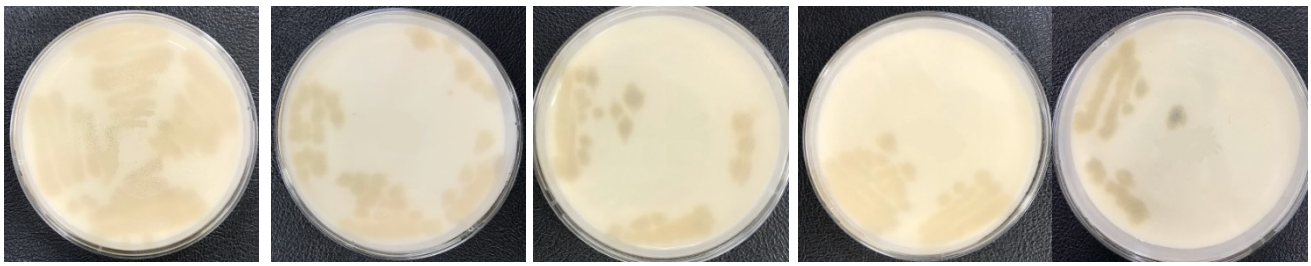

0 M 0.1 M 0.2 M 0.5 M 1.0 M

Figure 4. Growth of *Bacillus coagulans* DSM1on GYC agar after exposure to NaOH solution at the concentration of 0, 0.1, 0.2, 0.5, 1.0 M for 0, 1, 5 and 10 minutes.

Observation growth of B. coagulans DSM1 on GYC medium with and without neutralizing agent

Belong to the *B. coagulans* DSM1 shown less tolerant to each neutralizing agents that were used in this study. The growth in GYC, GY and GYN were observed for studying an effect of neutralizing agent on their growth. After incubated at temperature of 45 °C, the samples were collected every 6 hr and measured optical density at 600 nm and the pH value also. The results have shown in Figure 5.

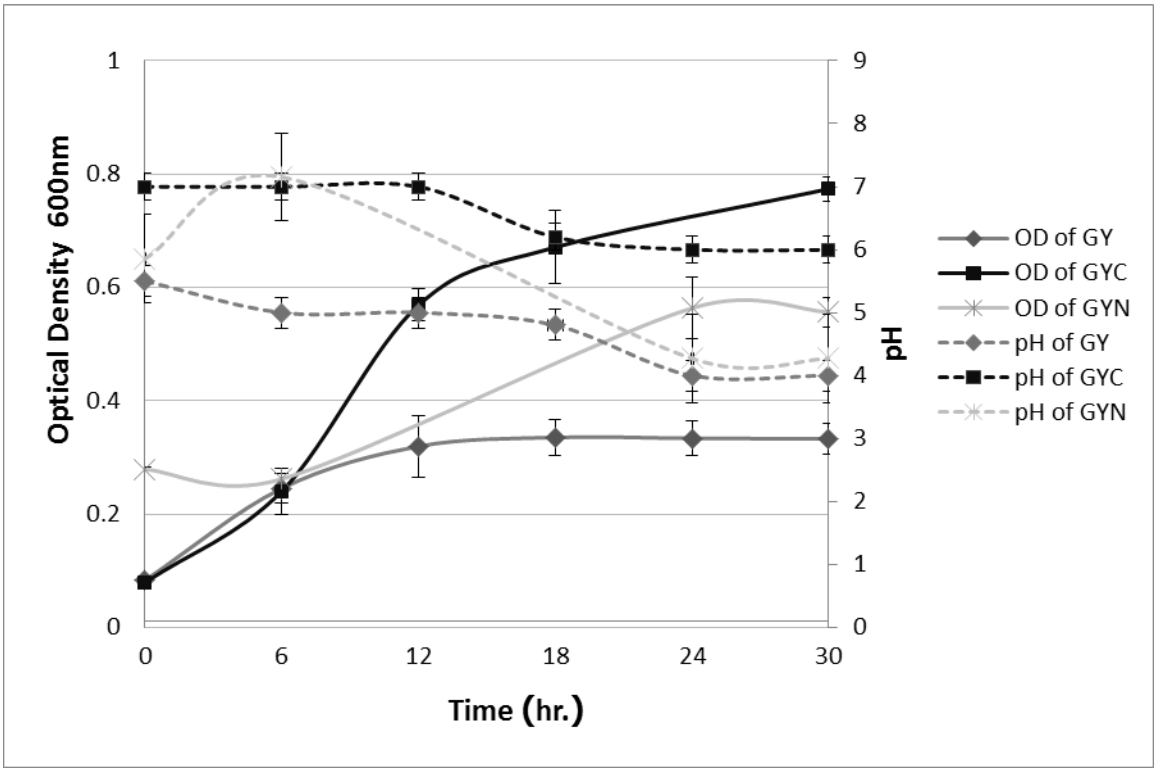

Figure 5. Growth curves of *Bacillus coagulans* DSM1 and pH values in GY, GYC and GYN medium. Each data point represents the average of three replicates, with the error bars representing the standard deviation.

When cultured *B. coagulans* DSM1 in GY medium (without neutralizing agent), a little bit growth was shown from 0 to 6 hr and then the growth was entering to stationary phase and the highest OD value of 0.3353 was achieved. As a result of the lactic acid production which released into medium, the pH was gradually decreased. In GYC medium which calcium carbonate is a neutralizing agent, the strain shown normally growth and the highest OD of 0.7741 was achieved. The pH of GYC medium was just slightly decreased through cultured time. In addition, when NaOH was added as a neutralizing agent in GYN medium at 6 hr of culture, *B. coagulans* DSM1 was shown growth better than in GY medium and the highest OD value of 0.5567 was achieved. It can be implied that the effect of neutralizing agent would be avoided the gradually decreased off pH and the effect of undissociated form of lactic acid because of the lactic acid can penetrate the bacterial membrane and strongly inhibit growth (Pieterse et al., 2005). Thus, the

fermentation process requires neutralization of the produced acid using a suitable neutralizing agent. However, $CaCO_3$ seem to the best neutralizing agent for *B. coagulans* DSM1 because of it promote the highest cell density than others neutralizing agents. Zhao (2012) and Hong-Wei (2010) had been reported that $CaCO_3$ is the most appropriate neutralizer by making lactic acid precipitate in the form of calcium lactate which facilitating the downstream separation of lactic acid. Moreover, the use of $CaCO_3$ would give higher lactic acid productivity than others neutralizing agent.

CONCLUSIONS

B. coagulans DSM1 shown less tolerant to each neutralizing agents that were used in this study and the neutralizing agent is still needed for cell growth and lactic acid fermentation. Thus, If lactic acid production from the strain need to be improved by using environmentally friendly neutralizer such as NaOH or KOH, the further studies have to find the method for developing the *B. coagulans* DSM1 to tolerant to the neutralizer.

ACKNOWLEDGEMENT

Authors would like to thank to Prof. Bo Yu at IMCAS for his support of *B. coagulans* DSM1.

REFERENCES

Bozell, J. J. and G. R. Petersen. 2010. Technology development for the production of biobased products from biorefinery carbohydrates—the US Department of Energy's "Top 10" revisited. Green Chemistry, 12(4): 539. doi: 10.1039/b922014c

Garlotta, D. 2001. A literature review of poly(lactic acid). J Polymers Envir. 9: doi:10.1023/A:1020200822435

Hong-Wei, Y., C.Tsia-Ju, P.Wei-Chin and W. Hsien-Jen. 2010. Effects of neutralizing agents on lactic acid production by *Rhizopus oryzae* using sweet potato starch. World J. Microbiol. Biotechnol. 26: 437–441. https://doi.org/10.1007/s11274-009-0186-0

Jiayang, Q., Z. Bo, W. Xiuwen, W. Limin, Y. Bo, M. Yanhe, M. Cuiqing, T. Hongzhi, S. Jibin and X. Ping 2009. Non-Sterilized Fermentative Production of Polymer-Grade L-Lactic Acid by a Newly Isolated Thermophilic Strain *Bacillus* sp. 2–6. PLoS One. 4(2): e4359. doi: 10.1371/journal.pone.0004359

John, R. P., K. M. Nampoothiri and A. Pandey. 2007. Fermentative production of lactic acid from biomass: an overview on process developments and future perspectives. Appl. Microbiol. Biotechnol. 74: doi: 10.1007/s00253-006-0779-6

Limin, W., B. Zhao, B. Liu, Y. Bo, M. Cuiqing, S. Fei, H. Dongliang, L. Qinggang, M .Yanhe and X. Ping. 2010.Efficient production of l-lactic acid from corncob molasses, a waste by-product in xylitol production, by a newly isolated xylose utilizing *Bacillus* sp. strain. Bioresour. Technol. 101(20): 7908-7915.

Limin, W., Z. Xue, B. Zhao, B. Yu, P. Xu and Y. Ma, 2013. Jerusalem artichoke powder: A useful material in producing high-optical-purity l-lactate using an efficient sugar-utilizing thermophilic *Bacillus coagulans* strain.Bioresour. Technol. 130: 174-180.doi: http://dx.doi.org/10.1016/j.biortech.2012. 11.144

Nair, L. S. and C. T. Laurencin. 2007. Biodegradable polymers as biomaterials. Prog. Polym. Sci. 32: doi: 10.1016/j.progpolymsci.2007.05.017

Nilnate, A., G. Deyong, Y. Bo, X. Yenfen. and M. YanHe. 2016. Efficient fermentative production of polymer grade d-lactate by an engineered alkaliphilic *Bacillus* sp. strain under non-sterile conditions. Microb. Cell Fact. 15:3.

Peng, L., L. Wang, C. Che, G. Yang, B. Yu and Y. Ma. 2013. *Bacillus* sp. strain P38: An efficient producer of l-lactate from cellulosic hydrolysate, with high tolerance for 2-furfural. Bioresour. Technol. 149: 169-176. doi: http://dx.doi.org/10.1016/j.biortech.2013.09.047

Pieterse, B., R. J. Leer, F. H. J. Schuren and M. J. van der Werf. 2005. Unravelling themultiple effects of lactic acid stress on *Lactobacillus plantarum* by transcription profiling. Microbiology.151: 3881–3894.

Södergård, A. and M. Stolt. 2002. Properties of lactic acid based polymers and their correlation with composition. Prog. Polym. Sci. 27. doi: 10.1016/S0079-6700(02)00012-6

Zhao, J. F., K. P. Li, Y. Z. Wang, J. H. Wang and S. D. Zhou. 2012. Effects of different neutralizing agents on D-(-)-lactic acid fermentation by *Escherichia coli*. W. Adv. Mat. Res. 463–464: 845–849. https://doi.org/10.4028/www.scientific.net/amr.463-464.845

EC-P005

SOY PROTEIN ISOLATE-BASED ADHESIVE FOR MANUFACTURING OF RICE STRAW FIBERBOARD

Kunat Kongsin[1,2], Chen Yu[3], Nutsinaporn Sinamonvech[4], Wuttinant Kongtud[1], Preeyanuch Srichola[1], and Rungsima Chollakup[1]*
[1] Kasetsart Agricultural and Agro-Industrial Product Improvement Institute, Kasetsart University, Chatuchak, Bangkok 10900, Thailand
[2] Biotechnology of Biopolymers and Bioactive Compounds Special Research Unit, Department of Biotechnology, Faculty of Agro-Industry, Kasetsart University, Chatuchak, Bangkok 10900, Thailand
[3] Panasonic Life Solutions Company, 1048, Kadoma, Osaka 571-8686, Japan
[4] Kokoboard Co., Ltd., Sam Khok, Pathum Thani 12160, Thailand
*E-mail: aaprmc@ku.ac.th

ABSTRACT
Conventional petroleum-derived thermosetting adhesives (urea–formaldehyde and phenolic resins) for wood-based panel manufacturing cause release of volatile organic compounds and formaldehyde, which contaminates the environment and affect to human health. Resulting in the development of alternative adhesives from biopolymers derived from renewable resources (e.g. protein, starch, lignin and tannin) due to their availability and sustainability. Therefore, this study was to elucidate the possibilities of using a bio-based adhesive from soy protein isolate (SPI) for rice straw fiberboard. To improve the SPI adhesive properties such as adhesion strength and water resistance, the SPI was denatured by react with urea under alkaline condition and then chemically modified by reactive epoxy groups of epoxy resin with amine hardener used as a curing agent. The rice straw fiberboards bonded with SPI based adhesive were prepared and characterized according to the Thai industrial standard for flat pressed particleboards (TIS. 876-2547) and compared with a commercial adhesive, methylene diphenyl diisocyanate (MDI). Results showed that the percentage of thickness swelling in water of the rice straw fiberboards prepared using SPI-based adhesives has lower than that of using commercial MDI. In considering, the production cost of SPI-based adhesives was still higher than commercial MDI around 7 times. However, the SPI-based adhesive is more easily biodegradable and being environmentally friendly without formaldehyde emissions.
Keywords: Soy protein isolate, Bio-based adhesive, Rice straw, Fiberboard

INTRODUCTION

Formaldehyde-based adhesives including phenol–formaldehyde, urea–formaldehyde resins and isocyanates have been mainly applied in pressed wood products such as particle board, plywood and fiberboard due to it provides durable adhesion performance (Pradyawong et al., 2017). However, formaldehyde-based resins negatively affect the environment and human health because it induces high carcinogenic and chronic toxic risks (Imam et al., 2013). Emissions of formaldehyde and the consumer awareness on unhealthy and non-environmentally products are important factor that facilitates the research and development on bio-based adhesive from natural renewable resources (Hemmila et al., 2017). Soy proteins, the main byproduct obtained from soybean oil production, are the most investigated natural compounds for producing adhesive due to their sufficient supply and low level of consumption by humans and animals (Wang et al., 2019). Soy proteins are already commercially used in wood adhesives, interior plywood and engineered wood flooring to replace formaldehyde-based adhesives (Vnučec et al., 2016). However, the application of soy protein-based adhesives have been limited due to high viscosity, short pot life, low bonding strength and poor water resistance (Ferdosian et al., 2017). To overcome this drawback, extensive researches have been conducted on improving the adhesive properties of SPI-based adhesives. There has been reported that adhesive properties of SPI based adhesives could be improve by different approach. For instance, using the modifying agents to denaturalize the higher order structure of soy protein such as alkaline chemicals, urea and sodium dodecyl sulfate to enhance the water resistance of the soy protein-based adhesive (Chen et al., 2015). Another research proposed to use cross-linker to react with the

amino group (-NH_2), carboxyl group (-COOH) and other exposed groups of soy protein to increase the cross-linking density of the soy protein-based adhesive. Epoxy crosslinking agents are commonly used to construct intra-penetrating or inter-penetrating networks with soy protein molecules for a stable crosslinking system (Pang et al., 2020).

In addition, rice straw is the main agricultural by-product of rice production at harvest. It is well documented that the rice straw open-field burning is practiced to facilitate quick planting of the next crop in many countries, including Thailand (Yodkhum et al., 2018). This improper rice straw management has promoted the utilization of rice straw for various applications in recent years. It has been found that rice straw could be recognized as an inexpensive natural lignocellulose resource, and it has the interesting characters of low density, biodegradability and high toughness with acceptable mechanical properties making it a potential candidate to replace wood four or fiber composites (Zhang et al., 2018).

Therefore, this study aimed to characterize the potential of rice straw for fiberboard manufacturing and develop the soy protein isolate-based formaldehyde-free adhesive by denaturalization of soy protein isolate using urea under the alkaline condition and chemical modification using epoxy resin with amine hardener used as a curing agent. The physical properties of the rice straw fiber were investigated. We compared this the soy protein isolate-based adhesive for rice straw fiber board with methylene diphenyl diisocyanate (MDI) adhesive which is a formaldehyde-free adhesive provided excellent mechanical board properties and lower levels of consumed resin but being a slight high resin cost.

MATERIALS AND METHODS

Preparation and characterization of rice straw and rice straw fiber

Rice straw was kindly provided from Kokoboard Co., Ltd., Thailand and then cut into chips with a length of 4-6 cm. Before further processing, the rice straw was dried in a hot air oven at 105 °C for at least 16 h to remove excess moisture content and then kept in a desiccator before used. The average moisture content of the dried rice straw was about 5-7%. In order to study the characterization of rice straw fiber, the cut rice straw was treated by an alkaline method using 15% of potassium hydroxide (% by oven dried weight of rice straw) at 100 ^{o}C for 1 h. Then, treated rice straw fiber was washed in water and dried at 60 ^{o}C.

The chemical compositions of the rice straw and rice straw fibers consisting of cellulose, hemicellulose lignin, ash and extractives were evaluated, followed by the standard method of the Technical Association of the Pulp and Paper Industry. The tensile properties (tensile strength, elongation at break and Young's modulus) of rice straw fibers were investigated by following the ISO 5076-1995(E) standard using a universal testing machine (Shimadzu AGS 5kN, Japan) with the gauge length of 15 mm and the cross head speed of 10 mm/min. In addition, water retention values of the rice straw fibers were determined following the ASTM D2402-01 standard. The rice straw fibers (approximately 0.10 – 0.15 g) were put into a net bag and then immerse into centrifuge tube containing distilled water and allowed to stand at room temperature for 3, 6, 9 and 24 h. To remove the excess water, the net bag containing rice straw fibers after the respective time of immersion was centrifuged at 100 rcf (relative centrifugal force), 25 °C for 5 min. The water retention value was then calculated by the equation (1);

$$\text{Water retention value (\%)} = [W_m - W_d]/W_d \quad (1)$$

where W_m = weight of the rice straw fiber after centrifuge and W_d = dried weight of the rice straw fibers after 24 h of immersion.

Preparation of soy protein isolate based adhesive

Soy protein isolate (SPI) based adhesive was prepared, followed by the method of Zhang et al. (2018) with some modifications. A suspension consisting of SPI/urea/distilled water was prepared in a weight ratio of 2:1:25 and the pH of the slurry were adjusted to 10.0 using 0.01 M of sodium hydroxide. The dispersion was stirred at 65 °C for 1 h, then epoxy resin YD580C (60 %wt of SPI) and hardener amine TH7257C (a curing agent for epoxy resin) was added to the dispersion. The obtained solution was continuously stirred for 2 h at the same temperature. The obtained glue was cool down to room temperature and immediately used.

Rice straw fiberboards manufacturing

The rice straw fiberboards were produced with a target density of 800 kg/m^3 with controlled of thickness at 4 mm. The rice straw was blended with the 10 %wt of SPI based adhesive in a plastic container by carefully hand mixing. The mixed rice straw fibers were transferred into a forming tool (90 x 90 x 10 mm) and then covered on both surfaces of the mixed rice straw with the Teflon sheets. The rice straw fiberboard was produced by the hot-pressing machine (mini test press, Toyoseiki 10, Japan) under 15 MPa at 150 °C for 15 min. The board was taken out of the hot-pressing machine and allowed to cool down at ambient conditions until further experiments.

Physical characterization of rice straw fiberboard

Physical properties of rice straw fiberboard were characterized according to the Thai industrial standard for flat pressed particleboards (TIS. 876-2547). The rice straw fiberboards were cut into rectangular pieces (50 x 50 x 4 mm) with a shape saw.

To calculate the density of the rice straw fiberboards, the lengths, widths and thicknesses of the test pieces were measured in millimeters by a vernier caliper and then there used to calculate its volume (lengths x widths x thicknesses). The density of the rice straw fiberboards was calculated by the equation (2);

$$\text{Density (kg/m}^3\text{)} = [m/v] \times 10^6 \quad (2)$$

where m = mass of fiberboard (g) and v = volume of fiberboard (mm^3)

The water absorption property of rice straw fiberboard was revealed by the measurement of thickness swelling in water. The test pieces were socked in tap water at 30 °C for 1 h, followed by drying at room temperature for 2 h. The thickness of the test pieces after immerse in water was measured and then calculated the percentage of thickness swelling by the equation (3);

$$\text{Thickness swelling (\%)} = [(t_2 - t_1)/t_1] \times 100 \quad (3)$$

where t_1 = the average thickness of the fiberboard before immersion in water and t_2 = the average thickness of the fiberboard after immersion in water.

RESULTS AND DISCUSSION

Chemical composition of the rice straw and alkaline treated rice straw fibers

Chemical composition of rice straw and are presented in Table 1. Rice straw showed high cellulose content around 25.01% and followed by 16.4 % of hemicellulose and 12% of lignin, respectively. In order to extract fiber from the rice straw fibers, the rice straw was treated with 15% (w/v) of potassium hydroxide at 100 ^{o}C for 1 h. This treatment was resulted to reduce hemicellulose and lignin, whereas its water-soluble extractives increased. However, the alpha-cellulose of the rice straw did not change with alkaline treatment.

Table 1 The chemical composition of rice straw and alkaline treated rice straw fibers

Chemical composition	**Content (% w/w)**	
	Rice straw	**Alkaline treated rice straw fibers**
Extractives	43.83 ± 0.20	54.42 ± 0.52
- Ethanol-benzene	5.42 ± 0.45	1.11 ± 0.02
- Ethanol	4.27 ± 0.35	0.38 ± 0.07
- Water	34.14 ± 0.99	52.93 ± 0.43
Holo-cellulose*****	41.41 ± 0.36	33.94 ± 0.28
Alpha-cellulose	25.01 ± 0.12	24.21 ± 0.02
Hemicellulose	16.40 ± 0.48	9.73 ± 0.26
Lignin	12.38 ± 0.22	6.71 ± 0.51
Ash	14.03 ± 0.01	13.16 ± 0.01

*****Holo-cellulose = Alpha-cellulose + Hemicellulose

Tensile properties of the rice straw fibers

The alkaline treated rice straw fibers were used to represent tensile properties and water retention property due to its purity and single fiber property. The tensile strength, elongation at break and Young's modulus of the alkaline treated rice straw fibers are showed in Table 2.

Table 2 Tensile properties of rice straw fibers

Tensile properties	
Tensile strength (MPa)	21.84 ± 8.43
Elongation at break (%)	7.27 ± 1.91
Young's modulus (MPa)	253.37 ± 99.78

Water retention property of the rice straw fibers

The water retention values of the rice straw fibers are shown in Figure 1. Rapidly increasing the water retention values (150%) were occurred in the initial time of water immersion, especially after 1 h. Then, the water retention values have slightly increased up to 200% at 24 h of water immersion.

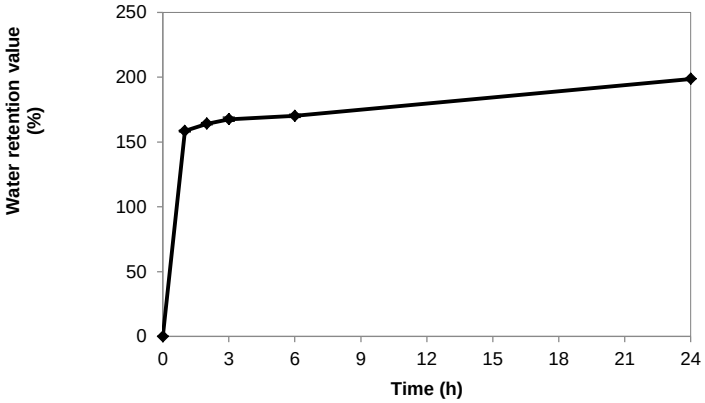

Figure 1. Water retention values of the rice straw fiber at different time of water immersion

The percentage of thickness swelling of the rice straw fiberboard prepared using SPI-based adhesives was lower than that of using the methylene diphenyl diisocyanate (MDI), a most common synthetic adhesive for wood-based panel industries (Table 3). This might be accomplished by the chemical reaction take place by functional groups of amino acid react with the carboxyl group in epoxy resin (Figure 2) and resulting in improving water resistance property of SPI-based adhesive.

Table 3 Physical characterization of rice straw fiberboards

Adhesives	**Density (kg/m^3)**	**Thickness swelling (%)**
Soy protein isolate-based adhesive	805.41	24.9
Methylene diphenyl diisocyanate (MDI)	869.90	28.3

Figure 2. Soy protein isolate reacted with urea and hydroxyl group (-OH) of cellulose of the rice straw.

Production cost of soy protein isolate-based adhesives

The production cost of soy protein isolate-based adhesives is estimated and presented in Table 4. The SPI-based adhesive has high production cost at 50.70 Baht/kg and 44.59 Baht per a rice straw fiberboard, which higher than that of the methylene diphenyl diisocyanate (MDI) for 7 times. The high price of raw materials for producing the SPI-based adhesive, especially the urea, was directly influenced by the overall production cost.

Table 4 Production cost of soy protein isolate-based adhesives for rice straw fiberboard and compared to MDI based adhesives.

Compositions	**Unit production cost (Baht/kg)**	**Content (g)**	**Production cost (Baht)**
Soy protein isolate (SPI)	180	20	12.60
Urea	650	10	22.70
Sodium hydroxide (NaOH)	320	250	6.70
Distilled water	10	0.88	8.70
Total	1160	280.90	50.70
Variable production cost per unit (1 unit per a rice straw fiberboard)			44.59
Methylene diphenyl diisocyanate (MDI)	130	49	6.37
Variable production cost per unit (1 unit per a rice straw fiberboard)			6.37

CONCLUSION

This work was demonstrated that the potential of rice straw for producing fiberboards using bio-based adhesive without formaldehyde emission. The water retention property of the SPI-based adhesive could be improved by adding urea and epoxy resin. Moreover, the rice straw fiberboard produced using the SPI-based adhesive has no toxicity and is easily biodegradable, which provides a sustainable solution to environmental concerns. However, the mechanical properties such as the internal bonging strength and bending strength of the rice straw fiberboard were needed for further analysis.

ACKNOWLEDGEMENTS

The authors would like to acknowledge the funding support from the Ministry of Higher Education, Science, Research and Innovation, Thailand under the Thailand Talent Mobility Program. The authors would also like to thank Ms. Chen Yu from the Panasonic Life Solutions Company, Japan for her suggestion and cooperation.

REFERENCES

Chen, M., Y. Chen, X. Zhou, B. Lu, M. He, S. Sun and X. Ling. 2015. Improving water resistance of soy-protein wood adhesive by using hydrophilic additives. Bio Res. 10(1): 41-54.

Ferdosian, F., Z. Pan, G. Gao and B. Zhao. 2017. Bio-based adhesives and evaluation for wood composites application. Polymers. 9: 70.

Hemmila V., S. Adamopoulos, O. Karlsson and A. Kumar. 2017. Development of sustainable bio- adhesives for engineered wood panels – A Review. RSC Adv. 7: 38604.

Imam, S. H., C. Bilbao-Sainz, B.-S. Chiou, G. M. Glenn and W. J. Orts. 2013. Biobased adhesives, gums, emulsions, and binders: current trends and future prospects. J Adhes Sci Technol. 27(18-19): 1972-1997.

Pang, H., S. Zhao, Z. Wang, W. Zhang, S. Zhang and J. Li. 2020. Development of soy protein-based adhesive with high water resistance and bonding strength by waterborne epoxy crosslinking strategy. Int J Adhes Adhes. 100: 102600.

Pradyawong, S., G. Qi, N. Li, X. S. Sun and D. Wang. 2017. Adhesion properties of soy protein adhesives enhanced by biomass lignin. Int J Adhes Adhes. 75: 66-73.

Vnučec, D., A. Kutnar and A. Goršek. 2016. Soy-based adhesives for wood-bonding – a review. Int J Adhes Adhes. 31(8): 910-931.

Wang, Z., Y. Chen, S. Chen, F. Chu, R. Zhang, Y. Wang and D. Fan. 2019. Preparation and characterization of a soy protein based bio-adhesive crosslinked by waterborne epoxy resin and polyacrylamide. RSC Advances. 9: 35273–35279.

Yodkhum, S., S. Sampattagul and S. H. Gheewala. 2018. Energy and environmental impact analysis of rice cultivation and straw management in northern Thailand. Environ Sci Pollut Res. 25: 17654-17664.

Zhang, W., H. Sun, C. Zhu, K. Wan, Y. Zhang, Z. Fang and Z. Ai. 2018. Mechanical and water-resistant properties of rice straw fiberboard bonded with chemically-modified soy protein adhesive. RSC Advances. 8: 15188–15195.

EC-P006

ENVIRONMENTALLY-FRIENDLY GREEN APPROACH FOR THE PRODUCTION OF ZINC OXIDE NANOPARTICLES FROM HERB AND FRUIT PEEL EXTRACTS

Prapassorn Rugthaworn*, Lalita Khacharat, Ketsaree Klinsukhon, Surisa Sakayaroj, Thipaporn Thongkum, Natthaporn Presunthiah, and Udomlak Sukatta
Kasetsart Agricultural and Agro-Industrial Product Improvement Institute (KAPI), Kasetsart University, Bangkok, Thailand
***E-mail: aappsr@ku.ac.th

ABSTRACT
Green synthesis of the nanoparticle is becoming popular due to its eco-friendliness, cost effectivity, and possibilities of large scale production. Zinc oxide nanoparticles (ZnO NPs) are known to be one of the most multifunctional inorganic nanoparticles with its application for use in various products. Recently zinc oxide nanoparticles have been well studied and used as a potential antimicrobial principle. This research study on biological synthesis of ZnO NPs using 15 Thai medicinal plant extracts. The result showed that lychee peel extract gave the high tendency to synthesize ZnO NPs which exhibited the sharpest absorbance peak at 365 nm [(Abs_{365}) 4.19]. The optimized parameters including concentration of Zinc Acetate $(CH_3COO)_2$ $Zn.2H_2O$, concentration of the extract and pH of the Zinc solution, that effect to synthesize ZnO NPs were determined to obtain high yield of ZnO NPs. The result reveal that the highest ZnO NPs synthesis was achieved by using Zinc Acetate $(CH_3COO)_2Zn.2H_2O$ at concentration 30 mM mixed with 10% w/v lychee peel extract and maintain the pH of solution at 12.0 and incubated at 90 °C for 2 h.
Keywords: Zinc oxide nanoparticles, Green synthesis, Plant extract, Nanotechnology

INTRODUCTION

Nanomaterial research has been developing rapidly and has potential in various areas, including biomedical, magnetics sciences, biosensors, optoelectronics, and catalysis. Zinc oxide nanoparticles (ZnO NPs), in particular, are environment friendly, offer easy fabrication and are non-toxic, biosafe and biocompatible making them an ideal candidate for biological applications (Mirzaei and Darroudi, 2017) due to their unique antibacterial and antifungal. Additionally, as per the US Food and Drug Administration, ZnO with other four zinc compounds have been listed as generally recognized as safe (GRAS) material (FDA, 2015). Various chemical methods have been proposed for the synthesis of ZnO NPs, such as reaction of zinc with alcohol, hydrothermal synthesis, wet chemical, chemical micro emulsion, vapor phase process, solvothermal, microwave-assisted combustion, chemical, direct precipitation and sono-chemical etc. (Elumalai and Velmurugan, 2015). However, these methods suffer various disadvantages due to the involvement of high temperature and pressure conditions and the use of toxic chemicals (Sabir et al., 2014). Green synthesis approaches are gaining interest circumventing the high costs and usage of toxic chemicals and harsh conditions for reduction and stabilization (Basnet et al., 2018). Physical, chemical, and biological methods have been used to synthesis ZnO NPs. Due to the increasing popularity of biological methods, different sources like bacteria fungus, algae, and plants have been used to produce ZnO NPs. Plant extract is used as an aid in the synthesis of NPs as it is cheap and safe to the environment.

Hence, this study was aimed to screen the kind of Thai herb and agro-industrial wastes for the selection of plant source having high potential for the synthesis of ZnO NPs. The study extent is to optimize the biosynthetic conditions for ZnO NPs production.

MATERIALS AND METHODS

Preparation of plant extract

Fifteen Thai medicinal plants were collected and cleaned by washing several times with running water and subsequently with distilled water. Plant samples were dried at room temperature in shade until all moisture was lost (12–14 days). Plant samples were then ground to yield coarse powder, 5 gm of which was

boiled in 100 mL of double distilled water for 30 min (Jamdagni et al., 2018). The aqueous extract was then cooled, filtered using Whatman No.1 filter paper and stored at 4 ^{o}C for further use.

Synthesis of zinc oxide nanoparticles

Zinc oxide nanoparticles were synthesized using zinc acetate dihydrate $Zn(CH_3COO)_2 \cdot 2H_2O$ as described previously by Gnanasangeetha and Thambavani (2013). Briefly, 10 mM solution of zinc acetate was taken and plant extract was added. Two milliliters of 5% plant extracts was added to 50 mL of zinc acetate solution. The pH of the mixture was maintained at 12.0 and the solution was stirred continuously for 2 h at 90 °C. A white precipitate resulted which was then dried at 60 °C overnight. Prior to drying, the precipitate was centrifuged at 15,000 rpm for 5 min and washed twice with sterile de-ionized water to remove any residue of the extract. Complete conversion to ZnO nanoparticles takes place during drying. All the experiments were performed in triplicate.

Optimization of synthesis parameters for zinc oxide nanoparticles

The synthesis conditions were optimized for the current reaction by varying various parameters involved in synthesis. Various concentrations of zinc acetate, from 5 mM to 50 mM were used as substrates. Lychee extract concentration, from 1% to 20% (w/v) were used as an effective chelating agent. Finally, the mixture was stirred continuously using a magnetic stirrer and was maintained at increasing pH values of 3, 7, 9, 12 and 14 using 2 M NaOH solution. The same temperature at which synthesis was carried out was used for overnight drying of the precipitate obtained.

UV–Visible spectroscopy

For UV–Visible spectroscopy, the resultant nanopowder from each of the reactions was re-suspended in equal amount of sterile de-ionized water and spectrum scans were performed using UV–Vis Spectrophotometer UV-1280 from Shimadzu, in the wavelength range of 200–800 nm.

FT-IR spectroscopy

Fourier transform infrared (FT-IR) spectroscopy helps establish the identity of various phyto-chemical constituents involved in the reduction and stabilization of the nanoparticles. FT-IR spectrum for dried and powdered ZnO NPs was obtained using Perkin Elmer FT-IR Spectrophotometer Frontier using the technique of Attenuated Total Reflectance (ATR) in the range of 4000–500 cm^{-1}.

Characterization

The surface morphology, particles size and composition of ZnO NPs were investigated by field emission scanning electron microscopy (FESEM) and energy dispersive X-ray spectroscopy (EDX, Zeiss Supra 35VP).

RESULTS AND DISCUSSION

Screening of plant for ZnO NPs biosynthesis

This study was aimed to screen the kind of Thai herb having high potential for the synthesis of ZnO NPs. After biosynthesis process, the nanopowder synthesized was stored in dried form in centrifuge tubes. The room temperature UV–Vis absorption spectrum of the ZnO NPs is shown in Figure 1. The ZnO NPs are dispersed in water with concentration of 0.1 wt.% and then the solution is used to perform the UV–Vis measurement. The spectrum reveals a characteristic absorption peak of ZnO NPs at wavelength of 365 nm (Jamdagni et al., 2018), which can be assigned to the intrinsic band-gap absorption of ZnO due to (Elumalai and Velmurugan, 2015).

Among 15 kinds of plants as shown in Table 1, only 1 kind could not synthesize ZnO NPs, which were rambutan peel. The result showed that lychee peel extract gave the high tendency to synthesize ZnO NPs (Table 1.) which exhibited the sharpest absorbance peak at 365 nm [(Abs_{365}) 4.19] as shown in Figure 1c. After synthesis, the appearances of ZnO NPs powder by lychee peel extract is shown in Figure 1b.

Table 1 A potential of Thai herbs and fruit peels on ZnO NPs biosynthesis.

Common name	Scientific name	Abs 365 nm
1. Mangosteen peel	*Garcinia mangostana* Linn.	2.64±0.30^{b}
2. Rambutan peel	*Nephelium lappaceum* Linn.	0.00±0.00^{f}
3. Longan peel	*Dimocarpus longan* Lour.	1.79±0.14^{cd}
4. Mango peel (var.Khiew Sawoey)	*Mangifera indica* Linn	1.28±0.45^{de}
5. Mango peel (var.Dawei)	*Manaifera indica* Linn	1.47±0.28^{de}
6. Banana peel	*Musa sapientum* Linn	1.79±0.14^{cd}
7. Lychee peel	*Litchi chinensis* Sonn.	4.19±0.71^{a}
8. Bora phet	*Tinospora crispa* (L.) Miers ex Hook.f. & Thoms	2.15±0.23^{bc}
9. Ginkgo leaves	*Ginkgo biloba* Linn	0.99±0.03^{e}
10. Edible-stemmed vine	*Cissus quadrangularis* Linn	1.53±0.10^{de}
11. Betel leaves	*Piper betle* Linn	2.47±0.28^{b}
12. Beleric Myrobalan	*Terminalia bellirica (Gaertn.)* Roxb.	0.34±0.18^{f}
13. Kariyat	*Andropraphis paniculata* (Burm.f.)	1.50±0.13^{de}
14. Emblica	*Phyllanthus emblica* Linn	1.37±0.19^{de}
15. Red Kwao Krua	*Butea superba* Roxb.	1.15±0.12^{e}

Optimization of parameters the biosynthesis of ZnO NPs

Increasing concentrations of zinc acetate (5, 10, 20, 30, 40, 50 mM) were used to optimize the synthesis. An increase in absorption was observed when increasing the concentration of zinc acetate from 5 mM to 30 mM accompanied by sharpening of peak. However, a further increase in concentration to 40 mM resulted in decrease in absorbance as well as substantial broadening of peak. Hence, it was concluded that increasing the concentration of metal ions beyond a threshold value led to decrease in the synthesis of nanoparticles (Figures 2 and 3).

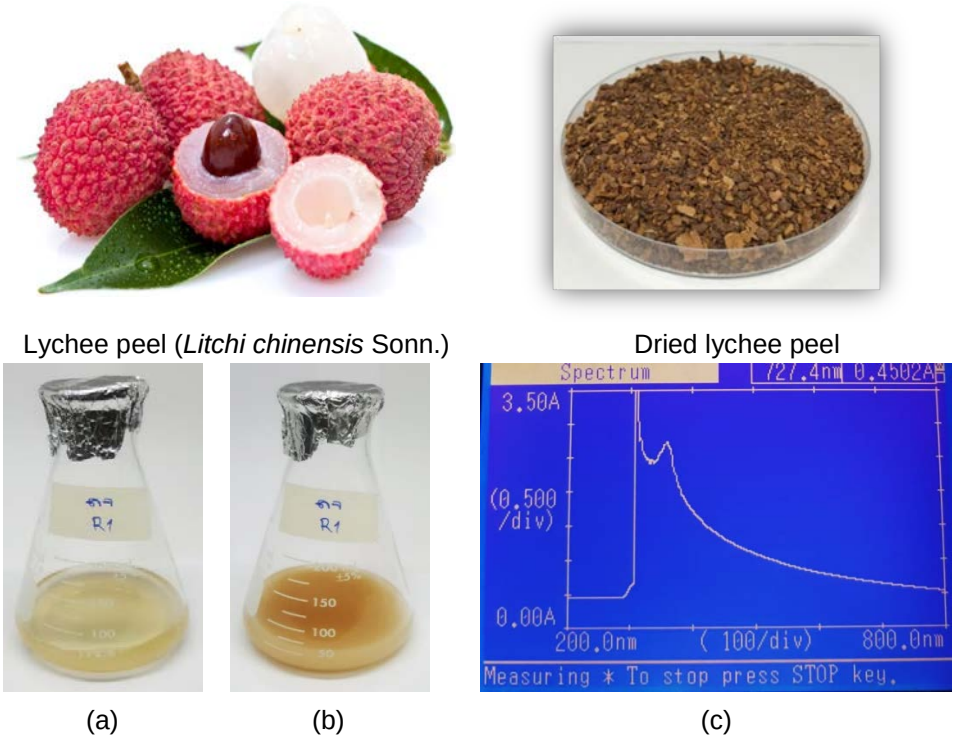

Figure 1. Green synthesis of ZnO NPs from lychee peel extract;
(a) = before synthesis, (b) = after synthesis and (c) = UV-Vis absorption spectrum

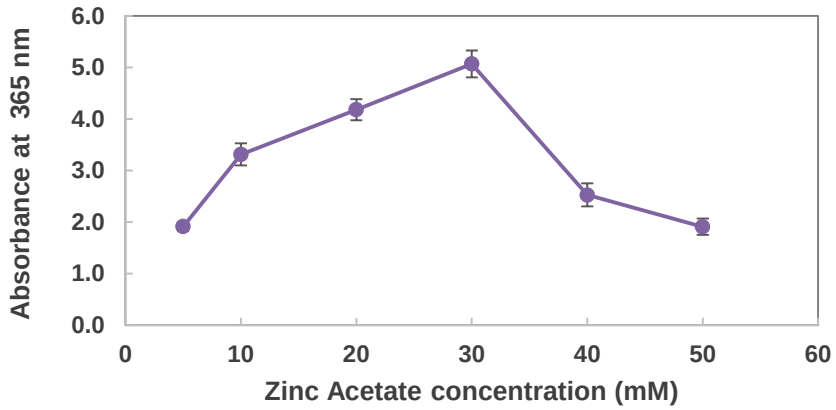

Figure 2. Difference of 365 nm absorption by ZnO NPs biosynthesis from lychee peel at different concentration of zinc acetate.

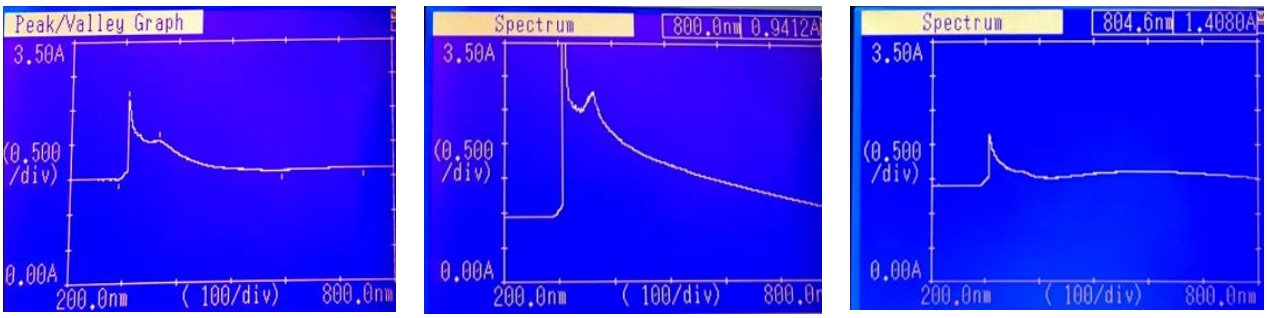

(a) (b) (c)

Figure 3. UV-Vis spectra of ZnO NPs biosynthesis at different concentration of zinc acetate: (a) 10 mM, (b) 30 mM and (c) 50 mM.

In this study, various concentrations of lychee peel extract (1,5,10,15,20 % w/v) were explored for optimum synthesis. A steady improvement in the absorption and peak prominence was observed when increasing the extract volume from 1% to 10%. Maximum absorption was observed with 10% of lychee peel extract in 50 mL of zinc acetate. Any increase or decrease in this volume led to decrease in the absorption values and hence, nanoparticle synthesis (Figure 4).

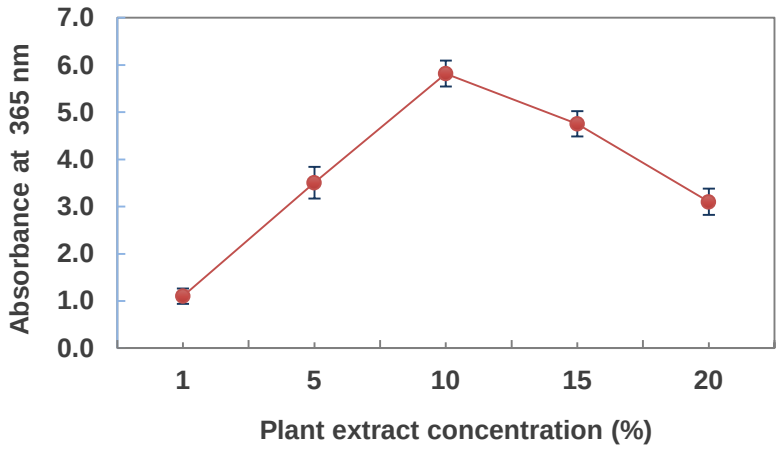

Figure 4. Effect of lychee extract concentration on ZnO NPs biosynthesis.

Other major governing factors in green synthesis of nanoparticles are the pH of the reaction mixture. In this study, it was noted that increase in pH from 9.0 to 12.0 led to increase in the absorbance of the final product. However, an almost straight absorption line with no peak at wavelength of 365 nm was observed from reaction mixture at pH 3.0 and 7.0 which exhibited the lower turbidity of reaction mixture than synthesis at pH 9.0 and 12.0 as shown in Figure 6. While, spectrum at pH 12.0 and 14.0 showed characteristic absorption peak. However, absorbance and sharpness both were recorded to be better at pH 12.0 (Figure 5), which related to turbidity, as turbidity is a measure of ZnO Nps synthesis (Gnanasangeetha and Thambavani, 2013)

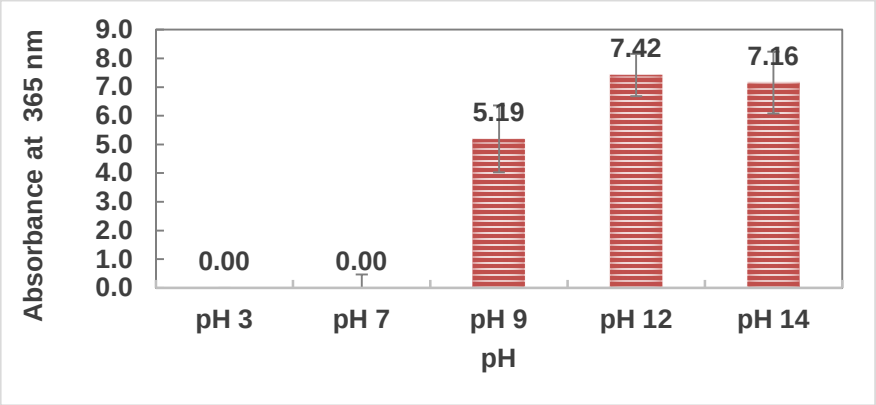

Figure 5. Effect of pH on ZnO NPs synthesis at various pH values.

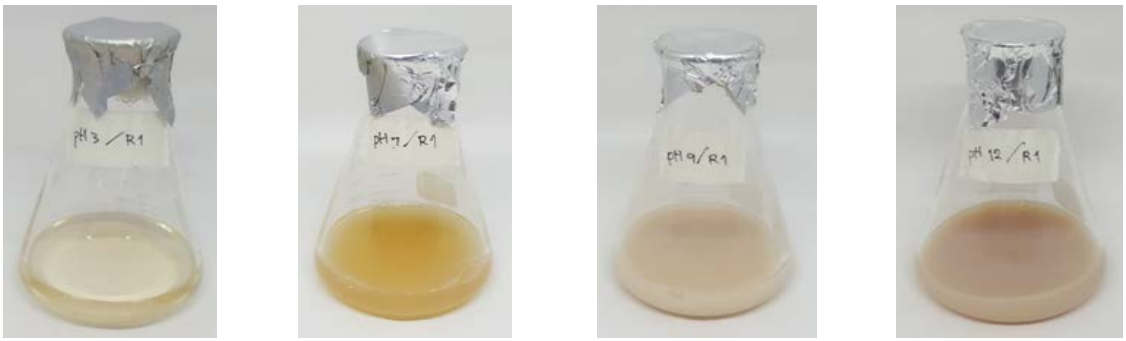

(a) (b) (c) (d)

Figure 6. Green synthesis of ZnO NPs synthesis at various pH values: (a) pH 3.0, (b) pH 7.0, (c) pH 9.0 and (d) pH 12.0.

Characterization of ZnO NPs

The morphology of the as-synthesized ZnO was examined by FESEM and the images are shown in Figure 7a. It can be seen that all the particles were in triangular-shaped with a wide particle size distribution of 39 –120 nm with well separated grain boundaries. The particles were found to be homogenously aggregated, resulting in the formation of a hierarchical sheet like appearance (Mucur et al., 2015).

The EDX studies, shown in Figure 7b, reveal the elemental composition of the ZnO samples, where it can be observed from nanopowder synthesized. Additionally, the values shown by these EDX studies corroborate the presence of zinc oxide in samples.

The FTIR spectra of the ZnO NPs are shown in Figure 7c. The analysis was performed in a frequency range of 4500–450 cm^{-1}, at room temperature. Different bands can be seen in the 1600–800 cm^{-1} region; these correspond to the organic content within the lychee peel extract. The absorption peaks at 1400.35 cm^{-1} can be attributed to the C–C stretching of aromatic rings. The spectrum presented a band at around 501 and 522 cm^{-1};

this signal is the characteristic bond signal of Zn–O, which confirms that the material is zinc oxide (Yuvakkumar et al., 2015).

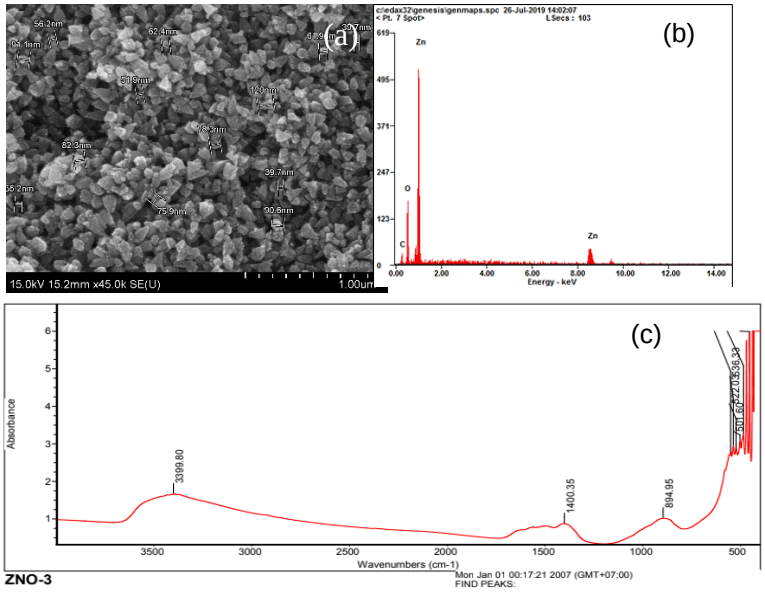

Figure 7. Biosynthesized ZnO NPs (a) FESEM (b) EDX spectrum and (c) FT-IR spectrum.

CONCLUSIONS

In this research ZnO NPs were produced through a green synthesis method using 15 medicinal plant extracts. The result showed that lychee peel extract gave the high tendency to synthesize ZnO NPs which exhibited the sharpest absorbance peak at 365 nm [(Abs_{365}) 4.19]. The optimized parameters including concentration of zinc acetate $(CH_3COO)_2Zn.2H_2O$, concentration of the extract and pH of the zinc solution that effect to synthesize ZnO NPs were determined to obtain high yield of ZnO NPs which related to their antifungal activity. The result reveal that the highest ZnO NPs synthesis was achieved by using zinc acetate $(CH_3COO)_2Zn.2H_2O$ at concentration 30 mM mixed with 10% w/v lychee peel extract and maintain the pH of solution at 12 and incubated at 90 ºC for 2 h.

ACKNOWLEDGEMENT

The research described herein was supported by the Kasetsart University Research and Development Institute (KURDI).

REFERENCES

Basnet, P., T. I. Chanu, D. Samanta and S. Chatterjee. 2018. A review on bio-synthesized zinc oxide nanoparticles using plant extracts as reductants and stabilizing agents. J. Photochem. Photobiol. B: Biol. 183: 201-221.

Elumalai, K. and S. Velmurugan. 2015. Green synthesis, characterization and antimicrobial activities of zinc oxide nanoparticles from the leaf extract of azadirachta indica (l.). Appl. Surf. Sci. 345: 329-336.

Gnanasangeetha, D. and D.S. Thambavani. 2013. Biogenic production of zinc oxide nanoparticles using acalypha indica. J. chem. biol. phys. sci. 4: 238.

Jamdagni, P., P. Khatri and J. Rana. 2018. Green synthesis of zinc oxide nanoparticles using flower extract of nyctanthes arbor-tristis and their antifungal activity. J. King Saud Univ. Sci. 30: 168-175.

Mirzaei, H. and M. Darroudi. 2017. Zinc oxide nanoparticles: Biological synthesis and biomedical applications. Ceram. Int. 43: 907-914.

Mucur, S. P., T. A. Tumay, S. Birdoğan, S. E. San and E. Tekin. 2015. Triangular-shaped zinc oxide nanoparticles enhance the device performances of inverted oleds. Nano-Struct. Nano-Objects. 1: 7-14.

Sabir, S., M. Arshad and S. K. Chaudhari. 2014. Zinc oxide nanoparticles for revolutionizing agriculture: Synthesis and applications. Sci. World J. 2014: Article ID 925494, 8 pages.

Yuvakkumar, R., J. Suresh, B. Saravanakumar, A. J. Nathanael, S. I. Hong and V. Rajendran. 2015. Rambutan peels promoted biomimetic synthesis of bioinspired zinc oxide nanochains for biomedical applications. Spectrochim. Acta A Mol. 137: 250-258.

EC-P007

EFFECT OF BLACK PEPPER EXTRACT ON BIODEGRADABLE ACTIVE PACKAGING FILM

Nattaporn Khanoonkon[1]*, Janista Nuntavisut[2], Tanyalak Oonnum[2], and Amnat Jarerat[2]
[1] Kasetsart Agricultural and Agro-Industrial Product Improvement Institute, Kasetsart University, Thailand
[2] Food Technology Program, Mahidol University, Kanchanaburi Campus, Thailand
*E -mail: aapnok@ku.ac.th

ABSTRACT
This study aims to investigate the feasibility of black pepper extract (BE) as an antioxidant in biodegradable carboxymethyl cellulose (CMC) packaging films. CMC/BE films were prepared by solution casting method using water as a solvent and glycerol as a plasticizer. BE contents used in this study were varied at 0, 0.25, 0.50, 0.75, 1.00, and 1.50% (w/v) of film solutions. Antioxidant activity and properties of films were investigated. CMC film was colorless and transparency, while CMC/BE film were yellowish and slightly opaque. The yellowness of the films increased with increasing black pepper extract contents (yellow index changed from 0.30 to 31.60). CMC/BE films exhibited antioxidant activity in the range of 21.36-41.27%. The antioxidant of films increased with increasing black pepper extract contents. The films showed ultimate tensile strength in the range of 14.91 to 19.90 MPa and elongation at break in the range of 2.90 to 10.61%. The addition of black pepper and increasing content improved tensile strength and stiffness of CMC films, while decreased their extensibility. Water vapor permeability of CMC films decreased, while their oxygen permeability increased when BE was added. The developed CMC/BE films were feasible for being used as antioxidant films for oxygen-sensitive food products.
Keywords: Black pepper extract, Carboxymethyl cellulose, Film, Biodegradable, Active packaging

INTRODUCTION

Nowadays, consumers require the high nutritional value of food which are fresh and natural products. To prolong the shelf life of these foods, chemical additives are usually added; however, these additives might be harmful to human health. The natural food additives might be the answer to this problem. The foods containing a high content of unsaturated fatty acids are easily subjected to lipid oxidation, which is the main cause of quality deteriorations leading to the formation of off-odours and off-flavours, texture, and colour changes (Domínguez et al., 2018). Black pepper (*Piper nigrum L*.) (BE) comprises various biologically active compounds, e.g. alkaloids, terpenes, flavones, steroids, and others. The major component of BE is Piperine (alkaloid) and there are also other active compounds providing the anti-inflammatory, antioxidant, and antimicrobial properties (Ozdemir et al., 2018). The study of total antioxidant activity on inhibited peroxidation of linoleic acid emulsion of black paper seed extracted with water and ethanol 95.5% and 93.3 %, respectively. This property was higher than that activity of standard antioxidants, i.e. butylated hydroxyanisole (BHA), butylated hydroxytoluene (BHT) and a-tocopherol, which showed 92.1%, 95.0%, and 70.4% inhibition on peroxidation of linoleic acid emulsion, respectively (Gülçin, 2005). Carboxymethyl cellulose or CMC, a polysaccharide biodegradable polymer, which good film-forming ability with can be used as a packaging film. However, this material does not present antioxidant ability (Riaz et al., 2020). To improve the functions and applications of biodegradable CMC film, natural extracts of BE with high potential as antioxidants are of interest due to the safety concern of customers. Therefore, this study aimed to investigate the effect of BE on antioxidant activity and properties of CMC film.

MATERIALS AND METHODS

Preparation of carboxymethyl cellulose/black pepper film

1.5 g of carboxymethyl cellulose powder (CMC) and 0.3 g of glycerol were dissolved in 100 mL of distilled water at 60 °C for 60 min with continuous stirring. After that, the temperature was cooled down to 40 °C prior to adding black pepper extract (BE) into the mixture. The concentrations of BE used were varied in the range of 0.25, 0.50, 0.75, 1.00 and 1.50% (w/v) of the mixture solutions. The mixtures were mixed by a homogenizer at the speed of 500 rpm for 30 min. The bubbles in the mixture solution were then removed by

placing the mixture solution beaker in an ultrasonic bath. The mixtures were poured into an acrylic plate and dried at 50 °C for 12 h. The CMC/BE films were then removed from the plates and kept in a desiccator containing silica gel prior to testing.

Film characterization and property testing

Determination of antioxidant

Antioxidant property of CMC/BE films was characterized using 2,2-diphenyl-1-picrylhydrazyl radical scavenging capacity assay (DPPH) method. The DPPH solution (0.1 mM in 95% ethanol) was prepared by added 0.00394 g of DPPH in 95% of ethanol in an ultrasonic bath for 5 min. The film samples were cut into small pieces. 0.01 g of film pieces were added into a centrifuge tube containing 10 mL of distilled water and the tube was placed in an ultrasonic bath for 5 min and centrifuge at 500 rpm for 10 min to dissolve the film. After that, the supernatant with a concentration of 10 mg/mL was used for antioxidant testing.

0.1 mL of supernatant (conc. 10 mg/mL) was pipetted into a test tube and 1 mL of DPPH solution was then added. The mixture was mixed using a vortex and kept in the darkroom for 30 min. The absorbance at 517 nm of the solution was measured using a spectrophotometer. The control (bank) sample used was a mixture of DPPH and distilled water. The oxygens scavenging of the samples was calculated following Equation (1)

$$\% \text{ Scavenging} = \left[\frac{\mathrm{OD}_{\mathrm{control}} - \mathrm{OD}_{\mathrm{sample}}}{\mathrm{OD}_{\mathrm{control}}}\right] \times 100 \quad (1)$$

Determination of water vapor permeability

Water vapor transmission rate (WVTR) was measured by a desiccant method according to ASTM E96 (ASTM, 2010). Film samples were cut into circular shapes with 7 cm in diameter and then sealed on top of a WVTR cup (inner diameter ~5.9 cm) containing dried silica gel (20 g) using molten beeswax. The sample assembly was weighed (initial weight) before storing it in a constant climate chamber (KBF 240; Binder, Tuttlingen, Germany) at 25 °C and 50% RH. The weight of the assembly was recorded once a day for 5 days. WVTR of the sample was calculated from the initial slope of the weight change (the weight difference at time t and initial time) versus time relationship divided by the absorption surface area. Five measurements were taken for each sample. WVP was then calculated from Equation (2):

$$\mathrm{WVP} = (\mathrm{WVTR} \times \mathrm{L})/\Delta p \quad (2)$$

where WVP is the water vapor permeability (g/m^2 s Pa), WVTR is the measured water vapor transmission rate through a sample (g/m^{2}s), L is the mean sample thickness (mm) and Δp is the partial water vapor pressure difference between two sides of the sample (Pa). The WVP data were averaged from five replicates to obtain a mean value ± standard deviation.

Determination of oxygen permeability

Film samples were cut into circular pieces with 13 cm in diameter and then conditioned in a closed chamber containing saturated calcium chloride salt solution at 25 °C (33% RH) for 48 h before measurement. Oxygen transmission rate (OTR) of the sample was measured according to ASTM D 3985-802 (ASTM, 2004) using an oxygen permeation analyzer (model 8501; Systech Illinois, Johnsburg, IL, USA) at 23 °C and 0% RH. Five specimens were tested for each sample. Oxygen permeability (OP) of the sample was then computed from Equation (3):

$$\mathrm{OP} = (\mathrm{OTR} \times \mathrm{L})/\Delta p \quad (3)$$

where OP is the oxygen permeability (cm^3.mm/atm.day.m^2), OTR is the measured oxygen transmission rate through a sample (cm^2/m^2 day), L is the mean sample thickness (mm) and Δp is the oxygen partial pressure difference between two sides of the sample (Pa). The OP data were averaged from five replicates to obtain a mean value ± standard deviation.

Tensile testing

Tensile properties, i.e. tensile strength, elongation at break and modulus of film samples were characterized following ASTM D 882-91 (ASTM, 2012) using a universal testing machine (Shimadzu AGS5kN, Tokyo, Japan) with a load cell of 20 N. The film specimens were cut into rectangular strips (12 cm x 1.5 cm) and then conditioned in a closed chamber containing a saturated solution of magnesium nitrate salt at 30 °C (51.4% RH) for 48 h before testing. The test was performed with an initial grip separation of 8 cm and a crosshead speed of 1 mm/min. Tensile strength (MPa) and elongation at break (%) were determined by TRAPEZIUM X software (Shimadzu, Tokyo, Japan). Young's modulus was calculated from the slope of the initial linear portion of the stress and strain curve. At least five specimens of each sample were tested.

Statistical analysis

Mean values and standard deviations (SD) were calculated and compared by one-way analysis of variance (ANOVA), with the value of statistical significance at $p < 0.05$, using the SPSS statistical software package. Multiple comparisons of group means were computed using Duncan's multiple range test (DMRT).

RESULTS AND DISCUSSION

Antioxidant property of films

DPPH is widely used to evaluate free radical scavenging activity of antioxidants effectiveness (Lü, Lin, Yao & Chen, 2010). In this work, the DPPH radical scavenging activity of BE and CMC/BE films were expressed as % scavenging (Table 1). The results suggested that the radical scavenging activity on DPPH radicals of CMC films was more pronounced as a function of BE concentration, implying improved antioxidant property of CMC film. The improvement of antioxidant properties might be according to a strong hydrogen donation ability, metal chelating ability, and their effectiveness as hydrogen peroxide, superoxide, and free radical scavengers of black pepper (Gülçin, 2005; Ozdemir et al., 2018)

Table 1 Antioxidant property, water vapor permeability, oxygen permeability of BE, CMC and CMC/BE Films.

Sample	Properties		
	Radical scavenging activity on DPPH radical (%)	WVP x 10^{-10} (g/m s Pa)	OP (cm^3.mm/atm. day. m^2)
BE	76.58 ± 3.30^{a}	-	-
CMC (Control)	ND	1.05 ± 0.01^{a}	0.51 ± 0.07^{c}
CMC/ 0.25BE	21.36 ± 1.06^{d}	0.91 ± 0.07^{a}	0.52 ± 0.03^{c}
CMC/ 0.50BE	33.12 ± 2.79^{c}	0.66 ± 0.02^{b}	0.69 ± 0.02^{b}
CMC/ 0.75BE	38.82 ± 2.74^{b}	0.46 ± 0.08^{c}	0.84 ± 0.28^{ab}
CMC/ 1.00BE	40.60 ± 1.11^{b}	0.36 ± 0.13^{c}	0.99 ± 0.30^{a}
CMC/ 1.50BE	41.27 ± 1.37^{b}	0.21 ± 0.04^{d}	0.84 ± 0.10^{ab}

Values reported are the mean ± SD.
ND is non-detected antioxidant activity.
Different letters (a-d) in the same column indicate a statistically significant difference ($p < 0.05$).

Water vapor permeability

Water vapor permeability (WVP) of the films was determined at 25 °C and 50% RH using a desiccant method. CMC film showed WVP of ~1.05×10^{-10} g/m s Pa, where the CMC/BE films exhibited WVP in the range of 0.21×10^{-10} to 0.91×10^{-10} g/m s Pa (Table 1). WVP values of the film decreased with incorporating BE and increasing its contents, implying improved water vapor barrier properties. The increment of this barrier properties possibly because the BE possessed a higher level of hydrophobic nature (Amalraj et al., 2020).

Oxygen permeability

Oxygen permeability (OP) of the films is shown in Table 1. CMC film showed OP of ~0.5 cm^3.mm/atm. day. m^2, whereas the CMC/BE films exhibited OP in the range of 0.52 to 0.99 cm^3.mm/atm. day. m^2 (Table 1). OP values of the film tended to increase with incorporating BE and increasing its contents, implying decreased oxygen barrier properties. The decrement of this barrier properties possibly because the BE possessed a higher level of hydrophobic nature (Amalraj et al., 2020).

Tensile properties

Tensile properties, i.e. tensile strength (TS), modulus and elongation at break (EB) of the films were determined from a stress–strain curve and the results are summarized in Table 2. Tensile strength and modulus of CMC film were increased, whereas elongation at break of the films was decreased with incorporating BE. These results suggested that the addition of BE can improve strength and stiffness of CMC films, whereas deteriorate extensibility of the films. This evidence might be due to the filler effect of BE. The highest tensile strength and stiffness were determined in the film containing 0.75% (w/v) of BE.

Table 2 Tensile properties, i.e. tensile strength, modulus, and elongation at break of CMC and CMC/BE films.

Sample	Properties		
	Tensile strength (MPa)	Young's modulus (MPa)	Elongation at break (%)
CMC (Control)	13.91 ± 1.40^{b}	629.51 ± 29.16^{c}	6.76 ± 0.80^{a}
CMC/ 0.25BE	14.23 ± 1.66^{b}	706.64 ± 79.68^{bc}	6.20 ± 2.34^{ab}
CMC/ 0.50BE	17.18 ± 0.72^{ab}	739.35 ± 48.73^{abc}	6.02 ± 2.75^{ab}
CMC/ 0.75BE	19.44 ± 0.82^{a}	849.95 ± 77.89^{a}	5.50 ± 1.25^{ab}
CMC/ 1.00BE	17.60 ± 2.65^{a}	783.12 ± 70.47^{ab}	4.29 ± 0.54^{ab}
CMC/ 1.50BE	17.01 ± 2.35^{ab}	833.73 ± 78.59^{ab}	3.39 ± 0.06^{b}

Values reported are the mean ± SD.
ND is non-detected antioxidant activity.
Different letters (a-d) in the same column indicate a statistically significant difference ($p < 0.05$).

CONCLUSIONS

Commercial black pepper extract composted of chemical compositions containing antioxidant activity. Black pepper extract can be used as an antioxidant in biodegradable carboxymethyl cellulose packaging films by enhancing antioxidant capacity as well as improving the strength, stiffness, and water vapor barrier of films.

ACKNOWLEDGEMENT

The authors also would like to thank Dr. Udomluk Sukutta and the team (Kasetsart Agricultural and Agro-Industrial Product Improvement Institute, Kasetsart University) for supporting the evaluation of free radical scavenging activity of BE and the CMC/BE film samples.

REFERENCES

Amalraj, A., J. T. Haponiuk, S. Thomas and S. Gopi. 2020. Preparation, characterization and antimicrobial activity of polyvinyl alcohol/gum arabic/chitosan composite films incorporated with black pepper essential oil and ginger essential oil. Int. J. Biol. Macromol. 151: 366–375.

ASTM. 2004. ASTM D3985-02: Standard test method for oxygen gas transmission rate through plastic film and sheeting using a coulometric sensor. West Conshohocken, PA: ASTM International.

ASTM. 2010. ASTM E96/E96M-14: Standard test methods for water vapor transmission of materials. West Conshohocken, PA: ASTM International.

ASTM. 2012. ASTM D882-12: Standard test method for tensile properties of thin plastic sheeting. West Conshohocken, PA: ASTM International.

Domínguez, R., F. J. Barba, B. Gómez, P. Putnik, D. B. Kovačević, M. Pateiro, E. M. Santos and J. M. Lorenzo. 2018. Active packaging films with natural antioxidants to be used in meat industry: A review. Food. Res. Int. 113: 93–101.

Gülçin, İ. 2005. The antioxidant and radical scavenging activities of black pepper (*Piper nigrum*) seeds. Int J Food. Sci. Nutr. 56(7), 491–499.

Lü, J. M., P. H. Lin, Q. Yao and C. Chen. 2010. Chemical and molecular mechanisms of antioxidants: experimental approaches and model systems. Cell. Mol. Med. 14(4): 840-860.

Ozdemir, N., C. C. Pola, B. N. Teixeira, L. E. Hill, A. Bayrak and C. L. Gomes. 2018. Preparation of black pepper oleoresin inclusion complexes based on betacyclodextrin for antioxidant and antimicrobial delivery applications using kneading and freeze drying methods: A comparative study. LWT – Food. Sci. Technol. 91: 439–445.

Riaz, A., C. Lagnika, H. Luo, M. Nie, Z. Dai, C. Liu, M. Abdin, M. M. Hashim, D. Li and J. Song. 2020. Effect of Chinese chives (*Allium tuberosum*) addition to carboxymethyl cellulose based food packaging films. Carbohydr. Polym. 235: 11594.

EC-P008

EFFECT OF CITRIC ACID ON PROPERTIES OF CASSAVA STARCH AND BIODEGRADABLE PACKAGING FOAM

Nattaporn Khanoonkon[1]*, Waratchaya Siangchin[2], Narinthorn Janprasatporn[2], and Amnat Jarerat[2]
[1] Kasetsart Agricultural and Agro-Industrial Product Improvement Institute, Kasetsart University, Thailand
[2] Food Technology Program, Mahidol University, Kanchanaburi Campus, Thailand
*E-mail: aapnok@ku.ac.th

ABSTRACT
Starch/natural fiber foam is biodegradable material that can be used for replacing non-biodegradable petroleum-based foam. However, the properties of starch/natural fiber foam became poor when using at high moisture content condition. The modified starch with citric acid (CA) might be the alternative way to solve this problem. Therefore, the objectives of this study were i) to study the effect of CA on properties of cassava starch and ii) to study the effect of citrate starch on properties of starch/natural fiber foam. The citrate starch was prepared by the interaction between cassava starch with CA by varying CA contents at 10% 20% 30% and 40% of starch dry weight (w/w). The properties of modified starch were investigated. FT-IR spectrum of modified starch exhibited new peak around 1722 -1726 cm^{-1}, which is associated with the stretching vibration of C=O bond from carbonyl groups of CA confirming that starch was cross-linked with CA. The degree of substitution of citrate starch increased with CA contents, resulting in decreased solubility of citrate starch. This modified starch was mixed with sugarcane bagasse fibers, water and glycerol and then heat pressed at 180 °C for preparing foam tray samples. The properties of foam trays were investigated. Biodegradable foam prepared from citrate starch was denser than those obtained from native starch. However, the citrate starch foam tray showed higher water absorption than native starch foam tray. Therefore, the utilization of these foam trays required further improvement, e.g. coating to enhance water resistance.
Keywords: Citric acid, Citrate starch, Foam, Biodegradable, Packaging

INTRODUCTION

Plastic foam or polystyrene foam are cellular polymers and expanded plastics, which has played a great role in everyday life. However, this foam cannot be degraded by microorganisms causing global warming and health problem. To replace polystyrene foam, starch foam has been developed, due to its biodegradability and safety for all organisms in the environment. However, starch foam exhibited high water absorption and poor mechanical properties. To reduce the water absorption of starch, the modification of starch with citric acid was of interest. The -OH functional groups of starch could be replaced by carboxylic groups of citric acid, which could form cross-linking between two starch molecules to provide strong granules and low water absorption of starch molecules. Moreover, the mechanical properties of starch foam can be improved by adding fibers. Sugarcane bagasse, waste from sugar industry, consists of fibers with high density and high strength. This material was used in fuel and textile industries. In this research we expected that addition of sugarcane bagasse to biodegradable foam resulted in the obtained foam with 100% biodegradability and improved mechanical properties. Therefore, the objectives of this study were i) to study the effect of citric acid content on the properties of modified cassava starch and ii) to study the effect of citrate starch on the properties of biodegradable citrate starch/sugarcane bagasse fiber foam.

MATERIALS AND METHODS

Modification of cassava starch with citric acid via crosslinking

Citric acid with varied of citric acid concentrations, i.e. 0 (CA0), 5 (CA5), 10 (CA10), 20 (CA20), 30 (CA30) and 40 (CA40) (w/w) of cassava starch were prepared. Citric acid was weighed and dissolved in distilled water. The pH of solution was adjusted to 3.5 by using 10 M NaOH, the distilled water was added into the solution to obtained 50 mL of citric acid solution. 50 g of cassava starch was weighed and mixed with the obtained citric acid solution. The mixtures were kept at room temperature for 16 h and dried at 60 °C

for 4 h in a hot-air oven. After that, the mixtures were heated at 140 °C for 1 h in the oven to finish the reaction and dried at 40 °C for 24 h prior to grinding into powders and sieving with a 150 μm sieve and keeping in zip lock bags before testing.

Citric acid modified cassava starch characterization and property testing

Chemical structure characterization

Chemical structure of citric acid modified starch was characterized by a Fourier transform infrared (FTIR) technique. The FTIR measurement was performed in an attenuated total reflection (ATR) mode by a Nicolet iS20 FTIR Spectrometer (Thermo Fisher Scientific™, United States) over a wavenumber range of 400–4000 cm^{-1} with 16 scans at a resolution of 4 cm^{-1}.

Degree of substitution determination

Degree of substitution (DS) of citric acid modified cassava starch was determine by titration technique. 2 g of cassava starch or modify cassava starch and 20 mL of distilled water were mixed. 2 droplets of phenolphthalein were added to the mixture solution prior to titration with 0.1 M NaOH until the color of phenolphthalein was changed from colorless to pink (end of titration). After that, 0.5 M NaOH (25 mL) was added to the mixture and mixed for 60 min at room temperature before titration with 0.5 M HCl acid until the reaction was ended (the color change from pink to colorless). Duplicate measurements were performed for each starch sample. DS of modified starch was calculated following the Equations: (1) and (2)

$$A = \frac{(V0-V1)x\ c\ x\ M\ x\ 100\%}{m} \quad (1)$$

$$DS = \frac{162A}{100M-(M-1)A} \quad (2)$$

where,

A	=	carboxyl content (%)
M	=	molecular weight of citrate (175 g/mol)
m	=	mass of starch sample (g)
c	=	concentration of HCl acid (0.5 M)
V_0	=	Volume of HCl used for titration with native starch (mL)
V_1	=	Volume of HCl used for titration with modified starch (mL)

pH measurement

pH of citric acid modified cassava starch was determined by using pH meter. 5 g of modified cassava starch was mixed with 25 mL of distilled water with stirring for 5 min prior to measuring pH of solution. Triplicate measurements were performed for each starch sample.

Moisture content determination

Moisture content of modified cassava starch was determined according to AOAC standard method (AOAC, 2000). Aluminum can was dried in a hot-air oven at 105 °C for 3 h and placed in a desiccator for 30 min and weighted and repeated until the weight of can was constant. 3 g of cassava starch was weighed and put on the can and dried in an oven using the same condition descripted above. The dried sample weight with aluminum can was used for calculating the moisture content of sample using the following Equation (3)

$$\text{Moisture content (\%)} = \frac{\text{Dried sample weight with aluminum can (g)} - \text{aluminum can weight (g)}}{\text{Sample weight (g)}} \text{ x } 100 \quad (3)$$

Solubility and swelling determination

1 g of native cassava starch or modified starch (W) was weighed and dissolved in breaker containing 30 mL of distilled water and placed in a water bath at 95 °C and 50 °C for 30 min. After that, the sample beakers were placed at room temperature allowing the sample temperature to cool down. The

sample was transferred into a centrifuge tube and centrifuged at 3000g for 10 min. The supernatant was placed in a container with known weight and dried at 105 °C for 2 h and weighed (soluble part, W2) and calculated the solubility of the sample using the Equation (4). The precipitated part (starch paste) in the centrifuge tube was weighed and calculated the swelling power following the Equation (5)

$$\text{Solubility (\%)} = \text{W2/W1 x 100} \quad (4)$$

$$\text{Swelling power} = \text{(Weight of starch paste)/(Weight of dry starch) x 100} \quad (5)$$

Preparation and property testing of citric acid modified starch/sugarcane bagasse fiber biodegradable packaging foam

Biodegradable packaging foam preparation

Native and modified starches with different citric acid contents were weighed (37.5 g) and dissolved in 150 mL of distilled waters prior to heated at 85 °C for 5 min with continuous stirring. Glycerol (1.49 mL) and sugarcane bagasse fibers (22.5 g) were added to the slurry and continued heating and stirring for 20 min. The slurry was then placed in an injection or compression? molding machine with setting temperature of 200 °C and pressed at pressure of 5 MPa for 2 min prior to opening the mold to remove pressure and pressed again for drying the sample. The biodegradable packaging foam was removed from the compression molding machine and kept in a Ziplock bag at room temperature before testing.

Determination and property testing of Biodegradable packaging foam

Determination of density

The density of biodegradable foam was determined from the ratio of weight and volume of packaging. The foam was cut into a sguare shape (2 cm × 2 cm) and measured for the dimensions and the thickeness with a digital gage prior to weighing the sample with the 4 digits weighing machine. The density of the sample was calculated according to the following Equation (6):

$$\text{Density (g/cm}^3\text{)} = \text{weight of sample (g) / volume of sample (cm}^3\text{)} \quad (6)$$

Determination of water absorption

Water absorption capacity (WAC) of biodegrable foam was determined. The foam sample was cut into a retangular shape (25 mm × 50 mm) and weighed (W_{dry}). After that the sample was immersed in a beaker containing distilled water and kept at room temperature for 1 min. The sample was removed from the beaker and the exceed water were removed from the samples by tissue paper. The sample was then weighed (W_{wet}). Water absorption of sample was calculated following the Equation (7)

$$\text{WAC\%} = \frac{(\text{Wwet} - \text{Wdry})}{\text{Wdry}} \text{ x } 100 \quad (7)$$

Tensile testing

Tensile properties, i.e. tensile strength, elongation at break and modulus of foam samples were characterized by a Testometric tensile testing machine (Testometric Micro 350, United Kingdom) with a load cell of 50 N. The specimens were cut into rectangular strips (2.5 cm x 15 cm) and then conditioned in a closed chamber containing a saturated solution of magnesium nitrate salt at 30 °C (51.4% RH) for 48 h prior to testing. The test was performed with an initial grip separation of 8 cm and a crosshead speed of 2 mm/min.

Statistical analysis

Mean values and standard deviations (SD) were calculated and compared by a one-way analysis of variance (ANOVA) with the value of statistical significance at $p < 0.05$, using the SPSS statistical software package. Multiple comparisons of group means were computed using a Duncan's multiple range test (DMRT).

RESULTS AND DISCUSSION

Citric acid modified cassava starch characteristics and properties

Chemical structure

Chemical structure of citric acid modified starch was characterized by FT-IR technique. FT-IR spectra of citrate starch exhibited new peaks around 1722 -1726 cm^{-1} (Figure 1b-e), corresponding to carbonyl group (C=O) formed between hydroxyl groups of starch and carboxylic groups of citric acid ester bonds. This result confirmed the successfully modified citrate starch (Pachuau et al., 2018).

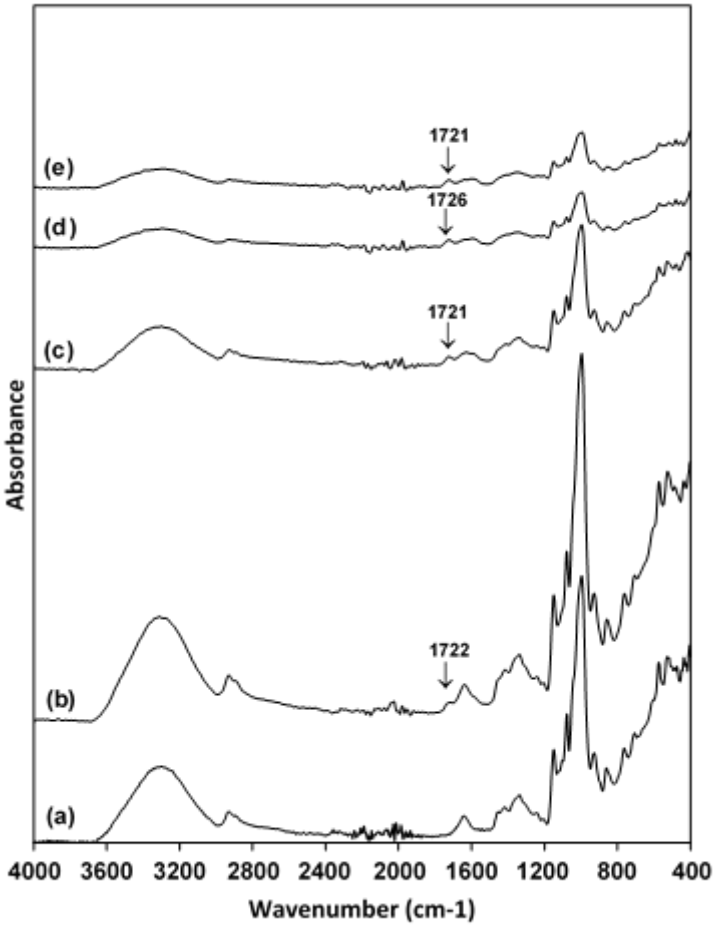

Figure 1. FT-IR spectra of (a) native starch and (b)- (e) citric acid modified starch with varied citric contents as: (b) 10%, (c) 20%, (d) 30% and (e) 40%.

Degree of substitution (DS)

The degree of substitution (DS) of citric acid modified starch was determined and the data are shown in Table 1. The degree of substitution (DS) of citrate starch were increased from 0.0248 to 0.3065, when citric acid contents increased from 10% to 30%, indicating the increased interaction between starch and citric acid. However, at 40% of citric acid content, DS of citrate starch became lower. This increase of citric acid to 40% resulting in a decrease in the DS maybe because citric acid was too concentrated and caused the steric effect resulting in the impedance of interaction between citric acid and starch (Mei et al., 2015). The highest DS (DS=0.31) was occur when using the citric content of 30%.

Table 1 Degree of substitution (DS) of modified cassava starch with different citric acid contents.

Sample	Properties		
	DS	pH	Moisture contents [ns] (%)
Native starch	-	5.43 ± 0.22[b]	13.25 ± 0.83
CA0	-	6.87 ± 0.12[a]	12.66 ± 0.54
CA10	0.03 ± 0.01[d]	5.15 ± 0.02[c]	12.95± 0.29
CA20	0.08 ± 0.01[c]	4.87 ± 0.012[d]	12.95 ± 1.12
CA30	0.31 ± 0.05[a]	4.73 ± 0.01[de]	13.77 ± 0.44
CA40	0.21 ± 0.05[b]	4.68 ± 0.01[e]	12.95 ± 0.05

Values reported are the mean ± SD.
Different letters (a-d) in the same column indicate a statistically significant difference ($p < 0.05$) and ns is not significant.

Acidity

pH of modified starch was measured by a pH meter and the results are shown in Table 1. The pH of starch decreased when modified with citric acid and increasing citric acid contents as the carboxyl group of citric acid that does not react with the starch molecules could show acidity properties and resulted in higher acidity of starch citrate as the amount of acid increased (Pachuau et al., 2018).

Moisture contents

Moisture contents of modified starch was measured according to the AOAC standard method and the results are shown in Table 1. The modification of cassava starch with citric acid and increasing its content did not influence the moisture content of starch.

Solubility and swelling power

Solubility of citric acid modified starch is shown in Figure 1. Below gelatinization temperature (50 °C) (Figure 2A), solubility of citrate starch was higher than that of native starch. This result might be because interaction of water and un-reacted carboxyl group of citrate starch, which could not form crosslinked with other starch chains, were more effective than that of water and native starch. However, at temperature higher than gelatinization temperature (95 °C), citrate starch exhibited lower solubility as compared with native one since partial cross-linked portions of citrate starch could restrict the starch granule deterioration by forming networking structure.

Swelling power of citric acid modified starch is shown in Figure 3. Below gelatinization temperature (50 °C), swelling power of citrate starch was higher than that of native starch as bulky group of citrate starch restricted H-bond formed between starch molecules, resulting in increased interaction with water molecules (Choi and Kerr, 2003). At temperature higher that gelatinization temperature (95 °C), swelling power of native starch and citrate starch were not significantly different except the citrate starch modified by 10% of citric acid which exhibited the highest swelling power. This might be due to the highest cross-linked starch.

Properties of biodegradable foam

Density

The density of biodegradable foam became higher when using citric acid modified starch and increasing citric acid contents from 10% to 20% (Table 2). However, the density was reduced when citric acid content increased to 30-40%. The highest density of foam occurred when preparing from 20% citric acid modified starch. This might be because the strength of the starch granular modified with citric acid was increased, resulting in stronger modified starch foam and more resistance to mechanical force than the foam made from native starch (Choi and Kerr, 2003).

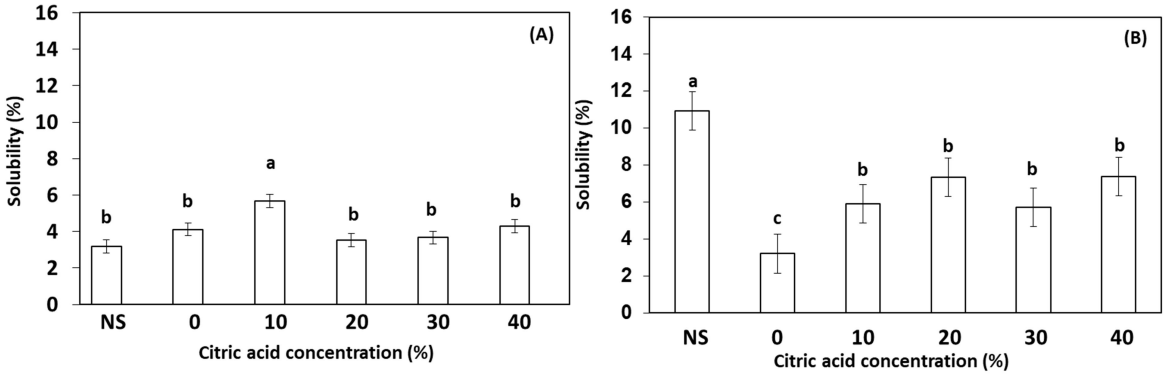

Figure 2. Solubility of citric acid modified starch at different temperature: (A) 50 °C and (B) 95 °C.

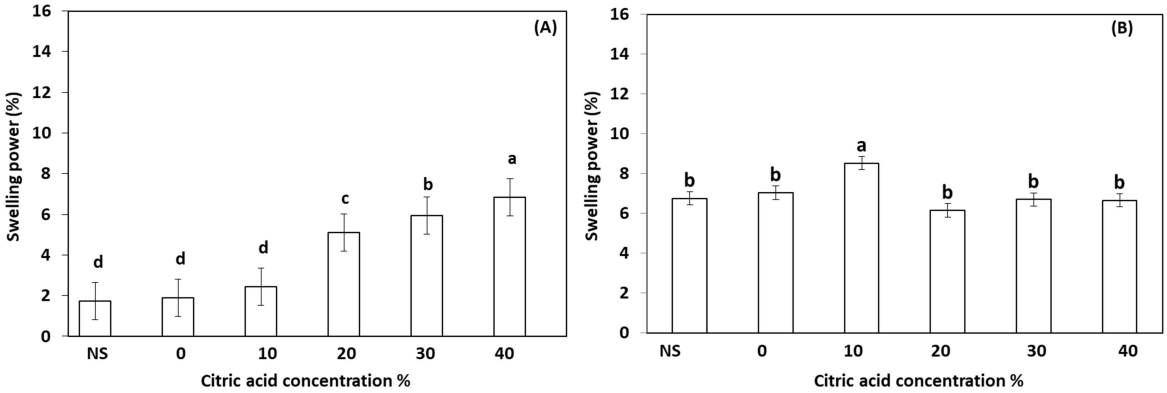

Figure 3. Swelling power of citric acid modified starch at different temperature: (A) 50 °C and (B) 95 °C.

Table 2 Density and water absorption of modified cassava starch with different citric acid contents.

Sample	Properties	
	Density (g/cm^3)	Water absorption (%)
Native starch	0.05± 0.00^{d}	22.39±0.91^{d}
CA0	0.06±0.01^{cd}	19.51±2.95^{d}
CA10	0.08±0.00^{c}	30.72±2.62^{c}
CA20	0.12 ±0.01^{a}	55.88±3.10^{b}
CA30	0.10± 0.00^{b}	> 99%^{a}
CA40	0.10±0.00^{bc}	> 99%^{a}

Values reported are the mean ± SD.
Different letters (a-d) in the same column indicate a statistically significant difference ($p < 0.05$) and ns is not significant.

Water absorption

Water absorption of biodegradable foam was shown in Table 2. The biodegradable packaging foam made from citric acid modified starch was significantly higher than those from native starch due to the corrosive ability of citric acid, which caused the damage of starch surface structure resulting in easily water molecule penetration (Hedayati et al., 2018).

Tensile properties

The tensile properties, i.e. max stress and max strain of biodegradable foam were shown in Figure 4. The results showed that tensile properties of the foam made from citric acid modified starch exhibited significantly higher values than those made from native starch as the carbonyl groups of citric acid could interact with starch molecules via hydrogen bonding. Moreover, the increased citric acid content (to 20%) could increase crosslinking of starch molecules which increased foam strength.

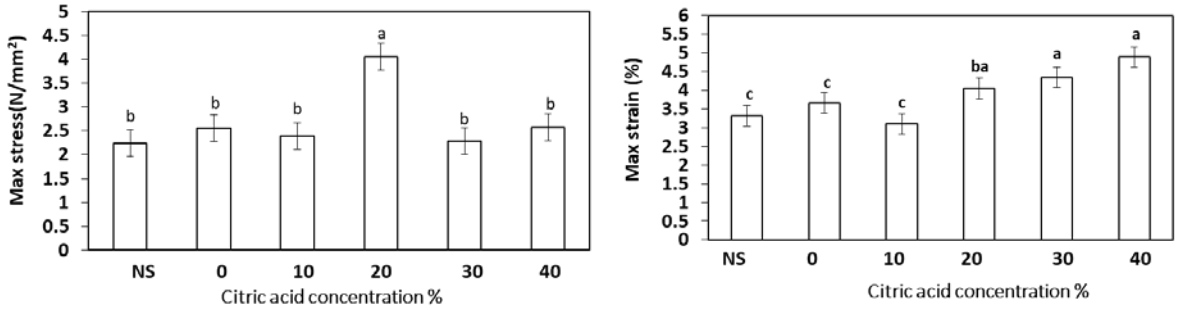

Figure 4. Tensile properties, i.e. (A) max stress and (B) max strain of biodegradable foam made from native starch and citric acid modified starch.

CONCLUSIONS

The FT-IR spectrum of citrate starch exhibited new peaks around 1722-1786 cm^{-1} confirming the successfully modified citrate starch, of which the highest DS was 0.3 (30% of citric acid content used). The solubilities of citrate starch were higher than that of native starch at the temperature below gelatinization temperature (50 °C), while these values became lower at gelatinization temperature (95 °C).

Biodegradable foam was successfully prepared from citric acid modified starch and sugarcane bagasse via compression molding technique. The density of biodegradable foam became higher when using citric acid modified starch as compared with the one prepared from native starch. However, water absorption of biodegradable foam from citric acid modified starch was significantly higher than the foam made from native starch. In addition, the tensile properties of biodegradable foam made from citric acid modified starch was significantly higher than the foam made from native starch.

ACKNOWLEDGEMENT

The authors also would like to thank Dr. Rungsima Cholakup and team (Kasetsart Agricultural and Agro-Industrial Product Improvement Institute, Kasetsart University) for supporting the equipments for testing the sample properties.

REFERENCES

Pachuau, L., R. S., Dutta, T. B. Devi, D. Deka and L. Hauzel. 2018. Taro starch (Colocasia esculenta) and citric acid modified taro starch as tablet disintegrating agents. Int. J. Biol. Macromol. 118: 397–405.

Mei, J. O., D. N. Zhou, Z. Y. Jin, X. M. Xu and H. Q. Chen. 2015. Effects of citric acid esterification on digestibility, structural and physicochemical properties of cassava starch. Food. Chem. 187: 378–384.

Choi, S. G. and W. L. Kerr. 2003. Effects of chemical modification of wheat starch on molecular mobility as studied by pulsed ^{1}H NMR. LWT. 51: 1–8.

Hedayati, S and M. Niakousari. 2018. Microstructure, pasting and textural properties of wheat starch-corn starch citrate composites. Food. Hydrocoll. 81: 1–5.

AOAC. 2000. The Association of Official Agricultural Chemists, seventeenth ed. Official Method of Analysis, Washington, DC, USA.

EC-P009

VALUE-ADDED DAIRY PRODUCTS FROM LOW PRICE LOCAL CORN

Gatesuda Foithongsuk[1], Thitiya Namnood[1], Antika Boondaeng[2], Pilanee Vaithanomsat[2], Waraporn Apiwatanapiwat[2], Phornphimon Janchai[2], and Nanthavut Niyomvong[1]*
[1] Department of Biology, Faculty of Science and Technology, Nakhon Sawan Rajabhat University, Nakhon Sawan 60000, Thailand
[2] Enzyme and Microbial Technology Laboratory, Kasetsart Agricultural and Agro-Industrial Product Improvement Institute (KAPI), Kasetsart University, Bangkok 10900, Thailand
*E-mail: nanthavut.ni@nsru.ac.th

ABSTRACT
Corn is an important economic crop that cultivated in Nakhon Sawan Province because it requires low humidity, fast and high-yielding under lack water condition. In Thailand, there are major problems in agricultural. The most important issue affecting the farmers' is a decline crop prices in every harvest season and farmers unable to processing corn to other products. Therefore, this research aims to study nutrition fact by explore the antioxidants from corn milk and amount of properly sugar in the corn yogurt and corn yogurt ice cream which produce from low price corn in the area. Study of sensory evaluation and consumer acceptability were performed in 10 people to collect the consumer acceptability scores by a 5-point hedonic scale (scale : 1-dislike extremely; 2-dislike slightly; 3-neither like nor dislike; 4-like slightly; 5-like extremely) to study the effects of sugar content at 3, 5 and 7% which consumers are most accepting at the amount of sugar at 5% (4.60±0.51). The production of corn yogurt ice cream by using corn yogurt and add a stabilizer which comparing carboxymethyl cellulose at concentrations of 0.2 and 0.4, sugar content at 6%, 10% and 11%, which consumers are most accepting at the carboxymethyl cellulose concentrations of 0.2% in 11% sugar (4.90±0.31). The nutrient fact analyze in yogurt and ice cream found that : moisture 76.57% protein 3.05% fat 2.29% ash 0.84% and carbohydrate 17.25%. The consumers were likely to rate the score in corn products in texture, taste and overall liking ratings at the high level, while the color and smell were at the moderate level. In conclusion, corn yogurt ratio 1:2 in the amount of sugar at 5% and corn yogurt ice cream at the ratio of 1:2 the concentration of carboxymethyl cellulose at 0.2% in the amount of sugar at 11%. The results found that those corn could represent as low-value corn for diary food product which advantage in economic value and this study could be able to further study in the development of local corn.
Keywords: Corn, Yogurt, Ice cream, Consumer, Acceptability, Stabilizer

INTRODUCTION

Corn is the third most important cereal in the world (Kyenpia et al., 2009). In Thailand, corn is considered an economic crop because it has rich nutritional especially starch, sugar and vitamins and corn crop can be process into various products. Farmers in many parts of Nakhon Sawan and Uthai Thani provinces will have locally grown sweet corn and ready for consumers in every month. Corn is also composed of carbohydrates as the main component and rich in vitamins B1 and B2 which help the body to take nutrients such as fats, carbohydrates and proteins to use in body pathway efficiently and vitamin A can helps the optical system and eyesight. Corn is rich in antioxidants which decrease the risk of many kind of disease, especially cancer and chronic diseases in digestive system. Therefore, processing corn into food products is an interesting choice with many advantage (Daila et al., 2020). Yogurt is considered one of the popular products because of a good smell and many benefits to health. In general, adding fruit make yogurt more tasty and more attractive (Huang et al., 2020). Another choice is blending the yoghurt into ice cream which made from the combination of sugar, stabilizer, emulsifier, add more attractive color and flavoring and pass through the pasteurization process, incubate and finally blend them into the ice cream. The development of yogurt, corn ice cream is an appropriate way to adding value. The research of corn in local is a one choice helps to promote the conservation of local corn varieties and establish the local agriculture market and then help consumers get more nutritious corn meal product. In addition, it is also creating new

products to provide more options in the market (Durmaz et al., 2020). The objective is adding value to cheap local corn by food product development.

MATERIALS AND METHODS

1. Corn milk

Corn milk was prepared by boiling corn (on the cob) at 80°C for 15-20 min, then blended the corn kernels with water at a ratio of 1:1 (w/v). After that, filtered through filter cloth (muslin) and pasteurized at 80°C for 3 min, stored at 4°C and prepare analyze antioxidants.

2. Corn Yogurt

2.1 Corn Yogurt preparation.

Corn Yogurt was prepared by blending the corn kernels with pasteurized milk at a ratio of 1:2 (w/v) then added yogurt starter and incubated at room temperature for 24 hr. then kept at 4°C.

2.2 The effect of sugar content

Design the experiment by add sugar content at 3,5 and 7% (w/v) store at 4°C. After that took the evaluation (color, odor, flavor, texture, smoothness and overall liking ratings) with Thai consumer. The samples were analyzed by analysis of variance (Analysis of variance: ANOVA) and determine differences between the treatment means by Duncan method (Duncan's Multiple Range Test: DMRT)

3. Corn yogurt ice cream

3.1 Corn yogurt ice cream preparation

Corn Yogurt ice cream was prepared from corn yogurt with suitable level of sugar content and spin with an ice cream maker for 2 hr. Then added 100 g of sweet boiled corn kernel per 300 ml of corn yogurt ice cream and stored at -20°C.

3.2 The effect of carboxymethylcellulose (CMC) stabilizer

Corn yogurt ice cream was prepared and added carboxymethylcellulose (CMC) at 0.2 and 0.4% (w/v).

3.3 The effect of sugar content

Prepared corn yogurt ice cream by added 0.2% CMC (w/v) then added 6,10 and 11% (w/v) sugar and kept at -20 °C. After that performed the sensory evaluation (color, odor, flavor, texture, smoothnessand overall liking) with general consumer. The samples were analyzed by analysis of variance (Analysis of variance: ANOVA) and determine differences between the treatment means by Duncan method (Duncan 'S Multiple Range Test: DMRT).

4. Consumer acceptance tests of corn yogurt products and corn yogurt ice cream

All 10 testers were interviewed about accepting and give a reasoning for 15 minute and the acceptability data were analyzed.

5. Nutrition fact in corn yogurt ice cream

The most accepted corn yogurt ice cream was analyzed for nutrient content (protein, fat, carbohydrates, ash and moisture)

5.1 Moisture using the method of In-house method WI-TMC-02 based on AOAC (2016) 925.45

5.2 Protein using the method of In-house method WI-TMC-02 based on AOAC (2016) 925.45

5.3 Fat using the method of In-house method WI-TMC-03 based on AOAC (2016) 991.20

5.4 Ash using the method of In-house method WI-TMC-100 based on AOAC (2016) 2003.05

5.5 Carbohydrates using the method of In-house method WI-TMC-01 based on AOAC (2016) 938.08

RESULTS AND DISCUSSION

1. Analysis of antioxidants in corn milk

Corn juice was analyzed for the antioxidant activity by ABTS assay. The ABTS assay value of corn juice was 42.06%.

Sample	ABTS assay (% scavenging)			
	Replication 1	Replication 2	Replication 3	Average
Corn milk	41.415	41.637	43.117	42.056
	ABTS assay (mg trolox/g sample)			
Corn milk	0.292	0.293	0.304	0.296

2. Studying of the effect of some suitable sugar in the corn yogurt.

From the test (Table 2) study of suitable sugar content in the corn yogurt which adding sugar at 3, 5 and 7% and then assess the sensory quality using the analysis of variance and compare differences of mean values by Duncan method. The result found that the smell and smoothness was not significantly different ($P > 0.05$). For the color, taste, texture and overall liking ratings was found that 5% of sugar ($P \leq 0.0$) was mostly accepted and we recommend this formulate for further production because it is suitable for health. In contrast, the sugar content at 3% has too little sugar sweetness and not suitable for marketing while the 7% of sugar content popular but is not good for health which mostly accepted for the Thai main stream consumers too. When compared with the research of (Choll et al., 2013), in terms of color, smell, texture, smoothness of both quantity is not different. We suggest 5% of sugar suitable to preparing for study in the next method.

3. Study the amount of stabilizer effect on the quality of corn yogurt ice cream.

From the experiment (Table 3), to study the amount of stabilizer on quality of ice cream, corn yogurt by adding stabilizer, carboxymethylcellulose at 0.2 and 0.4%, adjusted sugar at 6, 10 and 11%, the products were evaluated for quality by using the ANOVA method and comparing the differences in the mean values by the Duncan method. From the experimental results found that the smell was not significantly different ($P > 0.05$) but in terms of color, taste, texture, smoothness and overall liking was significantly different ($P \leq 0.05$). The highest concentration of carboxymethylcellulose at 0.2% and the sugar content at 11% were accepted. We also found that the addition of carboxymethyl cellulose stabilizers in various concentrations does not result in color, odor, smoothness but effect on the texture. When adding in a high concentration, the viscous texture is not suitable for consumers which is consistent with the research (Lucey et al., 2004). Carboxymethylcellulose stabilizers are not different in color, odor, and smoothness. But if put in a very high concentration that affects the texture and consumers.

4. To study the acceptance of the distribution of corn yoghurt and corn yogurt ice cream.

From the study (Table 4), it was found that interviewing all 10 people, all of them were accept the products (corn yoghurt and corn yogurt ice cream) for marketing as well as the qualitative data confirmed that a main reason is "The delicious taste, fragrant aroma, corn color, texture, overall liking ratings and suitable for consumers of all ages". Which is consistent with the research of (Haidar et al., 1997) by the interviewer's question and answer.

5. Nutrient Analysis in Corn Yogurt Ice Cream**.**

The nutrients of corn yogurt ice cream are presented in Table 1.

Table 1 Nutrient compositions of corn yogurt ice cream.

Test	%
Moisture	76.57
Protein	3.05
Fat	2.29
Ash	0.84
Carbohydrate	17.25
Energy, Kcal	101.81
Fat, Kcal	20.61

a b c d

Figure 1. corn milk (a) and corn yogurt (b) corn yogurt ice cream (c,d)

Table 2 Rating preferences of corn yogurt, consisting of 6 formulas.

Corn Yogurt :Fresh milk	Average preference score						
	Sugar (%)	Color	Smell	Taste	Texture	Smooth	Overall liking
1:2	3	4.30±0.48	3.20±0.78	2.80b±0.91	3.60b±0.78	3.50b±0.70	3.10c±0.56
1:2	5	4.50±0.52	3.70±0.67	4.30a±0.67	4.50a±0.52	3.80ab±1.03	4.60a±0.51
1:2	7	4.30±0.48	3.80±0.78	3.90ab±0.73	3.90b±0.47	4.00ab±0.47	4.00b±0.66

Table 3 The score of preference for ice cream, corn yogurt, amount 6 recipes.

Corn Yogurt : Fresh milk	Sugar (%)	Average preference score					
		Color	Smell	Taste	Texture	Smooth	Overall liking
0.2	6	3.80^{b}±0.42	3.70±0.48	3.00^{c}±0.47	3.50^{c}±0.52	3.60^{b}±0.51	3.70^{b}±0.48
0.2	10	4.20^{ab}±0.42	3.70±0.67	3.70^{b}±0.48	3.70^{bc}±0.67	3.90^{ab}±0.56	4.00^{b}±0.47
0.2	11	4.50^{a}±0.52	3.60±0.69	4.20^{b}±0.78	4.10^{b}±0.99	4.1^{ab}±0.99	4.20^{b}±0.76
0.4	6	4.10^{ab}±0.56	3.50±0.84	2.90^{c}±0.56	3.90^{bc}±0.31	3.70^{b}±0.48	3.70^{b}±0.67
0.4	10	4.30^{a}±0.48	3.80±0.63	3.90^{b}±0.56	4.00^{bc}±0.47	3.90^{ab}±0.56	4.00^{b}±0.47
0.4	11	4.40^{a}±0.51	3.90±0.73	4.80^{a}±0.42	4.90^{a}±0.31	4.50^{a}±0.52	4.90^{a}±0.31

Table 4 Accept and unaccepted consumers of corn yogurt products and corn yogurt ice cream.

produce	Assessment			
	Accept		Unaccepted	
	Number	%	Number	%
Corn yogurt	8	80	2	20
Corn ice-cream yogurt	10	100	0	0
Total	10	100	10	100

CONCLUSIONS

Corn yogurt and rice and yogurt ice cream developed from local corn is advantage with low cost and has high nutritional value. These products are the good texture and taste like yogurt which can be represent as another option for Thai people who need the healthy living. In addition, this research shows that the corn can be processing to a value-added product and show the efficacy for mass production in the future and put on another option in high nutrition food for health. The further study is fatty acid esters examine as well as the main flavor compounds in corn milk yogurt. Shelf-lives of corn milk and cow milk yogurts is an one target to explore.

ACKNOWLEDGEMENT

The grant bestowed by the National Research Council of Thailand (NRCT) is sincerely acknowledged. The authors also thank the Kasetsart Agricultural and Agro-Industrial Product Improvement Institute (KAPI; Bangkok, Thailand) for the support and all of the necessary facilities provided**.**

REFERENCES

Choll, M., D. Gille, A. Schmid, B. Walther, and P. Piccinali. 2013. Acceptance of sugar reduction in flavored yogurt. J. Dairy. Sci. 96: 5501–5511.

Durmaz, Y., M. Kilicli, O.S. Toker, N. Konar, I. Palabiyik. and F. Tamtürk. 2020. Using spray-dried microalgae in ice cream formulation as a natural colorant: Effect on physicochemical and functional properties. Algal. Res.47: 101811.

Hasneen, D.F., N.L. Zaki, M.S. Abbas, A.S. Soliman, I.S. Ashoush, and A.E. Fayed. 2020. Comparative evaluation of some herbs and their suitability for skimmed milk yoghurt and cast Kariesh cheese fortification as functional foods. Ann. Agric. Sci. 65(1): 6-12.

Haidar, A.H. 1997. Prospective chemistry teachers' conceptions of the-conservation of matter and related conceptions. J. Res. Sci. Teach. 34(1): 181-197.

Huang, Y.Y., J.J. Yu, Q.Y. Zhou, L.N. Sun, D.M. Liu, and M.H. Liang. 2020. Preparation of yogurt-flavored bases by mixed lactic acid bacteria with the addition of lipase. LWT. p.109577.

Jung, H., J.H. Moon, J.W. Park, and W.B. Yoon. 2020. Texture of surimi-canned corn mixed gels with conventional water bath cooking and ohmic heating. Food. Biosci. p.100580.

Ndimba, R.J., J. Kruger, L. Mehlo, A. Barnabas, J. Kossmann, and B.K. Ndimba. 2017. A comparative study of selected physical and biochemical traits of wild-type and transgenic sorghum to reveal differences relevant to grain quality. Front. Plant Sci. 8:952.

Lucey, J.A. 2004. Cultured dairy products: an overview of their gelation and texture properties. Int. J. Dairy Technol. 57: 77-84.

Pan, L.H., F. Liu, S.Z. Luo, and J.P. Luo, 2019. Pomegranate juice powder as sugar replacer enhanced quality and function of set yogurts: Structure, rheological property, antioxidant activity and *in vitro* bioaccessibility. LWT. 115: 108479.

Wang, K.J. and J.L. Zhao. 2019. Corn silk (*Zea mays* L.), a source of natural antioxidants with α-amylase, α-glucosidase, advanced glycation and diabetic nephropathy inhibitory activities. Biomed. Pharmacother.110: 510-517.

EC-P010

OPTIMIZATION OF BIOACTIVE COMPOUND EXTRACTION FROM KARANDA FRUIT AND ITS BIOLOGICAL PROPERTIES

Udomlak sukatta[1]*, Prapassorn Rugthaworn[1], Ketsaree Klinsukhon[1], Lalita Khacharat[1], Natedao Musigamart[1] Thanapoom Maneeboon[2] and Wetanee Suravanichnirachorn[3]
[1] Kasetsart Agricultural and Agro-Industrial Product Improvement Institute (KAPI), Kasetsart University, Bangkok, 10900 Thailand
[2] Scientific Equipment and Research Division, Kasetsart University Research and Development Institute, Kasetsart University, Bangkok, 10900 Thailand
[3] Department of Food Technology and Nutrition, Faculty of Home Economics Technology, Rajamangala University of Technology Krungthep, Bangkok, 10120 Thailand
*E-mail: aapuls@ku.ac.th

ABSTRACT
The present study was conducted to optimize total anthocyanin and total phenolic content from fruit of Karanda (*Carissa carandas*) using water extraction. Optimum extraction conditions were determined for the maximum extraction efficiency by using response surface methodology (RSM) with factorial design. The investigated factors including extraction temperature (50, 70 and 90 °C) and time (10, 20, 30 and 60 min). The result revealed that the optimum condition for extracting total anthocyanin and total phenolic was mixed dried fruit powder and water ratio of 1:20 (w/v), extraction temperature of 75.0±1 °C and extraction time of 40 min. This condition yielded Karanda fruit extract of 41.91%. The extract powder had red brown color with total anthocyanin content of 40.49+0.53 mg cyanidin-3-glucoside/100 g extract, cyanidin-3-glucoside and delphinidin-3-glucoside content of 19.88±1.40 and 4.18±0.36 mg/100 g extract, respectively, total phenolic content of 2051.81±5.71 mg GAE/100 g extract. Anti-free radical scavenging activities (IC_{50}) of Karanda fruit extract using DPPH and ABTS assay were 0.279±0.01 and 11.073±0.04 mg/ml, respectively. FRAP value of the extract was 248.48+2.43 µmol Fe (II)/g extract. Karanda fruit extract had high potent tyrosinase inhibitory effect and α-glucosidase inhibitory effect, with an IC_{50} of 26.36+1.35 mg/ml and 120.82±0.45 mg/ml, respectively.
Keywords: Karanda fruit, Extraction, Anthocyanin, Phenolic, Bioactivity.

INTRODUCTION

Carissa carandas, commonly known as Karanda belongs to Apocynaceae family and commonly found in various parts of Thailand. All parts of this plant can be used as traditional medicine. The unripe fruit was reported as an astringent, while the ripe fruit was taken as an antiscorbutic and remedy for biliousness. (Devmurari et al., 2010). The prominent biological activities have also been reported including antidiabetic, antimicrobial, cytotoxicity, anticonvulsant, hepatoprotective, antihyperlipidemic, cardiac depressant, analgesic, anti-inflammatory, antipyretic, and antiviral properties (Madhuri and Neelagund, 2019).

In this study, the extraction of anthocyanins and phenolic compounds from Karanda fruit was optimized by applying RSM of two-variable, three- and four levels, aiming to evaluate the influence of factors such as temperature and time on the process of extraction. In addition, anthocyanins in the fruit of Karanda were identified by high-performance liquid chromatography (HPLC). The crude extract obtained can be used as food, pharmaceutical and cosmetic products.

MATERIALS AND METHODS

1. Plant material preparation

The fully ripe of Karanda fruit were cleaned and cut into small pieces. Samples were dried in hot air oven at 45 °C and for 48 hours. The samples were then ground to a fine powder in a mechanical blender and stored in plastic bag at 4°C.

2. Extraction method

Optimum extraction conditions were determined for the maximum extraction efficiency by using response surface methodology (RSM) with factorial design. The investigated factors were extraction temperature (50, 70 and 90 °C) and time (10, 20, 30 and 60 min). Dried powder samples (10 g) were extracted with water under 1:20 solid–liquid ratio. The extracts were filtered through Whatman filter paper No. 1 and stored at 4 °C in storage vials for further analysis.

3. Determination of total phenolic content (TPC)

The total phenolic contents of the extract samples were measured using a modified colorimetric Folin-Ciocalteu method (Wolfe, et al., 2003).

4. Determination of total anthocyanin content (TAC)

The TAC was determined by the pH-differential method (Wrolstad et al., 2005). Absorbance was measured by a spectrophotometer-UV/VIS UVmini-1240 (Shimadzu, Japan) at 510 and 700 nm. Distilled water was used as blank. The TAC was calculated using Eq. (1) and expressed as cyanidin3-glucoside in mg/100 g sample.

$$\text{Total anthocyanins (mg/g)} = (A \times MW \times DF \times (V/G) / (\varepsilon \times l) \quad (1)$$

where A is absorbance = (A510nm – A700nm) pH 1.0 - (A510nm – A700nm) pH 4.5, ε is cyanidin-3-glucoside molar absorbance (26900L· (cm/mg), l is the cell path length (1 cm), MW is the molecular weight (449.2 g/L) and DF is the dilution factor.

5. Determination of individual anthocyanin by High-Performance Liquid Chromatography (HPLC)

Cyanidin-3-o-glucoside, Delphinidin, Pelargonidin and Malvidin were quantified by HPLC (Shimadzu, Japan) with an Inertsil ODS-3 C18 packed column (ID 5 µm, 250×4.6 mm). The HPLC analysis method used in this study was modified from the method of Salazar-González (2012).

6. In vitro free radical scavenging activity

In this study, three methods of free radical scavenging activity were evaluated for Karanda extracts. Vitamin C was used for reference of free radical scavenging activity.

DPPH radical scavenging activity

The scavenging effect of the extracts was assessed according to the DPPH assay described by Zhu et al. (2006) with some modifications. The percentage of inhibition (%inhibition) was calculated and IC_{50} which is an inhibitory concentration of sample required to reduce 50% of the DPPH radical was determined.

ABTS radical scavenging activity

The scavenging effect of the extracts was assessed according to the ABTS assay described by Re et al. (1999) with some modifications. The percentage of inhibition (%inhibition) was calculated and IC_{50} which is an inhibitory concentration of sample required to reduce 50% of the ABTS radical was determined.

Ferric reducing/antioxidant power (FRAP) assay

FRAP assay was based on the reduction of Fe^{3+}–TPTZ to a blue-coloured Fe^{2+}–TPTZ. The FRAP assay was adapted from Kubola and Siriamornpun (2008). The antioxidant potential of sample was determined from a standard curve plotted using the $FeSO_4$. $7H_2O$ linear regression equation to calculate the FRAP values of the sample with expressed as µmol of Fe (II)/g extract.

7. α-Glucosidase Inhibitory Assay

Alpha -glucosidase activity of extracts was carried out according to method of Kazeem et al. (2013) with some modification. The result was expressed as percentage inhibition.

8. Tyrosinase Inhibitory Assay

Tyrosinase-inhibition activity of extracts was performed according to method of Kubo et al. (2000) with slight modifications. The result was expressed as percentage inhibition.

9. Microbial analysis

Total plate count, yeast and mold count were conducted in accordance with AOAC methods (AOAC, 2000).

10. Data analysis

Analysis of variance (ANOVA), and mean separations were conducted using SPSS. Significant differences were determined at $p < 0.05$. STATISTICA software was employed for the regression analysis and graphical optimization.

RESULT AND DISCUSSION

In this study, factorial design (two variable, three and four levels) with the response surface methodology (RSM) was performed to evaluated the effect of extraction conditions using water as the extraction solvent on total anthocyanin content (TAC) and total phenolic content (TPC) of Karanda fruit extract. The effects of different extraction conditions on TAC and TPC were presented in Table 1. The results obtained during the optimization of the process showed that the highest amount of TAC and TPC were obtained at the condition of (70 °C and 10 min) and (90 °C and 30-60 min), respectively while the lowest amount of TAC and TPC were obtained with the same condition (50° C and 10 min). The extraction temperature and time was found to influence the TAC and TPC. In the case of TAC, extraction of Karanda fruit at 70 °C for long time (10-60 min) and 90°C for short time (10 min) provided high content of anthocyanin. In contrast, TAC was decreased as the extraction time was increase from 20-60 min at extraction temperature 90 °C. Anthocyanin pigments rapidly degrade during thermal processing because they are heat sensitive (Szalóki-Dorkó et al., 2015). For TPC, it was observed that increasing the extraction temperature and time resulted in higher phenolic content in Karanda fruit extract due to the high temperature condition has effect on the rupture of plant cell wall. In this way, polyphenols linked to the wall could be released from the cell wall matrix during the optimal temperature for extraction process. (Minatel et al., 2017).

Table 1 Effect of extraction conditions on TPC and TAC content of Karanda fruit extracts.

Parameters	time	Temperature		
		50	70	90
TAC (mg cyanidin-3-glucoside/100 g sample)	10	$31.44+0.89^{g}$	$44.67+0.29^{a}$	$44.66+0.37^{a}$
	20	$31.96+0.85^{fg}$	$42.37+0.33^{bc}$	$44.21+0.13^{ab}$
	30	$39.46+0.64^{de}$	$44.00+0.29^{ab}$	$41.35+0.12^{cd}$
	60	$37.95+0.28^{d}$	$43.49+0.11^{ab}$	$33.92+0.51^{f}$
TPC (mg GAE/100 g sample)	10	$1,095.76+33.10^{e}$	$1,239.77+12.52^{cd}$	$1,186.38+28.98^{de}$
	20	$1,198.71+45.66^{de}$	$1,342.53+52.17^{bc}$	$1,315.16+40.72^{bc}$
	30	$1,240.18+47.37^{cd}$	$1,383.36+72.10^{ab}$	$1,458.50+66.95^{a}$
	60	$1,229.23+11.34^{cd}$	$1,361.22+30.20^{ab}$	$1,468.32+30.20^{a}$

Mean values followed by different superscript in a column are significantly different ($p<0.05$).

All the responses were fitted to second-order polynomial equations. The equation for each variable showed in Table 2.

Table 2 The polynomial equation for TAC and TPC responses.

Response	Second degree polynomial equation	R^2	Model significance
TAC	$Y1 = -54.629 + 2.348x_1 + 0.792x_2 - 0.014x_1^2 - 0.009x_1x_2 - 0.003x_2^2$	0.773	0.000
TPC	$Y2 = 221.412 + 22.097x_1 + 11.738x_2 - 0.144x_1^2 + 0.075x_1x_2 - 0.191x_2^2$	0.794	0.000

X1 = Temperature(°C), X2 = time (min)

The generated response surface plots (Figure. 1) show the interactive effect of temperature and time on total anthocyanin and total phenolic content.

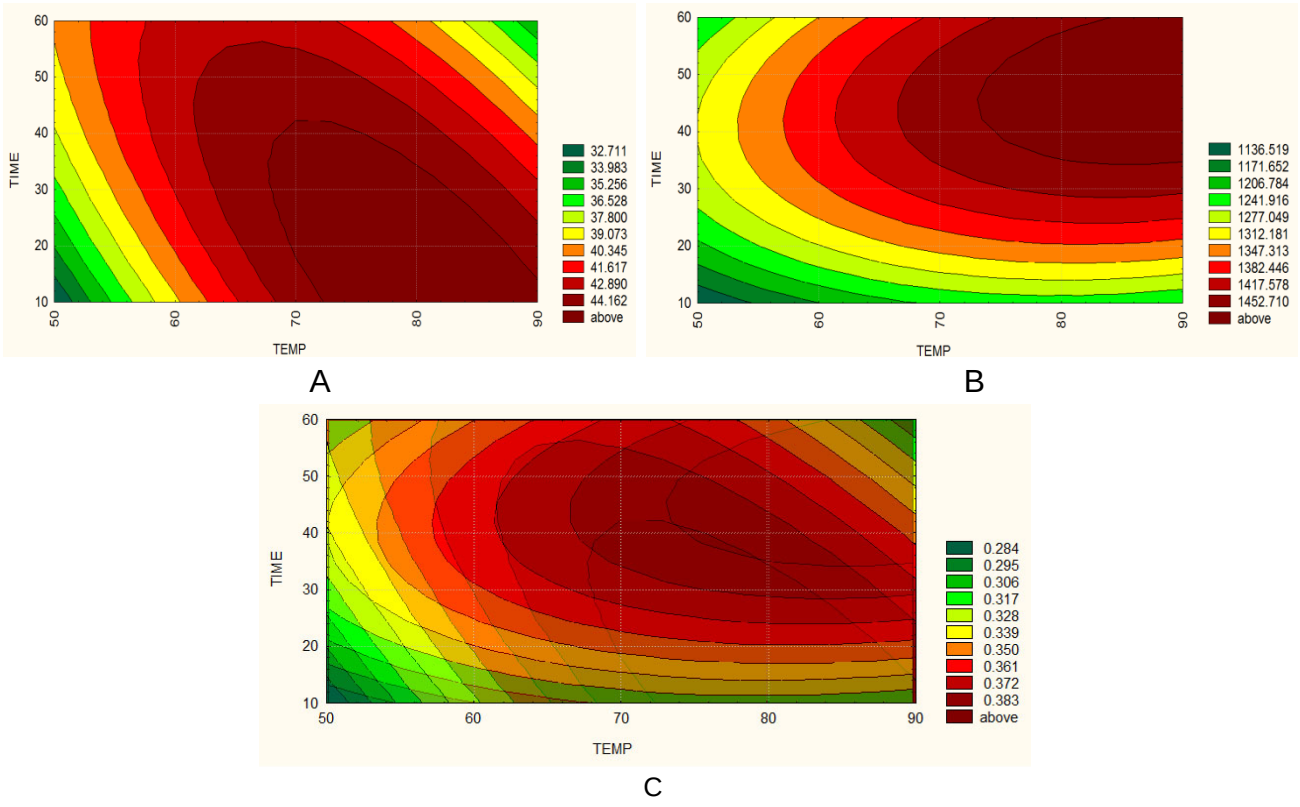

Figure 1. Response surface graphs, A = the interactive effect of temperature and time on total anthocyanin, B = the interactive effect of temperature and time on total phenolic content, C = the interactive effect of temperature and time on total anthocyanin and phenolic content.

The validation of the model was performed for three levels of extraction temperature; 70, 75, 80 °C and extraction time; 30 40 and 50 min (Table 3). Under optimal conditions the predicted TAC value was 42.60 mg cyanidin-3-glucoside/100 g sample and TPC value was 1,457.61 mg GAE/100 g sample. Triplicate experiments were carried out under the optimized conditions and the mean value of experimental results were 39.80 mg/100 g sample and 1,606.50 mg GAE/100 g sample. No significant difference ($p > 0.05$) was estimated between the experimental and predicted value that proved a good predictive capacity of the mathematical model and suitability of this model for optimizing extraction of anthocyanin and phenolic compounds from Karanda fruit.

Table 3 Validation of optimized model.

Temperature (°C)	Time (min)	TAC (mg/100 g sample)		TPC (mg GAE/100 g sample)	
		predicted value	experimental value	predicted value	experimental value
70.0±1	30.0	43.29	41.70[a]	1,400.34	1,558.07[b]
70.0±1	50.0	41.73	38.76[b]	1,434.50	1,603.05[ab]
75.0±1	40.0	42.60	39.80[ab]	1,457.61	1,606.50[ab]
80.0±1	30.0	43.07	40.31[ab]	1,427.81	1,607.66[ab]
80.0±1	50.0	35.80	35.80[c]	1,476.97	1,629.57[a]

Root mean square error (RMSE) of TAC and TPC are 2.55 and 59.75

The optimization results showed that the optimal conditions for maximum extraction of TAC and TPC from Karanda fruit was mixed dried fruit powder and water ratio of 1:20 (w/v), extraction temperature of 75.0 °C and extraction time of 40 min. The optimal condition was used for the upscale extraction of Karanda fruit. This process yielded extract 41.91% of dried fruit powder. The qualities and bioactivities of Karanda extract powder were shown in Table 4.

Table 4 Quality and bioactivity of Karanda extract powder.

Parameters	value
Yield (%)	41.91±1.37
TAC (mg cyaniding-3-glucoside/100 g extract)	40.49+0.53
cyanidin-3-glucoside content (mg/100 g extract)	19.88±1.40
delphinidin 3-glucoside content (mg/100 g extract)	4.18±0.36
TPC (mg GAE/100 g extract)	2051.81±5.71
Total plate count (CFU/g extract)	-
Yeast & Mold (CFU/g extract)	-
DPPH assay IC_{50} (mg/ml)	0.279±0.01
ABTS assay IC_{50} (mg/ml)	11.073±0.04
FRAP value (µmol Fe (II)/g extract)	248.48±2.43
α-glucosidase inhibition IC_{50} (mg/ml)	120.82±0.45
Tyrosinase inhibition IC_{50} mg/ml)	26.36±1.35

CONCLUSION

The use of RSM has effectively optimized extraction conditions. Optimized extraction parameters of 75.0°C for extraction temperature and 40 min for extraction time had successfully yielded optimal TAC and TPC in Karanda fruit. These results demonstrate that Karanda fruit extract contains high amount of anthocyanin and phenolic compounds can be used as active ingredient in food, pharmaceutical and cosmetic products.

ACKNOWLEDGEMENT

This work is supported by Kasetsart University Research and Development Institute, Kasetsart University.

REFERENCES

AOAC. 2000. Official Methods of Analysis of AOAC International, 15th ed. Association of Official Analytical Chemists. Virginia, USA.

Devmurari, V., P. Shivanand and N. P. Jivani. 2010. A review on Carissa congesta: phytochemical constituents, traditional use and pharmacological properties. Int. J. Chem. Sci. 8(1): 81-87.

Kazeem, M. I., J. O. Adamson and I. A. Ogunwande. 2013. Modes of inhibition of α-amylase and α-glucosidase by aqueous extract of *Morinda lucida* Benth leaf. Biomed Res. Int. 2013: 1-6.

Kubo, I., I. Kinst-Hori, S. K. Chaudhuri, Y. Kubo, Y. Sánchez and T. Ogura. 2000. Flavonols from Heterotheca inuloides: tyrosinase inhibitory activity and structural criteria. Bioorg. Med. Chem. 8(7): 1749-1755.

Kubola, J. and S. Siriamornpun. 2008. Phenolic contents and antioxidant activities of bitter gourd (*Momordica charantia* L.) leaf, stem and fruit fraction extracts in vitro. Food Chem. 110(4): 881-890.

Madhuri, S. and S. E. Neelagund. 2019. Antioxidant, antidiabetic activity and DNA damage inhibition activity of *carissa carandas* fruit. Int. J. Adv. Res. 4: 75-82.

Minatel, I.O., C.V. Borges, M.I. Ferreira, H.A.G. Gomez, C.Y.O. Chen and G.P.P. Lima. 2017. Phenolic Compounds: Functional Properties, Impact of Processing and Bioavailability, pp. 1–24. In: M. Soto-Hernández, M. Palma-Tenango, R. García-Mateos, (Eds.), Phenolic Compounds—Biological Activity. In Tech, London, UK.

Re, R., N. Pellegrini, A. Proteggente, A. Pannala, M. Yang and C. Rice-Evans. 1999. Antioxidant activity applying an improved ABTS radical cation decolorization assay. Free Radic. Biol. Med. 26(9-10): 1231-1237.

Salazar-González, C., F. T. Vergara-Balderas, A. E. Ortega-Regules and J. Á. Guerrero-Beltrán. 2012. Antioxidant properties and color of Hibiscus sabdariffa extracts. Cien. Inv. Agr. 39(1): 79-90.

Szalóki-Dorkó L, G. Végvári, M. Ladányi, G. Ficzek and M. Stéger-Máté. 2015. Degradation of anthocyanin content in sour cherry juice during heat treatment. Food technol. biotechnol. 53(3): 354-60.

Wolfe, K., X. Wu and R. H. Liu. 2003. Antioxidant activity of apple peels. Journal of agricultural and food chem. 51(3): 609-614.

Wrolstad, R. E., R. W. Durst and J. Lee. 2005. Tracking color and pigment changes in anthocyanin products. Trends Food Sci. Technol. 16(9): 423-428.

Zhu, K., H. Zhou and H. Qian. 2006. Antioxidant and free radical-scavenging activities of wheat germ protein hydrolysates (WGPH) prepared with alcalase. Process Biochem. 41(6): 1296-1302.

EC-P011

PROPERTIES AND BIOLOGICAL ACTIVITIES OF PROTEIN HYDROLYSATES FROM NIAW DAM MOR RICE BRAN

Phornphimon Janchai[1], Thanyaluk Seelachan[2], Waraporn Apiwatanapiwat[1], Pilanee Vaithanomsat[1], Antika Boondaeng[1], Jiraporn Meelaksana[1], and Sukantaros Tadakittisan[1]*
[1] Kasetsart Agricultural and Agro-Industrial Product Improvement Institute, Kasetsart University, Thailand
[2] Department of Agricultural Extension, Ministry of Agriculture and Cooperatives, Thailand
*E-mail: aapsrt@ku.ac.th

ABSTRACT
Niaw Dam Mor is a local black glutinous rice that has a soft texture when it is steam cooked. In the southern region of Thailand, the rice is commonly processed as a food supplement due to its high nutritional value and bioactive compounds. The objective of this research is to extract protein hydrolysate from Niaw Dam Mor bran by an enzymatic method at an optimized condition to be used as active ingredients in health supplements and cosmetic products. The protein phenolic compounds and anthocyanin in the extract were 23.92%, 7.63 g GAE/100g and 2.19 mg Cy3-glc E/g, respectively. The total amino acid content was 74.01 g/100g protein with glutamic acid, arginine and aspartic acid as the amino acids with highest composition (12.25, 7.90 and 7.02 g/100g protein, respectively). The highest vitamin content was vitamin B complex, including B3 (niacin), up to 45 mg/100 g, and magnesium was the highest mineral composition, 2.05 g/100g, followed by potassium and phosphorus (1.54 and 1.53 g/100 g). The protein hydrolysate extract exhibited antioxidant activity (DPPH IC_{50} = 0.102 mg/mL and FRAP = 762.88 µmol/g) and tyrosinase inhibition activity (IC_{50} = 9.07 mg/mL), which was comparable to the standard kojic acid (IC_{50} = 0.353 mg/mL). Overall, the protein hydrolysate from Niaw Dam Mor has a potential to be used as an ingredient in health supplements and cosmetic products.
Keywords: Niaw Dam Mor, Rice bran protein hydrolysate, Biological activity, Health supplement, Cosmetics

INTRODUCTION

Rice bran is an underutilized component obtained from milling process of paddy rice to produce white rice. Rice bran contains high quality protein with high amounts of essential amino acids, especially aromatic amino acids (9.46–11.41%) that act as strong antioxidants (Wang et al., 2017). Besides amino acids, rice bran also contains several vitamins and minerals such as Vitamin E, thiamine, niacin, aluminum, calcium, chlorine, iron, manganese (Saunders, 1990; Helm and Burks, 1996). Moreover, rice bran protein has various biological activities, including angiotensin converting enzyme (ACE) inhibitory activity (Chen et al., 2013), their cholesterol-lowering effect (Yang et al., 2013), and their antioxidant activities (Zhou et al., 2012 and Phongthai et al.,2016). However, nowadays, researchers and consumers are interested in colored rice due to their high nutritional properties. It contains anthocyanin, a substance that is beneficial to the body, has medicinal properties. It also has antioxidant properties, enhances in the circulation of the bloodstream, prevents the occurrence of cancer, diabetes, atherosclerosis and heart disease etc. Colored rice has a number of nutritional advantages over common rice, such as a higher content of protein, vitamins and minerals. However, the colored rice varies with cultivar and production location.

Niaw Dam Mor is a local black glutinous rice that has a soft texture when it is steam cooked. In the southern region of Thailand, the rice is commonly processed as a food supplement because it has high nutritional value and bioactive compounds including calcium, iron, and zinc. It also has high alpha-tocopherol vitamin E, vitamin B1, B3, B6, and high antioxidant activity. Tadakittasarn et al. (2017) extracted protein hydrolysate from white, red, and black rice bran and found that the black rice had the highest amount of anthocyanin, 1,696.08-7,319.48 ug/g, when compared with other rices (29.44-51.03 ug/g for red rice and 12.41-37.96 ug/g for white rice. This result was consistent with Laokulailok et al. (2011) which found the anthocyanin in the black rice to be 1,135-2,562 ug/g, similar to black soybean (220-1,870 ug/g, Xu et al. (2007)) and purple wheat bran (1,160 ug/g, Li et al. (2007)). Moko et al. (2014) reported that the colored varieties had better antioxidant properties than non-colored varieties and also concluded that color varieties

could be used as a material antioxidant sauce. Antioxidant activities of phenolic acid are higher than those of anthocyanin (Min et al., 2011, Chen et al., 2012 and Pitiga et al., 2013). Phenolic compounds also show higher reducing power compared with alpha-tocopherol (Laokuldilok et al., 2011). Therefore, the objective of this research is to extract the protein hydrolysate from Niaw Dam Mor rice bran, which contains important and bioactive compounds by an enzymatic method at the optimized condition for using as bioactive ingredients in health supplements and cosmetic products.

MATERIALS AND METHODS

Raw material and chemicals

Niaw Dam Mor Rice bran was obtained from Rice Department, Ministry of Agriculture and Cooperatives. The samples were packed in aluminum foil bags and kept at 4ºC until use.

Preparation of Niaw Dam Mor Rice bran protein hydrolysate (NDMRBPH)

Preparation of protein hydrolysate modified from the method of Yuan et al., 2008 and Silpradit et al., 2010. Rice bran was dissolved in 500 ml distilled water (1:5) weight by volume. The pH of homogenate was adjusted to pH 8 with 0.1 M NaOH, and was incubated at 63˚C followed by adding 1% alcalase enzyme, stirring at 300 rpm and controlling the pH value to 8 over 3 hours of incubation. After extraction, the enzyme was inactivated by heating at 85ºC for 10 min, then cooled down in cold water for 15 min. The protein supernatant was recovered using centrifugation at 8,000 g for 15 min at 4ºC. The protein solution was adjusted to pH 7.0 with 0.1 M citric acid. Then, RBPH solution was evaporated and freeze dried.

Composition, properties and biological activity of Niaw Dam Mor Rice bran protein hydrolysate (NDMRBPH)

Physical properties

The L*, a* and b* values for color of NDMRBPH were measured using Colour Measurement Spectrophotometer

Chemical properties

- Proximate analysis (AOAC,2006).
- Determination of total phenolic content (TPC)

The TPC of NDMRBPH was determined using Folin-Ciocalteu method according to Lim et al. (2007). The reaction mixture contained 300 µl of hydrolysate solution, 1.5 mL of Folin-Ciocalteu reagent (1:10 v/v) and 1.2 mL of 7.5% Na_2CO_3.The mixture was incubated in the dark at room temperature for 30 min. The absolute was measured at 765 nm. Distilled water was used as the control and gallic acid at 10-100 µg/ mL was used as a standard.

- The total amino acid was analyzed with HPLC (Water Alliance 2695 with heater) through Hypersil Gold column at 35ºC.
- Mineral analysis (USEPA, 1996) and vitamins (Chase et al., 1993)

Antioxidant properties

- DPPH radical scavenging activity

The scavenging effect of the extracts was assessed according to the DPPH assay described by Zhu et al. (2006) with some modifications. IC_{50} which is an inhibitory concentration of sample required to reduce 50% of the DPPH radical was determined.

- Ferric reducing/antioxidant power (FRAP) assay

FRAP assay was based on the reduction of Fe^{3+}–TPTZ to a blue-coloured Fe^{2+}–TPTZ. The FRAP assay was adapted from Kubola and Siriamornpun (2008). The antioxidant potential of sample was determined from a standard curve plotted using the $FeSO_4 7H_2O$ linear regression equation to calculate the FRAP values of the sample with expressed as µmol of Fe (II)/g extract.

- Inhibition of tyrosinase activity

Tyrosinase-inhibition activity of the extract of B. balsamifera DC leaves was performed by using L-DOPA as a substrate according to Kubo et al. (2000) and Saewan et al. (2011) with slight modification. The extract was first dissolved in DMSO at 1.0 mg/ml and then diluted to different concentration using

DMSO. Each sample (100 µl) was diluted with 1800 µl of 0.1 M sodium phosphate (pH 6.8) and 1000 µl of L-DOPA solution (with 0.1 M sodium phosphate, pH 6.8). Then, 100 µl of sample tyrosinase solution (138 units) was added in the reaction. The dopachrome formation was measured using UV-Vis spectrophotometer at 475 nm, for 6 min. The percentage of tyrosinase-inhibition activity was calculated.

RESULTS AND DISCUSSION

Composition, properties and biological activity of Niaw Dam Mor Ricebran protein hydrolysate

Physical properties

The color parameter of NDMRBPH was L*= 36.15±0.06, b*= 0.67±0.03 and a*= 0.14±0.03 (Figure 1). The NDMRBPH with purple to black had lower L* with dark Maroon color. Chen et al. (2016) evaluated the genotypic variation in red and purple bran of rice of diverse geographic origins for concentrations of oligomers and polymers of PAs, and their relationships to the total phenolic and flavonoid concentrations and antiradical capacity and identified purple rice bran had L*, a* and b*value of 28.90, 11.65 and 12.45, respectively.

Figure 1. Rice bran protein hydrolysate from Niam Dam Mor.

Chemical properties

Niaw Dam Mor Rice bran protein hydrolysate in Table 1 showed carbohydrate (54.23%) protein (23.92%), ash (11.20%), fat (5.61%), moisture (4.51%) and fiber (0.53%) respectively. Total phenolic contents (TPC) of NDMRBPH determined in this study was shown in Table 2. The results showed that NDMRBPH contained high amount of TPC (7.63±0.09 g GAE/100g). Comparable to Moongngarm et al., 2012 reported that TPC extracted from white red and black rice bran were 0.157, 0.439, 0.665 g GAE/ 100g DW, respectively. The total anthocyanin in black Niaw Dam Mor rice bran protein hydrolysate were 2.19 mg Cy3-glc E/g extract. Besides, Huang and Lai, 2016 reported that the Thai black rice bran contain highest total anthocyanins (11.27 mg Cy3-glc E/g DM) and also reported that red rice bran had only small amounts of anthocyanins 0.31-0.38 and 0.2- 0.28 mg Cy3-glc E/g DM in the outer and inner bran, respectively. Jangmesin et al., 2017 also reported that riceberry rice bran protein hydrolysate contained protein, TPC and anthocyanins 21.62%, 3.385 g GAE/100g 0.47 mg Cy3-glc E/g, respectively.

Table 1 Proximate composition of Niaw Dam Mor rice bran protein hydrolysate.

Sample	Protein (%)	Fat (%)	Ash (%)	Carbohydrate (%)	Fiber (%)	Moisture (%)
NDMRBPH	23.92±0.84	5.61±0.04	11.20±0.07	54.23±0.00	0.53±0.00	4.51±0.01

NDMRBPH = Niaw Dam Mor Rice bran protein hydrolysate

Table 2 Total phenolic content and total anthocyanin content of Niaw Dam Mor rice bran protein hydrolysate.

Sample	TPC (g GAE/100g)	TAC (mg Cy3-glc E/g Extract)
NDMRBPH	7.63±0.09	2.19±0.14

NDMRBPH = Niaw Dam Mor Rice bran protein hydrolysate, TPC=Total Phenolic content, TAC= Total anthocyanin content

The total amino acid compositions of NDMRBPH was shown in Table 3. The NDMRBPH contained high amount of glutamic acid 74.01 g/100g protein, arginine and aspartic acid as the amino acids with highest composition (12.25, 7.90 and 7.02 g/100g protein, respectively). The mineral composition of

NDMRBPH showed in Table 4 found that the NDMRBPH with the highest vitamin content was vitamin B complex, including B3 (niacin), up to 45 mg/100 g, vitamin B2 and B1 (0.31 and 0.032 mg/100 g respectively). The highest magnesium content was 2.05 g/100g, followed by potassium and phosphorus (1.54 and 1.53 g/100 g, respectively) in Table 5.

Table 3 Total amino acid composition (g/100g protein) of Niaw Dam Mor rice bran protein hydrolysate.

Total Amino	Amount (g/100g protein)
Aspartic acid	7.02
Serine	4.43
Glutamic acid	12.25
Glycine	5.10
Histidine	2.76
Arginine	7.90
Threonine	3.64
Alanine	5.52
Proline	3.43
Tyrosine	2.01
Valine	4.18
Lysine	4.10
Isoleucine	2.55
Leucine	5.69
Phenylalanine	3.43

Table 4 Vitamin B1, B2, B3 and B6 composition (mg/100g) of Niaw Dam Mor rice bran protein hydrolysate.

Sample	Vitamin B1 (mg/100g)	Vitamin B2 (mg/100g)	Vitamin B3 Niacin (mg/100g)	Vitamin B6 (mg/100g)
NDMRBPH	0.032	0.31	45.1	ND

NDMRBPH = Niaw Dam Mor Rice bran protein hydrolysate

Table 5 Mineral composition of Niaw Dam Mor rice bran protein hydrolysate.

Sample	P (g/100g)	K (g/100g)	Mg (g/100g)	Na (g/100g)	Ca (mg/100g)	Mn (mg/100g)	Fe (mg/100g)	Zn (mg/100g)	Se (mg/100g)
NDMRBPH	1.53	1.54	2.05	0.12	32.2	2.18	8.20	1.99	0.11

NDMRBPH = Niaw Dam Mor Rice bran protein hydrolysate

Antioxidant properties

The NDMRBPH was evaluated for its antioxidant activities with DPPH and FRAP assays. The IC_{50} value of NDMRBPH (Figure 2) was compared with ascorbic acid, α tocopherol and BHT. The result showed that DPPH radical scavenging activity of NDMRBPH (IC_{50} of 0.102 mg/mL) performed better oxidation inhibition than BHT (IC_{50} of 0.160 mg/mL). While FRAP assay had lower antioxidant properties than all standard (ascorbic acid, α tocopherol and BHT). Moongngarm et al. (2012) also reported that antioxidant activity of 1.03 and 1.15 mg/ml was observed in rice germ of black rice and red rice, respectively. Compared with the riceberry bran protein hydrolysate, it was found that DPPH radical scavenging activity of RBBPH (IC_{50} of 0.0517 mg/mL) performed better oxidation inhibition than BHT BHT (IC_{50} of 0.1299 mg/mL) (Jankmesin et al., 2017). However, the tyrosinase inhibition activity assay found that NDMRBPH had IC_{50} 9.07 mg/ml comparable with standard kojic acid (IC_{50} at 0.353 mg/mL) (Table 6). Thus, the NDMRBPH has potential to be used as an ingredient in cosmetic products.

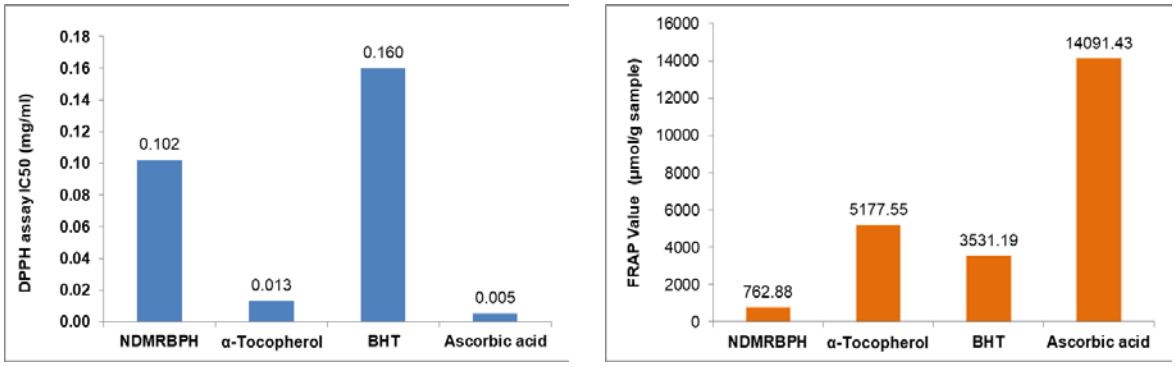

(A) **(B)**

Figure 2. Antioxidant properties of NDMRBPH (A) DPPH assay IC_{50} (mg/mL) and (B) FRAP Value (µmol/g sample).

Table 6 Tyrosinase Inhibit activity of Niaw Dam Mor rice bran protein hydrolysate.

Sample	Tyrosinase Inhibitory activity IC_{50} (mg/ml)
NDMRBPH	9.07
Kojic acid	0.353

NDMRBPH = Niaw Dam Mor Rice bran protein hydrolysate

CONCLUSIONS

The extraction of protein hydrolysate from Niaw Dam Mor rice bran have protein, phenolic compounds and anthocyanin of 23.92%, 7.63 g GAE/100g and 2.19 mg Cy3-glc E/g, respectively. It also contained carbohydrates (54.23%), protein, ash, fat, moisture and fiber (23.92%, 11.20%, 5.61%, 4.51% and 0.53%, respectively). The total amino acid content was 74.01 g/100g protein with glutamic acid, arginine and aspartic acid as the amino acids with highest composition (12.25, 7.90 and 7.02 g/100g protein, respectively). The highest vitamin content was vitamin B complex, including B3 (niacin), up to 45 mg/100 g, and magnesium was the highest mineral composition, 2.05 g/100 g, followed by potassium and phosphorus (1.54 and 1.53 g/100 g). The protein hydrolysate from Niaw Dam Mor rice bran had antioxidant activity (DPPH IC_{50} = 0.102 mg/mL and FRAP = 762.88 µmol/g) and tyrosinase inhibition activity (IC_{50} at 9.07 mg/mL), which was comparable to the standard kojic acid (IC_{50} = 0.353 mg/mL). Therefore, the protein hydrolysate from Niaw Dam Mor bran has a potential to be used as an ingredient in health supplements and cosmetic products.

ACKNOWLEDGEMENT

The financial support Rice Department, Ministry of Agriculture and Cooperatives.

REFERENCES

AOAC. 2006. Official Methods of Analysis of AOAC International, 17thed. The Association, Gaithersburg, MD.

Chase, G. W. Jr., W. O. Jr. Landen, A.M. Soliman and R. R. Eitenmiller. 1993. Liquid chromatographic analysis of niacin in fortified food products. J AOAC Int. 76: 390-393.

Chen, N., H. Yang, Y. Sun, J. Niu and S. Liu. 2012. Purification and identification of antioxidant peptides from walnut (*Juglans regia* L.) protein hydrolysates. Peptides, 38, 344–349.

Chen, J., S. Liu, R. Ye, G. Cai, B. Ji and Y. Wu., 2013. Angiotensin-I converting enzyme (ACE) inhibitory tripeptides from rice protein hydrolysate: Purification and characterization. J. Funct. Foods. 5, 1684–1692.

Chen, M. H., A. M. McClung and C. J. Bergman. 2016. Concentrations of oligomers and polymers of proanthocyanidins in red and purple rice bran and their relationships to total phenolics, flavonoids, antioxidant capacity and whole grain color. Food Chem. 208, 279-287.

Helm, R. M. and A. W. Burks. 1996. Hypoallergenicity of rice bran protein. Cereal Food World. 41: 839-843.

Laokuldilok, T., C. F. Shoemake and S. Jomgkaewwattana. 2001. Antioxidants and antioxidant activity of several pigmented rice brans. J. Agric. Food Chem. 59: 193–199.

Li W., M. D. Pickard and T. Beta. 2007. Effect of thermal processing on antioxidant properties of purple wheat bran. Food Chem. 104: 1080–1086.

Lim, Y. Y., T. T. Lim and J. J. Tee. 2007. Antioxidant properties of several tropical fruits: A comparative study. Food Chem. 103(3): 1003-1008.

Jangmesin, K., H. Rimkeeree and S. Tadakittisarn. 2017. Enzymatic optimization of riceberry bran protein hydrolysate extraction and characterization. Current Applied Science and Technology.17(2): 209-223.

Kubo I., I. Kinst-Hori, S. K. Chaudhri, Y. Kubo, Y. Sanchez and T. Ogura. 2000. Flavonols from Heterotheca inuloides: tyrosinase inhibitory activity and structural criteria. Bioorg Med Chem. 8:1749-1755.

Kubola, J. and S. Siriamornpun. 2008. Phenolic contents and antioxidant activities of bitter gourd (*Momordica charantia L*.) leaf, stem and fruit fraction extracts in vitro. Food Chem. 110: 881–890.

Min B., A. M. McClung and M. H.Chen. 2011. Phytochemicals and antiooxidant capacities in rice brans of different color. J Food Sci. 76: C117-126.

Moko, E. M., H. Purnomo, J. Kusnadi and F. G. Ljong. 2014. Phytochemical content and antioxidant properties of colored and non colored varieties of rice bran from Minahasa, North Sulawesi, Indonesia. Int. Food Res. J. 21(3): 1017-1023.

Moongngarm, A., N. Daomukdaa and S. Khumpika. 2012. Chemical compositions, phytochemicals and antioxidant capacity of rice bran, rice Bran Layer, and rice germ. APCBEE Procedia. 2: 73-79.

Phongthai, S., S. T. Lim and S. Rawdkuen. 2016. Optimization of microwave-assisted extraction of rice bran protein and its hydrolysates properties. J. Cereal Sci. 70, 146–154.

Pitija, K., M. Nakorniab, T. Sriseadka, A. Vanavichit and S. Wongpornchai. 2013. Anthocyanin content and antioxidant capacity in bran extracts of some Thai black rice varieties. Int. J. Food Sci. Technol. 48: 300-308.

Saewan N., S. Koysomboon and K. Chantrapromma. 2011. Anti-tyrosinase and anti-cancer activities of flavonoids from *Blumea balsamifera* DC. J. Med. Plant. Res., 5(6): 1018-1025.

Saunders, R. M. 1990. The properties of rice bran as a food stuff. Cereal Food World. 35: 632-662.

Silpradit, K., S. Tadakittasarn, H. Rimkeeree, S. Winitchai and V. Haruthaithanasan. 2010. Optimization of ice bran protein hydrolysate production using Alcalase. As. J. Food-Ind. 3(02): 221-231.

Tadakitisarn, S., S. Winitchai, U. Sukatta, N. Musigamart, S. Liengprayoon, P. Rugthaworn, P. Janchai, T. Seelachan and P. Vutdhipapornkul. 2017. The physicochemical properties and utilization of rice bran and rice bran oil for value. Final Report Year 2017.

Wang, X., H. Chen, X. Fu, S. Li and J. Wei. 2017. A novel antioxidant and ACE inhibitory peptide from rice bran protein: Biochemical characterization and molecular docking study. LWT - J Food Sci Technol. 75:93–99.

Xu, B. J., S. H. Yuan and S. K. Chang. 2007. Comparative analyses of phenolic composition, antioxidant capacity, and color of cool season legumes and other selected food legumes. J. Food Sci. 72(2): S167–176.

Yang, L., J. H. Chen, T. M. Xu, H. Nie and H. K. Yang. 2013. Hypocholesterolemic effect of rice protein is due to regulating hepatic cholesterol metabolism in adult rats. Gene, 512: 470–476.

Yuan, X., X. Gu and J. Tang. 2008. Optimization of the production of *Momordica charantia* L. Var. abbreviata Ser. protein hydrolysates with hypoglycemic effect using Alcalase. Food Chem. 111: 340-344.

Zhou, K., S. Sun and C. Canning. 2012. Production and functional characterisation of antioxidative hydrolysates from corn protein via enzymatic hydrolysis and ultrafiltration. Food Chem. 135: 1192–1197.

Zhu, K., Z. Huiming and Q. Haifeng. 2006. Antioxidant and free radical-scavenging activities of wheat germ protein hydrolysates (WGPH) prepared with alcalase. Process Biochem. 41(6): 1296-1302.

EC-P012

DEVELOPMENT OF NANOEMULSION FOR ELDERLY SKINCARE PRODUCT FROM SANGYOD AND TUBTIMCHUMPAE RED RICE BRAN OIL

Supanida Winitchai[1]*, Pavinee Yampeng[2], Hathairat Rimkeeree[2], Natedao Musigamart[1], Warawut Suphamitmongkol[1], Naddamas Tomon[1], and Siriluck Liengprayoon[1]
[1] Kasetsart Agricultural and Agro-industrial Product Improvement Institute (KAPI), Kasetsart University, Bangkok, 10900, Thailand
[2] Department of product development, Faculty of Agroindustry, Kasetsart University, Bangkok, 10900, Thailand
*E-mail: aappsw@ku.ac.th

ABSTRACT
Nanoemulsions are well recognized and widely applied in cosmetics due to their stability and permeation effectiveness. For elderly, skin structure and functions undergo degeneration with age increasing which makes skin prone to pervasive dryness, itching and cutaneous infection as well as the changes in personal appearances. To prevent water loss caused by skin aging, natural oils from different sources have been often applied in skincare products. However, slow permeability, viscous and stickiness after application are technical issues for oils. This study aims at developing the nanoemulsion using rice bran oils from two local red rice varieties which are Sangyod and Tabtimchumpae planted in the south of Thailand. These two varieties are well known for their cooking quality as well as bioactive compound richness. A pseudo-ternary phase diagram was constructed using a mixture of Sangyod (SRBO) and Tabtimchumpae rice bran oil (TRBO) as the oil phase (Omix) with surfactant/co-surfactant (Smix) and water through the aqueous titration method. A selected formulation which provided stable emulsion consisted of 4% Omix (SRBO/TRBO; 1:1), 16% Smix (Tween80/PEG400; 2:1) and 80% water. Nanoemulsion was produced from this formulation using microfluidizer under high pressure of 15,000 psi for 10 times. The obtained nanoemulsion appearance was almost transparent and low viscosity which indicated good stability. The average droplet size was 125.5 ± 3.80 nm with a polydispersity index of 0.37 and low negative charges with zeta potential value of -3.2 mV. The nanoemulsion was found to be stable after passing 6 cycles of heating-thawing test (45°C and 4°C) as the droplet size and zeta potential were not significantly different. The results suggested that nanoemulsion containing SRBO and TRBO could be potentially served as an ingredient in elderly skincare products to better prevent skin moisture loss and provide antioxidant activity.
Keywords : Nanoemulsion, Elderly, Rice bran oils, Sangyod and Tabtimchumpae rice bran oils

INTRODUCTION

Sangyod rice (*Oryza sativa*, L., var. indica) is one of special red rice, originally planted in Patthalung, a province in the south of Thailand, for a hundred years. This variety is known for the high content of minerals, vitamin B complex and bioactive compounds. For Tabtimchumpae, it is produced from hybridization between Hommali rice, Jasmine rice and Sangyod rice thus this variety is also having a red colour. Rice with red colour usually contains high amount of phenolics and flavonoids which is known for its antioxidant activity (Dajian et al., 2002). Beside edible products, rice bran oil obtained from conventional rice stains such as Jasmine rice as well as colour rice is also applied in cosmetic products due to their nutritional quality and emollient effect. However, the direct application of oils in cosmetic products is limited by its stickiness and skin permeation which impacts customer perception. Nanoemulsion is a technique widely used as a delivery system of lipophilic compounds as they support the skin penetration of active ingredients and thus increase their concentration in the skin which plays an important role in cosmetics product formulations. The cosmetic industry has shown an increased interest in nanoemulsion due to its active release efficiency on the skin, thus reducing the probability of skin irritation; excellent sensorial and aesthetic aspects; low viscosity; need for less surfactant; lower production costs; and higher stability (Fidel Villalobos-Castillejo, et al., 2018). These characteristics of nanoemulsion meets the fundamental process of formulating such products as body lotions, skin creams and sunscreens (Puglia, et al., 2010). Based on this information,

this study aims at developing nanoemulsion formulation containing Sangyod and Tabtimchumpae rice bran oil targeting the application for elderly skin. Suitable nanoemulsion formation is validated by the determination of physical and chemical property including stability of the nanoemulsion.

MATERIALS AND METHODS

Material

The materials used in this study were: Commercial Sangyod rice bran oil (SRBO) obtained from Patthalung province and Tabtimchumpae rice bran oil (TRBO) obtained from Kamphaeng Phet province. Both rice bran oils were extracted with a cold hydraulic press. The non-ionic surfactants, sorbitan monolaurate (Tween® 20), and sorbitan monooleate (Tween® 80) were purchased from Merck and co-surfactant, propylene glycol (PG) and PEG-400, were purchased from Namsiang Ltd, Thailand. Deionized water was used as an aqueous phase.

Preparation of pseudo ternary phase diagrams of nanoemulsion systems for SRBO and TRBO

The three phases in the nanoemulsion system consisted of SRBO and TRBO mixture (1:1, v/v) as oil phase (Omix), the mixture of surfactant and co-surfactant (Smix) and deionized water as aqueous phase. The four combinations of Smix were Tween 20: PG, Tween 20: PEG-400, Tween 80: PG and Tween 80: PEG-400. Each combination contained a mixture of surfactant and co-surfactant at the ratio of 1:1, 2:1 and 3:1 (v/v) so in total 12 formulas. The formulation between Omix and Smix were varied from 1:9 to 9:1. Total tested formulation used for nanoemulsion preparation was 108 formulas as illustrated in Figure 1. To develop a pseudo ternary phase diagram, each formulation was titrated with the constant volume of deionized water (200 µL, or 80% of total volume) and mixed with vortex and the quantity of Omix and Smix were calculated accordingly. After addition of water, the physical appearance of solution was daily observed during 3 days of storage at room temperature. Each formulation was visually graded from the transparent (A), slightly milky (B) and milky (C) according to the definition of Shafiq-un-Nabi, (2007). The observed physical appearance was plotted on a pseudo-three-component phase diagram with 1 axis representing the aqueous phase at a fixed volume ratio, the second representing the oil phase, and the third representing a mixture of surfactant and co-surfactant.

Preparation of nanoemulsion using microfluidizer and stability testing

The formulation provided the transparent (grade A) and slightly milky (grade B) solution was used to prepare emulsion using a high speed homogenizer (5,000 rpm for 5 minutes) and subjected to Microfluidizer (M-110L, USA) in order to obtain nanoemulsion. The studied parameters of microfluidization were pressure (10,000 psi and 15,000 psi) and the number of cycles (0 - 10). The nanoemulsion was then tested for their stability by heating-thawing at 45 °C for 24 hours and 4 °C for 24 hours for 6 times. The droplet size, polydispersity index and zeta potential of nanoemulsion were characterized using nanoparticle analyzer (Nanoplus HD, United States).

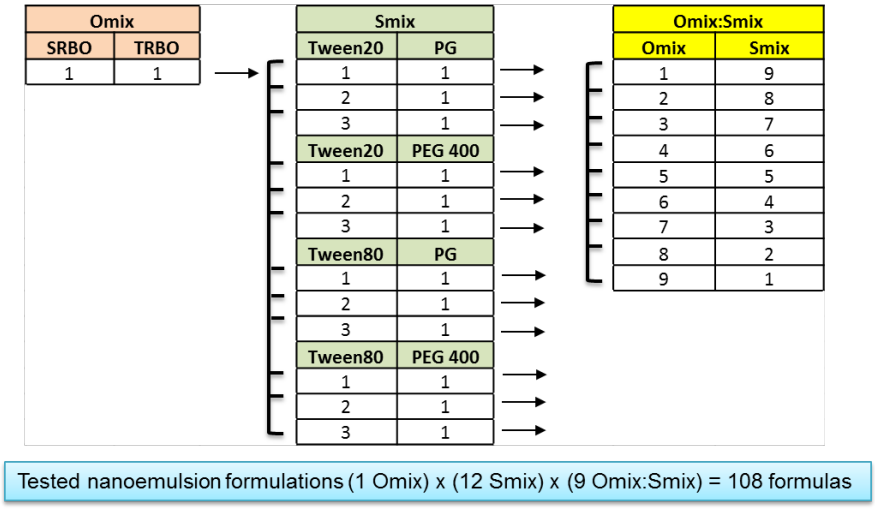

Figure 1. The full combination of studied nanoemulsion systems.

RESULTS AND DISCUSSION

Formulation selection

The nanoemulsion from the combination indicated in Figure 1 was prepared and visually graded. It was observed that only Smix prepared from Tween 80 and PEG400 from 1:1 and 2:1 ratio and Tween 20 and PEG400 at the ratio of 3:1 could provide nanoemulsion (Table 1).

Table 1 Evaluation of emulsion formation with grading system.

S:Co-S (Smix)	Omix:Smix	Grading System	Appearance
Tween 80: PEG400 (1:1)	1:9	Grade A	Clear appearance
	2:8	Grade B	Slightly less clear appearance
	3:7	Grade C	Milky
	4:6	Grade C	Milky
Tween 80: PEG400 (2:1)	1:9	Grade A	Clear appearance
	2:8	Grade B	Slightly less clear appearance
	4:6	Grade C	Milky
	5:5	Grade C	Milky
Tween 20: PEG400 (3:1)	1:9	Grade C	Milky
	2:8	Grade C	Milky
	3:7	Grade C	Milky
	4:6	Grade C	Milky
	5:5	Grade C	Milky

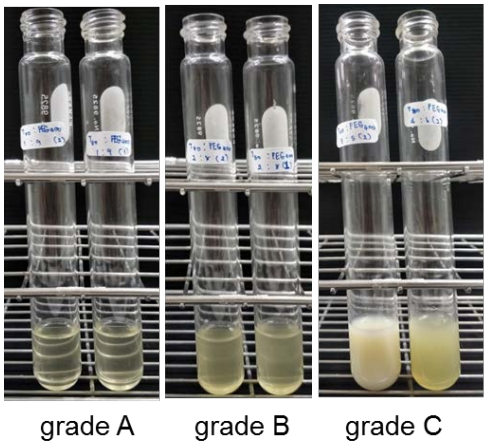

Figure 2. Physical appearance of nanoemulsion grade from transparent (grade A), slightly milky (grade B) and milky (grade C).

Smix of Tween 80 and PEG400 from 1:1 and 2:1 ratio could provide grade A and B nanoemulsion when Omix: Smix ratios were 1:9 and 2:8, respectively. Meanwhile, Smix composed of Tween 20 and PEG400 at the ratio of 3:1 from both 1:9 and 2:8 of Omix:Smix gave only milky nanoemulsion (grade C) as indicated in Table 1. Figure 2 showed the nanoemulsion defined as grades A, B and C. The pseudo-ternary phase diagrams of water, Omix and Smix (Tween 80: PEG 400 at the ratio of 1:1 and 2:1) is shown in Figure 3. The grey area in the diagram indicated the nanoemulsion region. At the fixed ratio of water (80%), the combinations of Omix and Smix that provided grade A and B nanoemulsion were selected. At Tween 80: PEG 400 at the ratio of 1:1 (grade A) the proportion of Omix and Smix were 2% and 18%, respectively. For 2:1 of Tween 80: PEG 400, the proportion of Omix was 4% and Smix was 16%. These formulations were further subjected to nanoemulsion preparation using a microfluidizer.

Preparation of nanoemulsion by microfluidizer

From the previous step, the selected formulation for nanoemulsion preparation by microfluidizer is indicated in Table 3. The tested pressures of microfluidizer were 10,000 and 15,000 psi. In fact, formulas 1-4 (set 1) were the same as set 2 (1-2 to 4-2) but prepared under the pressure of 15,000 psi. Before passing

through microfluidizer the mixture was homogenised at 5,000 rpm for 5 minutes and the initial droplet sizes were recorded as 0 cycles. After that, the sizes were recorded after every 2 cycles until 10.

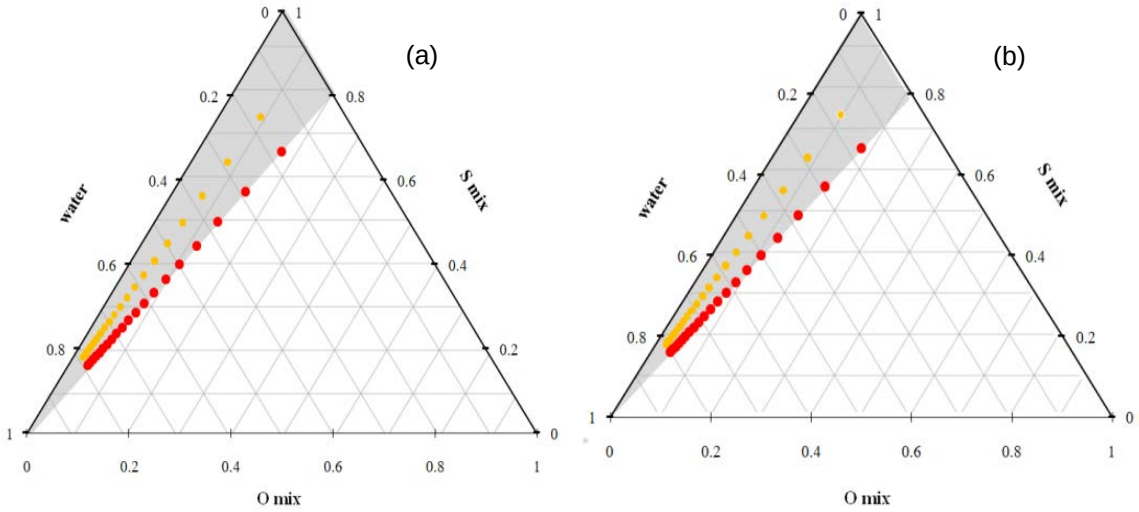

Figure 3. Pseudo-ternary phase diagram of water, Omix and Smix at the ratio Tween 80: PEG 400 at 1:1 (a) and 2:1 (b). Grade A (•) and grade B (•) nanoemulsion is indicated inside the nanoemulsion region (grey part).

Table 3 Selected formulas used for nanoemulsion preparation by microfluidizer.

Formula	grade	Smix	Omix:Smix	Omix (%)		Smix (%)		Water (%)	Total (%)	Pressure
				SRBO	TRBO	Tween 80	PEG400			
1-1	**A**	**1:1**	**1:9**	1	1	9	9	80	100	10,000psi
2-1	**B**	**1:1**	**2:8**	2	2	8	8	80	100	
3-1	**A**	**2:1**	**1:9**	1	1	12	6	80	100	
4-1	**B**	**2:1**	**2:8**	2	2	10.67	5.33	80	100	
1-2	**A**	**1:1**	**1:9**	1	1	9	9	80	100	15,000psi
2-2	**B**	**1:1**	**2:8**	2	2	8	8	80	100	
3-2	**A**	**2:1**	**1:9**	1	1	12	6	80	100	
4-4	**B**	**2:1**	**2:8**	2	2	10.67	5.33	80	100	

It was found that the pressure of 10,000 and 15,000 psi could provide the droplet sizes in the nanometre scale (150 – 350 nm at 2 cycles) according to the nanoemulsion definition (Nor Azrini Nadiha Azmi et al., 2019). However, the droplet size of emulsion from formula 2-1 (~200 nm) could not be reduced much at 10,000 psi pressure even 10 cycles but it could be lower to around 150 nm when 15,000 psi pressure applied (formula 2-2). For the other formulas, the droplet sizes were significantly decreased with number of cycles and pressure (Table 4). The smallest nanoemulsion droplet size was obtained from formula 4-2 with a diameter of 125 nm.

Table 5 shows the droplet sizes of nanoemulsion prepared from the same condition but subjected to heating and thawing at 45 °C for 24 hours and 4 °C for 24 hours for 6 times. It was observed that the droplet sizes were significantly increased with heating and thawing which could be due to the agglomeration of the phase. However, with the droplet size around 200 nm the agglomeration was less observed as compared to the bigger droplet size as seen in formula 1-1, 1-2, 3-1 and 3-2. Among tested formulas, formula 2 and 4 provided the smallest droplet size (~125 - 150 nm) even after stability test the size was less change (~200 nm) as compared to another formula. With satisfactory physical properties, formula 2 and 4 were further measured for zeta potential and the values were similar in the range of 1.72 to -3.17 mV which was also the same charge as the skin. It can be considered that these 2 formulas were suitable for further development of elderly skincare products.

Table 4 Nanoemulsion droplet sizes after 0 – 10 cycles of size reduction using microfluidizer at the pressure of 10,000 and 15,000 psi.

cycle	10,000 psi				15,000 psi			
	formula 1-1	formula 2-1	formula 3-1	formula 4-1	formula 1-2	formula 2-2	formula 3-2	formula 4-2
0	987.8 ± 50.7^{a}	238.4 ± 1.37^{a}	532.6 ± 25.5^{a}	345.3 ± 8.55^{a}	902.7 ± 84.4^{a}	270.6 ± 0.70^{b}	426.1 ± 99.7^{a}	373.9 ± 27.5^{a}
2	157.9 ± 3.25^{c}	222.7 ± 0.40^{b}	189. 5± 4.23^{e}	238.1 ± 4.46^{d}	348.6 ± 2.75^{c}	182.2 ± 13.5^{a}	162.3 ± 1.42^{b}	137.7 ± 0.85^{b}
4	275.9 ± 25.2^{c}	218.3 ± 1.15^{c}	453.2 ± 10.6^{c}	263.0 ± 14.6^{c}	390.7 ± 16.3^{c}	166.2 ± 2.74^{b}	158.7 ± 1.01^{b}	131.3 ± 3.34^{b}
6	212.9 ± 33.0^{d}	211.6 ± 0.20^{d}	350.9 ± 3.70^{d}	309.5 ± 4.26^{b}	565.3 ± 130.2^{b}	155.3 ± 2.15^{c}	147.3 ± 0.74^{b}	129.2 ± 6.59^{b}
8	243.2 ± 10.9^{cd}	202.1 ± 3.93^{e}	209.3 ± 3.41^{e}	351.9 ± 15.9^{a}	465.8 ± 41.6^{bc}	150.0 ± 2.10^{c}	138.9 ± 1.56^{b}	125.5 ± 2.99^{b}
10	339.2 ± 17.6^{b}	200.5 ± 1.53^{e}	490.8 ± 5.18^{e}	230.0 ± 8.76^{d}	928.1 ± 127.4^{a}	154.1 ± 1.21^{c}	141.3 ± 0.69^{b}	125.5 ± 3.80^{b}

The value was an average from 3 repetition ± SD, the same letter in the column indicates non-significant data

Table 5 Nanoemulsion droplet sizes of nanoemulsion after 0 – 10 cycles of size reduction using microfluidizer at the pressure of 10,000 and 15,000 psi measured after stability test (6 cycles of heating-thawing at 45 °C for 24 hours and 4 °C for 24 hours).

cycle	10,000 psi				15,000 psi			
	formula 1-1	formula 2-1	formula 3-1	formula 4-1	formula 1-2	formula 2-2	formula 3-2	formula 4-2
0	1198 ± 15.1^{a}	243.8 ± 0.63^{a}	194.9 ± 29.8^{d}	354.7 ± 0.42^{a}	1120.6 ± 55.2^{a}	184.5 ± 0.56^{a}	502.5 ± 37.7^{a}	459.3 ± 35.9^{a}
2	165.8 ± 0.78^{c}	223.1 ± 0.35^{b}	447.3 ± 5.65^{b}	241.8 ± 6.23^{c}	374.4 ± 2.55^{b}	271.5 ± 5.78^{a}	205.0 ± 1.63^{b}	238.4 ± 1.13^{b}
4	282.9 ± 16.5^{bc}	215.9 ± 1.41^{b}	258.4 ± 13.4^{c}	288.5 ± 20.6^{b}	468.2 ± 4.95^{b}	267.0 ± 0.07^{ab}	164.0 ± 0.07^{b}	204.5 ± 0.49^{b}
6	253.9 ± 45.7^{bc}	213.8 ± 0.14^{b}	210.4 ± 4.66^{d}	320.5 ± 3.81^{b}	620.2 ± 45.3^{b}	159.3 ± 2.05^{ab}	232.1 ± 0.78^{b}	191.8 ± 8.34^{b}
8	266.8 ± 15.3^{bc}	201.5 ± 4.74^{c}	494.9 ± 2.75^{b}	356.2 ± 20.4^{a}	491.4 ± 53.2^{b}	265.1 ± 1.41^{ab}	182.9 ± 2.19^{b}	178.9 ± 2.69^{b}
10	379.6 ± 4.53^{a}	198.4 ± 2.12^{c}	569.3 ± 5.65^{a}	238.3 ± 10.3^{c}	981.1 ± 77.2^{a}	251.8 ± 1.48^{a}	229.8 ± 0.64^{b}	202.5 ± 4.38^{b}

The value was an average from 3 repetition ± SD, the same letter in the column indicates non-significant data

CONCLUSIONS

The formulation of nanoemulsion using rice bran oil from two Thai rice varieties (Sangyod and Tabtimchumpae) which is well known for nutritional value and the antioxidant effect was developed. The pseudo-ternary phase diagram was constructed to identify a suitable formulation for further nanoemulsion preparation using a microfluidizer. The best condition was found to consist of 2% of SRBO and 2% of TRBO. The surfactant and co-surfactant used were Tween80 and PEG400 at 2:1 ratio and the suitable proportion in the formula was 16% and 80% of water. This formula could provide the smallest droplet size at 125 nm with 10 cycles of 15,000 psi pressure using a microfluidizer. The droplet size was slightly increased to around 200 nm when it was subjected to stability test. The zeta potential of around -3.2 mV was compatible with skin charge. In addition to the natural benefit of rice bran oil, with the characteristic obtained, the developed nanoemulsion could be potentially applied as an active ingredient for elderly skincare products.

ACKNOWLEDGEMENT

The authors are highly thankful for Kasetsart Agricultural and Agro-Industrial Product Improvement Institute (KAPI) and Department of Product Development. The partial financial support and research facility from Faculty of Agro-Industry is also appreciated.

REFERENCES

Dajian, H., O. Boxin. and H.W. Maureen, 2002. Development and validation of oxygen radical absorbancecapacity assay for lipophilic antioxidant using randomly methylated β-cyclodextrin as the solubility enhancer. J. Agric. Food Chem. 50: 1815-1821.

Villalobos, F., V. Granillo and D. Leyva. 2018. Fabrication of Nanoemulsions by Microfluidization, eds.

Puglia, C., L. Rizza, M. Drechsler and F. Bonina, 2010. Nanoemulsions as vehicles for topical administration of glycyrrhetic acid: Characterization and *in vitro* and *in vivo* evaluation. Drug Deliv. 17(3):123-129.

Shafiq-un-Nabi, S., F. Shakeel, S. Talegaonkar, J. Ali, S. Baboota, A. Ahuja, R.K. Khar and M. Ali, 2007. Formulation development and optimization using nanoemulsion technique: A technical note. AAPS Pharm Sci Tech. 8(2): pp: E1-E6.

Azmi, N.A.N., A.A.M. Elgharbawy, S.R Motlagh, N. Samsudin, H.M. Salleh, 2019. Nanoemulsions: Factory for Food, Pharmaceutical and Cosmetics. Processes. 7(9): 617

EC-P013

DEVELOPMENT OF HEALTH PRODUCTS TO SUSTAINABLE ENHANCE INCOME AND LIFE QUALITY IMPROVEMENT FOR BANG KA CHAO COMMUNITY

Punlapa Vutdhipapornkul, Paradee Asugovit, Siriorn Anootthato and Thotsaphon Umamanit*
Kasetsart Agricultural and Agro-Industrial Product Improvement Institute, Kasetsart University, Bangkok, Thailand.
***E-mail: aapthu@ku.ac.th

ABSTRACT
Bang Ka Chao is an agricultural area that has been called best urban oasis in Asia. It consists of 6 districts and one of them as Bang Kor Bua district, which has the most populated. Most community members are agriculture and traditional massage to earn extra income. The product from the member was used in massage to relieve pain as balm mixed with a body lotion, which is inconvenient and high cost. Therefore, the research team developed a massage oil product for the community uses and sells. To reduce cost, local herbs were used as an ingredient in this product for sustainable increases income and creates additional careers for the community. Local herbal ingredients in this product were Alata leaves, Tamarind leaves and Acanthus leaves which there were properties to relieve aches and muscle relaxation. The massage oil products were a clear yellow liquid with L* a* b* values of 49.10±0.20, -2.90±0.04 and 39.91±0.34, respectively. There was microbiological quality of product passed the Thai Industrial Standard basis. This product has a shelf life for 2 years. In this project, the extraction technology and the production massage oil products were propagated to people in the community. The Satisfaction score for the project was the most satisfactory level and made the community realize of the value of natural resources that can enhance income and improve the quality of life as well.
Keywords : Sustainable Development, Health Products Development, Massage Oil Product, Local Herbs, Bang Ka Chao

INTRODUCTION

The meaning of development is to create thing that doesn't exist before or improve to be more efficient and quality as well as improve things to be better. Sustainable development is a development that focuses on 3 components with consisted of economic, social and environmental. Development can create economic value, reduces environmental impact and improve the quality of life of the well-being of people. Sustainable development can be achieved successfully in society which have to a collaboration of all sectors to drive towards the goal. A purpose of this project is to sustainably enhance income and improve the quality of life for Bang Ka Chao community. Bang Kor Bua district is a large community which almost people is agriculture and traditional massage to earn extra income. This area has many local herbs that have properties to relieve aches and muscle relaxation.

Therefore, the researcher has an idea to bring a local herbs as raw materials in massage oil product development to add value and maximize the use of natural resources. In addition, the extraction technology and the production massage oil products were propagated to people in the community. Consequently, they can produce products for their own, which use and sale to increase income and create a career for the community. That is considered that a self-development in the economy, society and sustainable environment of the people in the community as well.

MATERIALS AND METHODS

Sample preparation

Local herbs were used in this product consisted of Plai (*Cassumunar ginger*), Turmeric, Tamarind leaves, Alata leaves and Acanthus leaves which have properties to relieve aches, sprains and muscle relaxation. The extraction used Maceration extraction method, using 95% ethyl alcohol as a solvent. At the laboratory scale, Tamarind leaves, Alata leaves and Acanthus leaves were washed with water and dried by

tray dryer at 40-50°C. Then, the sample were sliced, chopped into pieces and ground, after that packed into a cloth bag and added into a container with a lid. The samples were added 95% ethyl alcohol for 7 days. And then, the samples were filtered with filter paper and 95% ethyl alcohol was evaporated by rotary evaporator. The extract was dark green color, thick and sticky. On the other hand people in community do not have some Lab's instruments e.g. Tray dryer and Rotary evaporator. Therefore, some methods have been applied as follow Tamarind leaves, Alata leaves and Acanthus leaves were washed with water and dried in the sun until the sample dry (about 2-3 days). Sliced, chopped into pieces and ground of the sample and packed into a cloth bag and added into a stainless steel tank with a lid. The samples were added 95% ethyl alcohol for 7 days. And then, the samples were filtered with filter cloth and 95% ethyl alcohol was evaporated by heating through water.

For the extraction, Plai (*Cassumunar ginger*) and Turmeric will be fried with palm oil. Plai (*Cassumunar ginger*) and Turmeric were washed and sliced. Then, fried with palm oil until crispy and filtered with a filter cloth. The Plai (*Cassumunar ginger*) and Turmeric oil after filter were used in the recipe of massage oil products.

Product development

Developed massage oil products by using the extract of Tamarind leaves, Alata leaves, Acanthus leaves, Plai (*Cassumunar ginger*) and Turmeric oil were a recipe. Physical quality, Microbial quality and products shelf life were evaluated.

Product qualification

The property of massage oil products was tested. Physical quality was evaluated the appearance of products. Microbial quality was used the Colony plate count method of ISO 21149: 2017 and ISO 16212: 2017, examining the number of total bacteria, yeast and mold of products. Products shelf life was evaluated, testing the stability with the Heating and Cooling Cycle (40ºC – 4ºC) method for 8 rounds. (Leelapornpisid, 1989)

Technology transfer

The extraction technology and the production massage oil products technique were propagated to people in Bang Kor Bua community and evaluated the satisfaction of the project.

RESULTS AND DISCUSSION

The appearance of massage oil products was a clear yellow liquid which has the value of L* as 0.20 ± 49.10, a* as 0.04±2.90 and b* as 0.34±39.91, respectively. The sample did not detect the bacteria, yeast and mold in these products. After testing the stability of products by the Heating and Cooling Cycle (40 ºC – 4ºC) method for 8 rounds, founded that the product has good stability with no stratification and sedimentation. The shelf life of products can maintain for 2 years. The product's ingredients were shown in table 1.

Table 1 Massage oil product's ingredients.

Part	Ingredients
A	*Zingiber cassumunar* Roxb oil
	Curcuma longa L. oil
B	Paraffinum Liquidum
C	*Tamarindus indica* L. leaves extract
	Acanthus ebracteatus Vahl. extract
	Cassia alata (L.) Roxb. extract
D	Methyl salicylate
	Menthol
	Camphor
	Borneol camphor
E	*Eucalyptus Globulus* leaf oil

In this project, the researchers selected the suitable packaging and designed the label to be accurate in accordance with the notification of the Food and Drug Administration. The products will be packed in a clear glass bottle packaging due to the acidity of massage oil. Therefore, the glass bottle was suitable for this reason. The head was a roller for ease of use and for the purpose of using the product. The massage oil picture was shown in Figure 1.

Figure 1. Massage oil product's prototype.

In preparation technology, the extraction of Tamarind leaves, Alata leaves, Acanthus leaves and the oil extraction of Plai (*Cassumunar ginger*) and Turmeric were propagated to Bang Kor Bua community. Almost of people in this community was agricultural and traditional massage to earn extra income. The result of technology transfer was found that members of the community are very interested and attentive to study the extraction method and the production's technique. From the assessment of satisfaction in this project found the satisfaction score and was the most satisfactory level. The satisfaction assessment results on technology transfer were shown in Table 2 and the picture of technology transfer was shown in Figure 2.

Figure 2. The pictures of technology transfer activities at Bang Kor Bua community.

Table 2 Satisfaction assessment results on technology transfer.

Contents	score
Part 1 Knowledge content (High-Low = 10-1 score)	
1. What level of knowledge do you have before receive propagating the technology?	2±2
2. After propagating the technology, what level of knowledge do you have?	10±2
Part 2 Utilization (High-Low = 10-1 score)	
1. Herbal extraction techniques	10
2. Developing skills for product production	10
3. Product manufacturing techniques	10
4. Developing new products	10
5. Developing packaging	10
6. Creating market opportunities	10
7. Guidelines for applying to work	10
Part 3 Impact (High-Low = 10-1 score) Do you think that how does it affect your organization when participating in this activity?	
1. The propagation of knowledge gained from this activity to others in the community after the training	10
2. The knowledge is used to develop their capacity and responsibility	10
3. Attending this activity is worth the time	10
4. Able to apply knowledge to practical application	10
Part 4 The satisfaction of the service (The satisfaction scores were the highest, high, medium, little and least)	
1. The information received can be used as your requirement	the highest
2. Skills, knowledge, and ability of speakers	the highest
3. Etiquette, willingness and attention of speakers	the highest
4. Appropriateness of training duration	the highest
5. Availability of tools and equipment	the highest
6. Speakers give an opportunity to ask questions or participate	the highest

Business Model Canvas

Business Model Canvas				
Key Partners	**Key Activities**	**Value Propositions**	**Customer Relationships**	**Customer Segments**
People in community	Use of local herbs to create added value	Health products from research	Health products from research and safe	Elderly person
KAPI, Kasetsart University	Product development	Product that use natural extracts	Product that help relieve aches and muscle relaxation	People in community
Ministry of Tourism and Sports		Product that help people in community		Tourist
	Key Resources		**Channels**	People with aches and pains
	Researcher at KAPI, Kasetsart University		Bang Ka Chao community	Patients in community
Cost Structure	People in community	**Revenue Streams**	Booth exhibition	People from booth exhibition
Product's ingredients cost	Tourist	Revenue from sales of products		
Product development cost	Patients in community	Revenue from massage		
Packaging and Labels cost				
Package design cost				
Labor cost				
Cost of utilities				

CONCLUSIONS

This research was sustainable enhanced income and improves the life quality of Bang Ka Chao community. Technology transfer provided people in the community to realize the use of local herbs to create added value and adopt the maximum benefit. The extraction's technology and the product's production method were propagation to the community. Therefore, the community can produce products for their own use and sale. This way can enhance income and sustainable create a career for the community. The local herbal ingredients in this product were Alata leaves, Tamarind leaves and Acanthus leaves that can be planted in the area and have properties to relieve aches and muscle relaxation. The massage oil products were developed which have clear yellow liquid and have shelf life for 2 years. The satisfaction score of this research was the most satisfactory level.

ACKNOWLEDGEMENTS

This work was supported by Kasetsart University, Bangkok, Thailand.

REFERENCES

ISO 21149:2017 Cosmetics – Microbiology – Enumeration and detection of aerobic mesophilic bacteria.

ISO 16212:2017 Cosmetics – Microbiology – Enumeration of yesat amd mould.

Leelapornpisid, Pimporn. 1989. Cosmetic for skin care. Department of Pharmaceutical Technology, Faculty of Pharmacy, Chiang Mai University, Chiang Mai.

EC-P014

DEVELOPMENT OF MIXED FLOUR FOR GLUTEN-FREE AND LOW-GLYCEMIC INDEX STEAMED CAKE: VALUE-ADDED PRODUCT FROM JASMINE RICE AND ESTIMATION OF COST AND PROFIT

Jaruporn Rakmai[1]*, Pathama Chatakanonda[1], Usa Yonkoksung[2], and Chonlada Buratcharin[3]
[1] Biomass and Bioenergy Technology Division, Kasetsart Agricultural and Agro-Industrial Product Improvement Institute, Kasetsart University, Bangkok, Thailand
[2] National Center for Genetic Engineering and Biotechnology, National Science and Technology Development Agency (NSTDA), Pathum Thani, Thailand
[3] Research Commercialization and Information Technology Management, Kasetsart Agricultural and Agro-Industrial Product Improvement Institute, Kasetsart University, Bangkok, Thailand
*E-mail: aapjor@ku.ac.th

ABSTRACT
The objective of this research is to develop mixed rice flour for preparation of gluten-free and low-glycemic index (GI) steamed rice cake in order to increase the value of rice and decrease the effect of volatile rice price in the market. Because of its texture, aroma flavor and potential to be developed, Jasmine rice was chosen for this research. Optimization of process parameters including flour, fiber, sugar and low-calorie sweetener in preparation of low-GI gluten-free steamed cake was performed. Using low-GI formulation, the glycemic index decreased from 60 to 47. Sensory evaluation showed that the consumers preferred the low-GI steamed cake to the original one because of its softer texture. As the price increased about 2.6 times, the gross profit margin of low-GI rice mixed flour increased about 9.2 times from the Jasmine rice flour.
Keywords: Low-GI, Gluten-free, Jasmine rice, Steamed cake, Mixed flour

INTRODUCTION

Rice is one of the most important global agricultural products. It is the main food traded in Asia which is consumed by most Asian people. Although Thailand is a major producer and exporter of rice which is one of the most important agricultural products consumed by most Asian people, the overproduction of rice because of the mistake in estimating the demand and supply and the production of substitute food staple such as potato and corn caused rice price to fall. The current rice price is calculated based on the forecast of demand of consumers and future supply in the coming season. Thailand lacks a system to forecast rice supply based on the real data of national rice stocks of both the government and the private sector. Although, more farmers gain a higher price margin by turning themselves to sell their rice directly without passing through the middlemen, the development of rice to value-added products has been considered as a sustainable way to help Thai farmer together with government policy.

Jasmine rice is widely consumed in Southeast Asia, it has soft texture and aroma flavor. The 2-acetyl-1-pyrroline (2AP) is a key aroma compound among more than 140 volatile compounds of Jasmine rice (Mahatheeranont et al., 2001; Suwansri and Meullenet, 2004). Jasmine rice flour can be prepared using the broken Jasmine rice kernel during the processing of rice, which is an economical consideration for industrial cost (Clerici et al., 2009; Torbic et al., 2010; Qian and Zhang, 2013). Jasmine rice flour can be used to prepare gluten-free products for consumers with celiac disease. Celiac disease is a problem of certain protein absorption, especially gluten protein, in the diet (Schober et al., 2003). Celiac disease damages the villi of small intestine, it is an uncommon digestive disorder causing squeamish, diarrhea and bloating. Rice flour has been used as a non-allergenic raw material for preparation of gluten-free products including noodles, breakfast cereals, cereal bars, crackers and snacks (Deis 1997; Bond 2004). Previously, mixed Jasmine rice flour for preparation of steamed cake was developed. However, the occurrence of chronic metabolic diseases; such as diabetes, heart diseases and stroke, increases with an excessive consumption of highly refined sugars and high-calorie foods, especially snacks or bakery products. Dietary controls have been recommended to prevent those of metabolic diseases (American Diabetes Association, 2004; WHO, 2003). Consumption of low-glycemic index diets have been considered together with doing exercises. Therefore, the objective of this research is to develop value-added mixed Jasmine rice flour for

preparation of gluten-free and low-glycemic index steamed cake. So that it is expected to increase value of Jasmine rice in Thailand sustainably in the future.

MATERIALS AND METHODS

Preparation of steamed rice cake

The amounts of ingredient of steamed rice cake show in Table 1. Dry ingredients including Jasmine rice flour, sugar, baking powder and salt were mixed together and added to the homogenized wet ingredients consisting of eggs, fresh milk and vegetable oil. Dry and wet ingredients were mixed together. The batter was gently poured into a cup and steamed for 10 min. The steamed rice cakes were left for cooling and characterized in the next steps.

Table 1 Formulation of steamed rice cake.

Ingredient (g)	Quantity (g)
Flour	106.2
Sugar (Bakery sucrose)	96.3
Baking powder ($NaHCO_3$)	9.0
Salt	1.5
Fresh milk	140.0
Vegetable oil	36.0
Egg	100.0

Optimization of process parameters in preparation of low-GI gluten-free steamed cake

The flour combinations were varied in different proportions based on Jasmine rice flour and resistant maltodextrin. Sugar, bakery sucrose, was substituted by stevioside and sucralose with the same level of sweetness. Texture profile analysis, sensory evaluation and estimated glycemic index analysis were performed to characterize the steamed cake samples.

Texture profile analysis (TPA)

A piece of steamed cake sample (2 x 2 cm) was placed on the base plate. A two-cycle, force-versus-distance compression program was used to measure and calculate using a TA. XT-Plus Texture analyzer with a 50-kg load cell with a 35 mm cylindrical probe attachment (Stable Micro Systems Ltd., Surrey, UK). The TPA computer software was Texture Exponent 32 (Stable Micro Systems). The probe was allowed to descend at 1 mm/s. The steamed cake sample was compressed to 50% of its original height at a constant rate of 1 mm/s. After the first compression, the probe retracted off the steam cake and remained constantly for 5 sec followed by a second compression. For each replicate, texture measurements were conducted ten times. Texture parameters were derived from the TPA curve and calculated using the equations from Bourne (1978) (Table 2). Instrumental data were subject to one-way analysis of variance. A Tukey's test was used for means separation, when the effect of formulation was significant.

Table 2 Description of Texture Profile Analysis (TPA) parameters with calculations.

Parameter	Descriptive Definition
Hardness	Force required to compress steamed cake to 50% of original height (F1max) (g)
Hight1	Average height of one steamed cake (distance to reach F1max × 2/3) (cm)
Hight2	Average height of one steamed cake after first compression (distance to reach second F2max × 2/3) (cm)
Area1	Work of first compression (area under first curve to reach F1max) (g/mm)
Area2	Work of second compression (area under second curve to reach F2max) (g/mm)
Cohesiveness	Area2/Area1
Springiness	Height2/Height1
Gumminess	Hardness × Cohesiveness; i.e (F1max) × (Area2 / Area1)
Chewiness	Gumminess × Springiness; i.e (F1max) × (Area2 / Area1) × (Height2 / Height1)

Source: Finnie et al. (2006)

In vitro glycemic index analysis

Enzyme and Assay kits: Porcine pancreatic alpha-amylase and amyloglucosidase were purchased from Sigma-Aldrich (St Louis, MO). GOPOD (glucose oxidase and peroxidase) assay kits were purchased from Megazyme (Bray, Ireland). Alpha-amylase (6 g) was dispersed in 40-mL deionized water by magnetic stirring for 10 min. The dispersion was then centrifuged for 10 min at 30,000 g. The supernatant (32 mL) was transferred to a beaker, and amyloglucosidase (2 mL) and deionized water (3 mL) were added to prepare the enzyme solution. This solution should be freshly prepared for the digestion test.

Starch hydrolysis: The rate of starch hydrolysis was analyzed using the method reported by Goni et al. (1997). The in vitro digestion with enzyme was carried out at 37°C. Aliquots (1 mL) were sampled at intervals (0, 10, 20, 30, 60, 90, 120 and 180 min) and immediately boiled for 10 min to terminate the enzyme reaction. After centrifugation (1500 g, 10 min), the glucose contents in supernatant were determined by GOPOD assay kits.

The area under the hydrolysis curve (AUC) was calculated following the equation:

$$AUC = C_\infty(t_\infty - t_0) - (C_\infty/k)\,[1-\exp[-k(t_\infty - t_0)]]$$

where C_∞ corresponds to the equilibrium percentage of starch hydrolyzed after 180 min, t_∞ is the final time (180 min), t_0 is the initial time (0 min) and k is the kinetic constant.

The hydrolysis index (HI) was calculated as AUC of a sample as percentage of the corresponding AUC of reference (Goni et al., 1997). The white bread used as reference and the estimated glycemic index (eGI) was calculated according to equations:

$$GI = (0.549 \times HI) + 39.71$$

Sensory evaluation and consumer test

Sensory evaluation was conducted with untrained panelists, age 23-59 years, in individual testing booths. The panelists were asked to score characteristics of steamed cake samples including appearance, color, flavor, taste, texture and overall liking on a 9-point hedonic scale (1 = dislike extremely, 9 = like extremely). The computerized program was used to statistically calculate and determine the significance of the difference amongst formulations scored by panelists, a Tukey's test was used for means separation (Han et al., 2010).

RESULTS AND DISCUSSION

Texture profile analysis

The steamed cakes became softer with increased levels of resistant maltodextrin powder (Table 3). The internal resistance of steamed cake structure was expressed by cohesiveness. Springiness evaluates the elasticity of the steamed cake by determining the extent of recovery between the first and the second compressions. The springiness of sample decreased with an increase in resistant maltodextrin. Gumminess is the force required to break down the sample for swallowing, it is calculated by hardness multiplied by cohesiveness. Chewiness indicates the amount of energy needed to disintegrate a sample for swallowing. The gumminess and chewiness of steamed cake sample decreased with increase in resistant maltodextrin. Therefore, resistant maltodextrin helped the steamed cake became softer. However, the height of cake decreased with an increase in resistant maltodextrin from 33±0.8 to 31.5±1.3, 29.5±1.3 and 27.25±1.5 mm after substitution by 10, 20 and 30% resistant maltodextrin, respectively. Moreover, after substitution by ≥ 20% resistant maltodextrin, the texture of steamed cake was not firm and became friable (Figure 1).

Table 3 Texture profile of steamed cakes from Jasmine rice flour with different amount of resistant maltodextrin.

Samples	Hardness (Kg Force)	Cohesiveness	Springiness	Gumminess (Kg Force)	Chewiness (Kg Force)
J-0% RM	2.57 ± 0.20^{a}	0.72 ± 0.01^{a}	0.97 ± 0.01^{a}	1.84 ± 0.16^{a}	1.79 ± 0.15^{a}
J-10% RM	2.23 ± 0.21^{ab}	0.72 ± 0.08^{a}	0.95 ± 0.03^{ab}	1.63 ± 0.19^{ab}	1.55 ± 0.18^{ab}
J-20% RM	1.95 ± 0.18^{bc}	0.74 ± 0.08^{a}	0.94 ± 0.02^{ab}	1.44 ± 0.27^{b}	1.35 ± 0.25^{b}
J-30% RM	1.73 ± 0.18^{c}	0.75 ± 0.01^{a}	0.93 ± 0.01^{b}	1.30 ± 0.14^{b}	1.20 ± 0.12^{b}

* Mean values in the same column with different letters are significantly different ($p \leq 0.05$)

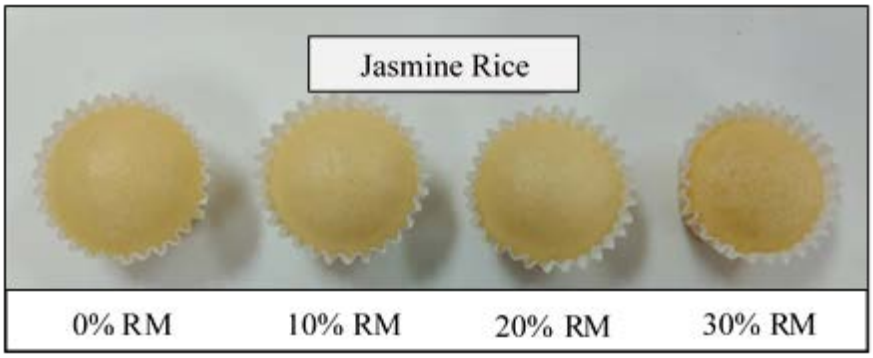

Figure 1. Steamed cakes form Jasmine rice with different levels of resistant maltodextrin.

In vitro glycemic index

Table 4 shows the estimated glycemic index (GI) of steamed cake formulations. The conventional steamed cake from Jasmine rice flour presented glycemic indexes of 60.4. This was classified as intermediate glycemic index foods (GI between 56 and 69) (American Diabetes Association, 2004). The GI reduced with a decrease in starch content by replacement of fiber. Substituting Jasmine rice flour by 10 percent resistant maltodextrin reduced glycemic index of steamed cake sample to 58.2. Dietary fiber is well known to contribute to reduction of glycemic index by several mechanisms (Brennan, 2005; Alongi et al., 2019; Weickert & Pfeiffer, 2018); however, 10 percent was not enough to prepare low-GI steamed cake. Substituting bakery sucrose by sucralose could be done up to 50 percent, replacement by 25 and 50 percent sucralose reduced glycemic index of steamed cake samples to 52.7 and 47.4, respectively which were classified as low-GI samples.

Table 4 Estimated glycemic index of steamed cake from different formulations.

Pancake formulation	Glycemic Index (GI)
Original steamed cake	60.4
Steamed cake substituted with 10% RM	58.2
Steamed cake substituted with 10% RM and 25% sucralose	52.7
Steamed cake substituted with 10% RM and 50% sucralose	47.4

White bread was used as a reference
RM: Resistant Maltodextrin

Sensory evaluation

Figure 2 shows sensory quality characteristics of steamed cakes with different proportions of sucralose; 0, 25 and 50 percent. There was no difference in the texture and overall liking between sample substituted by 25 and 50 percent sucralose. The taste of sample substituted by 50 percent sucralose, the flavor and the appearance of sample substituted by 25 percent sucralose showed higher score than those of other samples. The overall liking scores of the steamed cake substituted by 25 and 50 percent sucralose were 7.0-7.1 on a hedonic scale, indicating that these steamed cake products were highly acceptable compared to control samples which the overall liking score of 6.6. Therefore, a partial substitution of Jasmine rice flour with resistant maltodextrin and partial substitution of sucralose with bakery sucrose in steamed cakes was acceptable.

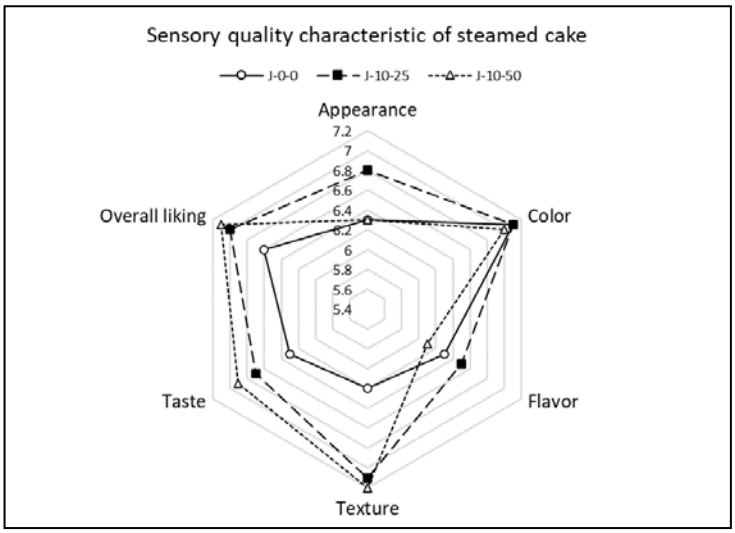

Figure 2. Sensory quality characteristics of steamed cakes with different proportions of sweeteners.

Estimation of costs and profits

Table 5 shows modern trade pricing structure and gross profit margin of Jasmine rice flour and its value-added products for steamed cake preparation. Gross profit margin is a metric analysts use to assess financial property by calculating the amount of money left over from product sales after subtracting the cost of goods sold (COGS) (Leahy, 2012). Sometimes referred to as the gross margin ratio, gross profit margin is frequently expressed as a percentage of sales. Although, the development of Jasmine rice flour to mixed Jasmine rice flour and low-GI mixed Jasmine rice flour costed higher expense, the price increased about 1.16 and 2.63 times and the estimated gross profit margins increased to 14.11 and 64.02 which were about 2.02 times and 9.19 times for the mixed rice flour and low-GI mixed rice flour, respectively.

Table 5 Modern trade pricing structure of Jasmine rice flour and its value-added products.

Modern Trade Pricing Structure	Jasmine Rice Flour (1 KG)	Mixed Jasmine Rice Flour for Steamed Cake (1 KG)	Mixed Jasmine Rice Flour for Low-GI Steamed Cake (1 KG)
1. Retail Selling Price (Include VAT)	95	110	250
2. VAT	6.21	7.20	16.36
3. Retail Selling Price (Exclude VAT)	88.79	102.80	233.65
4. Trade Margin	23.75	27.5	62.5
5. Listed Trade Price (LTP)	65.04	75.30	171.15
6. Advertising and Promotion	9.50	11	25
7. Market Hygiene	0.65	0.75	1.71
8. Standard Cost (Net Income)	54.88	63.55	144.43
9. Investment Unit Cost (COG)	47.91	49.44	80.41
10. Gross Profit Margin	6.97	14.11	64.02

CONCLUSIONS

A partial substitution of Jasmine rice flour with resistant maltodextrin and partial substitution of sucralose with bakery sucrose in steamed cakes was acceptable with overall liking score ≥ 7 on a hedonic scale. The GI reduced with a decrease in Jasmine rice flour and bakery sucrose content by replacement of 10 percent resistant maltodextrin and 25 percent sucralose, respectively. Resistant maltodextrin helped the steamed cake become softer; however, after substitution by ≥ 20%, the texture of steamed cake was not firm and became friable. The development of Jasmine rice flour to mixed Jasmine rice flour and low-GI mixed Jasmine rice flour increased the price about 1.16 and 2.63 times and the estimated gross profit margins increased to 14.11 and 64.02 which were about 2.02 times and 9.19 times, respectively.

ACKNOWLEDGEMENT

The research was supported by Kasetsart University Research and Development Institute (KURDI), Kasetsart University, Thailand.

REFERENCES

Alongi, M., S. Melchior and M. Anese. 2019. Reducing the glycemic index of short dough biscuits by using apple pomace as a functional ingredient. LWT - Food Sci. Technol. 100: 300–305.

American D. A. 2004. Nutrition principles and recommendations in diabetes. Diabetes Care. 27, S36-S46.

Bond, A. 2004. Consumer sensory characteristics of butter cake made from wheat and rice flour, p. 105. In: MS thesis. Baton Rouge, La.: Louisiana State Univ.

Brennan, C.S. 2005. Dietary fibre, glycaemic response and diabetes. Mol. Nutr. Food Res. 49: 560-570.

Clerici, M.T.P.S., C. Airoldi and A.A. El-Dash. 2009. Production of acidic extruded rice flour and its influence on the qualities of gluten-free bread. LWT – F Food Sci. Technol. 42: 618–623.

Deis, R.C.1997. Functional ingredients from rice. Food Prod Design. 7: 46–56.

Finnie, S.M., A.D. Bettge and C.F. Morris. 2006. Influence of flour chlorination and Iingredient formulation on the quality attributes of pancakes. Cereal Chem. 83: 684–691.

Goni, I., A. Garcia-Alonso and F. Saura-Calixto. 1997. A starch hydrolysis procedure to estimate glycemic index. Nutr. Res. 17: 427-437.

Han, J., J.A.M. Janz, M. Gerlat. 2010. Development of gluten-free cracker snacks using pulse flours and fractions. Food Res. Int. 43: 627-633.

Leahy, A.S. 2012. The Determinants of profitability In the pharmaceutical industry. Am. J. Health Sci. 3: 37-42.

Mahatheeranont, S., S. Keawsa-Ard and K. Dumri. 2001. Quantification of the rice aroma compound, 2-acetyl-1-pyrroline, in uncooked Khao Dawk Mali 105 brown rice. J. Agric. Food Chem. 49: 773-779.

Qian, H. and H. Zhang. 2013. Rice flour and related products, pp. 553-575. In: Handbook of food powders. Woodhead Publishing Ltd., Jiangnan University, China.

Schober, T.J., C.M. O'Brien, D. McCarthy, A. Darnedde and E.K. Arendt. 2003. Influence of gluten-free flour mixes and fat powders on the quality of gluten-free biscuits. Eur. Food Res. Technol. 216: 369–376.

Suwansri, S. and J.F. Meullenet. 2004. Physicochemical characterization and consumer acceptance by Asian consumers of aromatic jasmine rice. J. Food Sci. 69: 30–37.

Torbic, A., M. Hadnacev and T. Dapcevic. 2010. Rheological, textural and sensory properties of gluten-free bread formulations based on rice and buckwheat flour. Food Hydrocoll. 24: 626–632.

Weickert, M.O. and A.F.H. Pfeiffer. 2018. Impact of dietary fiber consumption on insulin resistance and the prevention of type 2 diabetes. J. Nutr. 148: 7–12.

WHO. 2003. Diet, nutrition and the prevention of chronic diseases. World Health Organization Technical Report Series. 916.

Author Index

ASEAN BIO energy & economy Conference 2020

conference.abb@gmail.com

http://www.abbconf.kapi.ku.ac.th/

https://www.facebook.com/KapiKuBiomass/